



Shri Gajanan Shikshan Sanstha's
SHRI SANT GAJANAN MAHARAJ COLLEGE OF ENGINEERING
SHEGAON – 444203, DIST. BULDHANA (MAHARASHTRA STATE),
INDIA

"Recognized by A.I.C.T.E., New Delhi" Affiliated to Sant Gadge Baba Amravati University, Amravati
"Approved by the D.T.E., M.S. Mumbai"

Ph +918669638081/82
Website- www.ssgmce.ac.in

Email. principal@ssgmce.ac.in,
registrar@ssgmce.ac.in

CRITERION III - RESEARCH, INNOVATIONS AND EXTENSION

Key Indicator 3.3 - Research Publications and Awards

Metric No	Assessment Indicators	Evidences
3.3.3	Number of books and chapters in edited volumes/books published and papers published in national/international conference proceedings	List of book chapter & Papers
		Copy of paper/Certificate



PRINCIPAL
Shri Sant Gajanan Maharaj
College of Engineering, Shegaon.



Shri Gajanan Shikshan Sanstha's
SHRI SANT GAJANAN MAHARAJ COLLEGE OF ENGINEERING
SHEGAON – 444203, DIST. BULDHANA (MAHARASHTRA STATE),
INDIA

“Recognized by A.I.C.T.E., New Delhi” Affiliated to Sant Gadge Baba Amravati University, Amravati
“Approved by the D.T.E., M.S. Mumbai”

Ph +918669638081/82
Website- www.ssgmce.ac.in

Email. principal@ssgmce.ac.in,
registrar@ssgmce.ac.in

List of Book Chapter & Papers

Name of the teacher	Title of the book/chapters published	Title of the paper
Mr. M.R.Chavan Dr. A.U.Jawadekar Danton Diego		SOBI-ANN Based Induction Motor Fault Classification
P.R.Bharambe Dr.S.R.Paraskar R. S. Kankale Dr.S.S.Jadhao	Recent Revolutions in Energy Drives and E-Vehicles	A Novel Algorithm for Discrimination of the Magnetizing Inrush Current and Internal Fault Current of a Transformer Using Teaser Energy Operator and Artificial Neural Network.
R. S. Kankale Dr.S.R.Paraskar Dr.S.S.Jadhao	Recent Revolutions in Energy Drives and E-Vehicles	Development of wavelet and ANN based algorithm in LABVIEW environment for classifying the power quality disturbances.
M. Bagde A.U.Jawadekar A. Sawalakhe	Recent Revolutions in Energy Drives and E-Vehicles	Enhancing performance of hybrid electric vehicle using optimized energy management methodology
Ravishankar S. Kankale, Dr. Sudhir R. Paraskar, Dr. Saurabh S. Jadhao	Futuristic Trends in Electrical Engineering, , IIP Series, Volume 3, Book 2, Part 6, Chapter 1	“Classification of Multiple and Multistage Power Quality Disturbances Using S-Transform and Feed Forward Neural Network”,
V.S.Karale, Dr. Sudhir R. Paraskar, Dr. Saurabh S. Jadhao,	Futuristic Trends in Electrical Engineering, e- ISBN: 978-93-6252-039-5, IIP Series, Volume 3, Book 2, Part 6, Chapter 4	Voltage Sag Reduction Using A UTVG Based Dynamic Voltage Restorer



Shri Gajanan Shikshan Sanstha's
SHRI SANT GAJANAN MAHARAJ COLLEGE OF ENGINEERING
SHEGAON – 444203, DIST. BULDHANA (MAHARASHTRA STATE),
INDIA

“Recognized by A.I.C.T.E., New Delhi” Affiliated to Sant Gadge Baba Amravati University, Amravati
 “Approved by the D.T.E., M.S. Mumbai”

Ph +918669638081/82
 Website- www.ssgmce.ac.in

Email. principal@ssgmce.ac.in,
registrar@ssgmce.ac.in

P.R.Bharambe Dr. Sudhir R. Paraskar, Dr. Saurabh S. Jadhao	Futuristic Trends in Electrical Engineering, IIP Series, Volume 3, Book 2, Part 7, Chapter 1	Discrimination of interturn faults from magnetizing inrush current in transformer: A wavelet transform Approach
Dr . A.U.Jawadekar G.G.Akotkar		Transformer Incipient Fault Diagnosis using Supervised Machine Learning
S. K. Khodke, R. S. Kankale and S. R. Paraskar		A Hilbert Transform Based Approach for Classification of Complex Power Quality Disturbances,"
Dr. S.R.Paraskar		Improvement of Power Quality in distributuin system using battery Energy storage system
Dr.S.R.Paraskar		Enhancing Reliability of Distribution system with Battery Energy Storage Systems
Dr . A.U.Jawadekar Samiksha Shahade		Advancement in Islanding Detection techniques: A Comprehensive Review
Neerja Dharmale		Application of OLCAO- GGA and OLCAO-MGGA Techniques forinvestigating properties of TiO ₂
Rupesh Mahamune		The multi-scale wavelet approach for the removal of eye-blink artifact from EEG Signals
Harshavardhan Patil		Elevating Canteen Management with a Modern Web Solution
S. P. Badar and K. Khanchandani		Efficient Implementation of Polar Decoder: Design and Performance Analysis
Dr D.D. Nawgaje		MDLGO: Integrated Multimodal Deep Learning Framework for Enhanced



Shri Gajanan Shikshan Sanstha's
SHRI SANT GAJANAN MAHARAJ COLLEGE OF ENGINEERING
SHEGAON – 444203, DIST. BULDHANA (MAHARASHTRA STATE),
INDIA

“Recognized by A.I.C.T.E., New Delhi” Affiliated to Sant Gadge Baba Amravati University, Amravati
 “Approved by the D.T.E., M.S. Mumbai”

Ph +918669638081/82
 Website- www.ssgmce.ac.in

Email. principal@ssgmce.ac.in,
registrar@ssgmce.ac.in

		Precision in Glaucoma Diagnosis Using OCT A-scans
Santosh B. Patil	Data Science and Big Data Analytics.Data Intensive Research	Transfer Learning by Fine-Tuning Pre-trained Convolutional Neural Network Architectures for Image Recognition
Santosh B. Patil	Artificial Intelligence, Machine Learning and User Interface Design	Enhancing Efficiency in Content Based Image Retrieval System Using Pre-trained Convolutional Neural Network Models .Published in a book “Artificial Intelligence, Machine Learning and User Interface Design”
Prof. Ganesh Wahile		Computational Analysis of Toroidal Propeller using CFD
Vishwanath S. Mahalle, Archana L. Rane,Debam Bhattacharya,Abhijit Banubakode and Vandana C. Bagal	Book Title: Artificial Intelligence, Machine Learning and User Interface Design Chapter Name: Knowledge representation in Artificial Intelligence- A Practical Approach	
Vishwanath S. Mahalle, Narendra M. Kandoi, Santosh B. Patil, Abhijit Banubakode and Vandana C. Bagal	Book Title: Artificial Intelligence, Machine Learning and User Interface Design Chapter Name: Enhancing Efficiency in Content-based Image Retrieval System Using Pre- trained Convolutional Neural Network Models	



Shri Gajanan Shikshan Sanstha's
SHRI SANT GAJANAN MAHARAJ COLLEGE OF ENGINEERING
SHEGAON – 444203, DIST. BULDHANA (MAHARASHTRA STATE),
INDIA

“Recognized by A.I.C.T.E., New Delhi” Affiliated to Sant Gadge Baba Amravati University, Amravati
“Approved by the D.T.E., M.S. Mumbai”

Ph +918669638081/82
Website- www.ssgmce.ac.in

Email. principal@ssgmce.ac.in,
registrar@ssgmce.ac.in

Prof. V. S. Mahalle, Narendra M. Kandoi, Santosh B. Patil	Book Title: Data Science and BigData Analytics Chapter: Transfer Learning by Fine Tuning Pre-Trained Convolutional Neural Network Architectures for Image Recognition	
Dr. Jaikumar M. Patil Dr. Aarti S. Zanwar Dr. Abhijit N. Merekar Dr. Smita A. Merekar Dr. Arvind R. Bhagat Patil	Book Name:Textbook of Quality Assurance	
Dr. N. M. Kandoi P. V. Kale A. G. Sharma	Book Name:AI-Driven Helthcare Transforming Diagnosis for Effective Treatment	
Vishwanath S. Mahalle, Chandrashekhar M. Mankar, Nikhil Prakash J. S., Debanjan Ghosh	Book Name: Cyber Security	
Dr. H M Jha "Bidyarthi", Dr. P. M. Kuchar, Dr. M. A. Dande, Dr. S. M. Mishra	Case studies on Leading and strategizing for organizations across contexts, Editor- Shreya Mishra,	Unchained: The On-going Rise of Chain Business- A case study of Shree Abhay Group of Industries



PRINCIPAL
Shri Sant Gajanan Maharaj
College of Engineering, Shegaon.

Department of Electrical Engineering

AY 2023-24

International Conference

Sl. No.	Name of the teacher	Title of the book/chapters published	Title of the paper	Title of the proceedings of the conference	Name of the conference	Year of publication	ISBN number of the proceeding	Name of the publisher
1	Mr. M.R.Chavan Dr. A.U.Jawadekar Danton Diego		SOBI-ANN Based Induction Motor Fault Classification	IEEE International Conference on Information Technology, Electronics and Intelligent Communication Systems (ICITEICS-2024)	IEEE International Conference on Information Technology, Electronics and Intelligent Communication Systems (ICITEICS-2024)	2024	ISBN:979-8-3503-8269-3	IEEE
2	P.R.Bharambe Dr.S.R.Paraskar R. S. Kankale Dr.S.S.Jadhao	Recent Revolutions in Energy Drives and E-Vehicles	A Novel Algorithm for Discrimination of the Magnetizing Inrush Current and Internal Fault Current of a Transformer Using Teager Energy Operator and Artificial Neural Network.	Lecture Notes in Electrical Engineering, vol 1162. Springer, Singapore.	Recent Revolutions in Energy Drives and E-Vehicles (REEDeV)	2024	ISBN 978-981-97-0762-1	Springer
3	R. S. Kankale Dr.S.R.Paraskar Dr.S.S.Jadhao	Recent Revolutions in Energy Drives and E-Vehicles	Development of wavelet and ANN based algorithm in LABVIEW environment for classifying the power quality disturbances.	Lecture Notes in Electrical Engineering, vol 1162. Springer, Singapore	Recent Revolutions in Energy Drives and E-Vehicles (REEDeV)	2024	ISBN 978-981-97-0762-1	Springer

4	M. Bagde A.U.Jawadekar A. Sawalakhe	Recent Revolutions in Energy Drives and E-Vehicles	Enhancing performance of hybrid electric vehicle using optimized energy management methodology	Lecture Notes in Electrical Engineering, vol 1162. Springer, Singapore.	Recent Revolutions in Energy Drives and E- Vehicles (REEDeV)	2024	ISBN 978-981- 97-0762-1	Springer
5	Ravishankar S. Kankale, Dr. Sudhir R. Paraskar, Dr. Saurabh S. Jadhao	Futuristic Trends in Electrical Engineering, , IIP Series, Volume 3, Book 2, Part 6, Chapter 1	“Classification of Multiple and Multistage Power Quality Disturbances Using S-Transform and Feed Forward Neural Network”,			2024	e- ISBN: 978-93- 6252-039-5	IIP Series
6	V.S.Karale, Dr. Sudhir R. Paraskar, Dr. Saurabh S. Jadhao,	Futuristic Trends in Electrical Engineering, e- ISBN: 978-93- 6252-039-5, IIP Series, Volume 3, Book 2, Part 6, Chapter 4	Voltage Sag Reduction Using A UTVG Based Dynamic Voltage Restorer			2024	e- ISBN: 978-93- 6252-039-5	IIP Series
7	P.R.Bharambe Dr. Sudhir R. Paraskar, Dr. Saurabh S. Jadhao	Futuristic Trends in Electrical Engineering, IIP Series, Volume 3, Book 2, Part 7, Chapter 1	Discrimination of interturn faults from magnetizing inrush current in transformer: A wavelet transform Approach			2024	e- ISBN: 978-93- 6252-039-5,	IIP Series
8	Dr . A.U.Jawadekar G.G.Akotkar		Transformer Incipient Fault Diagnosis using Supervised Machine Learning		International Conference on Recent Advances in Engineering and Computer Applications (ICRAECA-2023) 14th and 15th July 2023	2023	ISBN: 978-93- 92105-78-4	IFERP Explore

9	S. K. Khodke, R. S. Kankale and S. R. Paraskar		A Hilbert Transform Based Approach for Classification of Complex Power Quality Disturbances," ;		International Conference on Green Energy (ICOG 2023), Pune, India, May 2023.	2023		International Journal of Innovative Research in Electrical, Electronics, Instrumentation and Control Engineering (IJIREEICE)
10	Dr. S.R.Paraskar		Improvement of Power Quality in distributu in system using battery Energy storage system		Second international conference on Multidiciplinary Research and Innovation (ICMRI) 2024	2024		
11	Dr.S.R.Paraskar		Enhancing Reliability of Distribution system with Battery Energy Storage Systems		International Conference on Futuristic Trends in Science , Engineering and Management (ICFTSEM) 2024	2024		
12	Dr . A.U.Jawadekar Samiksha Shahade		advancement in Ilanding Detection techniques: A Comprehensive Review		Hinwis Second international Conference recent trends in Machine Learning and Image Processing LMIP 2023	2023		

SOBI-ANN Based Induction Motor Fault Classification

1st Mukesh Ravindra Chavan

2nd Anjali Uday Jawadekar

Department of Electrical Engineering
Shri Sant Gajanan Maharaj Collge Of Engineering
Shegaon, India
chavanmukesh38@gmail.com
anjali.jawadekar@gmail.com

3rd Danton Diego Ferreira

Department of Automation (DAT)
Federal University of Lavras
Lavras, Brazil
danton@ufla.br

Abstract—The Induction motor fault can lead to financial loss in any place where it is used. Hence, an early detection and diagnosis of fault and its classification becomes most important for the smooth working of the system. In this paper the study proposes an algorithm for fault classification. The second order blind identification method (SOBI) is used for calculating the estimates and these estimates are given to the ANN for fault classification. Result indicates the input requirements are reduced for the classification of faults when 14 statistical parameters of 2nd and 3rd estimates of SOBI are given to the ANN.

Index Terms—SOBI, BSS, ANN, Fault Classification

I. INTRODUCTION

The induction motor ranks among the most frequently employed motors within industrial settings. About 60% of the industrial load is induction motor load. The induction motor fault causes the industrial process to halt. This causes huge amount economic losses to the industries. The types of fault those an induction motor come across are rotor faults and stator faults. The rotor fault accounts for 20% faults on the induction motor. Rotor faults encompass categories such as rotor eccentricity, damage, fracture or deformation of rotor cage bars, and cracks or fractures in end rings, as well as rotor bowing [1]. The total faults of induction motor 40% faults reported are the bearing fault. Stator related issues generally be divided into two main groups: (i) faults related to laminations and the frame and (ii) faults associated with stator windings. These faults can occur in an induction motor due to various stress factors, including mechanical, thermal, electrical, and environmental factors, leading to potential fault conditions[2].

Numerous techniques and technologies are being suggested for identifying fault conditions in various systems. These methods include Employing electromagnetic field monitoring via coils wound around motor shafts particularly in context of axial flux detection and utilizing search coils, Utilizing infrared recognition, Monitoring radio-frequency and (RF) emissions, Assessing noise and vibration, Measuring acoustic noise, Implementing motor-current signature analysis (MCSA), Employing model-based, artificial intelligence based, and neural network-based approaches. Various techniques have been suggested for fault detection and classification,

including methods such as MCSA, Park's Transform, Artificial Neural Networks, Finite Element Method, Concordia Transform, Vibration Testing and Analysis, Multiple Reference Frames Theory, External Magnetic Field Analysis, Power Decomposition Technique, KU Transformation Theory and Wavelet Analysis. Among all the methods the MCSA, ANN and Wavelet Analysis method has been widely used because of the several advantages. For rotor faults detection and classification various methods have been used like Fast Fourier Transform (FFT), Short Time Fourier Transform (STFT), Discrete Wavelet Transform (DWT), finite element analysis, Vienna Monitoring Method, and wavelet transform based methods[3]. For stator faults mostly discussed and occurred fault is a bearing fault, then interturn faults are considered. To detect and classify bearing and interturn fault various methods for detection and classification have been proposed the negative and zero sequence currents for detection, checking for the additional air gap flux harmonics, instantaneous power signatures, random forest classifier, Park's Transform, Principal Component Analysis(PCA), Artificial Neural Network (ANN), Fuzzy classifier are used [2][3].

In addition to these approaches, researchers have delved into a novel realm of fault detection and classification known as blind source separation (BSS) methods. There are several algorithms in BSS like information maximization algorithm, Fixed point algorithms(ICA), JADE algorithm[4]. ICA uses the higher order statistical properties to linearly mixed signals into independent components, all without any prior information about original components or mixing process[5]. The ICA method is used over the FFT output and its standard deviation in region of interest were found to be fault discriminant [6]. The ICA method along with some constrained is used to classify the fault. The information is contained by the signals in terms of independent component is less so the c-ICA algorithms can classify the fault based only if prior knowledge of mechanical information is known as reference[7]. The ICA technique is employed to identify faults in induction motor by determining a threshold and triggering a fault detection if any condition surpasses this condition[8]. Form above results we come to the conclusion that ICA can be used for the fault

detection but will not be suitable for the fault classification. So another method and area of BSS algorithms is higher order statistics (HOS) called as Second Order Blind Identification method (SOBI). This paper is organized in eight chapters. The second chapter will explain about the SOBI method its advantages and disadvantages. Third chapter presents introduction to Artificial Intelligence. Fourth chapter presents feature extration. Fifth chapter will present the algorithm for classification of the faults of induction motor. Sixth chapter will discuss the experimental setup and observations. Seventh chapter will present the results and discussions. Eight chapter will present the conclusion and future scope.

II. SECOND ORDER BLIND IDENTIFICATION (SOBI) METHOD

The method was introduced by Belouchrani et al., in 1997 [9]. Second-Order Blind Identification (SOBI as introduced by Belouchrani et al. in 1997), leverages the temporal inter-dependencies of components through the joint diagonalization of one or multiple auto-covariance matrices. After that several authors have used this algorithm for source separation and finding out the valuable information for detection and classification in various area of application. The SOBI method has found application in various domains, including artifact removal from EEG data [9], the identification of significant signals in brain EEG data [10], the separation of vibrations originating from underground traffic, and the prediction of wind speed. SOBI has gained recognition as a well-established and extensively researched technique for separating uncorrelated weakly stationary time series. For different time series and BSS model this method has to be provided with some modification [11]. The SOBI method has been successfully implemented by the Oliveira et al. in 2020 for harmonic and inter harmonic classification of Power Quality disturbances. Applying the same concept here the induction motor fault classification is achieved [12]. The SOBI algorithm operates by approximating the joint diagonalization of two correlation matrices characterized by different delays. When $z[n]$ a whitened vector is provided, it investigates for a collection of r delayed correlation matrices for $z[n]$, denoted as $R_z(\tau_i)$ for $i = 1, \dots, r$. The objective of SOBI is to find a unitary transformation V such that:

$$V^T R_z(\tau_i) V = D_i \text{ for } i = 1, \dots, r \quad (1)$$

where, D_i refers to a collection of covariance related to the estimated signal $y[n]$. By working with several correlation matrices, SOBI reduces the probabilities of incorrect delay selection interfering with blind separation process. Put simply, the steps to execute the SOBI can be summarized as follows:

1. Evaluate the MxM correlation matrix $R_x(0)$ of signals $x[n]$ as:

$$R_x(0) = E[x(0)x^T(0)] = \frac{1}{N - M + 1} X X^T \quad (2)$$

where X is called as the Hankel matrix

2. Estimate the EVD of $R_x(0)$:

$$R_x(0) = V_x D_x V_x^T \quad (3)$$

where $V = [v_1, v_2, \dots, v_M]$ is an MxM unitary matrix having eigenvectors of $R_x(0)$ and D_x is an MxM diagonal matrix having eigenvalues $\lambda_1, \lambda_2, \lambda_3, \dots, \lambda_M$ of $R_x(0)$ prepared in descending order.

3. A white vector $z[n]$ is obtained by performing whitening of $x[n]$ through the whitening matrix Q ,

$$z[n] = Q_x[n] \quad (4)$$

Where,

$$Q = D_x^{-(1/2)} V_x^T \quad (5)$$

4. Calculate H delayed sample correlation matrices $R_z(\tau)$ from $z[n]$ for a set of fixed delays

$$\tau \in (\tau_j, j = 1, \dots, H); \quad (6)$$

5. Obtain the unitary matrix V , which is the joint diagonalizer of the set of correlation matrices $(R_z(\tau_j), j = 1, \dots, H)$, by applying the Givens Rotation method[12];

6. Estimate the output signals as:

$$y[n] = V^T Q_x[n] \quad (7)$$

And or the mixture matrix A , as $A=Q*V$.

Where $*$ denotes the Moore-Penrose pseudo-inverse.

Experimental findings have indicated that employing multiple correlation matrices is more effective and resilient in scenarios characterized by low signal-to-noise ratio (SNR) and/or sources with minimal spectral distinctions[12].

III. ARTIFICIAL INTELLIGENCE

Neural network is recognized as a biologically inspired computational method. It consists of the processing element, connections, and coefficients. The processing elements are neurons, connections are training and recall algorithms and coefficients are the weights given to connections. The Architecture of Artificial Neural Network is shown in Figure 1. Artificial neural networks possess key attributes such as adaptability in learning, the ability to generalize, parallel processing at scale, resilience, the capacity for associative information storage, and processing of spatiotemporal information [13]. Artificial intelligence is being used in various area of applications like pattern recognition, speech recognition, biomedical

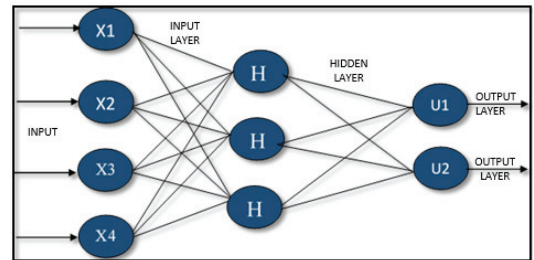


Fig. 1. Architecture of Artificial Neural Network

diagnosis applications, induction motor fault detection and diagnosis, and many more[14]. The neural network illustrated here is organized in three tiers: an output layer, a hidden layer and an input layer . The artificial feed-forward network topology is selected for simplicity. The choice for training input patterns involves utilizing a feedforward network, while error computation and weight adjustment based on error calculations are accomplished through backpropagation. The progression goes from input layer to hidden layer and to the output layer.

IV. FEATURE EXTRACTION

It is necessary to develop a feature extraction approach for classifying defects. Statistical parameters are extracted to classify the different faults. These statistical parameters include minimum, maximum, variance, average(mean), middle value(median), addition(sum), absolute addition(sum), shape factor, root mean square value(RMS value), kurtosis, energy, crest factor, standard deviation and skewness of captured stator current signals. The mathematical formula and its calculations can be referred in detail in [15].

V. PROPOSED ALGORITHM

Step1: Capture three phase current of the Induction motor for processing.

Step2: Take transpose if captured signal is in column and apply SOBI Algorithm to the signal

Step3: Calculate 14 statistical parameter of 2nd and 3rd estimate

Step4: Apply ANN classifier for the classification of the faults and obtain confusion matrix and the ANN classifier model

VI. EXPERIMENTAL SETUP AND OBSERVATIONS

For the purpose of experimentation and data generation, a squirrel cage induction motor with the following specifications is employed: 2 H.P, 3-phase, 4 poles, 415 volts, 50 Hz. The experimental set up is shown in *Figure 2*.

This motor has 24 coils distributed across 36 slots. Each phase consists of 8 coils, each comprising 300 turns. A tapping configuration is applied to each phase, with the tapping starting at 10 turns from the neutral point. With each group containing approximately 70 to 80 turns, tapping are drawn from these coils. To capture the current and voltage signals, an ADLINK DAQ system is used, operating at a sampling frequency of

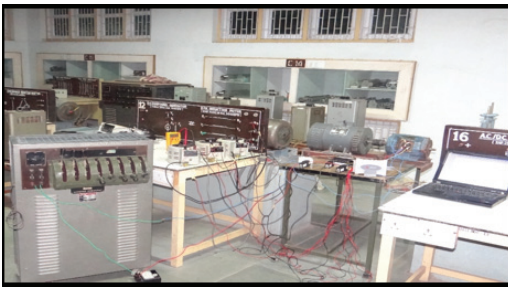


Fig. 2. Experimental Setup

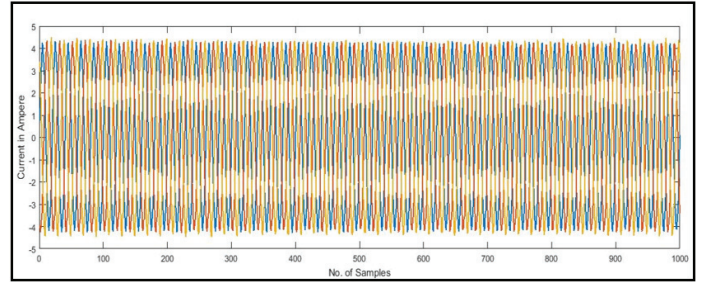


Fig. 3. 3-phase Current signal of the healthy condition of induction motor

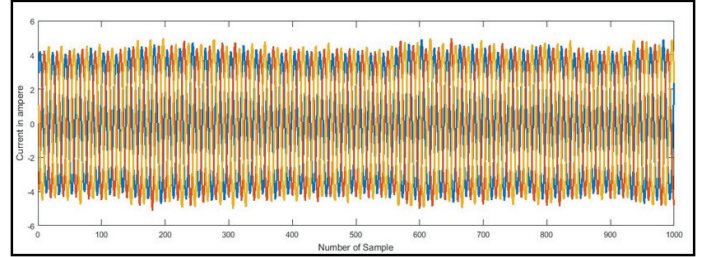


Fig. 4. 3-phase Current signal of the bearing fault of induction motor

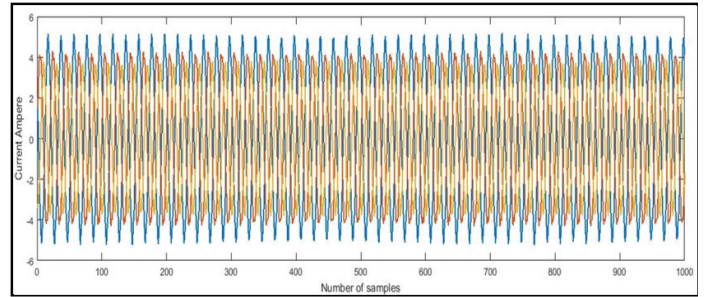


Fig. 5. 3-phase Current signals of inter turn fault of Induction motor

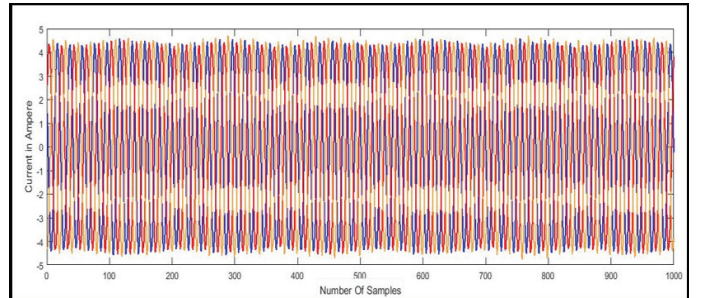


Fig. 6. 3-phase Current signal of rotor bar crack of Induction motor

1 kHz, and data is collected under various load and supply conditions for the specific cases outlined in *Figure 3* to *Figure 6*. The *Figure 3* to *Figure 6* display the 3-phase current signals corresponding to different fault conditions in the 3-phase induction motor.

The various condition of fault current are processed through the SOBI algorithm then 3 estimates are obtained. Note that the 3rd estimate and 2nd estimate shows the largest variations

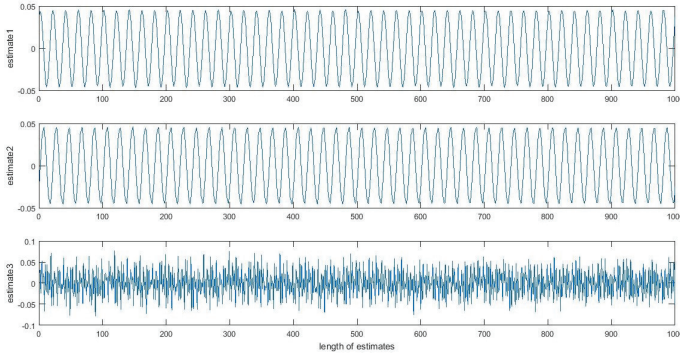


Fig. 7. SOBI demixing matrix estimates for healthy condition

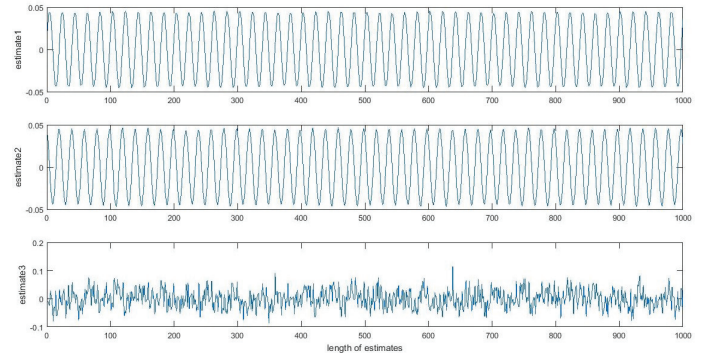


Fig. 10. SOBI demixing matrix estimates for Rotor-bar fault condition

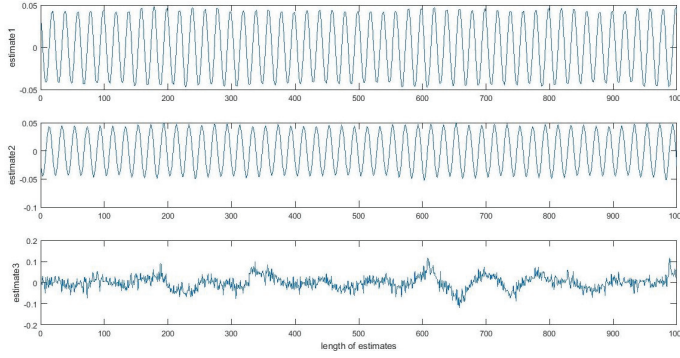


Fig. 8. SOBI demixing matrix estimates for bearing fault condition

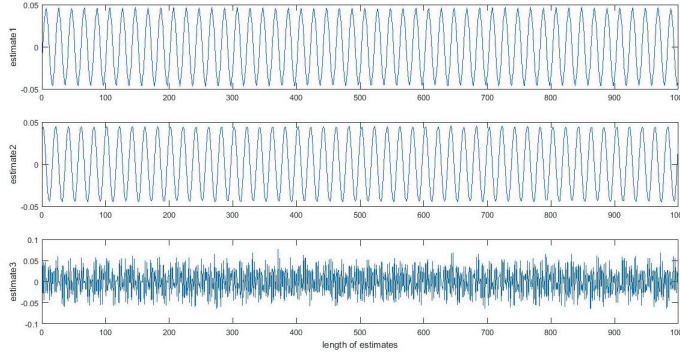


Fig. 9. SOBI demixing matrix estimates for Interturn Fault Condition

when compared with the healthy conditions and fault condition. The SOBI decompositions are as shown in *Figure7* to *Figure10* for various fault condition when motor is on load.

Form observation of *Figure7* to *Figure10* it is clearly visible that 3rd and 2nd estimates of faulty condition demonstrate the significant variation as compared to the healthy condition. Hence 14 statistical parameter has been calculated for both of the estimates. These 14 statistical parameters of 3rd and 2nd become the input to the ANN.

VII. RESULTS AND DISCUSSION

It is clearly seen that 3rd and 2nd estimate of the SOBI demixing matrix shows greater variations, so statistical parameter of 3rd and 2nd estimate has to be calculated. The total 10

reading are taken for each fault, hence 28x40 matrix of statistical parameters is obtain. An artificial neural network (ANN) with its strong pattern recognition abilities proves to be a valuable tool for the classification of faults in induction motors. This study utilizes a three-layer Feed Forward ANN (FFANN) trained through a supervised learning technique known as Back Propagation. The FFANN structure contains an input layer, hidden layer, and an output layer. The input layer comprises 28 nodes corresponding to statistical features derived from the 3rd and 2nd estimates of the SOBI demixing matrix, 12 neurons in the hidden layer. Meanwhile, the output layer is represented by four processing elements, each representing one of the following conditions: rotor bar crack, interturn fault, bearing fault and healthy condition. The ANN model obtained after training is shown in *Figure 11*. Randomized data is given as input into the network, to ensure generalization and the Transgmoid transfer function is employed for training purposes. This training process yields a percentage accuracy for classification. Considering these foundational principles, the research investigates the relationship between the accuracy percentage in categorizing induction motor states and the quantity of processing elements within the hidden layer. It can be clearly observed that the ANN is able to classify the faults with 100% accuracy considering the healthy condition. The

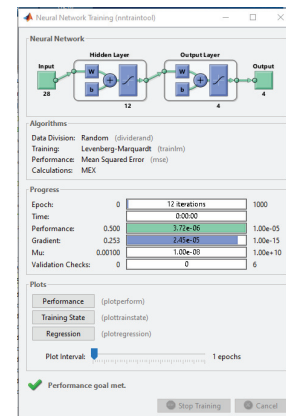


Fig. 11. ANN Training Model for induction motor fault classification

Confusion Matrix					
Healthy Condition ¹	20 25.0%	0 0.0%	0 0.0%	0 0.0%	100% 0.0%
Bearing Fault ²	0 0.0%	20 25.0%	0 0.0%	0 0.0%	100% 0.0%
Inter Turn Fault ³	0 0.0%	0 0.0%	20 25.0%	0 0.0%	100% 0.0%
Rotor Bar crack Fault ⁴	0 0.0%	0 0.0%	0 0.0%	20 25.0%	100% 0.0%
	100% 0.0%	100% 0.0%	100% 0.0%	100% 0.0%	100% 0.0%
	Healthy Condition	Bearing Fault	Inter Turn Fault	Rotor Bar crack Fault	Active

Fig. 12. Confusion Matrix for classification of induction motor fault

TABLE I
COMPARISON OF THE VARIOUS PARAMETERS OF ANN AND SOBI
ESTIMATES AND CLASSIFICATION RESULTS

Estimate No. selected for the statistical calculation and feed to ANN	Neuron Input	Neuron output	No. of hidden layers	No. of hidden Neurons	Confusion matrix classification
All 3 estimate	42	4	1	7	100%
Only 3rd estimate	14	4	1	11	98%
2nd and 3rd estimate	28	4	1	12	100%

confusion matrix obtained after training is shown in *Figure 12*. Table 1 displays the accuracy of classification when all the statistical features from the estimates are input to the ANN, resulting in a 100% classification accuracy rate. So as to check whether ANN can classify all the conditions with less number of input only the statistical parameter. The classification accuracy when the statistical parameter of only 3rd estimate is considered then only 98% classification accuracy is obtained. Hence to improve classification accuracy 2nd estimate along with 3rd is considered for processing and 100% classification accuracy is obtained here.

VIII. CONCLUSION AND FUTURE SCOPE

The paper proposes SOBI-ANN based induction motor fault classification. SOBI algorithm is used as signal separation method to identify the dominant fault signals and is given to the ANN after feature extraction for classification as ANN has good classifier properties. As this method is a time domain based method its computational complexity is less and time required to perform classification also reduced. Now this work could be extended by applying dimension reduction methods to select the dominant features after calculating the statistical parameter those are feed to ANN for classification.

REFERENCES

- [1] M. R. Mehrjou et al., "Wavelet-Based Analysis of MCSA for Fault Detection in Electrical Machine," in *Wavelet Transform and Some of Its Real-World Applications*, D. Baleanu, Ed., InTech, 2015. doi: 10.5772/61532.
- [2] R. Jigyasu, A. Sharma, L. Mathew, and S. Chatterji, "A Review of Condition Monitoring and Fault Diagnosis Methods for Induction Motor," in *2018 Second International Conference on Intelligent Computing and Control Systems (ICICCS)*, Madurai, India: IEEE, Jun. 2018, pp. 1713–1721. doi: 10.1109/ICCONS.2018.8662833.
- [3] R. N. Dash, S. Sahu, C. Ku. Panigrahi, and B. Subudhi, "Condition monitoring of induction motors: — A review," in *2016 International Conference on Signal Processing, Communication, Power and Embedded System (SCOPES)*, Paralakhemundi, Odisha, India: IEEE, Oct. 2016, pp. 2006–2011. doi: 10.1109/SCOPES.2016.7955800.
- [4] Y. Li, D. Powers, and J. Peach, "Comparison of Blind Source Separation Algorithms," *C 2000 WSES P18-21 Mastorakis2000 Adv. Neural Network. Appl. WSE*, p. 6.
- [5] A. Tharwat, "Independent component analysis: An introduction," *Appl. Comput. Inform.*, vol. 17, no. 2, pp. 222–249, Apr. 2021, doi: 10.1016/j.aci.2018.08.006.
- [6] J. E. Garcia-Bracamonte, J. M. Ramirez-Cortes, J. de Jesus Rangel-Magdaleno, P. Gomez-Gil, H. Peregrina-Barreto, and V. Alarcon-Aquino, "An Approach on MCSA-Based Fault Detection Using Independent Component Analysis and Neural Networks," *IEEE Trans. Instrum. Meas.*, vol. 68, no. 5, pp. 1353–1361, May 2019, doi: 10.1109/TIM.2019.2900143.
- [7] Z. Wang, J. Chen, G. Dong, and Y. Zhou, "Constrained independent component analysis and its application to machine fault diagnosis," *Mech. Syst. Signal Process.*, vol. 25, no. 7, pp. 2501–2512, Oct. 2011, doi: 10.1016/j.ymsp.2011.03.006.
- [8] I. Guney, E. Kilic, O. Ozgonenel, M. Ulutas, and E. Karadeniz, "Fault detection in induction motors with independent component analysis (ICA)," in *2009 IEEE Bucharest PowerTech*, Bucharest: IEEE, Jun. 2009, pp. 1–4. doi: 10.1109/PTC.2009.5282251.
- [9] A. Belouchrani, K. Abed-Meraim, J.-F. Cardoso, and E. Moulines, "A blind source separation technique using second-order statistics," *IEEE Trans. Signal Process.*, vol. 45, no. 2, pp. 434–444, Feb. 1997, doi: 10.1109/78.554307.
- [10] R. Sun, C. Chan, J. H. Hsiao, and A. C. Tang, "Validation of SOBI-DANS method for automatic identification of horizontal and vertical eye movement components from EEG," *Psychophysiology*, vol. 58, no. 2, p. e13731, Feb. 2021, doi: 10.1111/psyp.13731.
- [11] Y. Pan, M. Matilainen, S. Taskinen, and K. Nordhausen, "A review of second-order blind identification methods," *WIREs Comput. Stat.*, vol. 14, no. 4, Jul. 2022, doi: 10.1002/wics.1550.
- [12] D. R. De Oliveira, M. A. A. Lima, L. R. M. Silva, D. D. Ferreira, and C. A. Duque, "Second order blind identification algorithm with exact model order estimation for harmonic and interharmonic decomposition with reduced complexity," *Int. J. Electr. Power Energy Syst.*, vol. 125, p. 106415, Feb. 2021, doi: 10.1016/j.ijepes.2020.106415.
- [13] Subana Shanmuganathan and Sandhya Samarasinghe, *Artificial Neural Network Modelling*, vol. Volume

628. in *Studies in Computational Intelligence*", no. <http://www.springer.com/series/7092>, vol. Volume 628. SpringerNature. [Online]. Available: DOI 10.1007/978-3-319-28495-8
- [14] M. A. M. Sadeeq and A. M. Abdulazeez, "Neural Networks Architectures Design, and Applications: A Review," in *2020 International Conference on Advanced Science and Engineering (ICOASE)*, Duhok, Iraq: IEEE, Dec. 2020, pp. 199–204. doi: 10.1109/ICOASE51841.2020.9436582.
- [15] Anjali P. Wadekar and Anjali U. Jawadekar, "Fault Detection Of Induction Motor Through The Analysis Of Stator Current Data," *Int.J.Ind.Electron.Electr.Eng.*,no.8,[Online]. Available:[http : //pep.ijieee.org.in/journal_pdf/11 – 392 – 151703322731 – 35.pdf](http://pep.ijieee.org.in/journal_pdf/11-392-151703322731-35.pdf)

A Novel Algorithm for Discrimination of the Magnetizing Inrush Current and Internal Fault Current of a Transformer Using Teager Energy Operator and Artificial Neural Network



Purushottam Ramesh Bharambe, Sudhir Ramdas Paraskar, Ravishankar Shaligram Kankale, and Saurabh Suresh Jadhao

1 Introduction

The transformer is very important components of today's power system. Only because of availability of highly efficient transformer which changes the voltage level as per the requirement today's power system becomes much efficient and economic. In order to ensure the secure and proper operation of a transformer as well as the power system, a quick and reliable protection scheme is required [1].

Power transformers are protected using the differential protection technique. In differential protection scheme of a transformer, the differential relay compares the transformer's primary and secondary currents. Under normal operating condition, the magnitude of differential current is zero while a differential current exists when a transformer experiences an internal fault. As the differential current exists, then it will flow through the relay and the relay will generate the trip signal and operates circuit breakers on both primary and secondary side. In order to prevent the relay from tripping for through faults, the differential protection of the transformer uses a proportionate bias. The differential protection scheme of a transformer is shown in Fig. 1 [2].

P. R. Bharambe (✉) · S. R. Paraskar · R. S. Kankale · S. S. Jadhao
Shri Sant Gajanan Maharaj College of Engineering, Shegaon, India
e-mail: prbharambe@ssgmce.ac.in

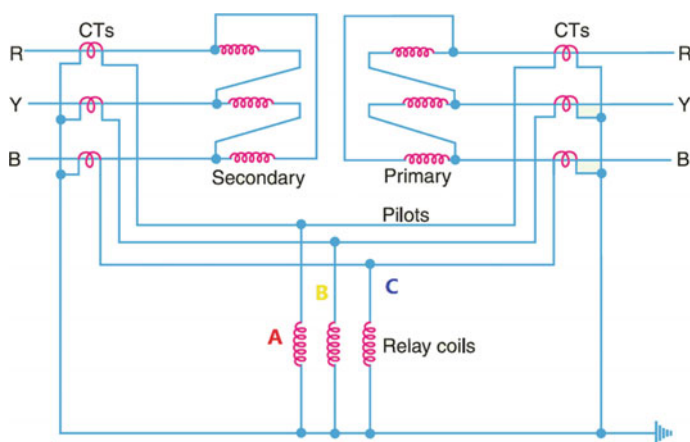


Fig. 1 Differential protection of transformer

Due to CT saturation, turn ratio variations brought on by changing taps, or magnetizing inrush current, the differential current can occasionally become large even in the absence of an internal problem. Avoiding the false tripping of the relay as a result of faulty discrimination between the magnetizing inrush current and internal fault current is the main difficulty in the differential protection of the power transformer [3]. When compared to the transformer's internal fault current, the magnetizing inrush current's magnitude is large. For the purpose of differentiating between inrush and internal fault current of the transformer, a number of protection schemes have been developed and presented in the literature which includes harmonic restrain scheme, flux restrain scheme, voltage restrain scheme, pattern recognition scheme, and artificial intelligence-based scheme. These methods have several advantages and disadvantages [4].

In this paper, a new algorithm is suggested in order to differentiate the inrush current from internal fault current of the transformer. In this algorithm first, calculate the Teager energy operator (TEO) of differential current and after comparing TEO with threshold value the occurrence of abnormality is detected. The statistical parameters are calculated from the differential current of the transformer as a feature.

Then, the training and testing of the ANN classifier are done using the features extracted from differential current to separate the internal fault current from inrush current of the transformer.

2 Teager Energy Operator (TEO)

The signal $x(t) = A \cos(w_c t + \emptyset)$ TEO $\psi[x(t)]$, is expressed as follows:

$$\varphi[x(t)] = [\dot{x}(t)]^2 - x(t) * \ddot{x}(t) \doteq A^2 w_c^2 \quad (1)$$

The discrete form representation of Eq. (1) by using approximation

$$\dot{x}[n] \approx \frac{x[n] - x[n-1]}{T},$$

when the value of T is small, it can define as

$$\Psi[x(n)] = ([x(n)]^2 - x(n-1)x(n+1))/T^2, \quad (2)$$

where T becomes the sampling time period between two consecutive samples, $x(n)$ and $x(n+1)$. In most of the cases assumption of $T=1$ is acceptable, due to information in discrete domain available after time interval T . Therefore, the discrete form representation of TEO

$$\Psi[x(n)] = [x(n)]^2 - x(n-1)x(n+1) \quad (3)$$

Equation (3) gives the information about magnitude and frequency of the sinusoidal signal. It requires only three samples of the discrete-time signals. The amplitude (A) of the TEO $\psi[x[n]]$ of the signal and frequency of the signal (Ω_c), is determined by using the separation method [2].

Let the signal with amplitude and frequency is denoted as $x(n) = A \cos(\Omega_c n + \emptyset)$. Therefore the discrete-time TEO is given by the following:

$$\psi[x(n)] = A^2 \sin^2(\Omega_c) \quad (4)$$

The TEO amplitude and frequency of the discrete TEO signal are determined by Eqs. (5) and (6), respectively.

$$A = \text{sqrt}\left(\frac{\psi[x(n)]}{\sin^2(\Omega_c)}\right) \quad (5)$$

$$\Omega_c = \cos^{-1}\left(1 - \frac{\varphi[x(n) - x(n-1)]}{\varphi[x(n)]}\right) \quad (6)$$

In this paper, the TEO is determined by using Eq. (5).

3 Artificial Neural Network (ANN)

The artificial neural network solves the problems that linear computers cannot as it operates in parallel. Pattern recognition and nonlinear system identification are the two common application of ANN where the formal analysis is either difficult or impossible. ANN consists of interconnection of simple elements working in parallel. The network's operation is determined by the connection weights. It is considered as the most basic type of available forward network. Using the training function, an artificial neural network must first be configured after creation. The network's elements are automatically modified to achieve a certain desired output for a particular input. Multiple layers are possible in a network. A weight matrix, a bias vector, and an output vector are present in each layer. Each neuron in a layer is directly connected to each neuron in the upper layer. The second class of feed-forward neural networks differs from the first by including one or more hidden layers, whose processing nodes are referred to as hidden neurons. The network's ability to extract higher order functions is enabled by increasing the number of layers and neurons. A feed-forward neural network is a well-liked ANN modeling technique. In a feed-forward neural network, there is no cycle in the connections between the nodes, making it a specific kind of artificial neural network. In order to distinguish between inrush and internal fault current of a transformer, a feed-forward neural network is employed as a classifier in this research work [1].

4 Proposed Algorithms

In this research work, the data required for the discrimination of the inrush current and internal fault current of a transformer is obtained from the experimental setup. This paper proposes two novel algorithms. In the first algorithm the differential current of a transformer is captured using the data acquisition system. This differential current is further used to calculate the TEO. The calculated value of TEO is compared with the threshold value (0.1). If the value of TEO exceeds the threshold then it indicates the occurrence of abnormality (inrush current or internal fault current). Once the abnormality is detected, the detection flag is set and statistical parameters such as standard deviation and variance are calculated as features from the differential current for the quarter cycle from that instant. A feature vector is created using the extracted features to train and test the ANN classifier [5]. The ANN classifier gives the decision about the class of abnormality. Figure 2 shows the flowchart of the proposed first algorithm. The detection of occurrence of abnormality is based on the TEO threshold. If the rating of the transformer is changed, then it is required to recalculate the threshold value of TEO. The rest of the algorithm remains same for discriminating the inrush and internal fault current of any transformer irrespective of its rating.

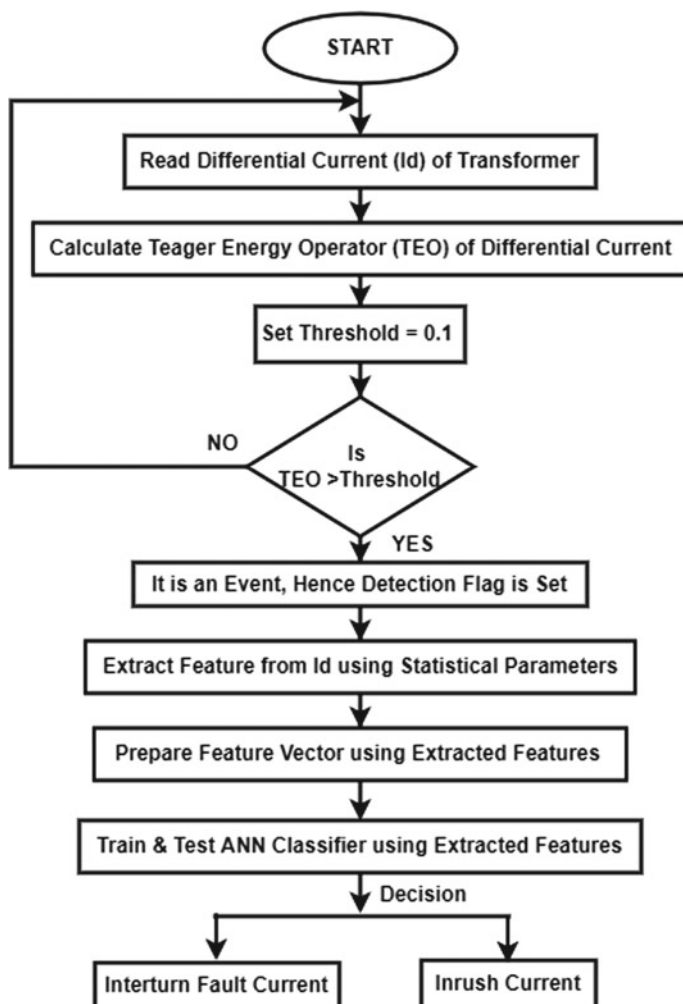


Fig. 2 First algorithm to discriminate inrush current and internal fault current

In the second algorithm, the differential current of a transformer is captured using the data acquisition system. This differential current is further used to calculate the TEO. The calculated value of TEO is compared with its threshold value (0.1). If the value of TEO exceeds the threshold, then it indicates the occurrence of abnormality (inrush current or internal fault current). Once the abnormality is detected the detection flag is set. In this algorithm, the detection flag is set for the duration of abnormality. If the duration of the detection flag is greater than a quarter cycle, then it is internal fault current else it is inrush current. Figure 3 shows the flowchart of the proposed second algorithm [2]. The detection of occurrence of abnormality is based on the TEO threshold. If the rating of the transformer is changed then it is required to

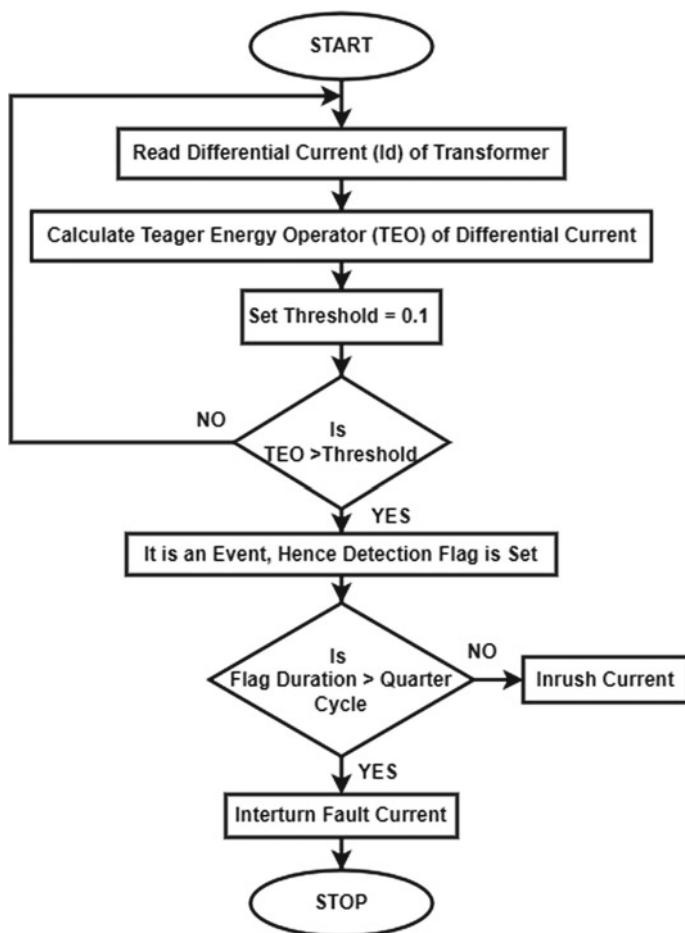


Fig. 3 Second algorithm to discriminate inrush current and internal fault current

recalculate the threshold value of TEO. The rest of the algorithm remains same for discriminating the inrush and internal fault current of any transformer irrespective of its rating.

5 Experimental Setup

The experimental setup used in this research work consists of a single-phase isolation transformer of rating 2 kVA, 230 V/230 V, 50 Hz with one-to-one tapings on both sides of the transformer to create internal faults. During the experimentation, a resistive load is connected with the transformer. The Adlink data acquisition system is used to

capture the differential current of a transformer with the sampling frequency of 1 kHz. The magnetizing inrush current of a transformer is captured at no-load condition and the internal fault current is captured under loading conditions by short-circuiting the few turns of transformer winding. A block diagram of the experimental setup is shown in Figs. 4 and 5 [2] shows the photograph of the experimental setup used for capturing the current signals of the transformer under different conditions.

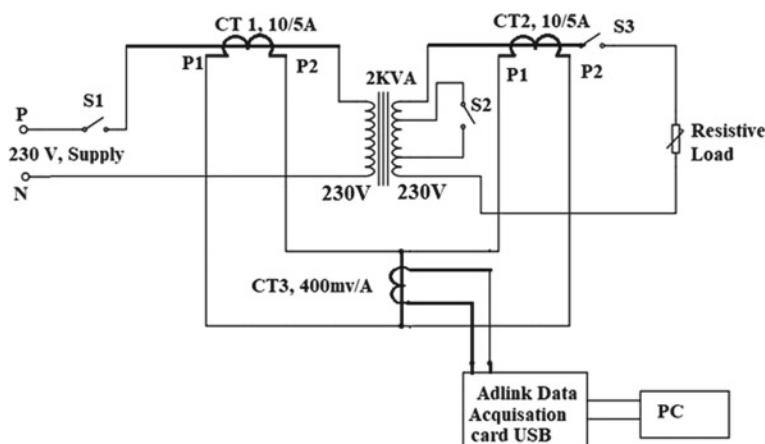


Fig. 4 Block diagram of experimental setup

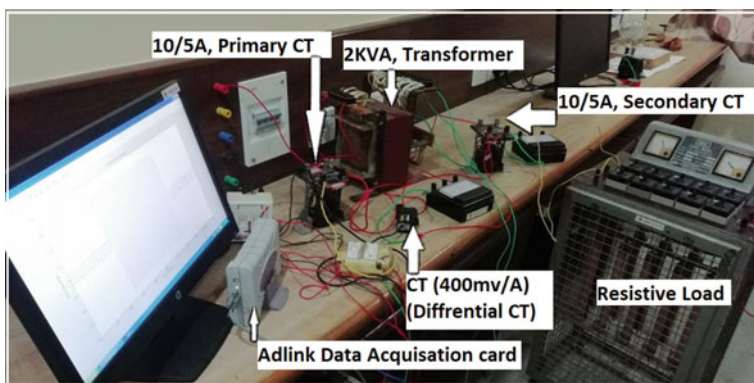


Fig. 5 Photograph of experimental setup developed in the laboratory

6 Result and Discussion

Step-1 Abnormality Detection Results

Case A: Transformer Under Normal Loading Condition

In the first case, the transformer is under normal loading conditions. The differential current corresponds to the normal loading condition is captured from the experimental setup using the data acquisition system. This differential current is further analyzed in MATLAB to obtain the TEO value. The calculated TEO value is then compared with the threshold value (0.1). The TEO value is less than the threshold hence the detection flag is not set. This indicates that the transformer is under normal condition. The threshold value is set to 0.1 by analyzing the differential current under different loading, inrush, and internal fault conditions. Figure 6 shows the TEO analysis of differential current under normal loading condition [6].

Case B: Transformer under Energization Condition

In this case, the transformer is under the energization condition. The differential current corresponding to the magnetizing inrush is captured from the experimental setup and further analyzed to calculate the TEO value. The TEO value and the threshold value are compared. If the TEO value exceeds the threshold value the detection flag is set which indicates the occurrence of an abnormal condition. The standard deviation (STD) and variance of the differential current are calculated for a quarter cycle from the instant of detection of abnormality. The feature vector is

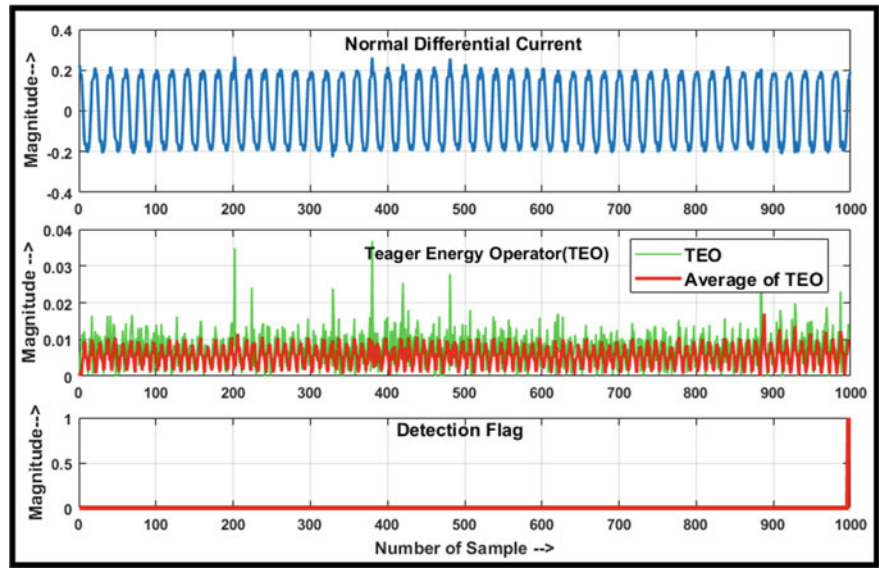


Fig. 6 TEO analysis of differential current under normal loading condition

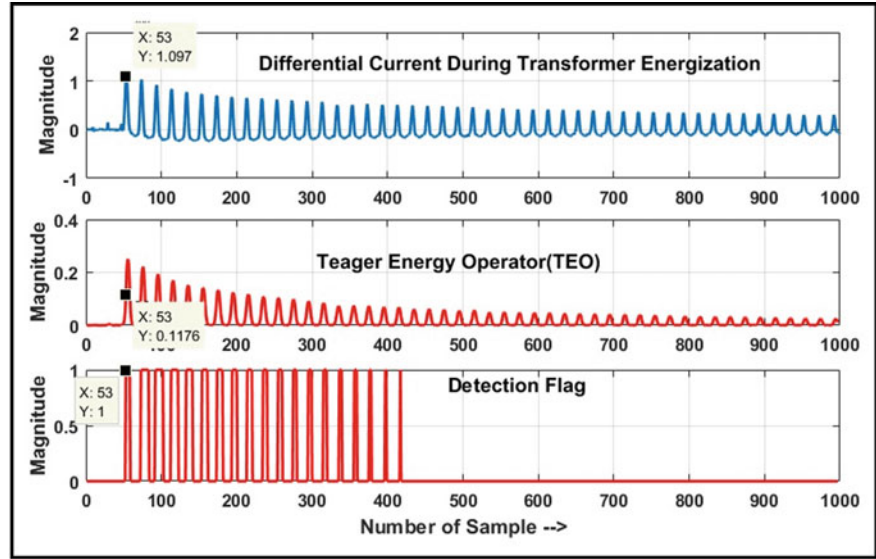


Fig. 7 TEO analysis of differential current under transformer energization condition

created using these statistical parameters which are further used to train and test the ANN. Figure 7 shows a TEO analysis of differential current under transformer energization condition [7].

Case C: Transformer Under Internal Fault Condition

In this case, the transformer is under the internal fault condition. The differential current corresponding to the internal fault is captured from the experimental setup and further analyzed to calculate the TEO value. The TEO value and the threshold value are compared and if the TEO value exceeds the threshold then the detection flag is set. This indicates the occurrence of an abnormal condition. The detection flag remains high till the fault persists. The standard deviation (STD) and variance of the differential current are calculated for a quarter cycle from the instant of detection of abnormality. The feature vector is created using these statistical parameters which are further utilized to train and test the ANN. Figure 8 [2] shows a TEO analysis of differential current under internal fault conditions [8].

Case D: Transformer Energization Followed by Internal Fault Condition

In this case, the transformer is initially under energization condition and followed by the internal fault condition. The differential current corresponds to the inrush and internal fault is captured from the experimental setup and further analyzed to calculate the TEO value. The TEO value is compared with the threshold value, as the TEO value exceeds the threshold value the detection flag is set. This indicates the occurrence of an abnormal condition. The detection flag is set under both inrush and internal fault conditions. The standard deviation (STD) and variance of the

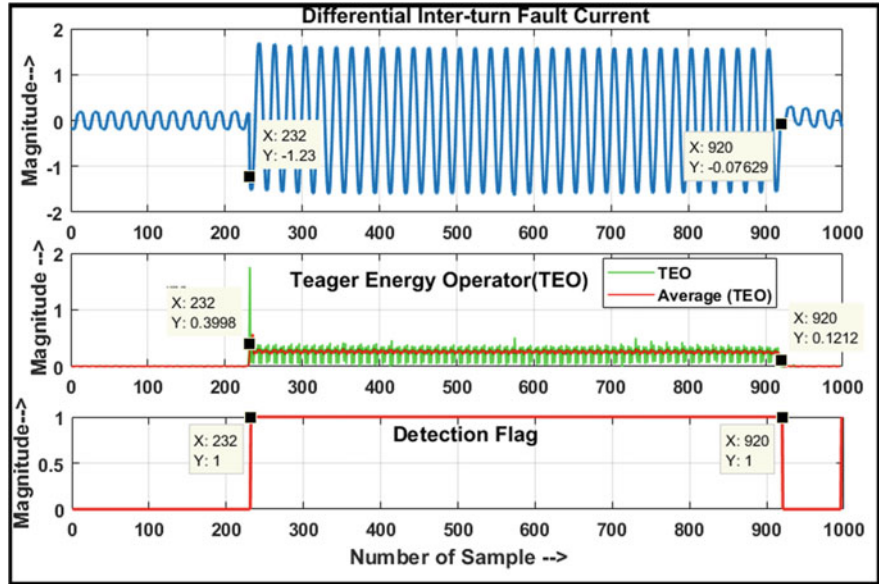


Fig. 8 TEO analysis of differential current during internal fault

differential current are calculated for a quarter cycle from the instant of detection of abnormality. The feature vector is created using these statistical parameters which are further utilized to train and test the ANN. Figure 9 shows a TEO analysis of differential current under internal fault conditions [7].

Step-2 Statistical Parameter Results

The standard deviation and variance of differential current are calculated for a quarter when an abnormal condition occurs as a feature. A feature vector is created using the values of standard deviation and variance for several cases of inrush and internal fault. Figure 10 shows the bar graph of standard deviation under inrush and internal fault conditions and Fig. 11 shows the bar graph of variance under inrush and internal fault conditions [9].

Step-3 Discrimination Results of First Proposed Algorithm

In the first algorithm, a transformer’s inrush and internal fault current are distinguished using a TEO along with ANN. In this algorithm, the feature vector is created using the extracted features which are further used to train and test the ANN classifier. In this research work, we have used the feed-forward neural network for discrimination [8]. Figure 12 shows the pattern recognition neural network model. The detail architecture of ANN classifier is shown in Table 1.

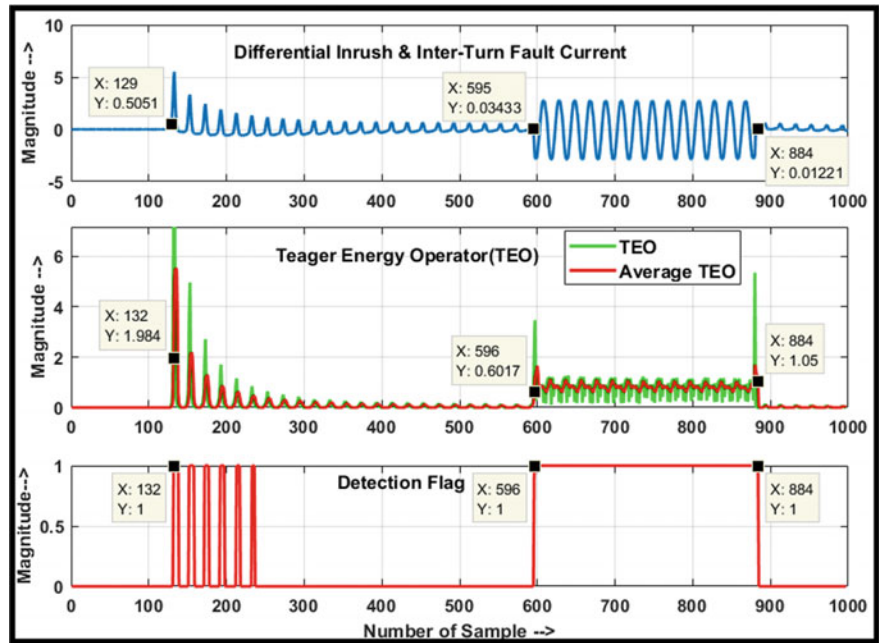


Fig. 9 TEO analysis of differential current during transformer energization and internal fault

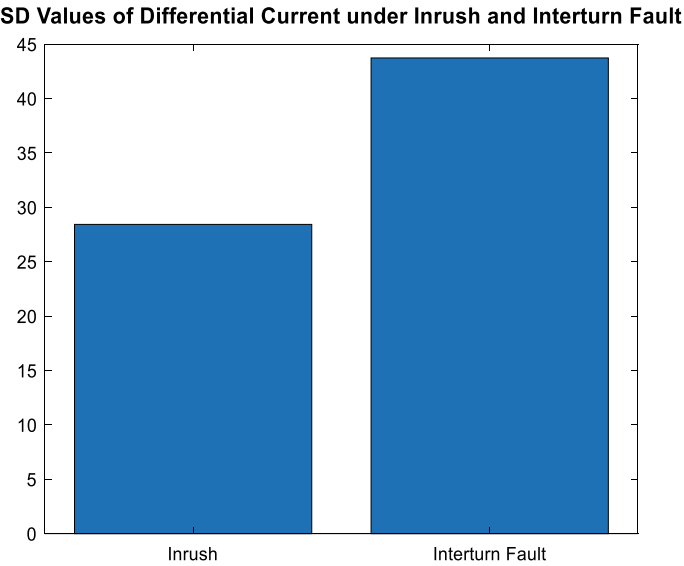


Fig. 10 Standard deviation value of differential current

Variance of Differential Current under Inrush and Interturn Fault

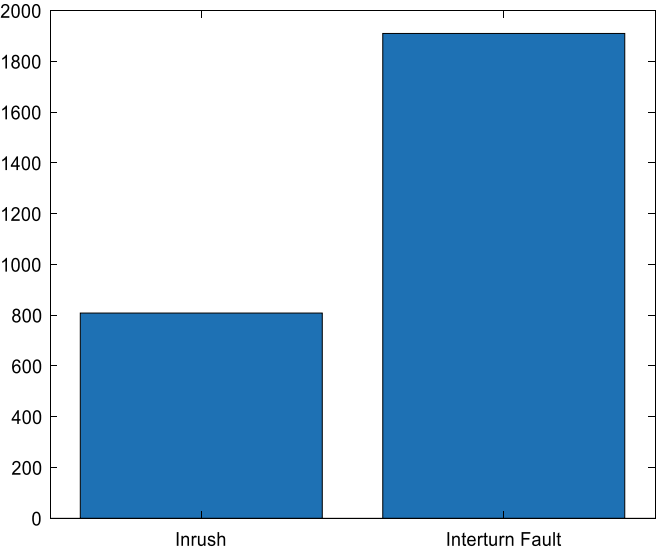


Fig. 11 Variance value of differential current

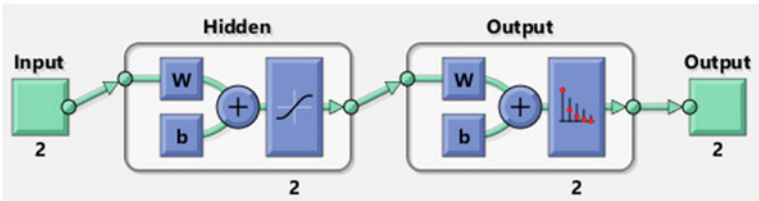


Fig. 12 Pattern recognition neural network

Table 1 Architecture of ANN classifier

Particulars	Number/percentage
Number of inputs	2
Number of outputs	2
Number of hidden layers	2
Training ratio	90%
Testing ratio	10%
Maximum number of epochs	500

The dataset required to train and test the ANN classifier is created using the extracted features. This dataset consists of total 30 test cases (15 cases of inrush and 15 cases of internal fault condition). In total, 90% of the dataset is used for training in the ANN algorithm, while the remaining 10% is used for testing. The results of ANN classifier are obtained in the form of confusion matrix. The diagonal elements of the confusion matrix show truly classified data and the non-diagonal elements shows misclassified data. The confusion matrix corresponds to the training shows 100% accuracy and the confusion matrix corresponds to testing also shows 100% accuracy. The overall confusion matrix shows that the proposed ANN algorithm discriminates the inrush and internal fault current accurately [10]. Figure 13 shows the training confusion matrix, Fig. 14 shows the testing confusion matrix and Fig. 15 shows the overall confusion matrix.

Discrimination Results of Second Proposed Algorithm

In the second algorithm proposed in this research paper after the detection of abnormality in differential current, the detection flag is set. In case of inrush current, the detection, flag is set only for the instance of peaks in differential current while the detection flag remains high till the duration of internal fault current. In order to discriminate between the inrush current and internal fault currents of a transformer,

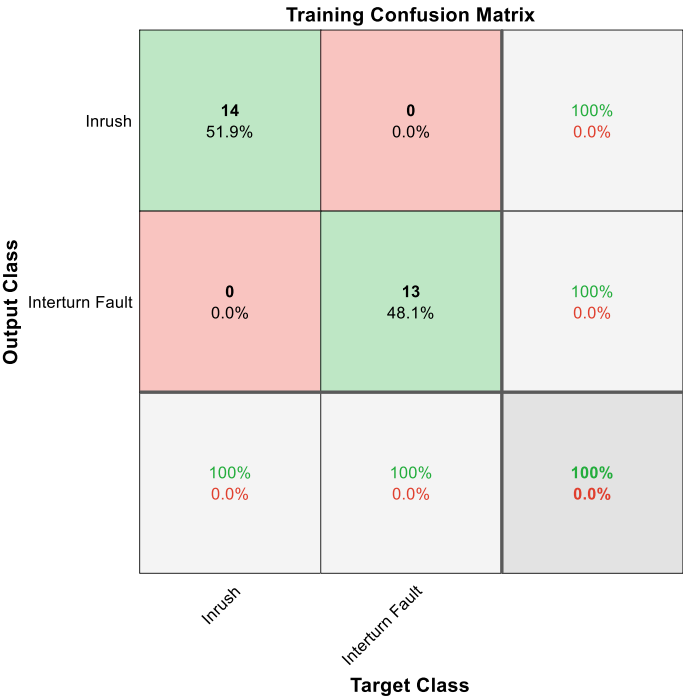


Fig. 13 Training confusion matrix

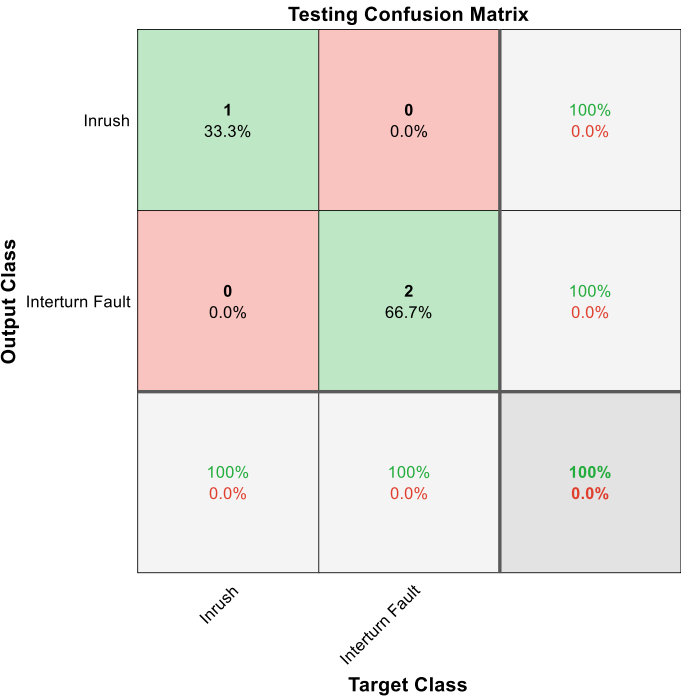


Fig. 14 Testing confusion matrix

the duration of the flag is compared with the quarter cycle duration. If the duration of the flag is less than the quarter cycle duration, then it is inrush current Fig. 16 shows this result in which the message box displays the name of event and corresponding action. In case of inrush, there will be no action. If the duration of the flag is greater than the quarter cycle duration, then it is an internal fault current [11]. Figure 17 shows this result in which the message box displays the name of event and corresponding action. In case of internal fault, a trip signal will be generated to trip the circuit breaker.

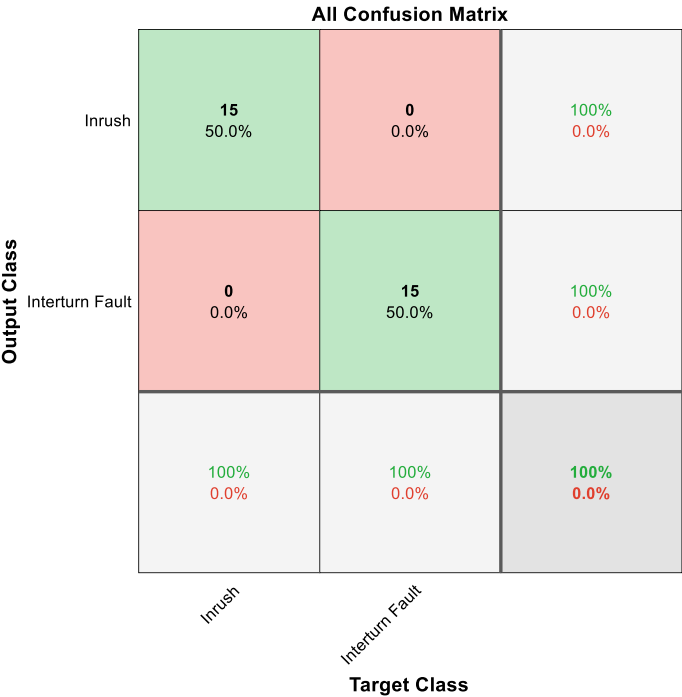


Fig. 15 All confusion matrix

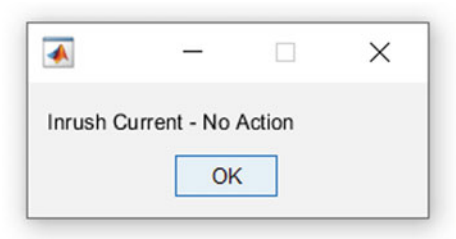


Fig. 16 Results of second algorithm corresponds to inrush current

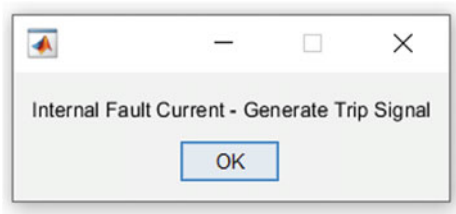


Fig. 17 Results of second algorithm corresponds to internal fault current

7 Conclusion

This section summarizes the work presented in this research paper. This paper proposes two novel algorithms to discriminate the inrush and internal fault current of a transformer. In the first algorithm, the unique combination of TEO-based threshold and ANN is proposed, this combination is found suitable to discrimination. In this algorithm three consecutive samples are used to detect the abnormality and quarter cycle of differential current is used for feature extraction. The computational time required for the execution of this algorithm is less and it is less complex. Hence, the implementation of this algorithm is easy and simple. The ANN classifier implemented with this algorithm gives 100% training and testing accuracy.

In the second algorithm, the duration of detection flag is used to discriminate between inrush and internal fault current of the transformer. Various cases of inrush and internal fault current are tested using this algorithm. It is observed that the proposed algorithm can reliably and truthfully differentiate between the inrush and internal fault current of the transformer under different cases. For discrete and finite length signals, the DFT is appropriate while the length of signals used in this study may have longer length. The implementation of DFT-based algorithm is more complex than TEO based algorithm. The computational time and complexity of DFT-based approach is more as compare to proposed approach. The algorithms proposed in this research work are tested using the experimental data and found efficient. This work can further be extended for discriminating the inrush and internal fault current of a transformer in real-time.

References

1. Paraskar SR (2022) Study on discrimination between inrush and fault in transformer: ANN approach. *Nov Perspect Eng Res* 8(2):11–23. <https://doi.org/10.9734/bpi/rtcams/v8/2606c>
2. Bonde G, Paraskar S, Jadhao S, Kothari D (2021) A novel approach to discriminate between inrush and interturn fault currents of transformer. *Int J Power Energy Syst* 41(3):175–182. <https://doi.org/10.2316/J.2021.203-0322>
3. Bharambe PR, Paraskar S, Jadhao SS (2021) A review of techniques used for discrimination of inrush current and internal fault current of a power transformer
4. Ahmadi M, Samet H, Ghanbari T (2015) Discrimination of internal fault from magnetising inrush current in power transformers based on sine-wave least-squares curve fitting method. *IET Sci Meas Technol* 9(1):73–84. <https://doi.org/10.1049/iet-smt.2014.0012>
5. Paraskar SR, Beg MA, Dhole GM, Khedkar MK (2010) A novel technique to discriminate inrush and fault in a single-phase transformer. *Int J Signal Imaging Syst Eng* 3(1):52–60. <https://doi.org/10.1504/IJSISE.2010.034632>
6. Han Z, Liu S, Gao S, Bo Z (2008) A novel detection criterion for transformer inrush based on short-window filter algorithm. In: *Proceedings of the universities power engineering conference*. <https://doi.org/10.1109/UPEC.2008.4651451>
7. Shah AM, Bhalja BR, Patel RM (2018) New protection scheme for power transformer based on superimposed differential current. *IET Gener Transm Distrib* 12(14):3587–3595. <https://doi.org/10.1049/iet-gtd.2018.0296>

8. Siddique MAA, Mehfuz S (2016) Artificial neural networks based incipient fault diagnosis for power transformers. In: 12th IEEE international conference on electronics, energy, environment, communication, computer, control (E3-C3), INDICON 2015, pp 1–6. <https://doi.org/10.1109/INDICON.2015.7443174>
9. Dolgicers A, Kozadajevs J (2015) Signal extraction from inrush current for inter-winding fault protection of power transformers. In: 2015 IEEE Eindhoven PowerTech, PowerTech 2015. <https://doi.org/10.1109/PTC.2015.7232721>
10. Li B, Yang X, Li B, Wen W, Chen X, Su J (2021) Differential current integral based bipolar short-circuit protection method for DC distribution network with blocking converters. *Electr Power Syst Res* 192. <https://doi.org/10.1016/j.epsr.2020.106977>
11. Hamouda AH, Al-Anzi FQ, Gad HK, Gastli A (2013) Numerical differential protection algorithm for power transformers. In: 2013 7th IEEE GCC conference and exhibition (GCC), pp 440–445. <https://doi.org/10.1109/IEEEGCC.2013.6705819>

Development of Wavelet and ANN-Based Algorithm in LabVIEW Environment for Classifying the Power Quality Disturbances



Ravishankar Shaligram Kankale, Sudhir Ramdas Paraskar,
and Saurabh Sureshrao Jadhao

1 Introduction

In the era of the industry 4.0 revolution, the technologies are changing rapidly. In today's world, factories are becoming smart due to the collaboration of technologies like artificial intelligence, smart automation, robotics, IoT, and cloud computing. In industry 4.0 everything is becoming smart. The architecture of this smart and digital industry comprises various sensors and hardware components. Everywhere we see automation most of the manual processes are nowadays replaced with smart automation. In this digital revolution, the energy demand is increasing at a significant rate. The technologies used in this revolution need good quality and reliable power supply for their operation.

In the emerging power system, Distributed Generation Systems based on renewable energy sources are employed in order to meet the ever-increasing power demand [1]. The Grid-connected solar photovoltaic systems and wind energy systems are the most commonly used DGs. The renewable energy resources-based DGs consist of power electronic devices such as converters and inverters [1]. The energy-efficient devices used nowadays also consist of power electric components. These power electronic components along with the conventional causes may lead to various power quality disturbances. These disturbances may cause maloperation or nuisance tripping of customers' sensitive loads which lead to heavy loss [2]. Hence, there is a necessity to develop a reliable and efficient power quality monitoring system. The power quality monitoring system must be simple and fast in operation [3]. It must accurately detect and classify the PQDs.

Many researchers have proposed a variety of power quality disturbance detection and classification techniques in the literature. In this research work, we have used

R. S. Kankale (✉) · S. R. Paraskar · S. S. Jadhao
Shri Sant Gajanan Maharaj College of Engineering, Shegaon, India
e-mail: ravi_kankale@rediffmail.com

the PQDs generated by utilizing the integral mathematical models of PQDs. The researchers have suggested different signal processing techniques for the analysis of PQDS. The PQD voltage signals are non-stationary in nature [1]. A signal whose frequency and magnitude change with respect to time is called a non-stationary signal. The statistical properties of such signals change with respect to time [4]. In the literature, people have proposed many signal processing techniques for analyzing the non-stationary signals related to PQDs. Wavelet transform-based multiresolution analysis is the simplest, reliable, and robust technique used in the study of non-stationary signals [5]. In this paper, we have used wavelet transform for the analysis of non-stationary signals corresponding to the PODs under study. The time–frequency localization obtained by the wavelet analysis is used for the feature extraction. As the statistical properties of non-stationary signals differ with respect to time, we have calculated the statistical parameters as a feature from the wavelet analysis. These features are then utilized for training and testing the artificial intelligence technique-based classifier. In the literature, various artificial intelligence-based soft computing techniques have been proposed. All techniques have some advantages and limitations.

2 Power Quality Disturbances

In the last three-four decades, Power Quality is the most often used keyword in the power sector. Both electric utilities and end users place more and more emphasis on the quality of the power they get. The term PQ is defined as “Any power problem which leads to the deviations in voltage, current, or frequency and results in failure or maloperation of end-users equipment” [6]. In electrical power system numbers of PQDs occurs, in this paper, we have considered the following commonly occurring PQDs.

2.1 Voltage Sag

A voltage sag is defined as a drop in root mean square (RMS) value of voltage between 0.1 and 0.9 pu at the rated frequency over periods ranging from 0.5 cycle to 1 min. The most frequent causes of voltage sag are switching a heavy load, turning on large induction motors, power system faults, and transformer energization. Voltage sag typically results in the malfunction or improper operation of end user equipment.

2.2 Voltage Swell

A voltage swell is defined as a rise in root mean square value of voltage between 1.1 and 1.8 pu at the rated frequency over a period of time between 0.5 cycle and 1 min. The most frequent causes of voltage swell are switching OFF of heavy load, faults in the distribution system, and energizing of large capacitor banks. Voltage swell can damage electronics and other sensitive equipment.

2.3 Voltage Interruption

A voltage interruption is defined as a dip in RMS value of voltage below 0.1 pu during a time frame shorter than a minute. The most frequent causes of voltage interruption are equipment failure, power system faults, insulation failure, and flashover of insulators. Therefore, a voltage interruption may result in damage as well as the full shutdown of equipment.

3 Discrete Wavelet Transform

The Discrete Wavelet Transform is one of the efficient tools used for time–frequency localization of signals. In the DWT analysis the input signal is divided into a number of sets. A discrete wavelet transform (DWT) divides an input signal into a number of sets. Each set includes a time series coefficient that displays the frequency band and signal variations over time. In this research work we have used Daubechies wavelet (db4) which is the most commonly used discrete wavelet transform used for the analysis of non-stationary signals corresponding to PQDs. The db4 wavelet has four scaling and wavelet functions coefficients. The DWT is defined as:

$$W_{\varphi}(j_0, k) = \frac{1}{\sqrt{M}} \sum_x f(x) \varphi_{j_0, k}(x) \quad (1)$$

$$W_{\Psi}(j, k) = \frac{1}{\sqrt{M}} \sum_k f(x) \Psi_{j, k}(x) \quad (2)$$

A scaling function $\varphi(x)$ is used to derive $\varphi_{j_0, k}(x)$ by translation and scaling using:

$$\varphi_{j_0, k}(x) = 2^{j/2} \varphi(2^j x - k) \quad (3)$$

A wavelet function $\Psi(x)$ is used to derive $\Psi_{j, k}(x)$ by translation and scaling using:

$$\Psi_{j,k}(x) = 2^{j/2} \Psi(2^j x - k) \quad (4)$$

The DWT can be modeled using a filtering method that uses a low-pass filter h_φ and a high-pass filter h_ψ , respectively. The approximate and the detail coefficients are computed using:

$$W_\psi(j, k) = h_\psi(-n) * W_\psi(j + 1, n)|_{n=2k, k \geq 0} \quad (5)$$

$$W_\varphi(j, k) = h_\varphi(-n) * W_\varphi(j + 1, n)|_{n=2k, k \geq 0} \quad (6)$$

The filter bank can be iterated to perform multiresolution analysis.

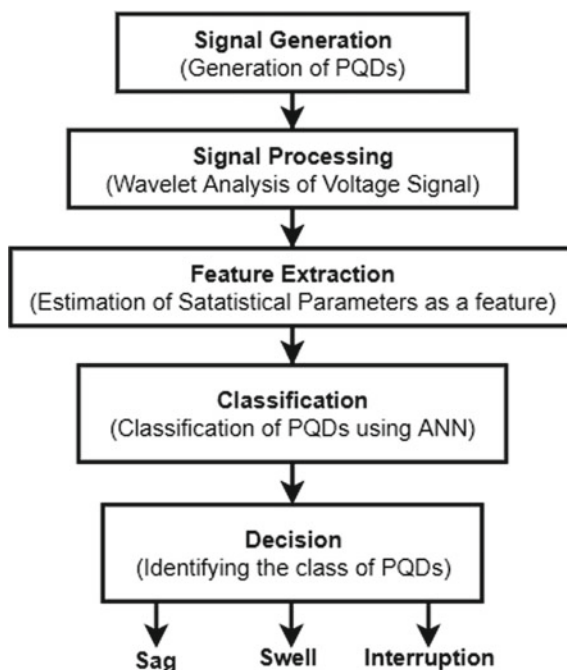
4 Artificial Neural Network (ANN)

A network built with artificial neurons is known as an artificial neural network. These neurons are linked in the same manner in which biological neurons are connected. An adaptive system that can alter its behavior in reaction to data entering and leaving the network can be built using a neural network. Applications like the classification of data and pattern recognition can be done using an ANN. In this research work, we have used a back propagation neural network algorithm for classification of voltage sag, swell, and interruption. A neural network can be trained using a training algorithm, which is a collection of learning strategies. The dataset input to the algorithm is utilized to train, validate, and test the classifier. When the error value is small enough, the training process will be finished. After the training process is finished, a trained network will be created. This trained network is validated and tested using the samples from the same dataset or new samples. The accuracy of the algorithm depends on the number of properly classified data samples.

5 Proposed Methodology

A wavelet and ANN-based method for classifying PQDs is suggested by this study. The LabVIEW software is used to implement the algorithm. The steps involved in the implementation of the proposed algorithm developed in LabVIEW are represented in the form of flowchart in Fig. 1. In this algorithm the voltage signals corresponding to three PQDs namely the sag, swell, and interruption are created utilizing the integral mathematical models of PQDs using Math script tool in the LabVIEW. The signals are recorded at a sampling rate of 10 kHz and analyzed using the wavelet transform. In wavelet analysis, we have used db4 wavelet for decomposing the voltage signal up to 6th level. The statistical parameters namely max, mean, median, variance, SD, kurtosis, energy, and skewness are calculated as features from the detailed coefficients

Fig. 1 Flowchart of proposed algorithm implemented in LabVIEW



of level 5 and 6. The dataset needed to train and to test the ANN classifier is created using these extracted features. Testing is done to identify the class of PQD after the ANN classifier has been trained using the extracted features.

6 Results and Discussion

6.1 Generation of PQDs

In this research work, the parametric equations of PQDs are implemented in the LabVIEW environment using the Math script tool to produce the data needed for Wavelet analysis [7] which is shown in Fig. 2.

The voltage signal with a 50% sag, i.e., 0.5 pu rms value for 0.08 s generated in the LabVIEW environment using the parametric equation of voltage sag is shown in Fig. 3. The duration of the signal is 0.2 s and the sampling rate is 10 kHz. To obtain the number of samples required to generate the dataset, the percentage and instant of sag is varied.

The voltage signal with a 50% swell, i.e., 0.5 pu rms value for 0.08 s generated in the LabVIEW environment using the parametric equation of voltage swell is shown in Fig. 4. The duration of the signal is 0.2 s and the sampling rate is 10 kHz. To obtain

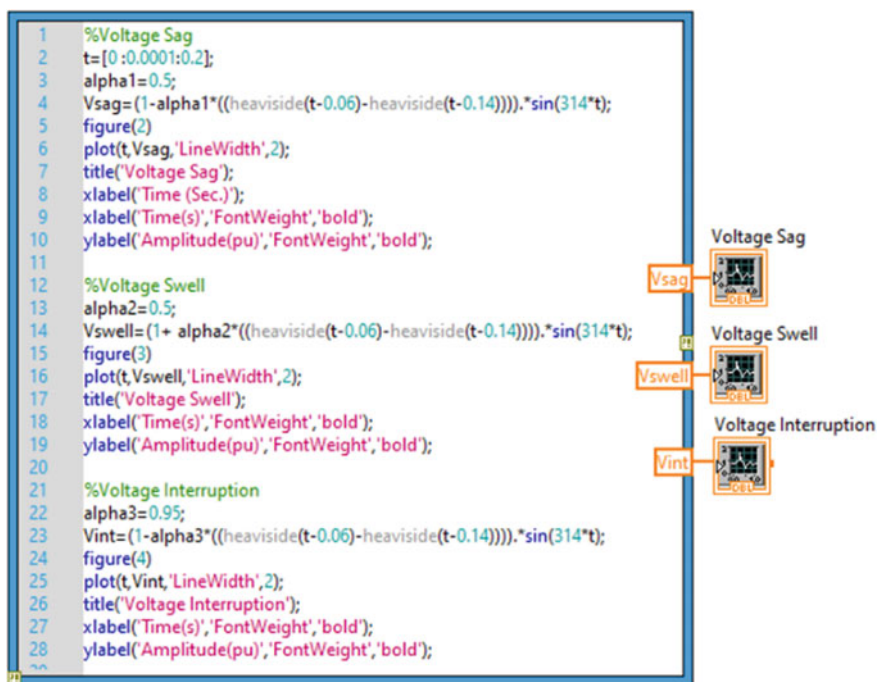


Fig. 2 Generation of PQDs using LabVIEW

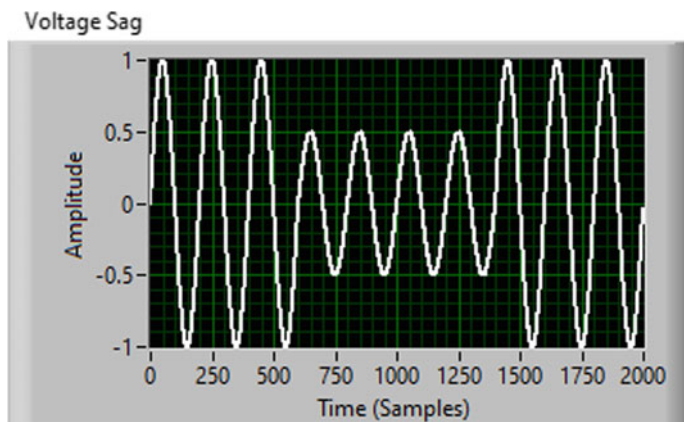


Fig. 3 Waveform of voltage signal with 50% sag

the number of samples required to generate the dataset, the percentage and instant of swell is varied.

The voltage signal with an interruption for 0.08 s generated in the LabVIEW environment using the parametric equation of voltage interruption is shown in Fig. 5. The duration of the signal is 0.2 s and the sampling rate is 10 kHz. To obtain the number of samples required to generate the dataset, the instant of interruption is varied.

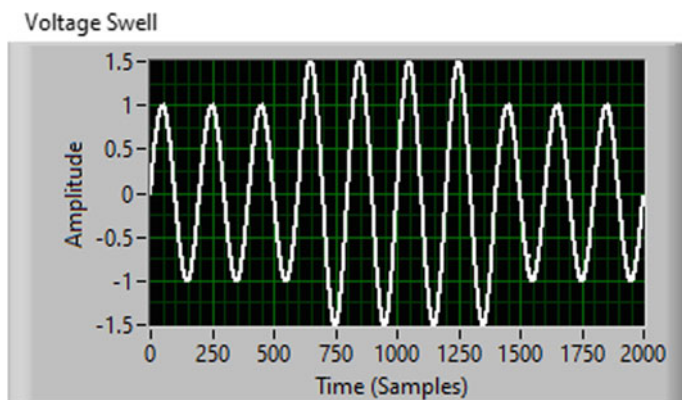


Fig. 4 Waveform of voltage signal with 50% swell

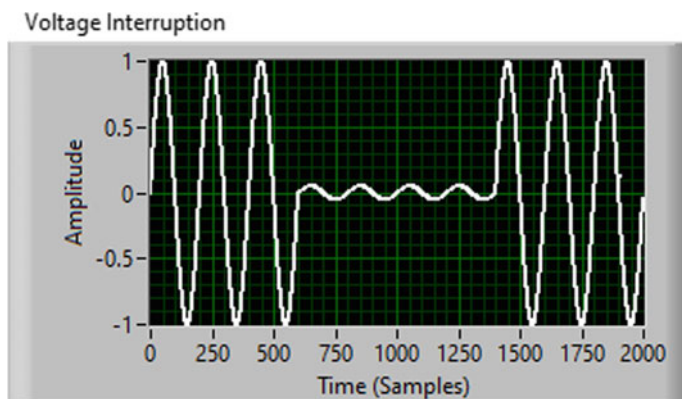


Fig. 5 Waveform of voltage signal with interruption

6.2 Wavelet Analysis Results

In the LabVIEW environment, a block diagram is created to process the voltage signals related to three PQDs using the Wavelet Transform as a signal processing tool. In the wavelet analysis, we have decomposed the voltage signal up to 6th level using db4 wavelet. Figure 6 shows the block diagram for wavelet analysis of voltage signals developed in LabVIEW.

Figure 7 shows the waveform of detailed coefficients of the 6th level obtained in the LabVIEW environment from the wavelet analysis of the voltage signal with sag.

Figure 8 shows the waveform of detailed coefficients of the 6th level obtained in the LabVIEW environment from the wavelet analysis of the voltage signal with swell.

Figure 9 shows the waveform of detailed coefficients of the 6th level obtained in the LabVIEW environment from the wavelet analysis of the voltage signal with interruption.

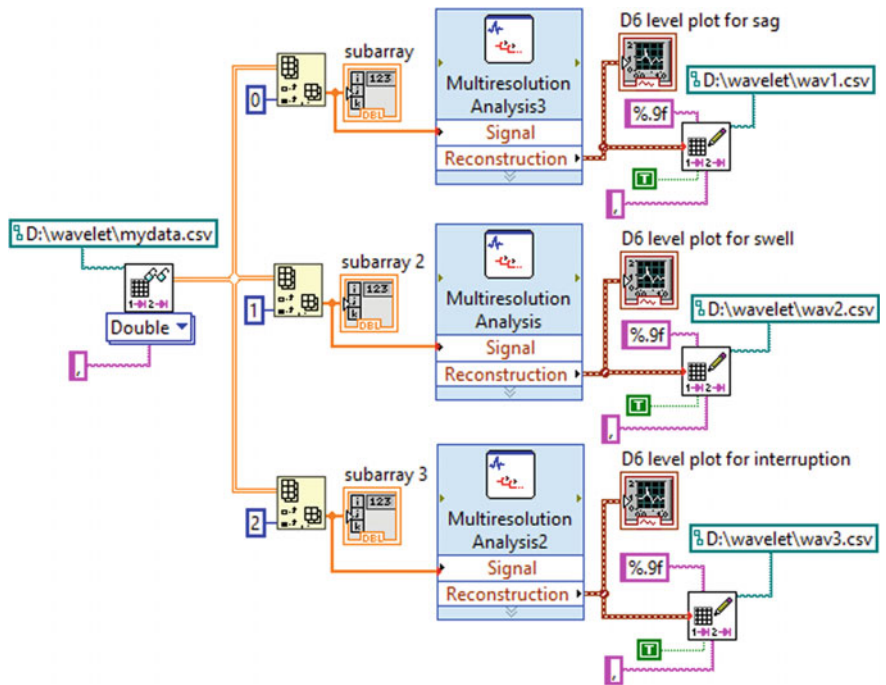


Fig. 6 Wavelet analysis block diagram developed in LabVIEW

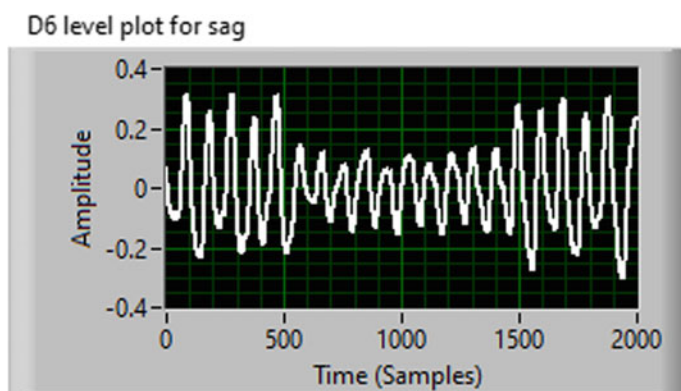


Fig. 7 Waveform of D6 level for voltage sag

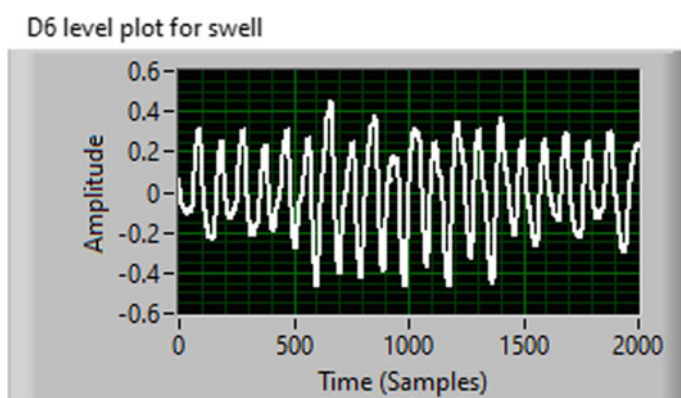


Fig. 8 Waveform of D6 level for voltage swell

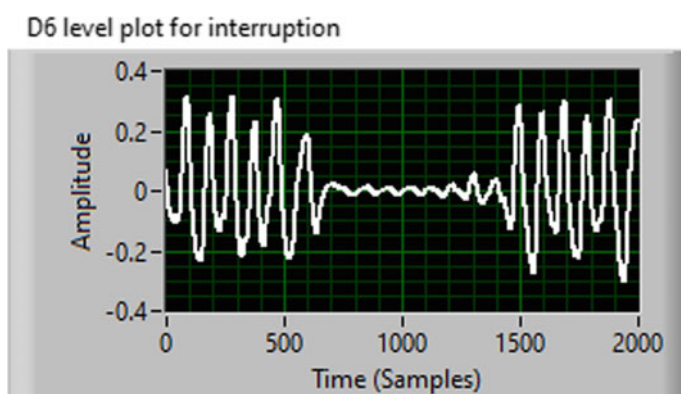


Fig. 9 Waveform of D6 level for voltage interruption

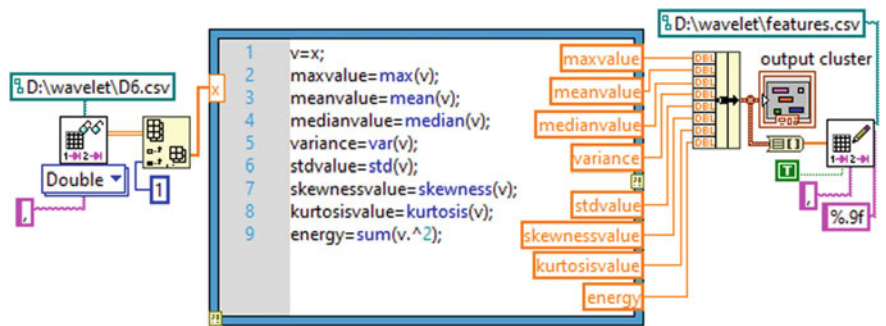


Fig. 10 Feature extraction block diagram developed in LabVIEW

6.3 Feature Extraction

The statistical parameters namely max value, mean value, median, variance, SD, skewness, energy, and, kurtosis are calculated from the detailed coefficients of 5th and 6th level for feature extraction. These extracted features are used to build the dataset needed to train and test the ANN classifier. Figure 10 shows the block diagram developed in LabVIEW for feature extraction.

6.4 ANN Classifier Architecture

In this research work, the back propagation algorithm is employed as an ANN classifier. In the ANN algorithm, we have evaluated the performance of the proposed ANN classifier using different combinations of extracted features, i.e., the variation in the number of inputs and training and testing ratios. Also, we have used the features extracted from detailed coefficient of 5th level. In this different combination, we got the most accurate results for the architecture shown in Table 1 and the pattern recognition neural network shown in Fig. 11.

Table 1 Architecture of ANN classifier

Particulars	Number
Number of inputs	8
Number of outputs	3
Number of hidden layers	1
Training ratio	80/100
Testing ratio	20/100
Maximum number of epochs	500
Network training function	‘trainlm’

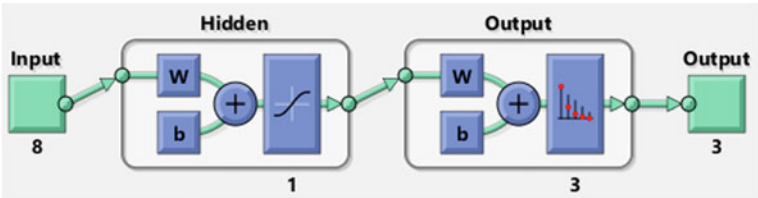


Fig. 11 Pattern recognition neural network

6.5 ANN Training Results

The dataset required to train and test the ANN consists of 63 samples (27 of sag, 27 of swell, and 9 of interruption). The 80% dataset, i.e., 50 samples are used to train the ANN. In Fig. 12, the outcomes of the ANN training are shown as a confusion matrix. From the confusion matrix it is seen that the training accuracy is found to be 100%. In the confusion matrix, the column displays the predicted class, while the rows represent the true class and the diagonal elements show correctly classified samples while the non-diagonal elements show incorrectly classified samples. The figure shows the training confusion matrix obtained by training the classifier using the features extracted from the detailed coefficients of the 6th level.

Fig. 12 Training confusion matrix

Training Confusion Matrix				
Output Class	SAG	SWELL	INT.	
	21 42.0%	0 0.0%	0 0.0%	100.0% 0.0%
	0 0.0%	22 44.0%	0 0.0%	100% 0.0%
	0 0.0%	0 0.0%	7 14.0%	100% 0.0%
				100% 0.0%
				100% 0.0%
				100% 0.0%
				100.0% 0.0%
				SAG
				SWELL
				INT.
				Target Class

Fig. 13 Testing confusion matrix

		Testing Confusion Matrix			
Output Class	SAG	6 46.2%	0 0.0%	0 0.0%	100% 0.0%
	SWELL	0 0.0%	5 38.5%	0 0.0%	100% 0.0%
	INT.	0 0.0%	0 0.0%	2 15.4%	100% 0.0%
		100% 0.0%	100% 0.0%	100% 0.0%	100% 0.0%
		SAG	SWELL	INT.	Target Class

6.6 ANN Testing Results

In the testing phase of the ANN 20% dataset, i.e., 13 samples are used. Figure 13 shows the outcomes of the ANN testing as a confusion matrix. From the confusion matrix it is seen that the testing accuracy is found to be 100%. The figure shows the testing confusion matrix obtained by testing the classifier using the features extracted from the detailed coefficients of the 6th level.

7 Conclusion

This paper presents a unique combination of wavelet transform and artificial neural network for the classification of PQDs. This paper mainly focuses on the development of PQDs classification algorithm in the LabVIEW environment. The wavelet transform is used as a signal processing tool for extracting the features required for discriminating the three power quality disturbances namely the voltage sag, swell, and interruption. WT is found to be more appropriate tool used for analyzing the non-stationary signals. The eight features extracted from wavelet analysis are found to be appropriate and sufficient to classify the PQDs with high accuracy. The results of the proposed algorithm are verified for different combinations of the input dataset. The training and testing accuracy for the ANN architecture discussed in the result section is found to be 100% for the dataset created using the features extracted from the detailed coefficients of the 6th level. We can infer from the results of this research that the proposed algorithm classifies PQDs accurately. The power quality monitoring system might be enhanced if these techniques are widely used. The work presented in this paper will be further extended to classify the PQDs in real time.

References

1. Kankale RS, Paraskar SR, Jadhao SS (2022) Classification of power quality disturbances in emerging power system using discrete wavelet transform and K-nearest neighbor. *ECS Trans* 107:5281–5291. <https://doi.org/10.1149/10701.5281ecst>
2. Zhang P, Feng Q, Chen R, Wang D, Ren L (2020) Classification and identification of power quality in distribution network. In: 2020 5th international conference on power and renewable energy, ICPRE 2020, vol 4, pp 533–537. <https://doi.org/10.1109/ICPRE51194.2020.92>
3. Zaro FR, Abido MA (2019) Real-time detection and classification of power quality problems based on wavelet transform. *JJEE* 5(4):222–242
4. Hole SD, Naik CA (2020) Power quality events' classification employing discrete wavelet transform and machine learning. In: 2020 1st IEEE international conference on measurement, instrumentation, control and automation, ICMICA 2020. <https://doi.org/10.1109/ICMICA48462.2020.9242894>
5. Pukhova VM, Ferrini G (2018) Time-frequency analysis of non-stationary signals, pp 1141–1145
6. Chawda GS, Shaik AG, Shaik M, Padmanaban S, Holm-Nielsen JB, Mahela OP, Kaliannan P (2020) Comprehensive review on detection and classification of power quality disturbances in utility grid with renewable energy penetration. *IEEE Access* 8:146807–146830. <https://doi.org/10.1109/ACCESS.2020.3014732>
7. Kankale RS, Paraskar SR, Jadhao SS (2021) Implementation of integral mathematical models of single and multiple power quality disturbances. *IARJSET* 8(6):330–336. <https://doi.org/10.17148/IARJSET.2021.8657>

Enhancing Performance of Hybrid Electric Vehicle Using Optimized Energy Management Methodology



Mahendra Bagde , Anjali Jawdekar , and Kunal Sawalakhe 

1 Introduction

The three most important and well-known engineering topics are freshwater, electricity, and the atmosphere because of their interdependence. Key issues that have been addressed include resource limitations and global warming [1]. Most fossil fuels used in transportation result in greenhouse gas emissions. Several attempts have been made in this field to increase the need for fuel cells (FCs) as a sustainable source of electrical energy that produces no greenhouse gases in transportation applications [2]. Fuel cells are a clean source of fuel for transportation and contribute to environmental protection when used in electric cars, trains, airplanes, etc. [3]. New energy conversion technologies such as fuel cells outperform conventional devices in many ways, including great energy efficiency, small size, environmental safety, long life, and many others. Because of its high power generation density and low heat generation—both essential in transportation applications—the proton exchange membrane fuel cell (PEMFC) appears to be the most suitable form for use in automotive applications. The limited dynamic response of fuel cells is their main disadvantage in transport applications. This means that the fuel cell is unable to respond adequately to sudden load changes because it lags behind the load changes.

As a result, the battery storage and ultracapacitor (UC) should be connected to the fuel cell [4], while the battery storage has high power density, having disadvantages, including low energy capacity, long charging time, short life, and high price. The most effective method to address these concerns is to use a hybrid FC/B/UC network. Hybrid sources can take advantage of their special qualities with this combination. The ultracapacitor provides short bursts of peak power, while the battery is used as an energy buffer. A power management scheme (PMS) is needed to achieve some hybridization and the main aim of spreading load demands across power sources.

M. Bagde (✉) · A. Jawdekar · K. Sawalakhe
S.S.G.M. College of Engineering, Shegaon, MS 444 203, India
e-mail: mabagde@gmail.com

PMS successfully maintains hydrogen consumption and improves energy efficiency by limiting fuel cell output to wider operating levels. A set of traditional PMS [5] has been implemented to manage the system load between these input sources.

They are Equivalent Consumption Minimization Scheme (ECMS), Fuzzy Logic Control (FLC), External Energy Minimization Scheme (EEMS), PI Control, State Machine Control (SMC), and Equivalent Consumption Minimization Scheme. Several other contemporary optimization-based techniques have also been developed. The battery bank, fuel cell, and ultracapacitors are included in the state machine control (SMC) power management technique that Wang et al. proposed in [6]. The authors of [7] implemented power management using the proportional integral (PI) technique to control the energy flowing between photovoltaics (PV), fuel cells (FC), batteries, and supercapacitors (SC). In [8], a rule-based energy management strategy was used to operate a hybrid device with B/SC/FC in many operating modes. Jiang et al. in Ref. [9] proposed a dynamic programming (DP) strategy to reduce the amount of hydrogen used in a hybrid power system that uses a fuel battery, cell, and supercapacitor to power the drivetrain. For the purpose of powering an electric car, Kamel et al. [10] devised a unique consumption control technique using rule-based fuzzy logic control with a number of multi-input sources, i.e., initially the input sources consist of B/FC and later input sources combination of FC/SC/B.

The authors present in [11] an adaptive neuro-fuzzy inference system (ANFIS) for efficient power management between FC and battery, which is often used to power electric vehicles (EV). To improve the output power in an electric car using neural networks, a power management technique with two sections—wavelet-based and radial-based solutions—was developed in [12]. In order to control the power between FC, B, SC, and EV, the authors developed a new power control mechanism that focuses on wavelet transform techniques. By Djerioui et al., the gray wolf optimizer (GWO) was created. A hybrid power system for electric vehicle applications considers FC/B/UC [13]. For parallel HEVs, an FLC-based method was designed to optimize the SoC, improve fuel efficiency, reduce nitrogen dioxide emissions, and guarantee better drivability. An FLC-based Intelligent Energy Management Agent (IEMA) was created to distribute energy among available resources. Energy requirements, vehicle speed, SoC, and FLC were constructed in [14] to improve system performance.

Colvin [15] presents a number of power management options for FC-powered EVs. Bison suggested a new optimization strategy based on a two-dimensional mechanism of the fuel efficiency of hybrid vehicles. Zhang et al. [16] used wavelet transform and fuzzy logic methodologies to improve the energy management of hybrid trams. The main goal of the project is the development of an ideal EMS to reduce hydrogen consumption and loss of FC functionality. All optimization problems are not fully solved by any of the different algorithms. This is consistent with the No Free Lunch Scientific Theory, which is explored in [17], and shows that there is a real need for new optimization techniques in the study of EV power management. One important problem that could be solved is the measurement of hydrogen consumption using a hybrid DC bus energy storage system. In addition, it combines each DC/DC converter into a single device. In this research paper, an innovative hybrid

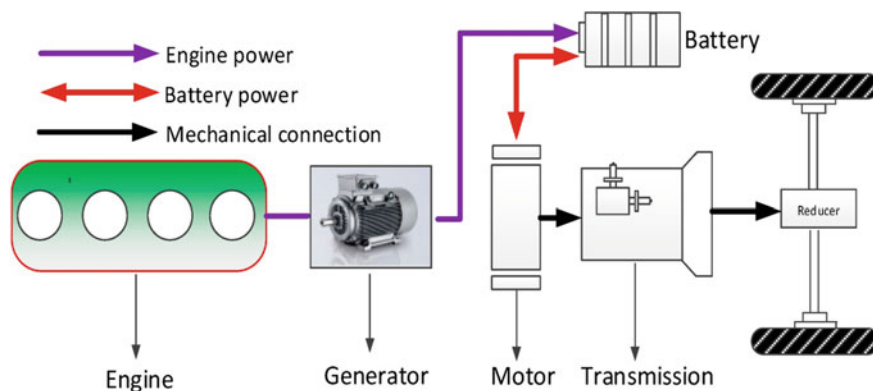


Fig. 1 Conventional diagram of hybrid E-vehicle

power management system that incorporates ANFIS and serves as an adaptive control system is used. This control system is modeled using MATLAB software to control hydrogen consumption in the FC and to keep the battery level (percentage of SoC) as high as possible in terms of life cycle costs and maintenance. With FC/B/UC and PMS settings, a hybrid power control scheme is proposed to improve the fuel economy of a hybrid electric vehicle, as shown in Fig. 1.

The essay is structured as follows. The literature review was described in Sect. 2 in relation to several problem statements. The proposed power management strategy (PMS) approach is presented in Sect. 3. The analysis of the comparative findings and the proposed technique are presented in Sect. 4. The primary findings that were derived from conducting this proposed work are presented in Sect. 5 as a final point.

2 Literature Survey

MATLAB/Simulink was used to model fuel cell, ultracapacitor fuel cell, and ultracapacitor fuel cell vehicles. Modeling features were included when they significantly affected the optimization goals (e.g., in accurate modeling of DC/DC converters) and excluded otherwise to achieve a good trade-off between accuracy and runtime (e.g., in simplified motor modeling). Based on efficiency, weight, and cost, the optimal powertrain topologies for use in this paper were selected through qualitative analysis. Selected powertrain topologies are shown in Fig. 1. All three vehicle types use a DC/DC converter to step up the fuel cell output voltage to match the motor controller input voltage (250–400 V is a common range [18]). This design allows the use of a smaller and therefore cheaper fuel cell, as the output voltage of the fuel cell can be lower than 250 V. The number of battery or ultracapacitor cells that can be connected in series with the ESS is limited because it is directly connected to the high-voltage bus (with the exception of the vehicle battery fuel cell-battery-ultracapacitor). This

limitation is acceptable because using a different DC/DC converter for the ESS would increase the weight and cost of the car and reduce the efficiency of the system.

2.1 Batteries

Due to their better power and energy density, lithium-ion batteries are currently widely considered to be the best option for energy storage in electric vehicles over lead-acid or nickel-metal hydride batteries [6]. The basis of the battery model used in this work is the high-performance lithium-ion cell ANR26650MI from A123 Systems. This paper exhibits great power density, high efficiency, and low cost compared to batteries used in earlier vehicle studies [19, 20]. The total resistance and the %V—SOC curves are determined by two variables, the number of cells in series and in parallel (batt s and batt p). The %V—SOC curve is a function of the percentage of peak voltage, as in the fuel cell model, allowing it to be applied to different serial numbers of cells. Estimates put Colombian efficiency at 95% [21].

The battery voltage is multiplied by the measured battery current. In order to add the energy entering or leaving the battery to the initial energy in the battery, this energy is integrated and then converted from joules to kilowatt hours (in kilowatt hours). The SOC of the battery in percent is then calculated by dividing the current energy output of the battery by its total capacity. This %SOC is converted to voltage using a lookup table based on the information for the ANR26650MI cell [22]. Since the bus voltage rating for the ESS battery is 346.5 V at 3.3 V per cell, the number of battery cells in series is fixed at 105 (with room to charge and discharge without exceeding the motor controller voltage limits). The battery voltage is chosen to be lower than the bus voltage for the battery-ultracapacitor ESS, which uses a two-quadrant DC/DC converter between the battery and the high-voltage bus. The maximum number of battery cells in series is 75, which allows the ultracapacitor bank to dissipate at 250 V. The weight of each cell is 70 g. The final weight per cell is 123 g after adding 53 g for packaging and cell balance. \$110 was quoted as the price for six articles [23]. It is estimated that the price may drop as low as \$100 for higher volume production. A final \$15 is added to each group of six cells for cell packing and balancing. Therefore, each cell is expected to cost \$19.15. The maximum current allowed is 70 A and the price per kilowatt is expected to be \$82.90/kW.

2.2 Fuel Cell Model

In order to vary the voltage of the fuel cell and battery independently of the voltage of the ultracapacitor, DC/DC converters coupled to the fuel cell and battery are essential components of the powertrain. If isolation is not required, as assumed in this paper, and if the voltage gain is not excessive, as in this paper, a non-isolated DC/DC

converter is suitable for use in fuel cell automobiles [24]. As a result, the fuel cell-battery-ultracapacitor vehicle uses a straight-line bidirectional converter (see Fig. 5) that connects the battery to the high-voltage bus, and all other types of vehicles use a straight-line unidirectional boost converter (the converter in Fig. 5 with switch S1 removed for ensuring unidirectional energy flow). This article uses basic hard-switching converter models to simplify modeling and avoid the in-depth topic of comparing different soft-switching methods based on efficiency, complexity, ease of control, weight, and cost. It is common practice to use interleaved and/or softswitch [25] converters at these high power levels.

Since the losses of the dynamic converter will impact the overall fuel consumption of the car [26] and because a high-performance converter can increase the volume and cost of the motor, it is essential to use a precise DC/DC converter. For example, when determining the true benefit of using a smaller fuel cell or battery, it is important to consider how much lighter and less expensive the accompanying DC/DC converter will be.

2.3 Ultracapacitor Vehicle

In a car using an ultracapacitor, the ultracapacitor stores energy from regenerative braking and offers additional power during acceleration. The energy storage capacity of the ultracapacitor is usually insufficient for vehicle movement at low speeds. Therefore, the control approach must guarantee that the energy storage capacity will be used as efficiently as possible. Mirjalili [27] examines three approaches and shows that optimal fuel efficiency is achieved by keeping the sum of the vehicle's kinetic energy and the energy stored in the ultracapacitor constant. This makes intuitive sense because the ultracapacitor will have enough room to absorb regenerative braking energy when the vehicle is braking, when its speed is high and its voltage is low. The low-pass coefficient is again chosen as the controller variable. The power supply of the fuel cell and the EZS are separated from the necessary electrical energy by means of a filter. All ESS (transient) power is supplied by the ultracapacitor within its current and voltage limitations. The battery supplies the remaining energy needed in case the voltage of the ultracapacitor drops below its lower limit (250 V). If the fuel cell is unable to provide electricity, or if the current consumption of the fuel cell is less than 7.55%, the battery supplies additional energy.

3 Proposed Hybrid Power Management System

A hybrid energy storage system (HESS) consists of a supercapacitor, Li-ion batteries, and a PEMFC. To ensure that the load has sufficient reliable power, these three sources are often considered FCHEVs. Figure 1 shows the hybrid system analysis configuration. The three power sources in this system are the capacitors, the fuel

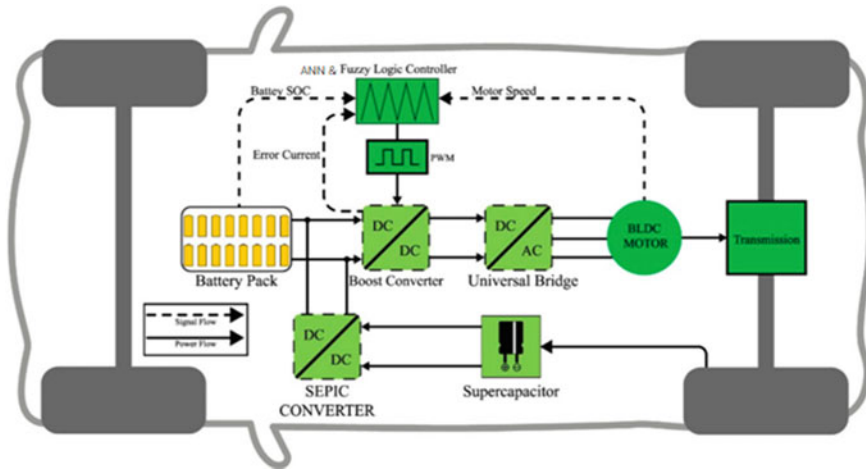


Fig. 2 Proposed hybrid power management system

cell, and the rechargeable battery. The fuel cell is equipped with a DC/DC boost converter that rises its voltage level to the expected level and maintains it at the outputs. A DC/DC bidirectional power supply device that converts variable power into a fixed voltage is found in batteries. Supercapacitors have been included in bidirectional converters that allow energy to be exchanged in both directions, similar to some other capacitors (Fig. 2).

3.1 Fuel Cell

Various fuel cell technologies exist, and they are divided into groups based on the electrolytes they use. Proton exchange membrane fuel cells (PEMFC) are a different kind of fuel cell that are frequently utilized in automotive applications. There are a number of novel fuel cell prototypes, each having a unique set of advantages and disadvantages depending on the subject being viewed. Additionally, this study proposes a straightforward electrochemical model that might be utilized to predict how such a fuel cell will behave under both dynamic and static circumstances [28]. The relationship between the fuel cell voltage level and the absolute pressures of hydrogen, water, and oxygen is the basis for the hydrogen fuel design used in this work. Table 1 provides an illustration of the fuel cell stack's specs. The relative pressures of oxygen and hydrogen, the temperature at which the membrane hydrates chemically, and the output current all affect the fuel cell's voltage. Below is the mathematical model.

$$V_{FC} = E_{Nernst} - V_{act} - V_{ohmic} - V_{con} \quad (1)$$

Table 1 Fuel cell specifications

Fuel cell model (input parameters)	Specifications
Voltage	53.5 V
No. of fuel cell	65
Operating temperature	43 °C
Nominal efficiency of the fuel stack	55%
Response time of fuel cell voltage	1 s
Voltage undershoot	2 V

where E_{Nernst} represents the mean value of thermodynamic potential in every single cell unit.

Here,

V_{act} = Activation voltage drop,

V_{ohmic} = Ohmic voltage drop,

V_{con} = Concentration voltage drop.

Hence, for N number of cells connected in series, the stack voltage V_{stack} is described as

$$V_{\text{stack}} = N \cdot V_{\text{FC}}$$

(2)

3.2 Supercapacitors

One of the most recent developments in power storage technology, particularly for integrated devices, is the use of supercapacitors. In this configuration, a series resistance (R_{sc}) comparable to a capacitance (C_{sc}) is connected. In Table 2, the UC’s specifications are displayed. The supercapacitor voltage (V_{sc}), which results from the SC current (I_{sc}), is calculated using the formula [29].

$$V_{\text{sc}} = V_1 - R_{\text{sc}} \times I_{\text{sc}} = \frac{Q_{\text{sc}}}{S_{\text{sc}}} - R_{\text{sc}} \times I_{\text{sc}}.$$

(3)

An electric vehicle that uses supercapacitors as its storage system must be built with a set of cells where N S cells are connected in series and N P cells are connected in parallel.

Table 2 Supercapacitor specifications

Supercapacitor model (input parameters)	Specifications
Surge voltage	306 V
Capacitor number in series	6
Capacitor counts in parallel	1
Rated voltage	290 V
Rated capacitance	14.5 F
Operating temperature	24 °C

Table 3 Li-ion battery specifications

Battery model (input parameters)	Specifications
Minimal voltage	48 V
Determined capacity	40 Ah
Esteemed capacity	40 Ah
Nominal voltage capacity	35.15 Ah
Response time of battery voltage	29 s
Fully charged voltage	55.77 V

3.3 Battery

A tiny controlled power supply is built into the battery in series with a fixed resistance like this [20]. Table 3 lists the requirements for Li-ion batteries. The battery voltage V_{bat} is specified in Eq. (1).

$$V_{\text{bat}} = E - R_{\text{bat}} \cdot I_{\text{bat}} \tag{4}$$

3.4 Adaptive Network-Based Fuzzy Interface System (ANFIS)

Power management techniques have emerged to support industrial work, such as fuzzy approaches, which are more used in systems control, by automating the learning experience. ANFIS is a key method that combines rule-based fuzzy logic control methodology and artificial neural network (ANN) learning ability to develop a complete set of all different kinds of feed-forward neural networks using supervised learning functions [31]. The ANFIS strategy is used as a hybrid training procedure based on relevant data, input/output, and coupling factors.

The architecture is shown in Fig. 3 as having only one hidden layer. The input node is represented by layer 1, the fuzzification nodes are in layer 2, the result nodes (hidden) are in layer 3, the defuzzification nodes are in layer 4, and the output node

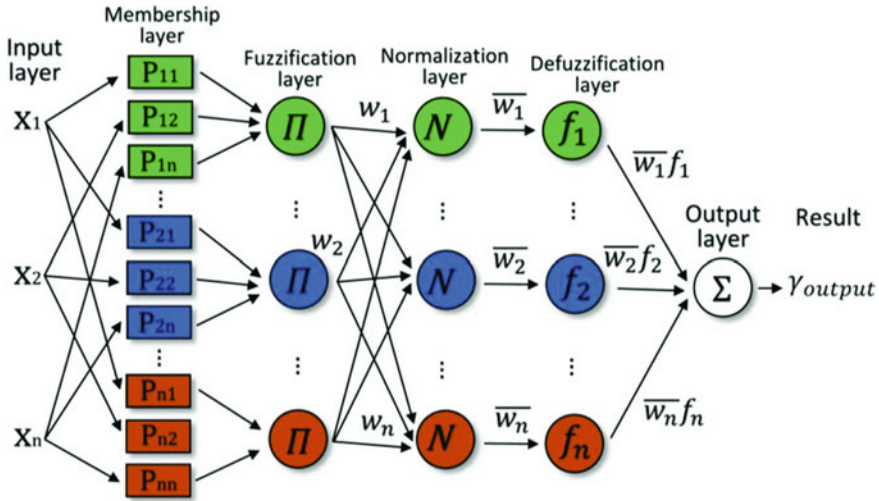


Fig. 3 ANFIS five layer structure

is represented by layer 5 []. A node can also be updated, at which point it will be divided into dynamic and static categories. Layers 2 and 4 are examples of dynamic nodes, while layers 1 and 3 are examples of stable nodes. The Li-ion battery SoC with three membership functions (MF) and the vehicle energy load represented by Pload are both used as inputs of the ANFIS control technique to predict the output power of the fuel cell [31]. The predicted proportional benefit from the PEMFC level is the result of ANFIS. ANFIS uses proportional variables to quickly measure and change standards.

4 Results and Discussion

The performance of EV driving just with the battery, fuel cell, and supercapacitor has been compared with the performance of EV driving in order to assess the efficacy of the proposed ANFIS energy management method (Figs. 4, 5, 6). The primary simulation parameters are listed in Table 4.

Moreover, the most successful offline global optimization method, dynamic programming, was compared with the proposed EMS for an online driving cycle in this study. The priority and effectiveness of the proposed approach will be guaranteed by its advantage over the dynamic programming method. In addition, the dynamic programming method does not limit the power generated by the PEMFC to specific operating locations. The simulation results of the proposed strategy are contrasted with the results of the dynamic programming approach, the most successful offline global optimization technique. For example, the fuel consumption in the proposed

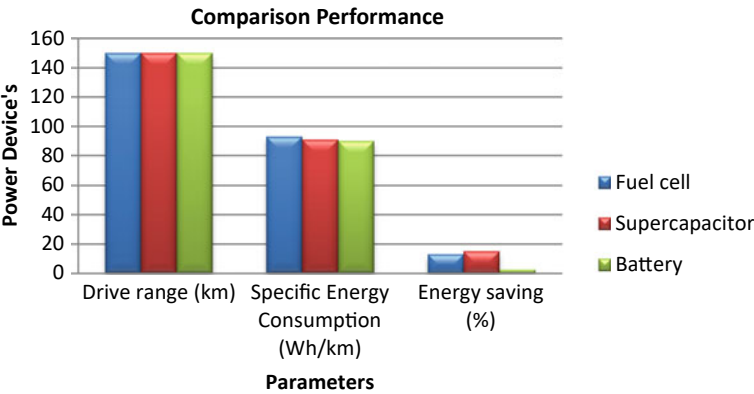


Fig. 4 Comparison performance

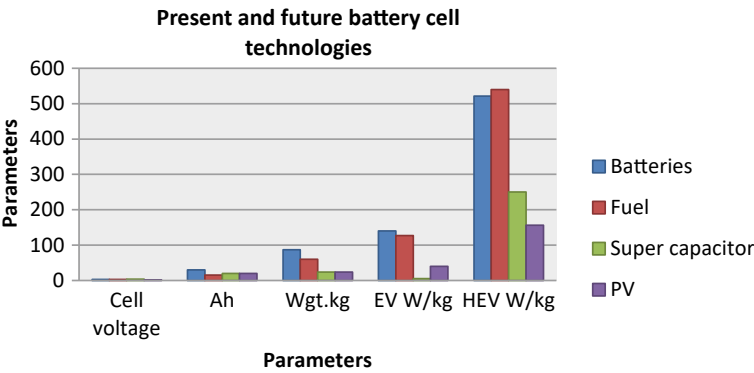


Fig. 5 Characteristics of cell present and future battery technologies for EVs

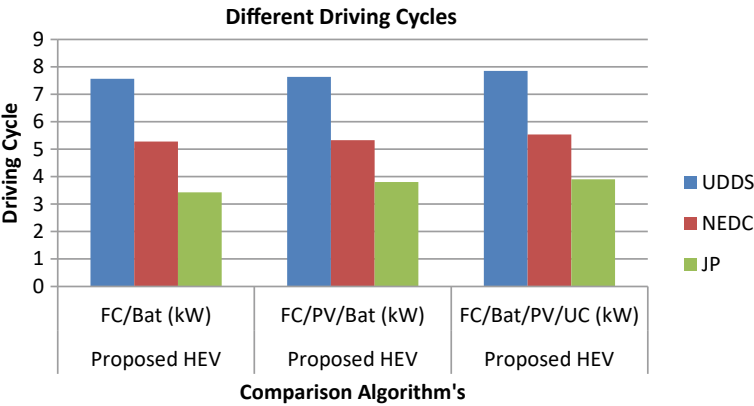


Fig. 6 Simulation results comparison for different driving cycles

Table 4 Comparison performance [32]

Power device's	Drive range (km)	Specific energy consumption (Wh/km)	Energy saving (%)
Fuel cell	150	93	+ 13
Supercapacitor	150	91	+ 15
Battery	150	90	+ 2.5

Table 5 Characteristics of cell present and future battery technologies for EVs [33]

Parameter's	Cell voltage	Ah	Wgt kg	EV W/kg	HEV W/kg
Batteries	2.8	30	87	140	521
Fuel	2.7	15	60	127	540
Supercapacitor	3.4	20	24	5.5	250
PV	1.5	20	24	40	156

Table 6 Simulation results comparison for different driving cycles [34]

Driving cycle	Proposed HEV FC/Bat (kW)	Proposed HEV FC/PV/Bat (kW)	Proposed HEV FC/Bat/PV/UC (kW)
UDDS	7.57	7.64	7.85
NEDC	5.28	5.33	5.54
JP	3.43	3.81	3.90

EMS is 7.64 MPG, while the fuel consumption in the DP strategy is 7.65 MPG in the UDDS driving cycle for an identical FC/battery/UC structure. As a result, the fuel consumption of the proposed EMS is roughly equivalent to that of the DP technique. Table 4 also lists battery power fluctuations. According to the findings, the FC/battery/UC arrangement with the proposed EMS has the least performance variation compared to the alternative tactics (Tables 5, 6).

5 Conclusion

In order to save gasoline as much as possible, this study proposes an ANFIS for power management in hybrid electric vehicles, with fuel cell (FC) as the primary energy source and batteries (BB) and ultracapacitors (UC) as secondary sources. The battery SoC is controlled by battery performance penalty coefficients in ECMS, a cost-based optimization approach. UC efficiency is not considered in this optimization strategy. Once the UCs are depleted, they can be recharged with the same power from the battery bank thanks to converters in the battery bank that control the DC bus voltage profile. During the load cycle, the battery and FC balance the load demand. This study recommends ANFIS for power management in hybrid electric vehicles, with

fuel cell (FC) as the main energy source and batteries (BB) and ultracapacitors (UC) as secondary sources to save as much oil as possible. The battery SoC is controlled by battery penalty coefficients in ECMS, which is a cost-based optimization method. This optimization technique does not consider the utility of UC. The battery bank has converters that regulate the DC bus voltage profile so that if the UCs are depleted, they can be recharged with the same power from the battery bank. The battery and FC balance the load demand during the load cycle.

References:

1. Zhang F, Wang L, Coskun S, Pang H, Cui Y, Xi J (2020) Energy management strategies for hybrid electric vehicles: review, classification, comparison, and outlook. *Energies* 13:3352
2. Duhr P, Christodoulou G, Balerna C, Salazar M, Cerofolini A, Onder CH (2021) Time-optimal gearshift and energy management strategies for a hybrid electric race car. *Appl Energy* 282:115980
3. Guo N, Zhang X, Zou Y, Guo L, Du G (2021) Real-time predictive energy management of plug-in hybrid electric vehicles for coordination of fuel economy and battery degradation. *Energy* 214:119070
4. Li Q, Chen W, Liu S, You Z, Tao S, Li Y (2012) Power management strategy based on adaptive neuro-fuzzy inference system for fuel cell-battery hybrid vehicle. *J Renew Sustain Energy* 4:013106
5. Allahviridzadeh Y, Mohamadian M, HaghiFam MR, Hamidi A (2017) Optimization of a fuzzy-based energy management strategy for a PV/WT/FC hybrid renewable system. *Int J Renew Energy Res* 7:1686–1699
6. Yavasoglu HA, Tetik YE, Ozcan HG (2020) Neural network-based energy management of multi-source (battery/UC/FC) powered electric vehicle. *Int J Energy Res* 44:12416–12429
7. Montazeri-Gh M, Pourbafarani Z (2017) Near-optimal SOC trajectory for traffic-based adaptive PHEV control strategy. *IEEE Trans Veh Technol* 66:9753–9760
8. Singh KV, Bansal HO, Singh D (2021) Development of an adaptive neuro-fuzzy inference system-based equivalent consumption minimization strategy to improve fuel economy in hybrid electric vehicles. *IET Electr Syst Transp* 11:171–185
9. Suhail M, Akhtar I, Kirmani S, Jameel M (2021) Development of progressive fuzzy logic and ANFIS control for energy management of plug-in hybrid electric vehicle. *IEEE Access* 9:62219–62231
10. Kamel AA, Rezk H, Abdelkareem MA (2021) Enhancing the operation of fuel cell-photovoltaic-battery-supercapacitor renewable system through a hybrid energy management strategy. *Int J Hydrogen Energy* 46:6061–6075
11. Song Z, Hofmann H, Li J, Hou J, Han X, Ouyang M (2014) Energy management strategies comparison for electric vehicles with a hybrid energy storage system. *Appl Energy* 134:321–331
12. Gaber M, El-Banna S, El-Dabah M, Hamad O (2021) Designing and implementation of an intelligent energy management system for electric ship power system based on adaptive neuro-fuzzy inference system (ANFIS). *Adv Sci Technol Eng Syst J* 6:195–203
13. Tian X, He R, Xu Y (2018) Design of an energy management strategy for a parallel hybrid electric bus based on an IDP-ANFIS scheme. *IEEE Access* 6:23806–23819
14. Ding N, Prasad K, Lie TT (2021) Design of a hybrid energy management system using designed rule-based control strategy and genetic algorithm for the series-parallel plug-in hybrid electric vehicle. *Int J Energy Res* 45:1627–1644
15. Colvin R (2019) *Advances in automotive technologies*, vol 84. Springer, Berlin/Heidelberg
16. Zhang X, Guo L, Guo N, Zou Y, Du G (2021) Bi-level energy management of plug-in hybrid electric vehicles for fuel economy and battery lifetime with intelligent state-of-charge reference. *J Power Sources* 481:228798

17. Cai CH, Du D, Liu ZY (2003) Battery state-of-charge (SOC) estimation using adaptive neuro-fuzzy inference system (ANFIS). *IEEE Int Conf Fuzzy Syst* 2:1068–1073
18. Shaik RB, Kannappan EV (2020) Application of adaptive neuro-fuzzy inference rule-based controller in hybrid electric vehicles. *J Electr Eng Technol* 15:1937–1945
19. Karaboga D, Kaya E (2019) Adaptive network-based fuzzy inference system (ANFIS) training approaches: a comprehensive survey. *Artif Intell Rev* 52:2263–2293
20. Zhang F, Hu X, Langari R, Wang L, Cui Y, Pang H (2021) Adaptive energy management in automated hybrid electric vehicles with flexible torque request. *Energy* 214:118873
21. Zhang L, Ye X, Xia X, Barzegar F (2020) A real-time energy management and speed controller for an electric vehicle powered by a hybrid energy storage system. *IEEE Trans Ind Inform* 16:6272–6280
22. Zhang Q, Li G (2019) A predictive energy management system for hybrid energy storage systems in electric vehicles. *Electr Eng* 101:759–770
23. Zhang Q (2020) Applied sciences strategy for hybrid electric vehicles based on driving cycle recognition. *Appl Sci* 10:696
24. Wiecezorek M, Lewandowski M (2017) A mathematical representation of an energy management strategy for hybrid energy storage system in electric vehicle and real-time optimization using a genetic algorithm. *Appl Energy* 192:222–233
25. Sarkar J, Bhattacharyya S (2012) Application of graphene and graphene-based materials in clean energy-related devices Minghui. *Int J Energy Res* 33:23–40
26. Gomes GF, da Cunha SS, Ancelotti AC (2019) A sunflower optimization (SFO) algorithm applied to damage identification on laminated composite plates. *Eng Comput* 35:619–626
27. Mirjalili S, Gandomi AH, Mirjalili SZ, Saremi S, Faris H, Mirjalili SM (2017) Salp swarm algorithm: a bio-inspired optimizer for engineering design problems. *Adv Eng Softw* 114:163–191
28. Mirjalili S, Mirjalili SM, Hatamlou A (2016) Multi-verse optimizer: a nature-inspired algorithm for global optimization. *Neural Comput Appl* 27:495–513
29. Saremi S, Mirjalili S, Lewis A (2017) Grasshopper optimisation algorithm: theory and application. *Adv Eng Softw* 105:30–47
30. Mirjalili S, Mirjalili SM, Lewis A (2014) Grey wolf optimizer. *Adv Eng Softw* 69:46–61
31. Abdalla O, Rezk H, Ahmed EM (2019) Wind-driven optimization algorithm based global MPPT for PV system under non-uniform solar irradiance. *Sol Energy* 180:429–444
32. Tolba M, Rezk H, Diab AAZ, Al-Dhaifallah M (2018) A novel robust methodology based salp swarm algorithm for allocation and capacity of renewable distributed generators on distribution grids. *Energies* 11:2556
33. Yadav N, Yadav A, Bansal JC, Deep K, Kim JH (2019) Harmony search and nature inspired optimization algorithms: theory and applications, vol 741. In: *ICHSA 2018*. Springer, Berlin/Heidelberg
34. Mirjalili S (2019) Particle swarm optimization. *Stud Comput Intell* 780:15–31

CLASSIFICATION OF MULTIPLE AND MULTISTAGE POWER QUALITY DISTURBANCES USING S-TRANSFORM AND FEED FORWARD NEURAL NETWORK

Abstract

The reliable and uninterrupted supply of electrical power is fundamental to modern society's functioning. However, Power Quality Disturbances (PQDs), encompassing a diverse range of transient events such as voltage sags, swells, harmonics, and interruptions, can compromise the stability and effectiveness of power systems. Detecting and accurately classifying these disturbances, particularly those involving multiple and multistage events, is pivotal for mitigating their adverse effects. In response to this challenge, this research paper presents an in-depth investigation into the use of the S-Transform, a time-frequency analysis technique, for the detection and classification of multiple and multistage PQ disturbances. We propose a comprehensive methodology that integrates the S-Transform with advanced classification techniques, including Feed Forward Neural Network (FFNN). The effectiveness of the proposed methodology is demonstrated through the PQ disturbance datasets. The results showcase the S-Transform's aptitude in revealing fine-grained time-frequency structures inherent in multistage disturbances. Furthermore, the integration of advanced classification techniques yields robust and accurate identification of disturbance types, ensuring timely and appropriate responses to mitigate their impact.

Keywords: Power Quality Disturbances, Feed Forward Neural Network, S-Transform.

Authors

Ravishankar S. Kankale

Department of Electrical Engineering
SSGMCE, Shegaon
India
rskankale@ssgmce.ac.in

Dr. Sudhir R. Paraskar

Department of Electrical Engineering
SSGMCE, Shegaon
India
srparaskar@ssgmce.ac.in

Dr. Saurabh S. Jadhao

Department of Electrical Engineering
SSGMCE, Shegaon
India
ssjadhao@ssgmce.ac.in

I. INTRODUCTION

In modern society, the uninterrupted supply of electric power has become an indispensable necessity for the operation of various critical infrastructures, industrial processes, and domestic activities. However, the reliability and quality of power supply are often challenged by a multitude of disturbances that can disrupt the normal functioning of electrical systems. Power Quality (PQ) disturbances encompass a wide array of transient and non-stationary events, such as voltage sags, swells, interruptions, harmonics, and flicker, among others. These disturbances can lead to severe economic losses, equipment damage, and operational disruptions, underscoring the significance of accurate and timely detection and classification.

To address these challenges, researchers and practitioners have focused their efforts on developing advanced techniques for the detection and classification of PQ disturbances. Traditional methods often rely on Fourier Transform-based techniques, which are suitable for stationary signals but fall short when analyzing non-stationary and time-varying disturbances. In response to this limitation, the S-Transform, also known as the Stockwell Transform, has emerged as a promising tool for the simultaneous analysis of signals in both the time and frequency domains. Its ability to provide enhanced time-frequency resolution makes it well-suited for the detection and classification of multistage PQ disturbances.

This research paper presents a comprehensive investigation into the application of the S-Transform for the detection and classification of multiple and multistage PQ disturbances. We delve into the underlying principles of the S-Transform and its advantages over conventional techniques in handling transient and non-stationary disturbances. Leveraging this transformative analysis method, our study aims to not only enhance the accuracy of detection but also enable the differentiation of complex PQ disturbance patterns that may involve multiple stages of events.

II. RELATED LITERATURE

The research conducted by Kuo et al. (2009) presented a novel approach for the detection and classification of multistage power quality disturbances using the S-Transform and probabilistic neural networks. The study highlighted the effectiveness of the S-Transform in capturing time-frequency features of PQ disturbances, enabling improved discrimination between different disturbance types. The integration of probabilistic neural networks provided accurate classification results, enhancing the overall reliability of the detection system.

Chandrasekaran and Sankaranarayanan (2010) proposed a method for PQ disturbance classification using the S-Transform and an adaptive network-based fuzzy inference system (ANFIS). The researchers showcased the ability of the S-Transform to capture transient and non-stationary features of PQ disturbances. The ANFIS-based classification demonstrated the system's adaptability to varying disturbance patterns, making it suitable for real-world applications.

Messina et al. (2011) contributed to the field by developing an automatic detection and classification framework for power quality disturbances using the S-Transform and fuzzy

c-means clustering. The study emphasized the effectiveness of fuzzy clustering in identifying clusters of similar disturbance patterns, which facilitated accurate classification. The combination of the S-Transform and fuzzy clustering provided a robust solution for handling multistage disturbances.

In another study by Cheng et al. (2011), the authors investigated the automatic detection and classification of power quality disturbances using the S-Transform and a probabilistic neural network. The research highlighted the S-Transform's ability to reveal intricate time-frequency structures in disturbance signals. The probabilistic neural network demonstrated its proficiency in effectively distinguishing between various PQ disturbance types, enhancing the overall reliability of the classification process.

Yu et al. (2012) contributed to the field by presenting a power quality disturbance detection and classification methodology based on the S-Transform and probabilistic neural network. The research showcased the potential of the S-Transform in characterizing complex disturbances with multiple stages. The integration of a probabilistic neural network ensured accurate classification, underscoring the practicality of the approach for real-world power systems.

Collectively, these research papers highlight the significance of the S-Transform as a valuable tool for capturing time-frequency features of PQ disturbances, particularly those involving multiple and multistage events. The incorporation of advanced classification techniques, such as probabilistic neural networks and fuzzy clustering, further enhanced the accuracy and reliability of detecting and classifying these disturbances. The studies underscore the importance of these methodologies in ensuring the stability and reliability of power systems, particularly in the presence of intricate PQ events that can lead to significant operational and economic consequences.

III. S-TRANSFORM

The S-Transform, also known as the Stockwell Transform, is a time-frequency analysis technique used to analyze signals in both the time and frequency domains simultaneously. Unlike traditional Fourier-based techniques that provide a static frequency representation of a signal, the S-Transform captures the dynamic changes in frequency content over time, making it particularly useful for analyzing non-stationary and transient signals, such as those found in power quality disturbances, seismic signals, and biomedical data.

At its core, the S-Transform combines the concepts of the Short-Time Fourier Transform (STFT) and the windowed Fourier Transform. While the STFT uses a fixed window to analyze signal segments, the S-Transform employs an adaptive window that adjusts its length according to the local frequency characteristics of the signal. This adaptive window allows the S-Transform to provide higher time resolution in regions with fast frequency variations and higher frequency resolution in regions with slow variations.

CLASSIFICATION OF MULTIPLE AND MULTISTAGE POWER QUALITY DISTURBANCES USING S-TRANSFORM AND FEED FORWARD NEURAL NETWORK

The mathematical representation of the S-Transform of a signal $x(t)$ at a specific time t and frequency f is given by:

$$S_x(t, f) = \int_{-\infty}^{\infty} x(\tau) g(t - \tau) e^{-2\pi i f (t - \tau)} d\tau \quad (1)$$

Here

$x(t)$ is the input signal

$g(t)$ is the analyzing window function

f represents frequency

t denotes time

i is the imaginary unit

The result of the S-Transform is a complex-valued matrix where the magnitude represents the amplitude of the frequency component at a specific time and frequency, and the phase represents the phase information.

IV. FEED FORWARD NEURAL NETWORK (FFNN)

Feedforward neural network is a fundamental architecture in artificial neural networks that models the relationship between input data and corresponding output predictions. It is a form of supervised learning where the network learns to map input features to desired output labels through a series of interconnected layers. Feedforward neural networks are widely used for various tasks, including pattern recognition, classification, regression, and function approximation.

A feedforward neural network consists of layers of interconnected nodes, commonly referred to as neurons. These neurons are organized into three main types of layers: input layer, hidden layers, and output layer. Information flows from the input layer through the hidden layers to the output layer without any feedback loops, hence the term "feedforward."

Each neuron in a layer is connected to all neurons in the previous layer and to all neurons in the subsequent layer. These connections are associated with weights that determine the strength of the connection. The process of learning in a feedforward neural network involves adjusting these weights to minimize the difference between the network's predictions and the actual target values, typically using optimization algorithms like gradient descent.

The output of each neuron is determined by an activation function. Common activation functions include the sigmoid function, rectified linear unit (ReLU), and hyperbolic tangent (tanh). These functions introduce non-linearity to the network, enabling it to model complex relationships within the data.

The operation of a feedforward neural network occurs in two main steps: forward propagation and backpropagation. During forward propagation, input data is fed into the input layer. The input is multiplied by the weights and passed through the activation functions in each subsequent layer, ultimately producing an output prediction in the output layer.

Mathematically, the output O_j of a neuron j in a layer can be expressed as:

$$O_j = f(\sum_i \omega_{ij} \cdot o_i + b_j) \quad (2)$$

Here:

ω_{ij} is the weight of the connection between neuron i in the previous layer and neuron j in the current layer.

o_i is the output of neuron i in the previous layer.

b_j is the bias term associated with neuron j .

f is the activation function.

Feedforward neural networks provide a powerful framework for learning complex relationships in data. By organizing neurons into layers and using activation functions, they can model intricate patterns within input data and generate meaningful predictions. The training process, involving forward propagation and backpropagation, enables these networks to adapt their weights and biases to optimize their performance on specific tasks. As a foundational concept in artificial intelligence and machine learning, feedforward neural networks continue to drive advancements in various fields by enabling computers to learn from data and make informed decisions.

V. PROPOSED METHODOLOGY

In this algorithm the PQ disturbance signal is processed using S-Transform. The resultant S-Transform complex matrix is obtained. To obtain the maximum voltage amplitude versus time contour, the maximum of the absolute value of S-Transform matrix has been taken for analysis. It provides the absolute value of the fundamental frequency element present in the PQ disturbance signal. Figure 1 shows the flowchart of the proposed methodology adopted in this research work.

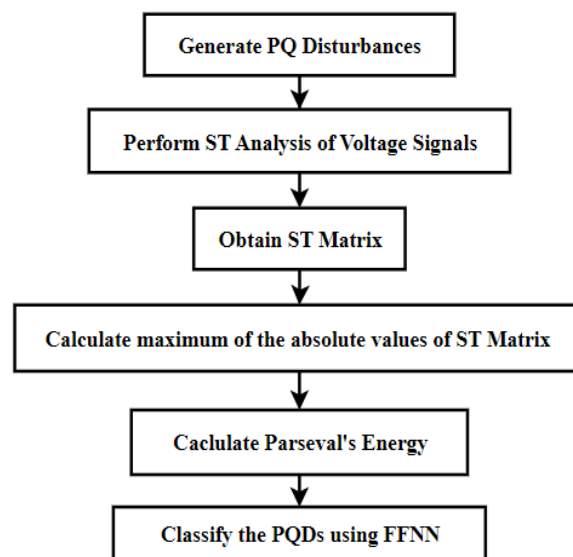


Figure 1: Flowchart of proposed methodology

VI. GENERATION OF POWER QUALITY DISTURBANCES

The Power Quality Disturbances required for the evaluation of the performance of proposed algorithm are generated by using the integral mathematical models of PQDs as per the standards. By varying the parameters of the models, we obtained different dataset of PQDs. The details of the multiple and multistage PQDs considered under study is given below.

- 1. Multiple Power Quality Disturbances:** The superim position of more than one type of PQ disturbances during the same period corresponds to multiple PQ disturbances e.g., voltage sag with flicker, voltage swell with harmonics, transient with harmonics, flicker with harmonics, interruption with harmonics, voltagesag with harmonics, etc. These disturbances are generated by the addition/multiplication of single-stage PQ disturbances. PQ variation such as harmonics which always exists in a power distribution network, when multiplied with single-stage PQ disturbances, produces multiple PQ disturbances. The multiple PQ disturbances have been generated as shown in Figure 2-4. The selection of parameter values of these disturbances has been performed as per Table 1.

Table 1: Mathematical Modeling of Multiple PQ Disturbances

PQ disturbance	Mathematical model	Parameter range
Sag with harmonics	$V(t) = \left(1 - \beta \left(u(t - t^*) - u(t - t^{**})\right)\right) \left(\beta_1 \sin(\omega t) + \beta_3 \sin(3\omega t) + \beta_5 \sin(5\omega t) + \beta_7 \sin(7\omega t)\right)$	$0.1 \leq \beta \leq 0.9, T \leq t^{**} - t^* \leq 9T$ $0.05 \leq \beta_3, \beta_5, \beta_7 \leq 0.15,$ $\sum \beta_i^2 = 1$
Swell with harmonics	$V(t) = \left(1 + \beta \left(u(t - t^*) - u(t - t^{**})\right)\right) \left(\beta_1 \sin(\omega t) + \beta_3 \sin(3\omega t) + \beta_5 \sin(5\omega t) + \beta_7 \sin(7\omega t)\right)$	$0.1 \leq \beta \leq 0.8, T \leq t^{**} - t^* \leq 9T$ $0.05 \leq \beta_3, \beta_5, \beta_7 \leq 0.15,$ $\sum \beta_i^2 = 1$
Interruption with harmonics	$V(t) = \left(1 - \beta \left(u(t - t^*) - u(t - t^{**})\right)\right) \left(\beta_1 \sin(\omega t) + \beta_3 \sin(3\omega t) + \beta_5 \sin(5\omega t) + \beta_7 \sin(7\omega t)\right)$	$0.9 \leq \beta \leq 1.0, T \leq t^{**} - t^* \leq 9T$ $0.05 \leq \beta_3, \beta_5, \beta_7 \leq 0.15,$ $\sum \beta_i^2 = 1$

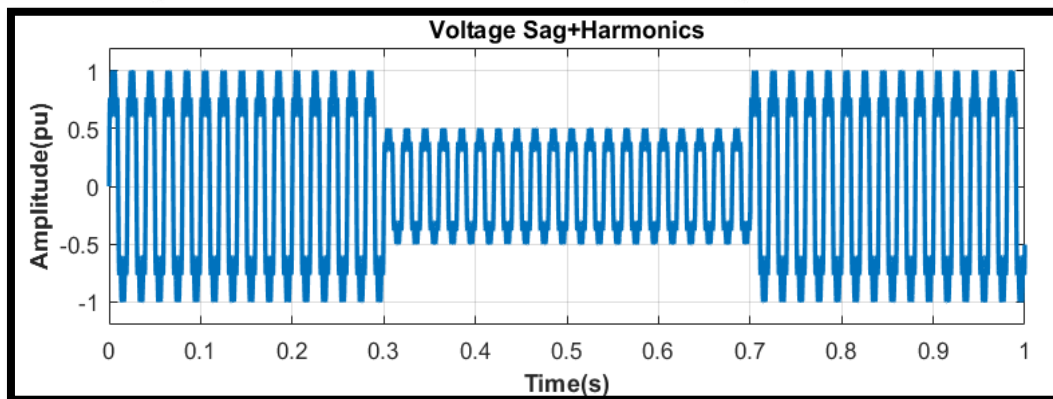


Figure2: Simulated sag with harmonic signal

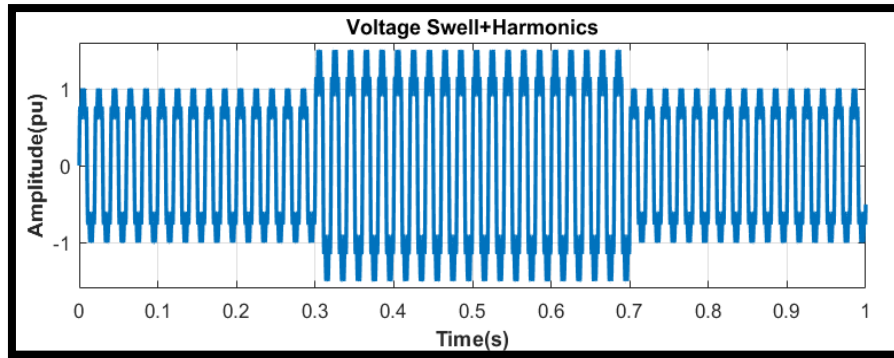


Figure 3: Simulated well with harmonic signal

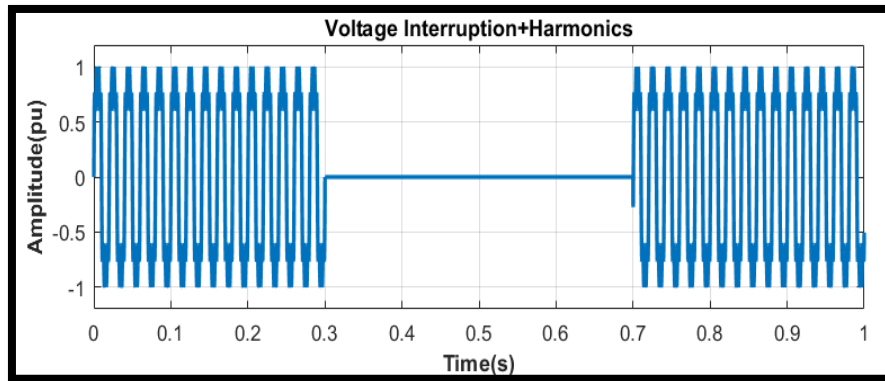
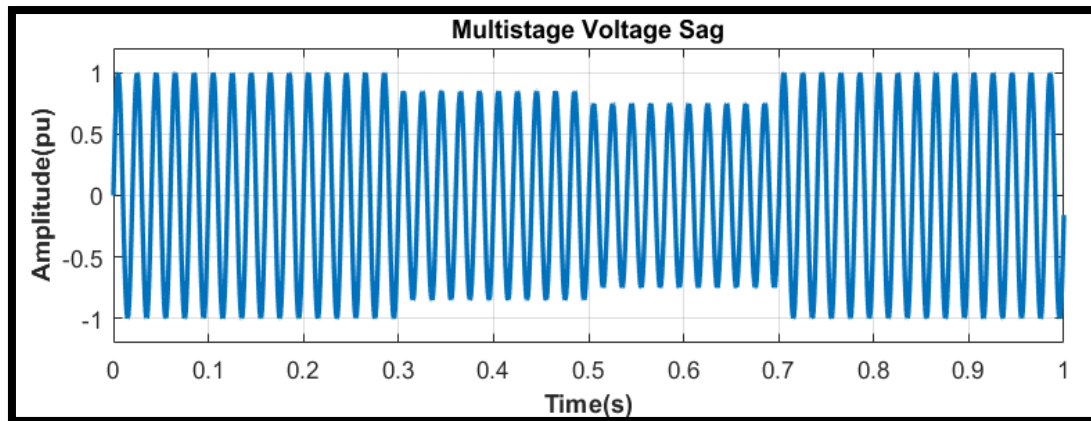
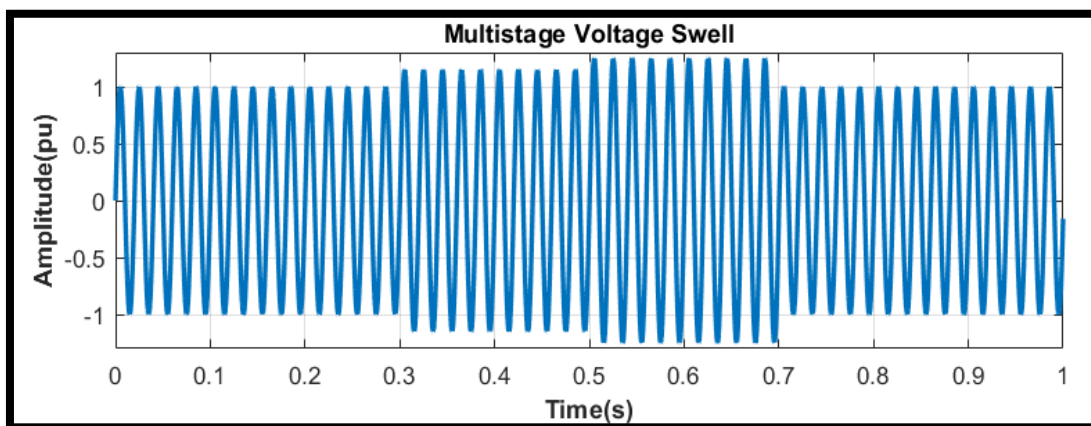
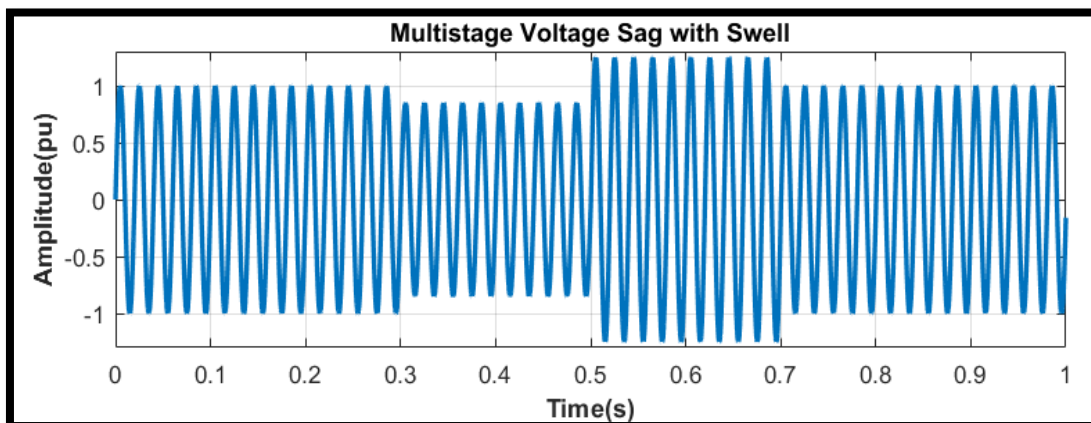


Figure 4: Simulated interruption with harmonic signal

2. **Multi Stage PQ Disturbances:** Multi-stage PQ disturbances are defined as the single-stage PQ disturbance followed by some other PQ disturbance before the recovery of the former disturbance e.g., voltagesag followed by swell, voltages well followed by sag, transient followed by sag, transient followed by swell, etc. These disturbances change their parameters before recovery. It is formed using the addition of single-stage PQ disturbances. Several generated multi-stage PQ disturbances (two stages) are shown in figure 5-7. The parameters of these disturbances are selected as per Table 2. Likewise, the multi-stage PQ disturbances having more than two stages which may be possible due to the complexity of the power system, can be synthetically generated.

Table2: Mathematical Modelling of Multi-Stage PQ Disturbances

PQ disturbance	Mathematical model	Parameter range
Multi-stage sag	$V(t) = \left[\begin{aligned} &1 - \beta_1 \left(u(t-t^*) - u(t-t^{**}) \right) + \\ &1 - \beta_2 \left(u(t-t^{**}) - u(t-t^{***}) \right) \end{aligned} \right] \sin \omega t$	$0.1 \leq \beta_1, \beta_2 \leq 0.9, T \leq t^{**} - t^* \leq 9T,$ $T \leq t^{***} - t^{**} \leq 9T,$
Multi-stage Swell	$V(t) = \left[\begin{aligned} &1 + \beta_1 \left(u(t-t^*) - u(t-t^{**}) \right) + \\ &1 - \beta_2 \left(u(t-t^{**}) - u(t-t^{***}) \right) \end{aligned} \right] \sin \omega t$	$0.1 \leq \beta_1, \beta_2 \leq 0.8,$ $T \leq t^{**} - t^* \leq 9T,$ $T \leq t^{***} - t^{**} \leq 9T$
Multi-stage sag with swell	$V(t) = \left[\begin{aligned} &1 - \beta_1 \left(u(t-t^*) - u(t-t^{**}) \right) + \\ &1 + \beta_2 \left(u(t-t^{**}) - u(t-t^{***}) \right) \end{aligned} \right] \sin \omega t$	$0.1 \leq \beta_1 \leq 0.9,$ $0.1 \leq \beta_2 \leq 0.8,$ $T \leq t^{**} - t^* \leq 9T,$ $T \leq t^{***} - t^{**} \leq 9T$

**Figure 5:** Simulated multi-stages ag signal**Figure 6:** Simulated multi-stages well signal**Figure 7:** Simulated multi-stages ag with swell signal

VII. S-TRANSFORM ANALYSIS RESULTS

The voltage signals corresponding to multiple and multistage Power Quality Disturbances are processed using S-Transform. The results of the ST analysis is discussed in this section. Figure 8 (a) – 10 (a) show the three types of multiple PQ disturbances and Figure

8 (b) – 10 (b) show their voltage amplitude versus time vectors respectively. Three cases of multistage PQ disturbance have been shown in Figure 11 (a) – 13 (a) with their voltage amplitude versus time vectors as shown in Figure 11 (b) – 13 (b). From the figures obtained from ST analysis it is cleared that the time versus normalized amplitude plot obtained from the maximum of the absolute value of S-Transform matrix forms an important aspect for the classification of both multiple and multistage PQDs. These characteristics found to be distinct for different PQDs.

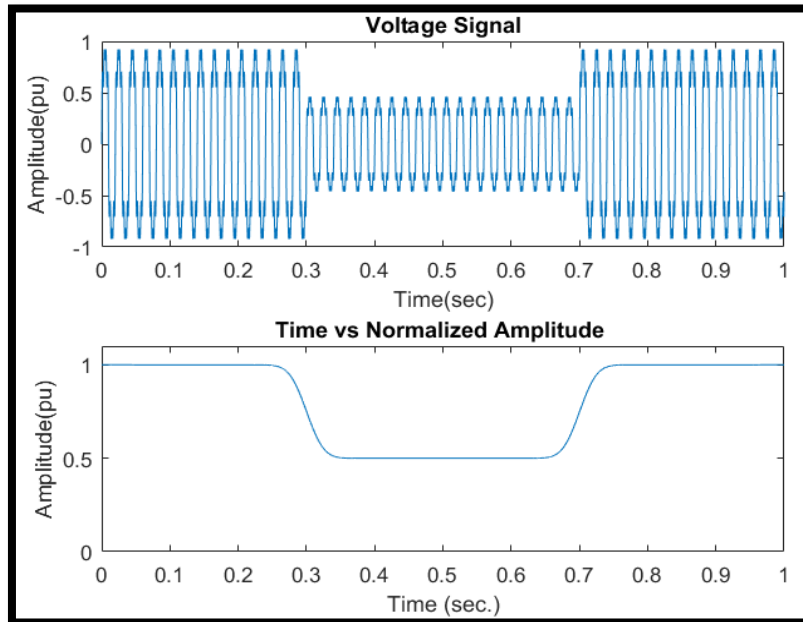


Figure 8: (a) Sag with harmonics (b) Voltage amplitude vs time vector

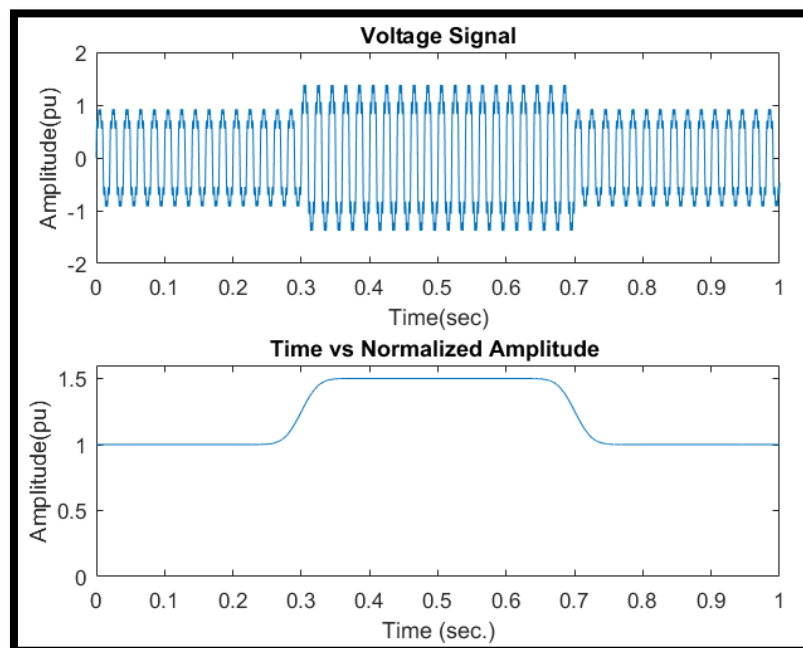


Figure 9: (a) Swell with harmonics (b) Voltage amplitude vs time vector

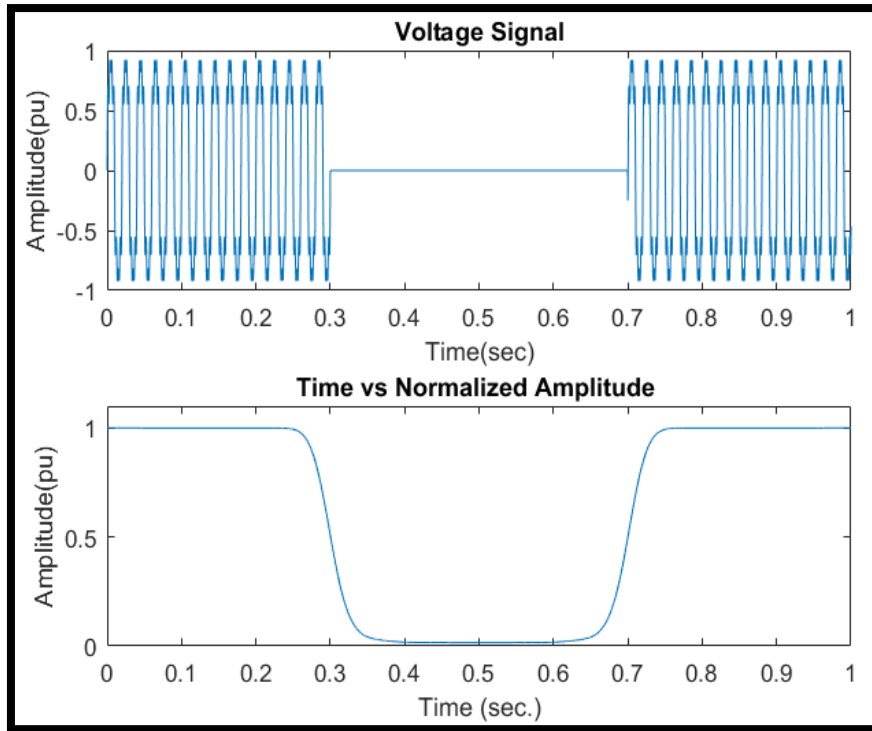


Figure 10: (a)Interruption with harmonics (b)Voltage amplitude vs time vector

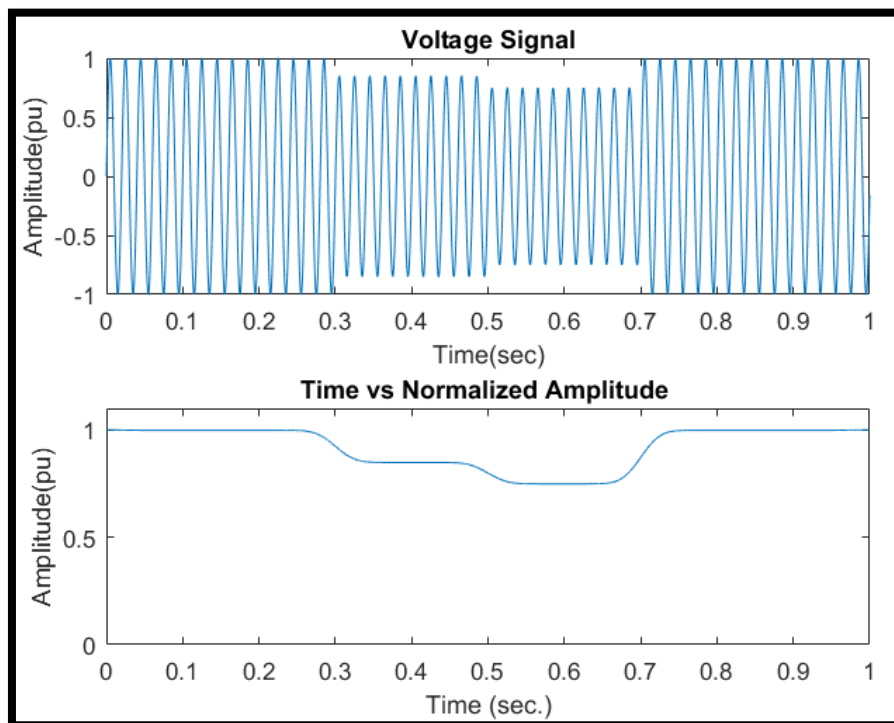


Figure 11: (a) Multi stage sag (b) Voltage amplitude vs time vector

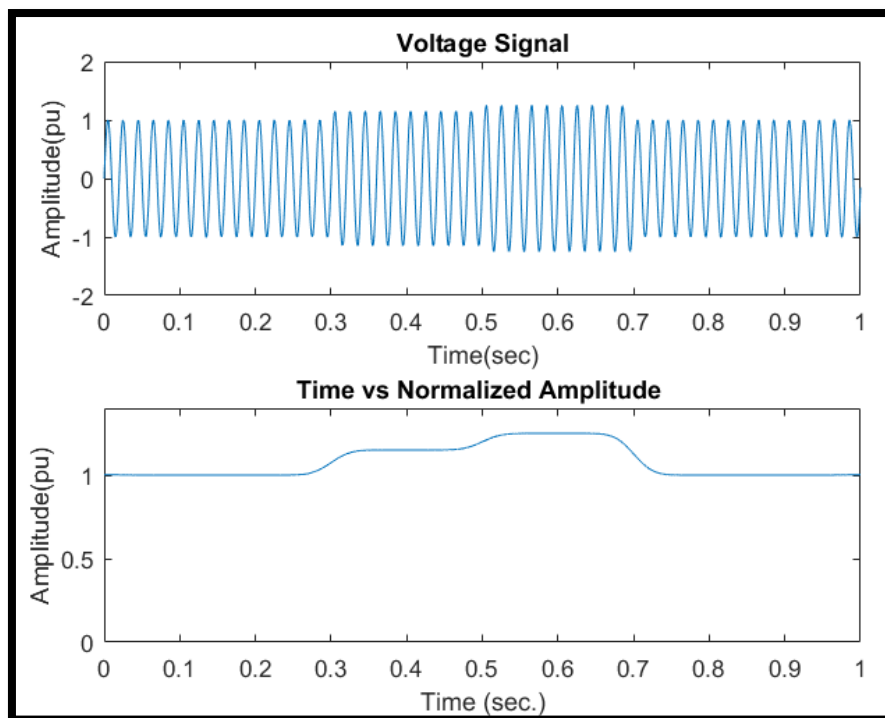


Figure 12: (a) Multi stages well (b) Voltage amplitude vs time vector

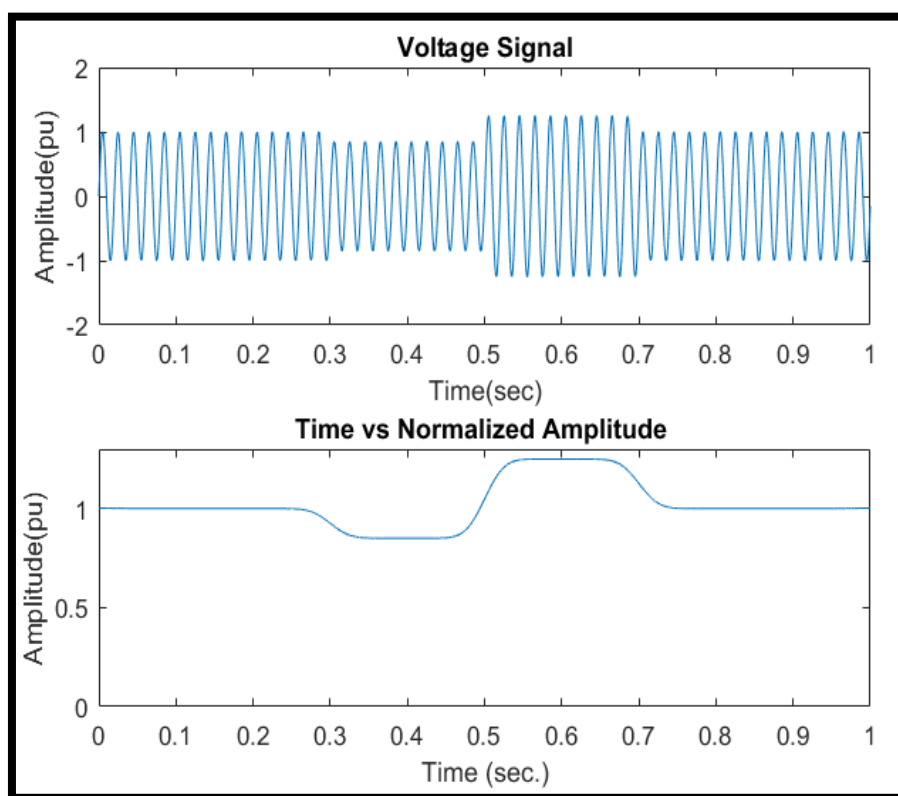


Figure 13: (a) Multi stages ag with swell (b) Voltage amplitude vs time vector

VIII. FEATURE EXTRACTION FROM S-TRANSFORM ANALYSIS

The existing literature focuses on detection and recognition of single-stage PQ disturbances. So, this work emphasizes on the detection and classification of multiple and multistage PQ disturbances using S-Transform. Voltage amplitude versus time vector obtained from S-Transform complex matrix clearly depicts the PQ disturbance behavior. Further, features extracted from the transformed signals are used for automatic identification of multiple and multistage PQ disturbances. The Parseval's energy calculated from the magnitude of time vs normalized amplitude plot is used to classify the multiple and multistage power quality disturbances. Figure 14 shows the Parseval's energy plot of both multiple and multistage PQ disturbances. By calculating the values of energy corresponding to different PQ disturbances a dataset is created for the classification of disturbances.

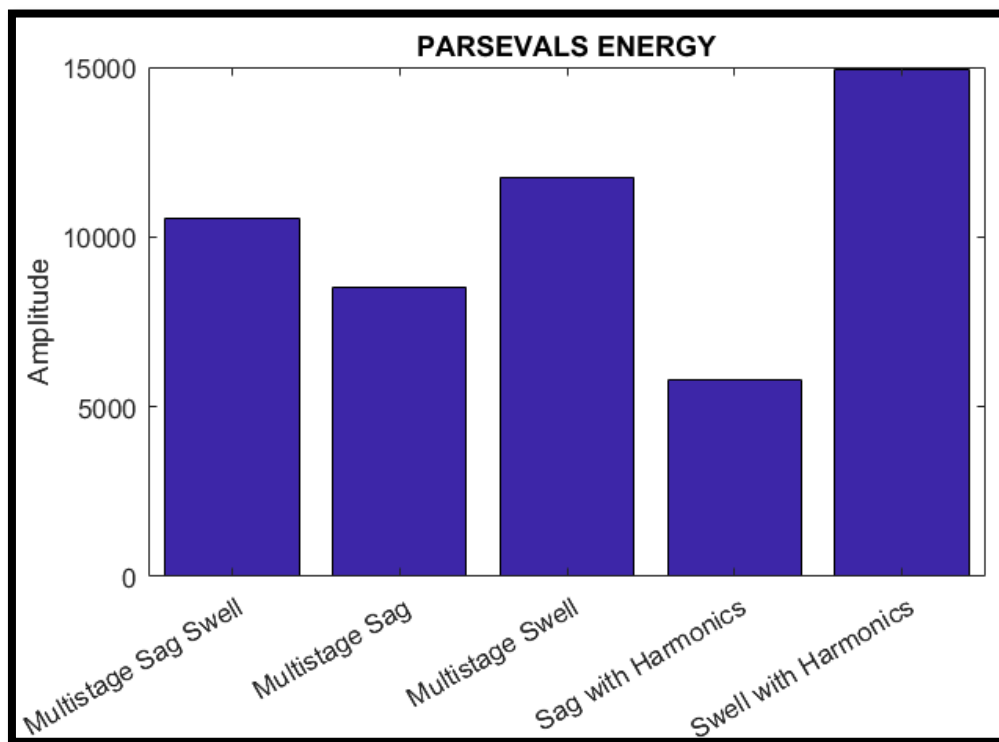


Figure 14: Parseval's Energy calculated for multiple and multistage PQ disturbances

IX. FEED FORWARD NEURAL NETWORK CLASSIFIER RESULTS

The feature vector of 20 datasets of each disturbance is created by computing the Parseval's energy of different PQDs from the ST analysis. The training and testing of Feed Forward Neural Network (FFNN) are done using the extracted feature vector. Table 3 shows the results of the FFNN classifier represented in the form of confusion matrix. In the confusion matrix the diagonal elements denote correctly classified PQDs, while the non-diagonal elements denote misclassification. All diagonal elements are averaged to calculate overall accuracy.

CLASSIFICATION OF MULTIPLE AND MULTISTAGE POWER QUALITY DISTURBANCES USING S-TRANSFORM AND FEED FORWARD NEURAL NETWORK

Table 3: Confusion Matrix of FFNN Classifier

Class	C1	C2	C3	C4	C5	C6
C1	20	-	-	-	-	-
C2	-	20	-	-	-	-
C3	-	-	20	-	-	-
C4	-	-	-	20	-	-
C5	-	-	-	-	19	1
C6	-	-	-	-	-	20

Inordertoevaluateandexaminetheperformanceofthedetectingalgorithm, a classification system technique is needed. In this research work Feed Forward Neural Network (FFNN) is used as a classifier. Table 4 shows the results of FFNN.

Table 4: Classification accuracy of FFNN with hidden layers

Class	PQDs	1 hiddenlayer	2 hiddenlayers
C1	Sag with Harmonics	100.00 %	100.00 %
C2	Swell with Harmonics	100.00 %	100.00 %
C3	Interruption with Harmonics	95.00 %	100.00 %
C4	Multistage Sag	100.00 %	100.00 %
C5	Multistage Swell	95.00 %	95.00 %
C6	Multistage Sag and Swell	100.00 %	100.00 %
	Overall Accuracy	98.33 %	99.17 %

X. CONCLUSION

In the S-Transform based multiple and multistage PQ disturbances detection and classification approach the normalized amplitude versus time vector is obtained from the S-Transform matrix clearly shows the behavior of PQ disturbance. The features extracted from the transformed signals are used for automatic classification of multiple and multistage PQ disturbances. The Parseval's Energy computed using the normalized amplitude found sufficient to categorize the PQ disturbances based on threshold values. The computational complexity and time of S-Transform is high which limits its application in real-time detection of PQ disturbances. The FFNN trained and tested using the Parseval's energy gives accuracy of 95% and above for individual disturbance and overall accuracy is more than 98%.

REFERENCES

- [1] C. L. Kuo, C. W. Liu, Y. C. Cheng, T. H. Huang, "Detection and Classification of Multistage Power Quality Disturbances Using S-Transform and Probabilistic Neural Networks", IEEE Transactions on Power Delivery, Vol. 24, Issue 1, pp. 292-301, Jan 2009.
- [2] S. Chandrasekaran, V. Sankaranarayanan, "Power Quality Disturbance Classification Using S-Transform and Adaptive Network-based Fuzzy Inference System (ANFIS)", IEEE Transactions on Power Delivery, Vol. 25, Issue 2, pp. 905-912, April 2010.
- [3] G. G. Messina, J. I. Yuz, L. A. N. Lorena, D. A. A. M. G. Monteiro, "Automatic Detection and Classification of Power Quality Disturbances Using S-Transform and Fuzzy C-Means Clustering", IEEE Transactions on Power Delivery, Vol. 26, Issue 4, pp. 2634-2641, Oct 2011.

CLASSIFICATION OF MULTIPLE AND MULTISTAGE POWER QUALITY DISTURBANCES USING S-TRANSFORM AND FEED FORWARD NEURAL NETWORK

- [4] Y. C. Cheng, C. L. Kuo, J. C. Wang, C. M. Huang, "Automatic Detection and Classification of Power Quality Disturbances Using S-Transform and Probabilistic Neural Network", IEEE Transactions on Power Delivery, Vol. 26, Issue 1, pp. 197-205, Jan 2011.
- [5] Y. J. Yu, J. S. Hsu, T. F. Wu, C. T. Su, "Power Quality Disturbance Detection and Classification Using S-Transform and Probabilistic Neural Network", IEEE Transactions on Power Delivery, Vol. 27, Issue 1, pp. 56-63, Jan 2012.
- [6] R. Kankale, S. Paraskar and S. Jadhao, "Classification of Power Quality Disturbances in Emerging Power System using S-transform and Support Vector Machine," 2021 IEEE 2nd International Conference on Electrical Power and Energy Systems (ICEPES), 2021, pp. 1-6, doi: 10.1109/ICEPES52894.2021.9699673.
- [7] R. Kumar, R. Kumar, S. Marwaha and B. Singh, "S-Transform Based Detection of Multiple and Multistage Power Quality Disturbances," 2020 IEEE 9th Power India International Conference (PIICON), Sonapat, India, 2020, pp. 1-5, doi: 10.1109/PIICON49524.2020.9112945.
- [8] Umamani Subudhi, Sambit Dash, "Detection and classification of power quality disturbances using GWO ELM", Journal of Industrial Information Integration, Volume 22, 2021, 100204, ISSN 2452-414X,
- [9] Dash, Sambit Supriya and Umamani Subudhi. "Multiple power quality event detection and classification using modified S-transform and WOA tuned SVM classifier." International Journal of Power and Energy Conversion (2019): n. pag.
- [10] Minh Khoa, Ngo, and Le Van Dai. 2020. "Detection and Classification of Power Quality Disturbances in Power System Using Modified-Combination between the Stockwell Transform and Decision Tree Methods" *Energies* 13, no. 14: 3623. <https://doi.org/10.3390/en13143623>

VOLTAGE SAG REDUCTION USING A UVTG-BASED DYNAMIC VOLTAGE RESTORER

Abstract

Unnecessary clash is caused through voltage dips or sags on both the utility and consumer sides. In order to correct voltage sag. In this Paper, a custom power Device (DVR) with voltage source converter (VSC) topology is used. A modified power device called a dynamic voltage restorer (DVR) is used to decrease power quality concerns in the electrical power system network and promote voltage stability. DVRs are normally installed in the delivery network between load feeders and sources. This study discusses a method of voltage sag correction unit vector template generation (UVTG)-based and a dynamic voltage restorer. The results are acquired following simulation with the MATLAB program.

Keywords: Dynamic voltage restorer, sensitive load, and voltage sag.

Authors

V.S. Karale

Assistant Professor
Department of Electrical Engineering
Shri sant Gajanan Maharaj college of Engineering
Shegaon, India.
vskarale04@gmail.com

Dr. S. S.Jadhao

Assistant Professor
Department of Electrical Engineering
Shri sant Gajanan Maharaj college of Engineering
Shegaon, India.
ssjadhao@ssgmce.ac.in

Dr. Sudhir R. Paraskar

Professor & Head
Department of Electrical Engineering
Shri sant Gajanan Maharaj college of Engineering
Shegaon, India.
srparaskar@ssgmce.ac.in

I. INTRODUCTION

The primary concept in today's power delivery systems is power quality. Poor power quality has a number of repercussions on energy consumers, including production loss, appliance damage, increased power losses, interference with communication lines, & so on. The basic purpose of electrical utility providers is to deliver continuous, constant-magnitude sinusoidal voltage to its customers [1,2]. To improve power quality, custom power devices are employed. Hingorani initially suggested customized power in 1995 [16]. Custom power (CP) is a term that refers to the usage of electronic controllers in power system networks. A few examples of specialist power units include the Distribution Statcom (D-STATCOM), Dynamic Voltage Restorer (DVR), and Unified Power Quality Conditioner (UPQC). Battery Systems (BESS), Distribution Series Capacitors (DSC), and Surge Arresters (SA), Uninterruptible Power Supplies (UPS), Solid-State Fault Current Limiters (SSFCL), Solid-State Transfer Switches (SSTS), and Static Electronic Tap Changers (SETC) are all examples of solid-state devices. Either in series, shunt, or a combination of the two connections are used to connect the CPD devices. Power systems ensure high-quality electrical power supplies, which calls for balanced, sinusoidal voltage and current waveforms. Additionally, the system's voltage level torque should be within a safe range, often within $100\pm 5\%$ of its rated value. The performance of the equipment is compromised if the voltage is greater or lower than this predetermined value. There is a requirement for voltage adjustment because when the voltage is low, the television's picture begins to roll and the induction motor's velocity is reduced to the square of the voltage. Today, the electric utility grid's focus on power quality is crucial. Voltage conflict at the PCC causes sensitive industrial equipment to malfunction, which results in the failure of grid component [5, 6]. For reducing this voltage disturbance and safeguard sensitive loads from it, dynamic voltage restorations are an effective solution. The voltage level on the system should also be within a secure range, often within $\pm 5\%$ of their rated value if the voltage is more or less than this precise value, performance of the voltage sag, which is the majority significant voltage disturbance. The VSC that add a series voltage into the line is known as a DVR. DVR have the ability to function as series active power filters. The UVTG control approach, which is DVR-based, is used to compensate for voltage sag in this paper.

II. DVR CONFIGURATION

A dynamic voltage restorer's main components are the insertion transformer, harmonic filter, VSC, and energy storage control [9].

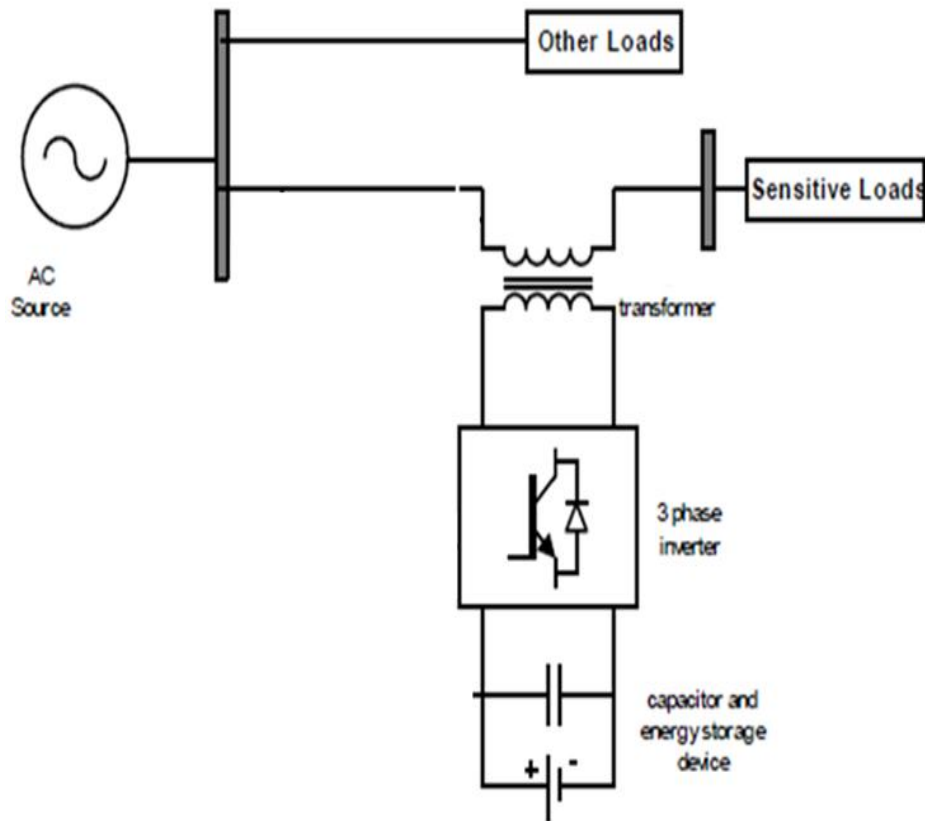


Figure 1: DVR Configuration

The DVR is a device that is associated in series to remove voltage sag. The dynamic voltage restorer solutions for the supply voltage issue by injecting a voltage series into the line, resulting in distortion-free voltage at the load terminal. The subsequent equation illustrates the series converters.

$$V_{\text{injected}}(\omega t) = V_{\text{Load}}(\omega t) - V_{\text{Source}}(\omega t) \quad (1)$$

$V_{\text{Injected}}(t)$, $V_{\text{Load}}(t)$, and $V_{\text{Source}}(t)$ are the voltage to be added, load side voltage, and genuine supply voltage of a series converter, respectively."Figure 1.shows the configuration of DVR. The DVR is separated into two sections: a) The power circuit and PI controllers, and b) Circuit that to be controlled. The main circuit i.e. Power is made up of a voltage source converter (VSC), a series linked booster transformer, a passive filter, and some storing energy devices. The DVR circuit is used to compute the responses of the control signal that should be injected from side to side DVR, such as amplitude, frequency, and phase shift. In response to this control signal, the main part of circuit is use for injection of voltage. To remain the load side voltage to susceptible loads within safe limits, the DVR compensates for voltage sag. The DVR is designed to eliminate voltage sag of varying magnitudes for varying durations. Because the delta-star transformer connection in the distribution system does not permit zero sequence voltage to pass through, only positive sequence voltage restoration and negative sequence voltage compensation are essential. The Voltage source Converter employs an insulated gate. i.e. Thyristors are used. It is fueled by an power source and uses an inverter to produce modified Sinusoidal voltage. The filter suppresses switching

harmonics and corrects the compensated voltage to be injected. An insertion transformer connected in sequence with the distribution line connects the DVR to the system. The three single phase insertion transformer is used to insert voltage into PCC that is not present. This study's major purpose is to adjust for both symmetrical and unsymmetrical voltage sags.

III.DC CAPACITOR SELECTION

The value of dc capacitance is selected on the basis of amount of transient energy required when the load varies. The energy stored in the capacitor is used to meet the energy demand of the load for a fraction of the power cycle.[18]

$$\left(\frac{1}{2}\right)\{C_{DC}(V_{DC}^2 - V_{DC1}^2)\} = 3V_f I_f \Delta t(4)$$

Where V_{DC} is the rated voltage, V_{DC1} is the voltage drop allowed during the transient, t is the time required for support, and C_{DC} is the DC bus capacitance.

IV. CONTROL ALGORITHM AND METHDOLOGY

In this part the suggested control technique for the DVR. As demonstrated in figure. 2, the UVTG technique is employed to regulate the DVR in the controlled block diagram DVR in order to provide a reference voltage signal.[2][3][4]

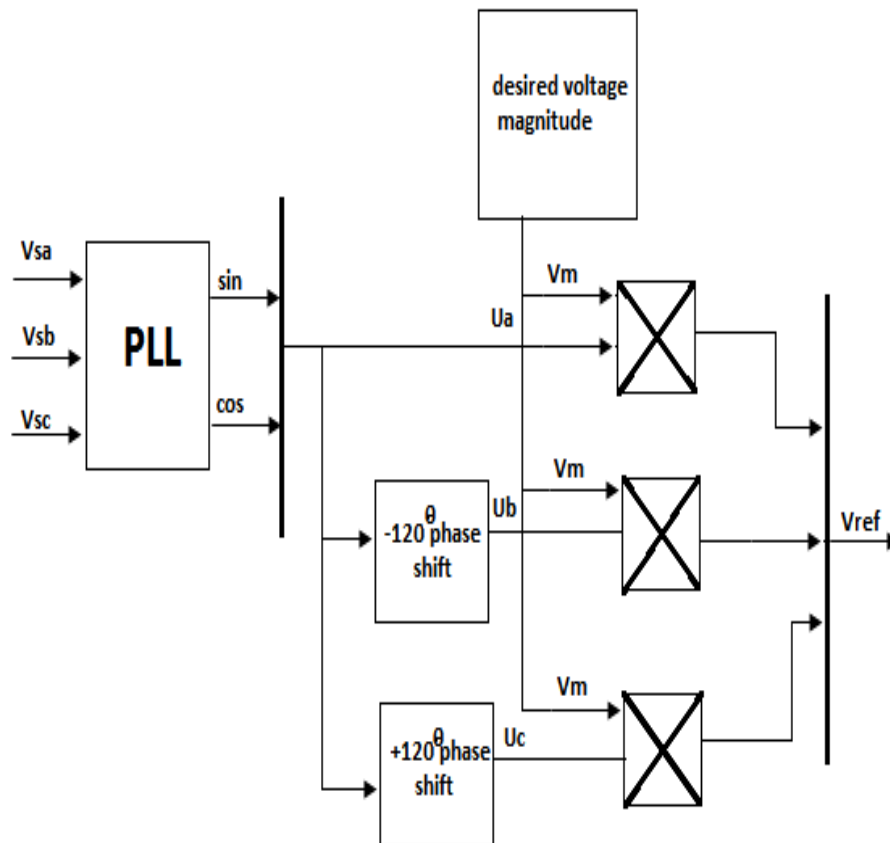


Figure 2: Shows a Overall Control Algorithm

Voltage between the PCC and the load side voltage is controlled by the series filter component (DVR) such that it is balanced, distortion-free, and maintains the appropriate range. The input voltage may be not proper, or power quality problems may exist on the system. To produce the controlled voltage signal by UVTG, the input supply voltage is measured and multiplied by gain equal to $1/V_m$ (V_m is the maximum value of the reference voltage). The PLL is used to coordinate the supply voltage. The equation below shows how to use UVTG and a PLL to generate a three-phase voltage reference signal for a series APF. Three-phase voltage is distorted. Voltages are sensed and sent through a PLL, which generates two quadrature unit vectors (\sin_{wt} and \cos_{wt}). The in-phase sine and cosine outputs of the PLL are used in equation to compute the supply in phase, 120° displaced three unit vectors (u_a, u_b, u_c) as follows:

$$\begin{bmatrix} u_a \\ u_b \\ u_c \end{bmatrix} = \begin{bmatrix} 1 & 0 \\ -1/2 & -\sqrt{3}/2 \\ -1/2 & \sqrt{3}/2 \end{bmatrix} \begin{bmatrix} \sin \theta \\ \cos \theta \end{bmatrix} \quad (2)$$

The three-phase reference voltages are obtained by multiplying with U_a, U_b, U_c by the needed peak value of the phase voltage (V_m).

$$\begin{bmatrix} V_{la} \\ V_{lb} \\ V_{lc} \end{bmatrix} = V_m \begin{bmatrix} u_a \\ u_b \\ u_c \end{bmatrix} \quad (3)$$

338 Volts is the required maximum range of voltage under consideration. The calculated voltages from the reference voltages from Equation (2) are then feed into the comparator device, together with the sensed three phase load voltages. In this way error signal is generated.

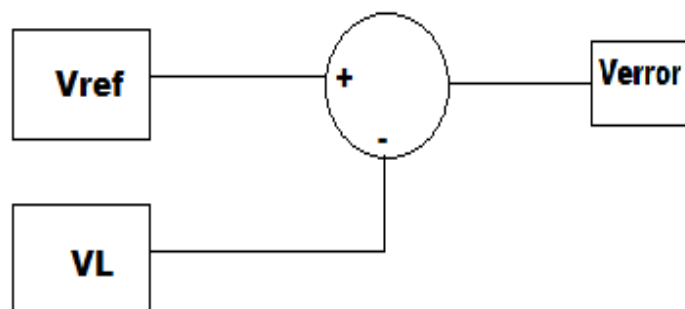


Figure 3: Error signal generation

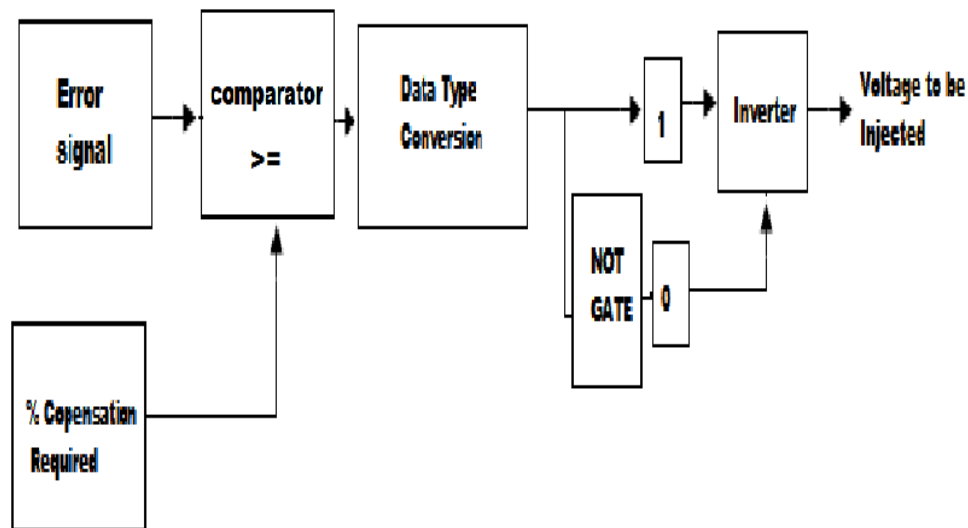


Figure 4: Creating pulses to triggered the Gate

Above figure shows the creation of pulses from an error indication as well as the required corrected to be needed. The error signal is compared to the needed % correction, and the output data type is changed with respective required logic. The consistent operation of the signal generates the required pulses for the inverter, which get required correction in the system voltage.

V. CONTROL ALGORITHM

This controlled algorithm perform the operations like voltage sag detection , various distortion, and harmonics in the system; calculated the voltage correction; generating pulses for triggering the inverter to the PWM-based DC-AC inverter; correcting any anomalies in the series voltage injection; and terminating the trigger pulses when the event has passed. The controller can also be used to convert the DC-AC inverter into rectifier mode and charge the capacitors in the DC energy link in the absence of voltage sags. The control strategy proposed for the system is based on a comparison of a voltage reference and the measured terminal voltage (V_a , V_b , V_c). When the supply falls below a particular threshold, voltage sags are detected at 20% of the reference voltage. The error signal is used as a modulation signal to generate a commutation pattern for the voltage source converter's power switches (IGBTs). The commutation pattern is formed using The sinusoidal pulse width modulation (SPWM) technique; the modulation controls voltages. The phase locked loop circuit is intended to produce a single alternating current wave In-phase with the system voltage.

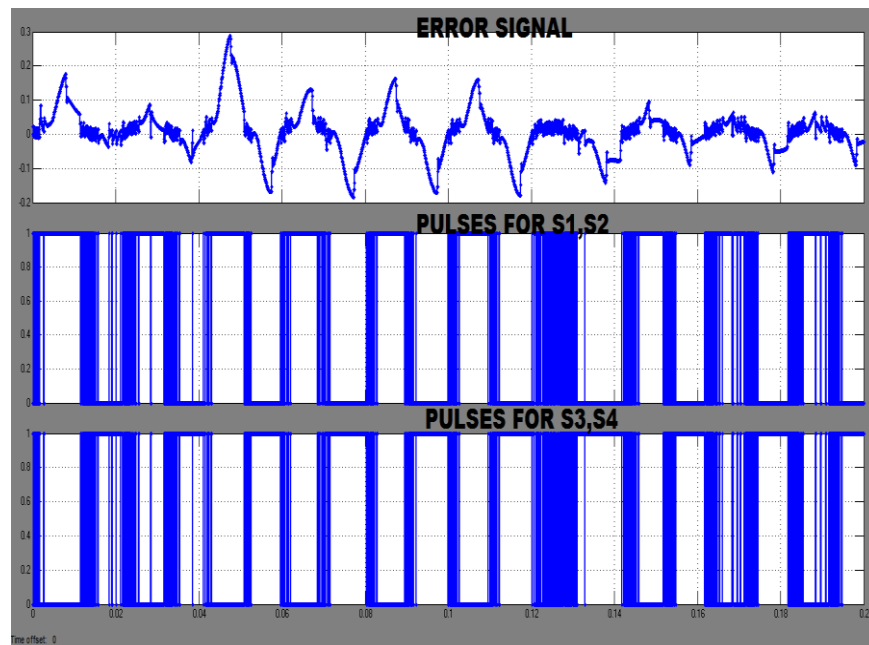


Figure 5: Required Pulses for triggering

The comparator creates switching waveform for Series filters. It generates the essential signals for swathing to convert the voltage signal at system to the suitable reference voltage. Consequently, the ripple filter voltage applied to the series transformer effectively eliminates both balanced and unbalanced voltage sags within the power supply.

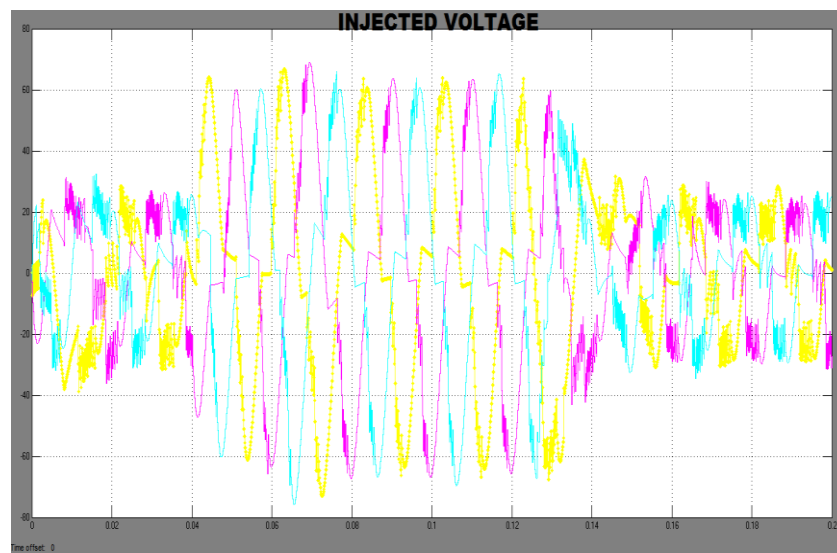


Figure 6: Output of transformer

Above displays the voltage signal that will be inserted in series with the load voltage signal. The injected voltage is the somewhat sine wave voltage induced by winding inductance of transformer.

VI. RESULTS AND SIMULATION MODELLED

Simulation and results for DVR voltage sag correction using a proposed technique is approach. The UVTG control technique was used to evaluate two situations for the DVR, which are listed below using MATLAB software.

- 1. Mitigation of 20% Voltage sag from all three Phases:** Sag is usually caused by faults or the start of a sudden significant load. The system under consideration as follow.

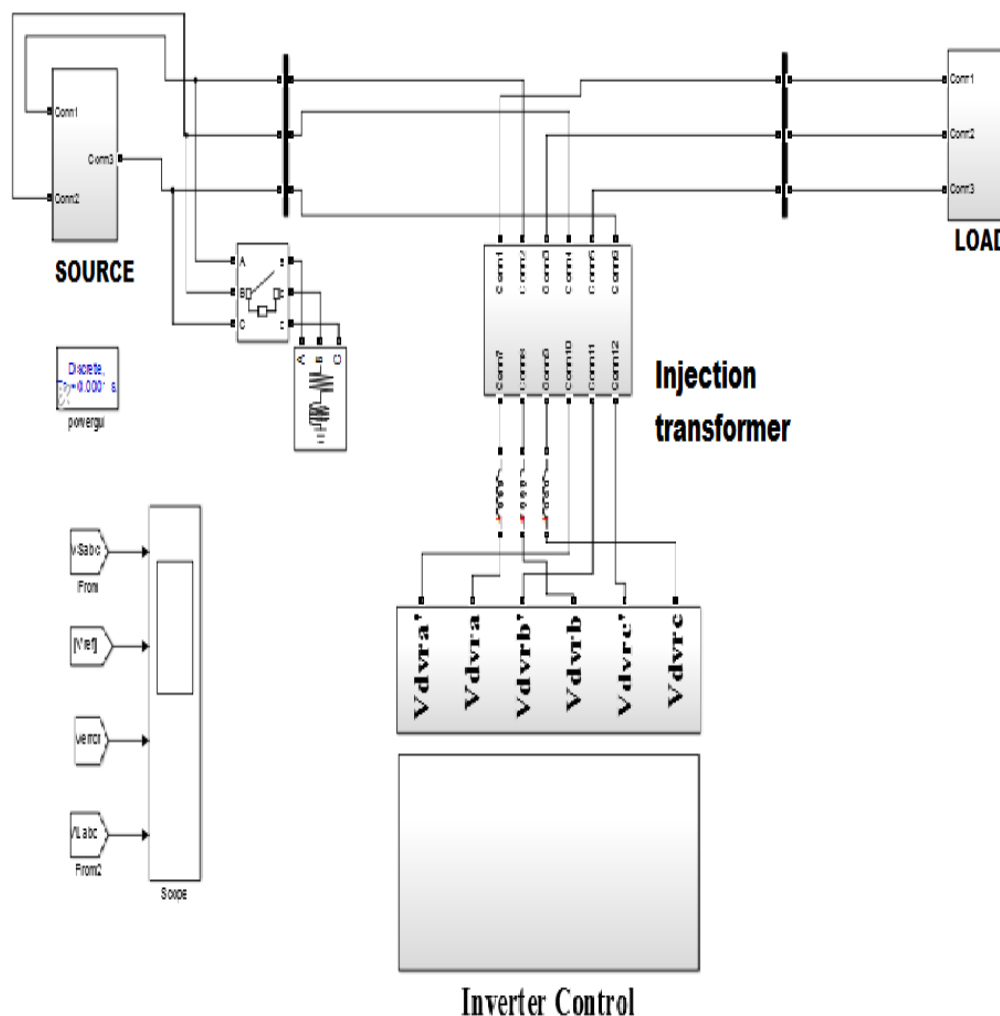


Figure 7: System Under Consideration

The below figure shows the results of 20 percent supply balance voltage sag developed in every phases due to addition of non linear load at 0.04 Second and reduce at 0.12 second displayed in below results. The DVR is in operation and insert the required sag voltage during the disturbance when the supply voltage sag occurs at 0.04 second.

VOLTAGE SAG REDUCTION USING A UVTG-BASED DYNAMIC VOLTAGE RESTORER

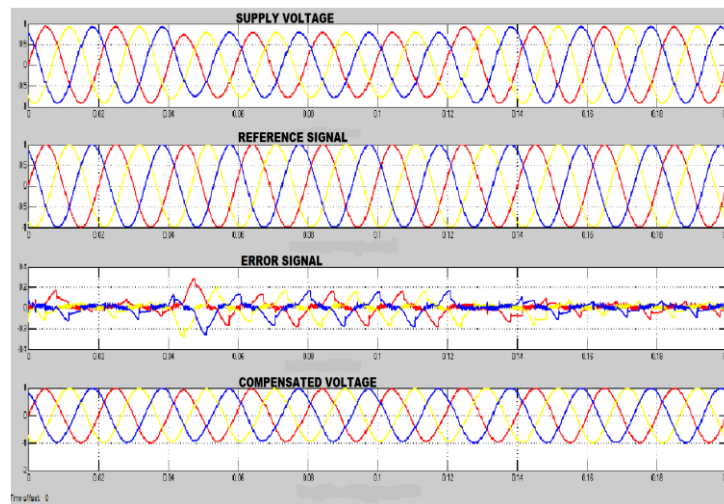


Figure 8: Case I simulation and results are shown

System Voltage	Sag	Inserted voltage	Mitigated voltage
415.00Volts	0.2 per unit	0.2	1 per unit

Table 1: Case I Observed Output

2. 25% Voltage sag in three phases:

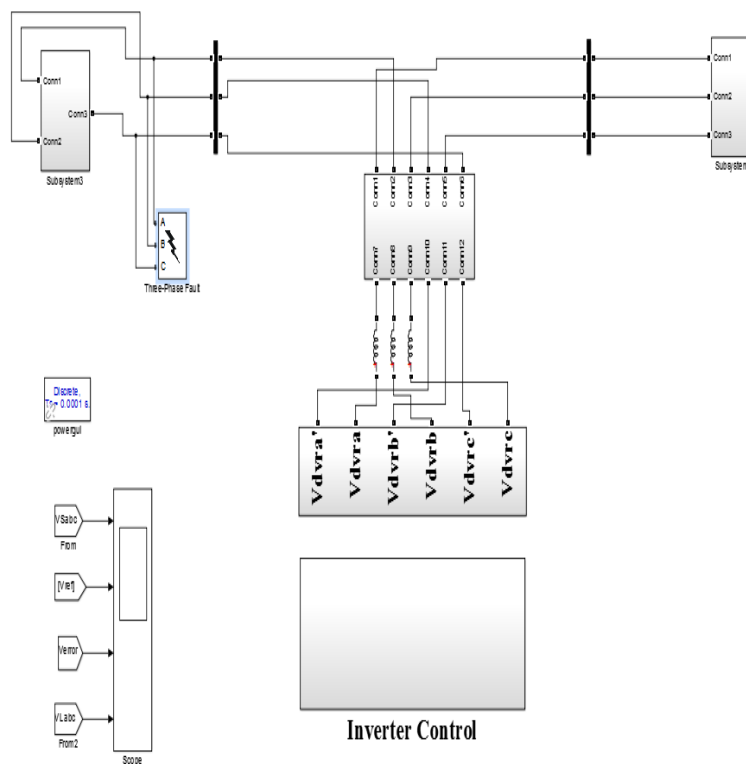


Figure 9: System Under Study

The below figure shows that a 25 Percent Source voltage sag is developed by a LLL-G Fault for the duration of 0.08 second is given in the figure. When the supply voltage reduces, the DVR comes into the actions and compensate the required voltage.

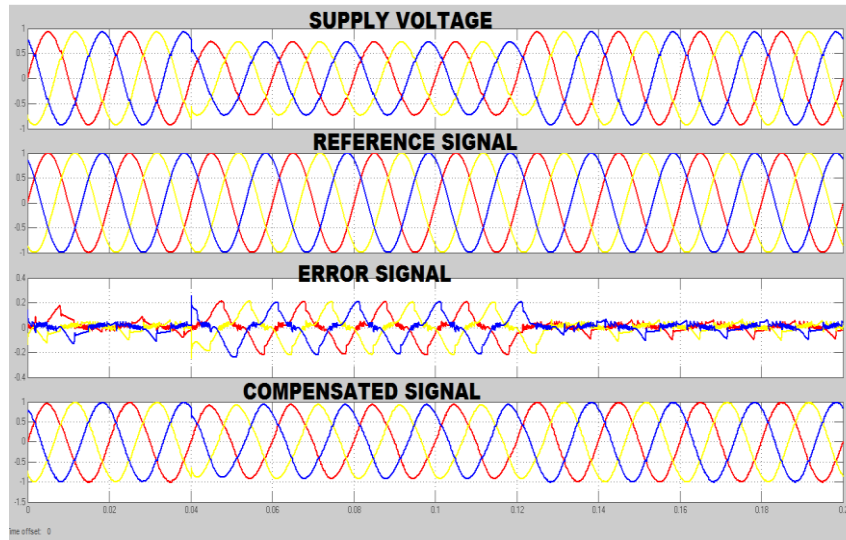


Figure 11: Signals of simulated results.

System Voltage	Sag	Inserted Voltage	Compensated voltage
415Volts	0.25 per unit	0.125×2	1 per unit

Table 2: Case II Observed Output

3. **25 Percent sag compensation in R phase:** The below figure shows that 25 percent sag is developed by L-G faults for the duration of 0.08 Second, then the DVR comes into the action and will inject the required magnitude when sag happened at 0.04 second

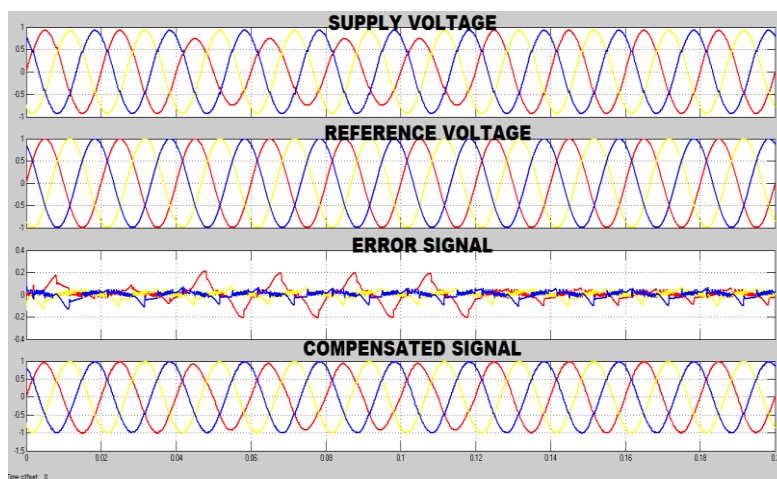


Figure 12: waveform of Results 3.

System Voltage	Sag	Inserted voltage	Compensate Voltage
415.00Volts	0.25 per unit	0.125*2	1 per unit

Table 3: Output Seen It is demonstrated in both cases that the voltage injected by the inverter equals 1- (Error Voltage) = Sag in per Unit

VII. CONCLUSION

The designing and MATLAB results of a DVR is describe. A projected control algorithm for DVR based on UVTG. The proposed control approach was put to the check using MATLAB models. The results show that the DVR performs adequately in terms of minimizing Power Quality disturbances. The Observations also disclose that the DVR adjusts prompt to sags and has immense voltage directive. The DVR can effortlessly handle various situations of disturbances and compensate the essential voltage component to swiftly rectify any cause in the source voltage for clearing the power quality disturbances.

REFERENCES

- [1] Rosli Omar and Nasrudin Abd Rahim "Mitigation of voltage sag/swell by using DVR" ARPN Journal of Engineering and Applied Sciences, vol. no 4, June 2009.
- [2] Bhim Singh and venkateswarlu.P "A simplified control algorithm for three-phase , four wire unified power quality conditioner" Presented at journal of power electronics ,vol no.1, January 2010
- [3] S. N. Gohil, M.V.Makwana, K.T. Kadivar,G.J.Tetar "Three phase unified power quality conditioner(UPQC) for power quality improvement using UVTG Technique" 2013 International conference on renewable energy and sustainable energy [ICRESE'13].
- [4] B.Singh, a chandra and k al haddad "review of active filters for power quality improvement" IEEE trans. Industrialelectronics,vol 46, No 5,pp.960-97, oct. 1999
- [5] IEEE Std. 1159 – 1995, "Recommended Practice for Monitoring Electric Power Quality".
- [6] Vijay Karale and Saurabh jadhao "voltage sag mitigation using dynamic voltage restorer" proceeding of 2nd international conference on innovative in electrical & electronics engineering (ICIEE)., No.184, Aug 2015.
- [7] P.Boonchiam and N. Mithulananthan, Thammasat "Understanding of Dynamic Voltage Restorers through MATLAB Simulation," Int. J. Sc. Tech., Vol. 11, No. 3, July-Sept 2006.
- [8] J. G. Nielsen, M. Newman, H. Nielsen,and F. Blaabjerg, "Control and testing of a dynamic voltage restorer (DVR) at medium voltage level," IEEE Trans.Power Electron., vol. 19, no. 3,p.806, May 2004.
- [9] Ghosh and G. Ledwich, "Power Quality Aamir Hanif, Mohommad Ahmed Choudhary,and Tahir Mehmood "Feed-Forward Control Strategy for the VSC of DVR for Smooth and Clean Power Flow to Load".
- [10] Hideaki Fujita and Hirofumi Akagi, "The Unified Power Quality Conditioner", IEEE transaction on power electronics, VOL. 13, NO. 2, MARCH 1998
- [11] H. Awad, J.Svensson, M. Bollen, "Mitigation of Unbalanced Voltage Dips Using Static Series Compensator", IEEE Trans. On Power Elec., Vol. 19, No. 13, May 2004
- [12] Hochgraf, R. Lasseter, "Statcom controls for Operation with Unbalanced Voltages", IEEE Trans. On Power delivery, Vol. 13, No. 2, April 1998.
- [13] Gunther, E.W., Mehta, H.: A survey of distribution system power quality. In: IEEE Trans. on PowerDelivery, vol.10 (1995), No.1, Jan.1995, pp.322-329.

- [14] IEEE recommended Practices and Recommendations for harmonics Control in Electric Power Systems. In:IEEE std.519, 1992.
- [15] Kotwal, C., Pillai, G. N., Gupta, H. O.: Modeling and Simulation of Different Topologies for VSI Based Static Synchronous Series Compensator. In: JEE, Vol.10(2010), Edition-4.
- [16] H. Hingorani “Introducing custom power” IEEE spectrum, vol.32 no.6,June 1995 p 41- 48.
- [17] Bhim Singh ,Amrish Chandra And Kamal AL-Haddad “Power quality problems and mitigation techniques” Published by 2015 John Wiley & Sons,Ltd

DISCRIMINATION OF INTER-TURN FAULTS FROM MAGNETIZING INRUSH CURRENT IN TRANSFORMER: A WAVELET TRANSFORM APPROACH

Abstract

To distinguish the magnetizing inrush current and internal fault accurately & quickly is a crucial issue in the transformer protection. .. This paper describes a novel and simple technique to discriminate the magnetizing inrush current and inter-turn fault using the wavelet transform avoiding rigorous mathematics. This method is independent of setting any threshold for discrimination amongst these, and capable of detecting interturn short circuit involving few turns also, which is otherwise very difficult to detect. With a thorough explanation of the proposed criterion, practical results for the specially constructed transformer are shown. The difference between the two-peak amplitudes of wavelet coefficients in a given band is used to build a discriminating function for feature extraction. This differentiation will help in the creation of an automatic detection system that will provide information to anticipate the failure in advance and allow the appropriate corrective actions to be made to decrease downtime and avoid outages.

Keywords: Inter-turn fault, Magnetizing inrush current, wavelet transform

Authors

P.R. Bharambe

Assistant Professor
Department of Electrical Engineering
Shri Sant Gajanan Maharaj College of
Engineering
Shegaon, Maharashtra, India

Dr. S. S. Jadhao

Associate Professor
Department of Electrical Engineering
Shri Sant Gajanan Maharaj College of
Engineering
Shegaon, Maharashtra, India

Dr. S. R. Paraskar

Professor & Head
Department of Electrical Engineering
Shri Sant Gajanan Maharaj College of
Engineering
Shegaon, Maharashtra, India

I. INTRODUCTION

The transformer, an important part of electric power systems, is crucial to the power system's secure operation. Due to its straightforward operating principle and sensitivity, differential protection has long served as the transformer's primary method of protection [1],[16]. How to distinguish a magnetising inrush from an internal failure, nevertheless, is a key differential protection problem. The traditional method uses the second harmonic component of differential currents to limit the differential relay's operation so as to prevent tripping during conditions of magnetising inrush. [2].

It is commonly known that this strategy falls short in various ways when it comes to protecting modern power transformers. High performance relays are also necessary for the modern power system, particularly in terms of operating speed. The peaked wave characteristics of the transformer core's asymmetric saturation are also present in the magnetising inrush. These features enable a new field of investigation for increasing the relays' working speed by identifying magnetising inrush [15].

The power industry is becoming more and more regulated in the modern world. There is fierce competition because there are more utilities providing power. Customers want a "Good quality" of electric supply. Therefore, it is crucial in this situation to reduce the frequency and length of unwelcome distribution transformer outages.

Since the second harmonic component may also be introduced during an internal fault due to a variety of other factors, such as current transformer saturation or the presence of a shunt capacitor, it is no longer possible to distinguish between an internal fault and a magnetising inrush current by looking for the presence of a second harmonic component in the inrush current [2], [10].

Transformer inductance during saturation, flux derived from the voltage integral, and differential current are examples of earlier work on transformer protection. Fuzzy logic and ANN are two recent methodologies that have been utilised. Additionally, a few methods have been used to detect internal defects and the magnetising inrush [16],[8]. For this, a system based on microprocessors and modal analysis was deployed as a tool. In [16], the discriminating factor is the active power coming into the transformer, which is nearly zero in the event of energization.

A wavelet-based system is employed in [11]. For the study and feature extraction of power system transients, a wavelet-based signal processing technique is useful [2]. There have been reports of the technique's use in data compression, protection, study of power quality issues, fault detection, and power quality assessment.

An innovative wavelet-based technique is put out in Paper [11] to detect inrush current from internal problems and identify it. The asymmetrical magnetization that is unique to the inrush is described by the second harmonic component. The wavelet transform idea is first applied. It is described how wavelets' ability to have multiple resolutions in time and frequency allows for accurate transient component time location while also preserving data on the fundamental frequency and its lower order harmonics, making it easier to spot transformer inrush currents. Using a data window smaller than half a power frequency cycle,

the approach extracts the wavelet components present in the line currents to detect inrush currents. The findings demonstrate that the suggested method can provide the desired responses and can be applied as a quick, accurate way to distinguish between inrush magnetising and power frequency issues.

In this study, a wavelet-based method for identifying inrush current and differentiating it from internal defects is devised. The data from the controlled studies were gathered in the lab using a specially constructed single-phase transformer. A wide range of potential failure scenarios on the transformer's primary and secondary windings were purposefully introduced in these controlled testing. For reaching the goal, a schematic algorithm is created; the suggested scheme does not call for any threshold settings.

II. WAVELET TRANSFORM

The wavelet transforms associated with fast electromagnetic transients are typically non-periodic signals, which contain both high-frequency oscillations and localized impulses superimposed on the power frequency and its harmonics. The entire frequency spectrum may be impacted if signals are altered in a specific localised time instant. The short-time Fourier transform (STFT) is employed to lessen the impact of non-periodic signals on the DFT. It presupposes local periodicity within an ongoing time window of translation..The process for implementing a Discrete Wavelet Transform is shown in Fig. 1, where S represents the original signal and LPF and HPF stand for low-pass and high-pass filters, respectively. An initial signal is split into two portions, each with a frequency bandwidth of half, and delivered to the LPF and HPF in the first step. The output of the LPF is then further reduced by halving the frequency bandwidth before being delivered to the second stage. This process is repeated until the signal has been divided into its component parts to the predetermined level. According to Nyquist's theorem, the original signal could only contain frequencies up to $F_s/2$ Hz if it were sampled at F_s Hz. The first detail, number 1, would show this frequency at the high pass filter's output; similarly, detail 2, number 2, and so on, would show the band of frequencies between $F_s/4$ and $F_s/8$. The frequency levels of the wavelet function coefficients are shown in Table 1. In this research, the sampling frequency is assumed to be 10 kHz.

Table 1: Frequency Levels of Wavelet Functions Coefficients

Decomposition Level	Frequency Components
D1	5000-2500
D2	2500-1250
D3	1250-625
D4	625-312.5
D5	312.5-156.25
A5	0-156.25

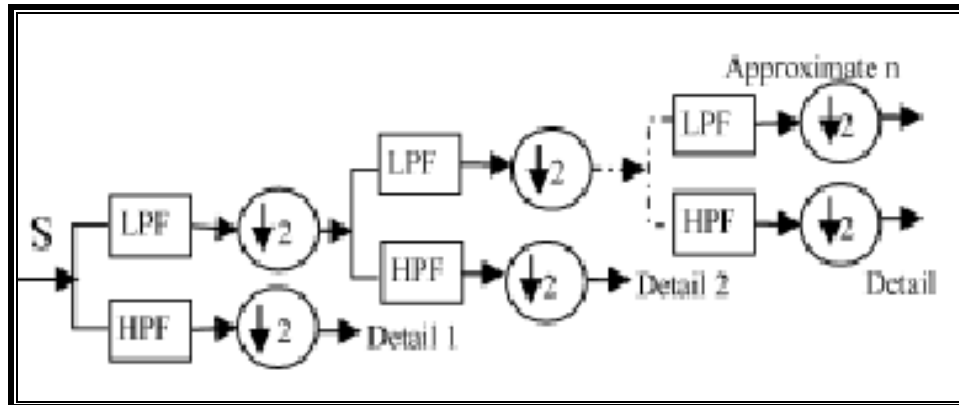


Figure 1: Implementation of DWT

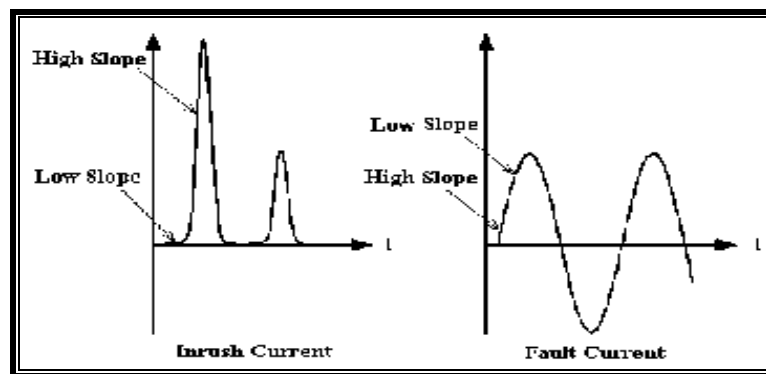


Figure 2: Different Behavior of Fault and Inrush Current

III. PROPOSED METHOD

Figure 2's waveform of the inrush differential current makes it obvious that its initial slope is less than that of the fault differential current, which grows after lowering initially. High frequency components are present when the slope has a high value. These characteristics are depending on the different types of current and transformer parameters and are independent of the associated power supply. The initial slope of the differential current owing to fault and that due to magnetising inrush current differ significantly from one another, and this difference has been utilised to distinguish between inter-turn fault and magnetising inrush current. According to the suggested approach for internal fault (in one scenario, an inter-turn short circuit), the high frequency's initial amplitude is high and then it gradually drops. Therefore, as illustrated in Figure 3, high frequency components are recorded in the first two levels, D1 and D2. In contrast, in an inrush current, the high frequency component's initial amplitude is lower and then grows. Therefore, nothing can be seen at the first two levels, D1 and D2, whereas at D3 (see Fig. 4), a significant amplitude can be noticed.

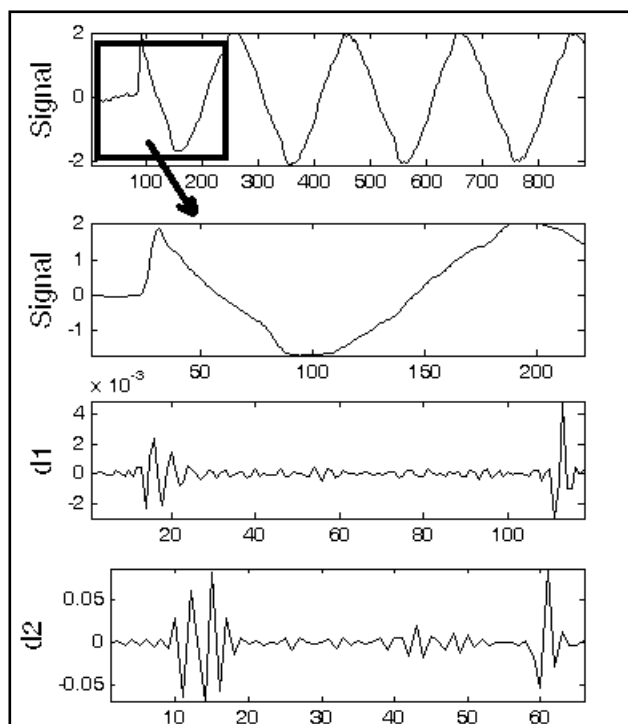


Figure 3: Illustration of Wavelet Decomposition of Fault Current

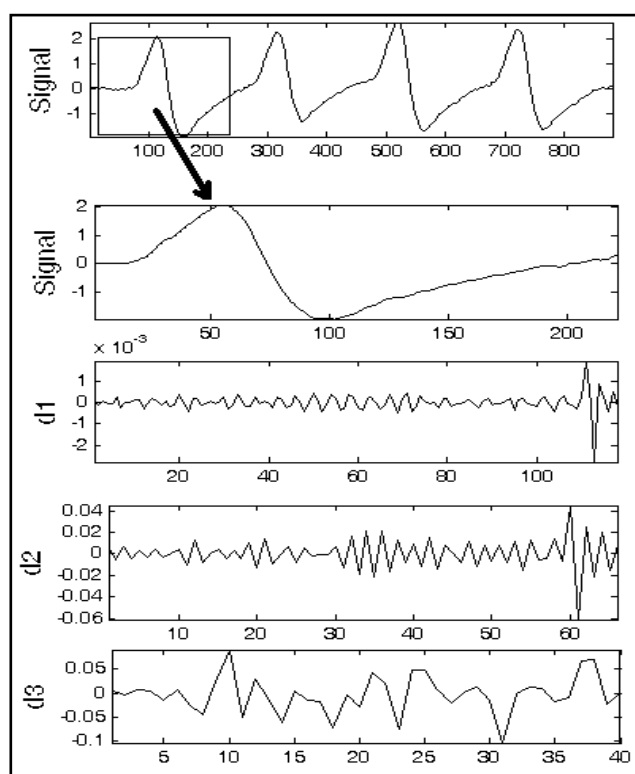


Figure 4: Illustration of Wavelet decomposition of Inrush Current

IV. EXPERIMENT SETUP

A specially constructed 220V/220V, 2KVA, 50Hz, single-phase transformer with externally accessible taps on both the primary and secondary to introduce faults is used in the experiment setup. There are 272 turns between windings.

The secondary's load is made up of Induction motor and static components. The voltage and current readings were recorded using Tektronix Instruments' data acquisition card. 10,000 samples per second was the sample rate used to record these signals.

On the custom-built transformer, several inrush current and inter turn short circuit events were staged by changing the parameters, which drastically altered the properties of these currents. The voltage angle at the time of switching and the residual core flow are these parameters. The effects of the number of shorted turns on the primary or secondary, and load conditions are taken into account when staging various inter turn short circuit instances. The custom-built transformer was used for the ensuing the following tests.

- The primary current was measured in an unloaded state to ensure good health.
- By keeping four percent (10 turns) of the primary turns short-circuited while under load, the transformer was powered up and differential current was acquired.
- The identical process was carried out again for secondary winding short circuits.

On the specially made transformer, the suggested algorithm was put to the test. The experiment setup is depicted in Figure 5

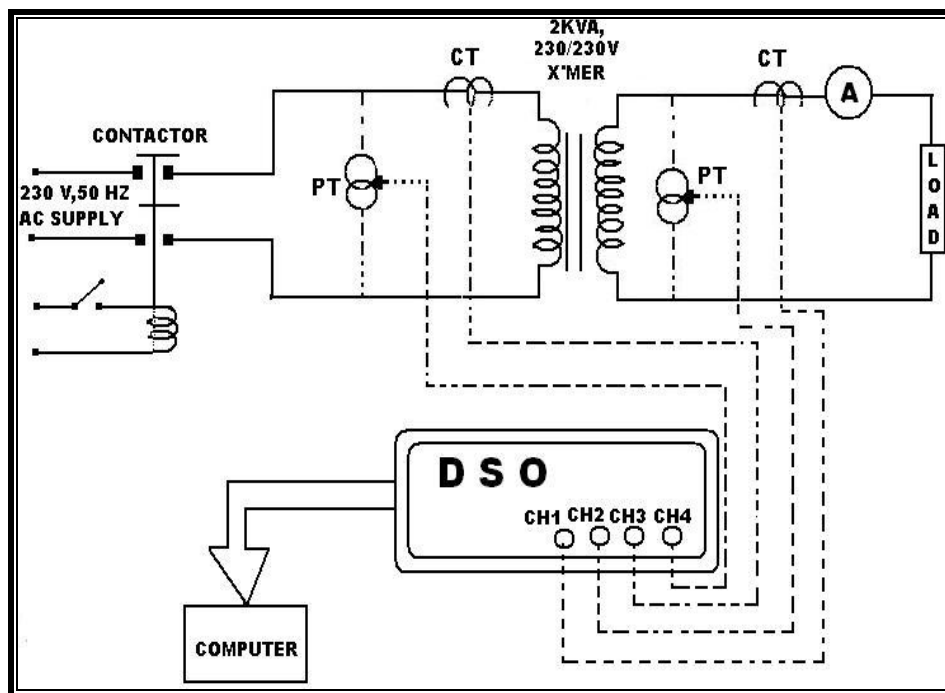


Figure 5: Experimental Setup

V. RESULT AND DISCUSSION

Figure 6 displays the differential current (labelled "Signal") caused by an inter-turn short circuit in a primary winding with a 4% winding that is close to neutral, together with their specific coefficients from Wavelet Transform up to D5 level. In this case, the desired wavelet coefficients are obtained using the daub- 4-mother wavelet.

The detailed coefficients of levels 1 to 5 of decomposition are shown in this image as d1 through d5, with level 5's estimated coefficients shown as a5. The absolute value of d5 is displayed at the bottom of this figure. Below is a full explanation and interpretation of Figure 6:

- The figure's 'Signal' represents the original differential current signal that was recorded using the data acquisition technology previously mentioned. The fault starts at sample number 39 (about), and it is indicated in the graphic as "x." The first negative differential current peak, indicated by 'Y' in the picture, is seen at sample number 50.
- Peaking of the wavelet coefficient is seen in decomposition level 'd1', roughly from samples 39 to 64. The magnitude of these oscillations then starts to decay.
- At the 'd2' level, the sudden shifts in the signal during samples 39 to 64 are more clearly visible, and sample number 45 has the highest positive peak.
- In 'd3' level, high frequency components that were present in d2 are filtered off. The apex of the waveform was once more seen at sample number 45.
- At the d4 level, sample 39 exhibits the first positive peak with a magnitude of 0.3571 while sample 50 exhibits the first negative peak with a magnitude of -0.3651. This is a close representation of the 'x'-'y' curve.
- The first positive peak in the d5 level is seen at sample 39 and has a magnitude of 0.4041, while the first negative peak is seen at sample 59 and has a value of -0.5657. The slopes of faults and inrush currents can therefore be measured precisely at the d5 level.

As a result, the first two successive peak values following the fault moment are the best approximations for the initial slope changes in the fault and inrush current, taking the absolute value of |d5| as indicated in the figure.

Consequently, the following can be used to select the discriminating function for fault and inrush current:

$$\Delta M\{d5\} = \{First\ Peak\ after\ fault\ initiation\} - \{Second\ Peak\ after\ fault\ initiation\} \quad (1)$$

$$\Delta M\{d5\} = A - B \quad (2)$$

Hence, for inrush current $\Delta M < 0$ and for fault current $\Delta M > 0$.

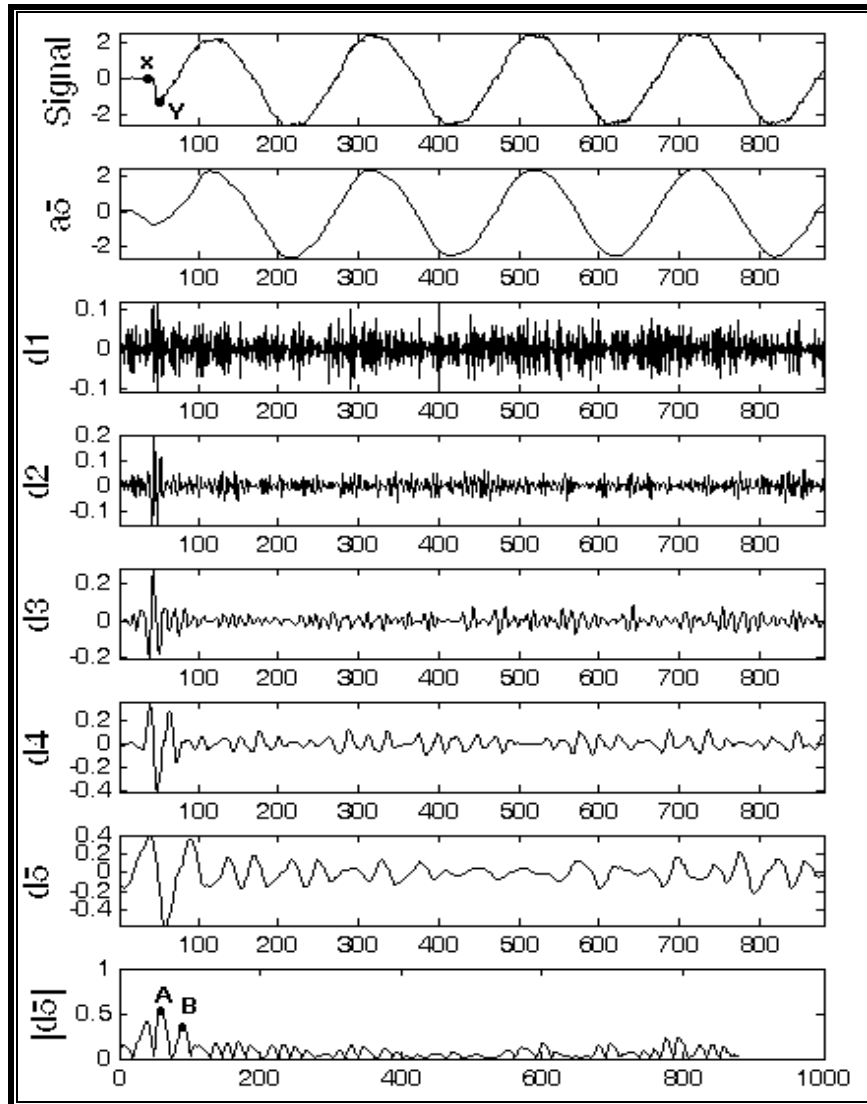


Figure 6: Wavelet Decomposition of Differential Current for Fault in Primary Winding

Figure 7 displays the wavelet decomposition of the differential current measured during the interturn fault of the secondary winding's 10 turns. Similar high frequency components were seen in primary winding faults.

For high initial slope of fault current, high frequency components were seen at decomposition level d1-d4. As was previously discussed, as the fault develops, the slope of the fault current gradually diminishes. High frequency components with large amplitudes at the time of the fault and fading trends afterwards are clearly discernible from time-frequency localization in the d1-d3 levels.

Filtration of this high frequency up to the d5 level produces some really intriguing fault and inrush current discrimination criteria. The bottom of this illustration displays the coefficients of the d5 waveform's absolute value. The first two peaks after the disturbance in this have amplitudes A and B. The figure shows that for the inter-turn fault, $A > B$. The quarter cycle can be used to issue commands in the event of an $A > B$ journey. Typically, the

characteristics required for diagnosis appear in the high frequency range rather than the lower frequency range.

Figure makes clear that the wavelet coefficients in D5 have bigger amplitudes than those in D1 through D4. Many wavelets were tested as analysis wavelets, but Daubechies 4 (Db4) ultimately provided reassuring and distinctive properties.

The size of the two successive peaks A and B likewise exhibits the same relationship, namely, $A > B$.

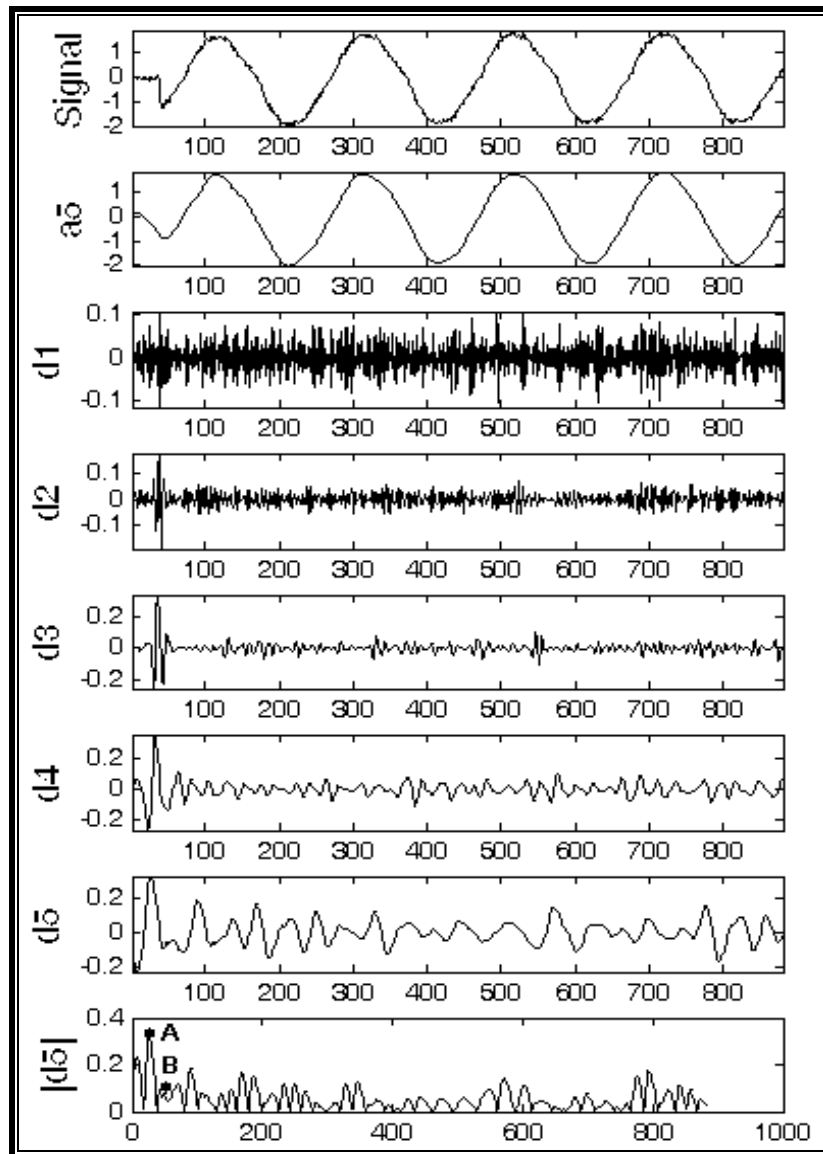


Figure 7: Wavelet Decomposition of Differential Current for Fault in Secondary Winding

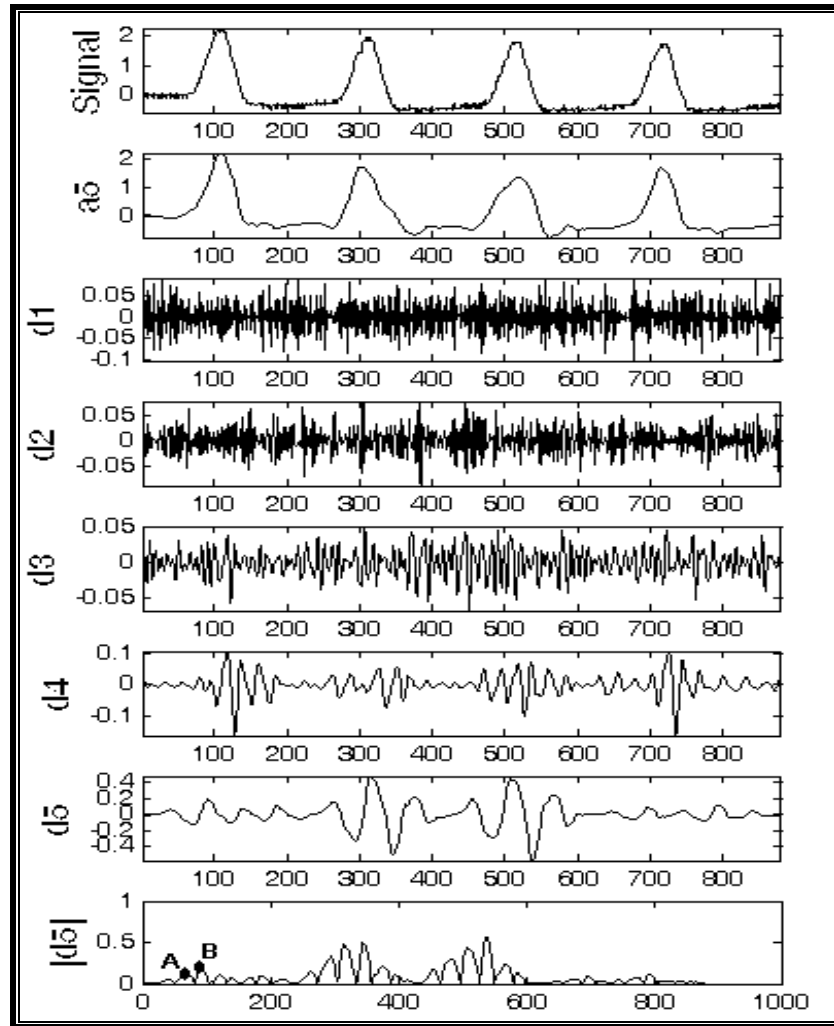


Figure 8: Wavelet Decomposition of Differential Current During Inrush

Despite having a similar amplitude, inrush current differs from fault current in behaviour or features. Low slope inrush current begins and increases quickly after. In fig. 8, this trait is illustrated. The signal for the acquired inrush current is divided into five levels. As was the case with the inter-turn fault, there was no peaking at the initial instant in the d1-d2 level. However, because high slope follows low slope in inrush current, high frequency oscillations can be observed in these levels. As a result, in contrast to the preceding situation, repeated oscillations are reported at the d4 level that match the steep inrush current slope. The consecutive peaks A and B can be found from the d5 and $|d5|$ and compared. It should be observed that $A > B$ for inrush.

In line with the prior discussion, the proposed technique does not call for a threshold value to distinguish between the transformer's magnetizing inrush and inter-turn failures. The following is a presentation of the discrimination algorithm:

- Under the aforementioned events, measure the differential current with an acceptable sample frequency.

- Use the MRA method to get the discrete wavelet transform up to the fifth level of decomposition.
- Obtain $|d5|$
- Discover $|d5|$'s first two peak values, A and B.
- Determine $M=A-B$.
- If M is negative, inrush current is present.
- If M is positive value, it is fault condition and will sound an alarm or trip signal.

The wavelet decompositions of fault and inrush currents at various switching instants are shown in Figures 9 and 10.

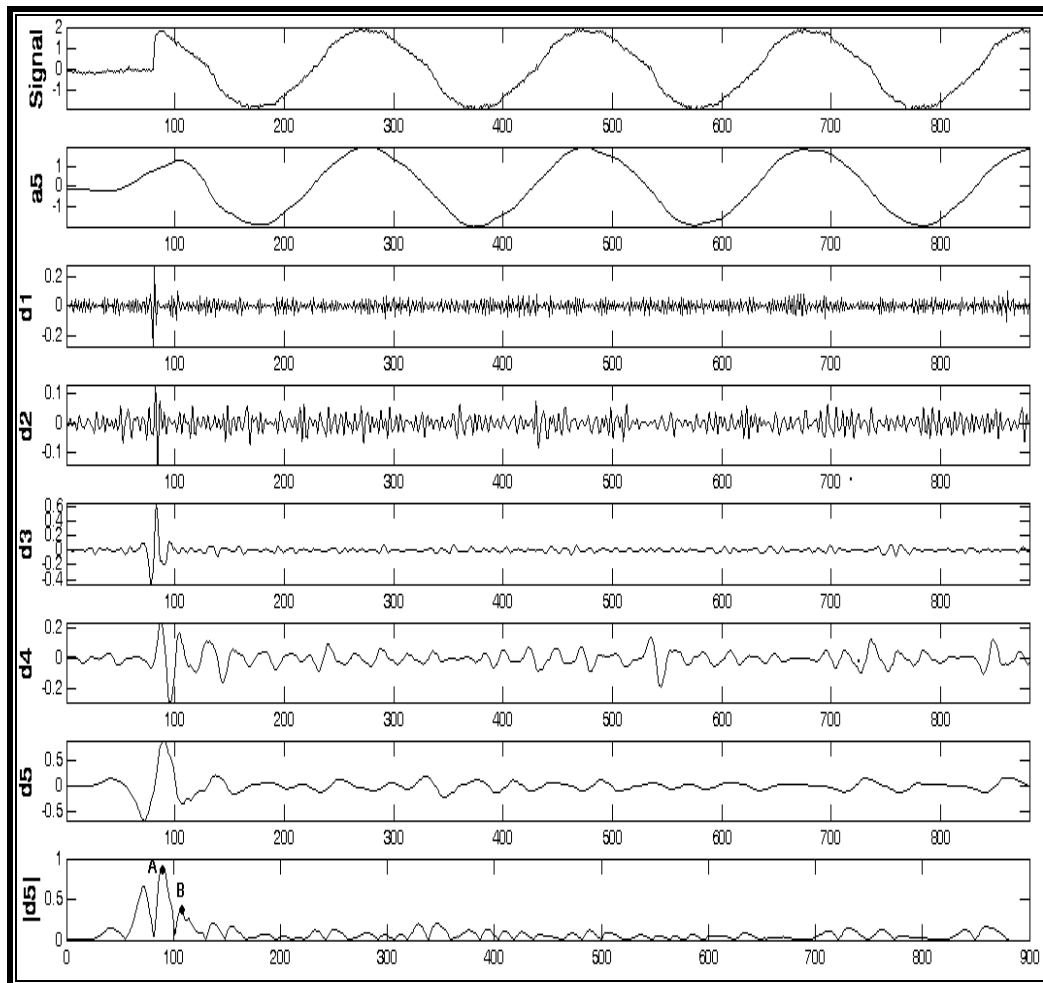


Figure 9: Wavelet Decomposition of Differential Current During Fault

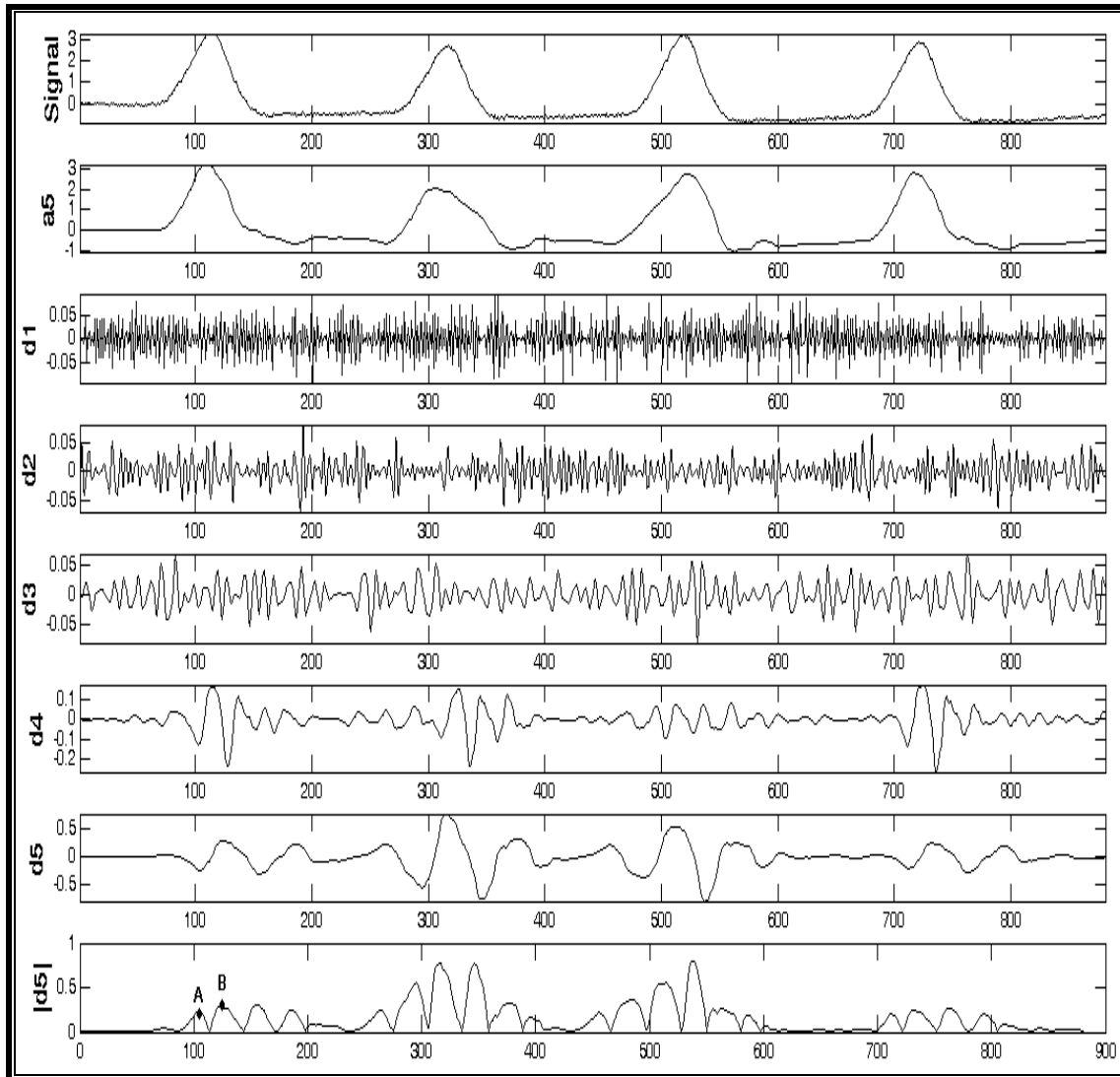


Figure 10: Wavelet Decomposition of Inrush Current

VI. CONCLUSION

This work introduces a new method that distinguishes between the inter-turn fault and the magnetising inrush current. Wavelet coefficients served as the algorithm's discriminating function. To differentiate the situations under study, two peaks at the $|d5|$ level immediately following the fault moment are used. Since the criteria for this algorithm compare the two peaks, no threshold adjustments are required. The proposed method is thoroughly detailed and shown to be effective using a custom-built transformer.

VII. REFERENCES

- [1] Karen L Butter-pury & Mustafa bagriyanik, "Characterization of transients in Xmer using DWT" IEEE Transactions on power system, Vol.18 No.2 may 2003.
- [2] Jawed Faiz, "A Novel Wavelet-based algorithm of internal faults" from magnetizing inrush currents in power transformers." IEEE Transactions on power delivery, Vol.21 No.4 Oct 2006.

- [3] Karen L Butter-pury, "Identifying Transformer Incipient Events fir maintaining Distribution system reliability" Proceedings of the 36th Hawai International Conference on system sciences 2003.
- [4] M.A.Rahman and B Jeyarurya "A state of art reviews of transformer protection algorithm, "IEEE Transactions on power delivery, Vol.3 PP 534-544 Apr-1988.
- [5] P.M.Anderson, Power system protection. Piscataway NJ: IEEE press 1999.
- [6] H.Wang and K.L.Butter "Modelling transformers with internal incipient faults." IEEE Transactions on power delivery, Vol.17 PP 500-509 Apr-2002.
- [7] P.L.Mao and R.K Agrawal, "A wavelet transform based logic method for discrimination between internal faults and inrush currents in power transformers," Electrical Power and Energy system," Vol.22 PP 389 – 395, 2000.
- [8] P.L.Mao and R.K.Agrawal "A novel approach to the classification of the transient phenomena's in power transformers using combine wavelet transform and neural network, "IEEE Transactions on power delivery, Vol.16 No.4 PP 654-660 Oct 2001.
- [9] Y.Y.Hong and C.W.Wang, "Switching detection / classification using discrete wavelet transform and self organizing mapping network " IEEE Transactions on power delivery, Vol.20 No.2pt II PP 1662 – 1668 APR – 2005.
- [10] S.A.Saleh and M.A.Rahman , "Modelling and protection of three phase power transformer using wavelet packet transform" IEEE Transactions on power delivery, Vol.20 No.2pt II PP 1273 – 1282 APR – 2005.
- [11] O.A.S.Yousef, "A wavelet based technique for discrimination between faults and magnetizing inrush currents in transformer" IEEE Transactions on power delivery, Vol.18 No.1 PP 170 – 176 Jan – 2003.
- [12] C.K.Chui, ed: Wavelets: - A tutorial in theory and application academic Press. Inc. 1992.
- [13] G.Kaiser, A Friendly guide to wavelets, Birk base 1994.
- [14] S Mallat, "A theory for multi resolution signal decomposition: the wavelet representation," IEEE Transactions on power Anal and much Intel, Vol.111 PP 674 – 693 Jul 1989.
- [15] Benteng He,Xuesong Zhang,and Zhiqian Q.Bo "A New Method to Identify Inrush Current Based on Error Estimation ". IEEE Transactions on power delivery, Vol .21,NO 3 JULY 2006.
- [16] Y. Kukaki, "Power differential method for discrimination between fault and magnetizing inrush current in transformer" IEEE Transactions on power delivery, Vol .12,pp1109-115, JULY 1997.

INTERNATIONAL CONFERENCE ON RECENT ADVANCES IN ENGINEERING AND COMPUTER APPLICATIONS-2023

14th & 15th July 2023 | Hybird Conference

Certificate No: ICRAECAP20231415-95140

This is to Certify that **Dr. Anjali U Jawadekar** of
Associate Professor, SSGMCE Shegaon, Sant Gadge Baba Amravati University, Amravati, India presented his/her worthy
presentation titled *"Transformer Incipient Fault Diagnosis using supervised Machine Learning"*

during the "International Conference on Recent Advances in Engineering and Computer Applications (ICRAECA 2023)" Organized by LJ School
of Computer Applications, LJ University, Ahmedabad, in Association with Institute For Engineering Research and Publication (IFERP) held on
14th & 15th July 2023 in Ahmedabad, India.



Mr. Alok Manke
Director
LJ School of Computer Applications
LJ University



Mr. Siddh Kumar Chhajer
MD & Founder, IFERP
Technoarete Group



Mr. Rudra Bhanu Satpathy
CEO & Founder, IFERP
Technoarete Group





AISSMS

COLLEGE OF ENGINEERING

ज्ञानम् सकलजनहिताय

Approved by AICTE, New Delhi, Recognized by Government of Maharashtra
Affiliated to Savitribai Phule Pune University and recognized 2(f) and 12(B) by UGC
(Id.No. PU/PN/Engg./093 (1992))
Accredited by NAAC with "A+" Grade



ICOGE 2023



Certificate of Participation

This is certified that Dr. / Mr. / Ms. / Mrs. Ravishankar S. Kankale of SSGMCOE
is appreciated his / her Presentation / Participation for **International Conference on Green
Energy 2023** held on 16th & 17th May, 2023 organized by AISSMS College of Engineering, Pune,
Under the Aegis of Western Regional Chapter of Solar Energy Society of INDIA (SESI).

Mr. N. P. Mawale
Convener, ICOGE-2023

Dr. D. S. Bormane
Principal
Conference Chair, ICOGE-2023



TRIZ Association of ASIA





AISSMS

COLLEGE OF ENGINEERING

ज्ञानम् सकलजनहिताय

Approved by AICTE, New Delhi, Recognized by Government of Maharashtra
Affiliated to Savitribai Phule Pune University and recognized 2(f) and 12(B) by UGC
(Id.No. PU/PN/Engg./093 (1992))
Accredited by NAAC with "A+" Grade



ICOGE 2023



Certificate of Participation

This is certified that Dr. / Mr. / Ms. / Mrs. Dr. Sudhir R. Paraskar of SSGMCOE
is appreciated his / her Presentation / Participation for **International Conference on Green
Energy 2023** held on 16th & 17th May, 2023 organized by AISSMS College of Engineering, Pune,
Under the Aegis of Western Regional Chapter of Solar Energy Society of INDIA (SESI).

Mr. N. P. Mawale
Convener, ICOGE-2023

Dr. D. S. Bormane
Principal
Conference Chair, ICOGE-2023



TRIZ Association of ASIA





**RSP
CONFERENCE
HUB**
Lighting the path to success

CERTIFICATE of Participation

Proudly Presented to

Dr. Sudhir R Paraskar

Professor, Department of Electrical Engineering, SSGM College of Engineering, Shegaon

for Attending & Giving an oral Presentation for the Paper Entitled

Improvement of Power Quality in distribution system using Battery Energy Storage System

In Second International Conference on Multidisciplinary Research & Innovation (ICMRI) 2024 – Jointly Organized by Department of Mechanical Engineering, Radhakrishna Institute of Technology and Engineering, Bhubaneswar, Odisha, India & RSP Conference Hub, Coimbatore, Tamil Nadu, India on 27/03/2024 & 28/03/2024.

Dr. Chandrabhanu Malla

Conference Co-convener & Dean Academics,
Radhakrishna Institute of Technology and
Engineering, Bhubaneswar, Odisha, India.

Dr. Subash Ranjan Kabat

Principal & Conference Convener,
Radhakrishna Institute of Technology and
Engineering, Bhubaneswar, Odisha, India.





Global Conference Hub

CERTIFICATE of Participation

Proudly Presented to

Dr. Sudhir R Paraskar

Professor, Electrical engineering department, SSGM College of engineering, Shegaon, Maharashtra, India

for Attending & Giving an oral Presentation for the Paper Entitled

Enhancing Reliability of Distribution system with Battery Energy Storage Systems

in **International Conference on Futuristic Trends in Science, Engineering and Management (ICFTSEM) 2024** – Jointly Organized by Department of Business administration, St. Xavier's College of Management & Technology (SXCMT), Patna, Bihar, India & Global Conference Hub, Coimbatore, Tamilnadu, India on 23/02/2024 & 24/02/2024.

Mr. Piyush Ranjan Sahay

Coordinator, Department of Business Administration, St. Xavier's college of Management & Technology, Patna, India

Fr. Dr. Martin Poras SJ

Principal, St. Xavier's college of Management & Technology, Patna, India



CERTIFICATE OF PRESENTATION & PUBLICATION



Hinweis Second International Conference on Recent Trends
in Machine Learning and Image Processing, MLIP-2023

December 22-23, 2023

<http://mlip.thehinweis.com/2023>

Dr. Anjali U. Jawadekar
SSGMCE Shegaon, Maharashtra, India

Author of a Research Paper titled **Advancements in Islanding Detection Techniques for Microgrid Systems: A Comprehensive Review** has submitted the paper which has been approved and presented for publication in the Hinweis Second International Conference on Recent Trends in Machine Learning and Image Processing, MLIP-2023.

Dr. Yogesh Chaba
General Chair



Dr. Janahanlal Stephen
General Co Chair



Shri Gajanan Shikshan Sanstha's
SHRI SANT GAJANAN MAHARAJ COLLEGE OF ENGINEERING
SHEGAON – 444203, DIST. BULDANA (MAHARASHTRA STATE), INDIA
"Recognized by A.I.C.T.E., New Delhi" Affiliated to Sant Gadge Baba Amravati University, Amravati
"Approved by the D.T.E., M.S. Mumbai"

Ph : +918669638081/82

Fax : 091-7265-252346

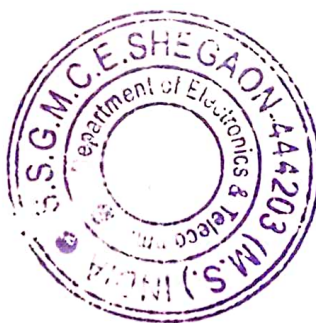
Email: principal@ssgmce.ac.in, registrar@ssgmce.ac.in

Website- www.ssgmce.ac.in

3.3.2: Number of books and chapters in edited volumes/books published and papers published in National/ International conference proceedings per teacher during year

2023-24

Sr. No.	Evidences
1	List of papers/Books
2	Copy of Paper/Certificate



V. S. Ingole

Prof. V. S. Ingole
Prepared By

Dr. M. N. Tibdewal

Dr. M. N. Tibdewal
HOD, Electronics and Telecommunication
Engineering



Shri Gajanan Shikshan Sanstha's
**SHRI SANT GAJANAN MAHARAJ COLLEGE OF ENGINEERING
SHEGAON - 444203, DIST. BULDANA (MAHARASHTRA STATE), INDIA**

"Recognized by A.I.C.T.E., New Delhi" Affiliated to Sant Gadge Baba Amravati University, Amravati
"Approved by the D.T.E., M.S. Mumbai"

Ph : +918669638081/82

Email: principal@ssgmce.ac.in, registrar@ssgmce.ac.in

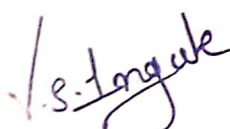
Fax : 091-7265-252346

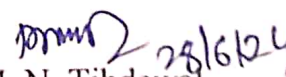
Website- www.ssgmce.ac.in

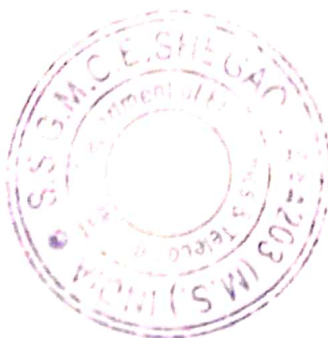
3.3.2 Number of books and chapters in edited volumes/books published and papers published in national/ international conference proceedings per teacher during year

2023-24

Cri. No.	Key Aspects	Assessment Indicators	Total
3.3.3	Number of books and chapters in edited volumes/books published and papers published in national/ international conference proceedings per teacher during year	Books and chapters in edited volumes/books published and papers published in national/ international conference proceedings per teacher during year	07


Prof. V. S. Ingole
Prepared By


Dr. M. N. Tibdewal
HOD, Electronics and Telecommunication
Engineering





Shri Gajanan Shikshan Sanstha's
SHRI SANT GAJANAN MAHARAJ COLLEGE OF ENGINEERING
SHEGAON - 444203, DIST. BULDANA (MAHARASHTRA STATE), INDIA
"Recognized by A.I.C.T.E., New Delhi" Affiliated to Sant Gadge Baba Amravati University, Amravati
"Approved by the D.T.E., M.S. Mumbai"

Ph : +918669638081/82
Fax : 091-7265-252346

Email: principal@ssgmce.ac.in, registrar@ssgmce.ac.in
Website- www.ssgmce.ac.in

Sr No	Name of the teacher	Title of the book/chapters published	Title of Paper	Title of proceedings of the conference	Name of Conference	National / International	Year of publications	ISBN/ISSN number of proceeding	Affiliating institute at the time of publication	Name of the publisher
1	Neerja Dharmale		Application of OLCAO-GGA and OLCAO-MGGA Techniques for investigating properties of TiO ₂	NA	3rd International Conference on Emerging Electronics and Automation (E2A-2023) organized by Department of Electronics and Instrumentation Engineering, National Institute of Technology Silchar, Assam, India on 15th to 17th December 2023.	International	NA	NA	Shri Sant Gajanan Maharaj College of Engineering, Shegaon	NA
2	Rupesh Mahamune		The multi-scale wavelet approach for the removal of eye-blink artifact from EEG Signals	NA	3rd International Conference on Emerging Electronics and Automation (E2A-2023) organized by Department of Electronics and Instrumentation Engineering, National Institute of Technology Silchar, Assam, India on	International	NA	NA	Shri Sant Gajanan Maharaj College of Engineering, Shegaon	NA



Shri Gajanan Shikshan Sanstha's
SHRI SANT GAJANAN MAHARAJ COLLEGE OF ENGINEERING
SHEGAON - 444203, DIST. BULDANA (MAHARASHTRA STATE), INDIA
"Recognized by A.I.C.T.E., New Delhi" Affiliated to Sant Gadge Baba Amravati University, Amravati
"Approved by the D.T.E., M.S. Mumbai"

Ph : +918669638081/82
Fax : 091-7265-252346

Email: principal@ssgmce.ac.in, registrar@ssgmce.ac.in
Website- www.ssgmce.ac.in

					15th to 17th December 2023.					
3	Harshavardhan Patil		Elevating Canteen Management with a Modern Web Solution	2024 IEEE International Students' Conference on Electrical, Electronics and Computer Science, 2024, DOI: 10.1109/SCEE CS61402.2024 .10482188	2024 IEEE International Students' Conference on Electrical, Electronics and Computer Science	International	2024	Electronic ISSN: 2688- 0288 Print on Demand(Po D) ISSN: 2688-027X DOI: 10.1109/SC EECS61402. 2024.10482 188 Publisher: IEEE	Shri Sant Gajanan Maharaj College of Engineering, Shegaon	IEEE
4	S. P. Badar and K. Khanchandani		Efficient Implementatio n of Polar Decoder: Design and Performance Analysis	NA	3rd International conference on "Computational Electronics for Wireless Communications" held at NIT Jalandhar during December 22-23, 2023.	International	NA	NA	Shri Sant Gajanan Maharaj College of Engineering, Sh egaon	NA



Shri Gajanan Shikshan Sanstha's
SHRI SANT GAJANAN MAHARAJ COLLEGE OF ENGINEERING
SHEGAON - 444203, DIST. BULDANA (MAHARASHTRA STATE), INDIA
"Recognized by A.I.C.T.E., New Delhi" Affiliated to Sant Gadge Baba Amravati University, Amravati
"Approved by the D.T.E., M.S. Mumbai"

Ph : +918669638081/82
Fax : 091-7265-252346

Email: principal@ssgmce.ac.in, registrar@ssgmce.ac.in
Website: www.ssgmce.ac.in

5	Dr.D.D.Nawgaje		MDLGO. Integrated Multimodal Deep Learning Framework for Enhanced Precision in Glaucoma Diagnosis Using OCT A- scans	2024 International Conference on Emerging Smart Computing and Informatics (ESCI)	International Conference on Emerging Smart Computing & Informatics 2024	International	2024	Electronic ISBN 979-8- 3503-0661-3 Print on Demand(PoD) ISBN 979- 8-3503-0662- 0	Shri Sant Gajanan Maharaj College of Engineering, Shegaon	IEEE
6	Dr.Santosh B. Patil	Data Science and Big Data Analytics. Data Intensive Research	Transfer Learning by Fine-Tuning Pre-trained Convolutional Neural Network Architectures for Image Recognition	Proceedings of IDBA 2023 (Springer).	International Conference on Data Science and Big Data Analysis	International Conference	2024	ISSN 2731- 555X ISSN 2731-5568 (electronic) Data- Intensive Research ISBN 978- 981-99-9178- 5 ISBN 978- 981-99-9179- 2 (eBook)	Shri Sant Gajanan Maharaj College of Engineering, Shegaon	Springer, Singapore



Shri Gajanan Shikshan Sanstha's
SHRI SANT GAJANAN MAHARAJ COLLEGE OF ENGINEERING
SHEGAON - 444203, DIST. BULDANA (MAHARASHTRA STATE), INDIA
"Recognized by A.I.C.T.E., New Delhi" Affiliated to Sant Gadge Baba Amravati University, Amravati
"Approved by the D.T.E., M.S. Mumbai"

Ph : +918669638081/82
Fax : 091-7265-252346

Email: principal@ssgmce.ac.in, registrar@ssgmce.ac.in
Website- www.ssgmce.ac.in

7	Dr. Santosh B. Patil	Artificial Intelligence, Machine Learning and User Interface Design	Enhancing Efficiency in Content Based Image Retrieval System Using Pre-trained Convolutional Neural Network Models Published in a book "Artificial Intelligence, Machine Learning and User Interface Design"		NA	NA	2024	eISBN: 978-981-5179-60-6, 2024 ISBN: 978-981-5179-61-3	Shri Sant Gajanan Maharaj College of Engineering, Shegaon	Bentham Science
---	----------------------	---	--	--	----	----	------	---	---	-----------------

V. S. Ingole

Prof. V. S. Ingole
Prepared By



Dr. M. N. Tibdewal 28/6/24

Dr. M. N. Tibdewal
HOD, Electronics and Telecommunication Engineering

3rd International Conference on Emerging Electronics and Automation



E2A
2023



Organized by

Department of Electronics and Instrumentation Engineering
National Institute of Technology Silchar, Assam, India

Certificate of Participation

This is to certify that **Dr. Neerja Dharmale** has presented a paper entitled "**Application of OLCAO-GGA and OLCAO-MGGA Techniques for investigating properties of TiO₂**" in the 3rd International Conference on Emerging Electronics and Automation (E2A-2023) organized by Department of Electronics and Instrumentation Engineering, National Institute of Technology Silchar, Assam, India on 15th to 17th December 2023.

Prof. Dilip Kumar Baidya
Director, NIT Silchar

Dr. Shivendra Kumar Pandey
General Chair

Prof. Shahedul Haque Laskar
General Chair

3rd International Conference on Emerging Electronics and Automation



E2A
2023



Organized by
Department of Electronics and Instrumentation Engineering
National Institute of Technology Silchar, Assam, India

Certificate of Participation

This is to certify that **Rupesh Mahamune** has presented a paper entitled ***“The Multi-Scale Wavelet Approach to Remove the Eyeblink Artifacts from EEG Signals”*** in the 3rd International Conference on Emerging Electronics and Automation (E2A-2023) organized by Department of Electronics and Instrumentation Engineering, National Institute of Technology Silchar, Assam, India on 15th to 17th December 2023.

Prof. Dilip Kumar Baidya
Director, NIT Silchar

Dr. Shivendra Kumar Pandey
General Chair

Prof. Shahedul Haque Laskar
General Chair



IEEE MANIT STUDENT BRANCH

MP Section



CERTIFICATE OF PRESENTATION

The Institute of Electrical and Electronics Engineers - MANIT Student Branch (IEEE-MSB)
extends this Certificate of Authorship to

Harshavardhan Patil

acknowledging their exceptional impact on the realm of research and technology
at SCEECs'24 held on 24th - 25th February, 2024.

We eagerly anticipate looking forward to seeing more of your valuable
contributions to shaping the industry ahead.

As you embark on your journey towards continued success, IEEE-MSB conveys our
sincere congratulations and best wishes for your continued innovation.

Devansh Kapri
Branch Chairperson
IEEE MSB

Dr. Jyoti Singh
Branch Counsellor
IEEE MSB

Conferences > 2024 IEEE International Stude... ?

Elevating Canteen Management with a Modern Web Solution

Publisher: IEEECite ThisPDF

<< Results

H. B. Patil ; Mr. Mohit Rathi ; Vishakha G. Wankhade ; Mrunali Darokar ; Yash Wankhade ; Neerja DharmaleAll Authors

18FullText Views

Alerts

Manage Content AlertsAdd to Citation Alerts

Abstract

Document Sections

I. Introduction

II. Literature Survey

III. Working

IV. Architecture

V. Computational methodology

Show Full Outline

Authors

Figures

References

Keywords

Metrics

More Like This

Download PDF

Abstract:

In this paper, the author aims to remove the hassle of cash transactions from college canteen payments by streamlining the process. The present reliance on currency frequ... **View more**

Metadata

Abstract:
In this paper, the author aims to remove the hassle of cash transactions from college canteen payments by streamlining the process. The present reliance on currency frequently proves inconvenient, particularly when precise amounts are needed, making change provision difficult. Educational establishment's conventional canteen management scenario must improve with inefficiencies from manual record-keeping, monetary transactions, and user annoyances. This study offers a cutting-edge web-based system that could completely transform canteen operations in response to these issues. Our approach offers device-independent accessibility, unlike existing systems that are device-bound. The suggested system fully addresses these issues, guaranteeing a smooth and inclusive user experience across various devices. It is focused on essential areas like User Authentication and Profile Management, E-wallet Recharge, Database Management System Setup, Admin Access, and Transaction Notifications.

Published in: 2024 IEEE International Students' Conference on Electrical, Electronics and Computer Science (SCECS)

Date of Conference: 24-25 February 2024

DOI: 10.1109/SCECS61402.2024.10482188

Date Added to IEEE Xplore: 02 April 2024

Publisher: IEEE

► ISBN Information:

Conference Location: Bhopal, India

▼ ISSN Information:

☰ Contents

I. Introduction

Canteen operations are now manual, which adds complexity and inefficiency to the entire process, from placing orders to delivering food. When there is no automatic system in place, computations must be done by hand, which increases the possibility of errors. One of the biggest obstacles is that each student's food intake is not precisely recorded, which results in inconsistent statistics and makes it hard to monitor consumption trends. The consequences encompass inaccuracies in invoicing, disparities in inventory, and inefficiencies in operations, which eventually affect the precision of finances and the caliber of services rendered [6].

Authors	▼
Figures	▼
References	▼
Keywords	▼
Metrics	▼

Back to Results

More Like This

Transforming a database systems and design course for non computer science majors
Proceedings Frontiers in Education 1995 25th Annual Conference. Engineering Education for the 21st Century
Published: 1995

Research-in-progress: User experience evaluation of Student Centered E-Learning Environment for computer science program
2014 3rd International Conference on User Science and Engineering (i-USEr)
Published: 2014

Show More



ICCWC-2023

ICCWC/NITJ/2023/46

3rd International conference on
Computational Electronics for Wireless Communications
December 22-23, 2023

This is to certify that Professor/Dr/Mr/Ms **Swapnil Panjabrao Badar** has participated and presented a paper entitled **EFFICIENT IMPLEMENTATION OF POLAR DECODER: DESIGN AND PERFORMANCE ANALYSIS** co-authored with **Kamlesh Khanchandani** in 3rd International conference on "Computational Electronics for Wireless Communications" held at NIT Jalandhar during December 22-23, 2023.

Dr. Manjeet Singh
Organizing Secretary

Dr. Pawan Kumar Verma
Organizing Secretary

Dr. Nitesh Kashyap
Organizing Chairman

Dr. Ashish Raman
Organizing Chairman

Conferences > 2024 International Conference... ?

MDLGO: Integrated Multimodal Deep Learning Framework for Enhanced Precision in Glaucoma Diagnosis Using OCT A-scans

Publisher: IEEE

Cite This

PDF

<< Results

Rupesh Goverdhan Mundada ; Devesh D. Nawgaje All Authors ...

26
Full
Text Views



Alerts

Manage Content Alerts

Add to Citation Alerts

Abstract

Document Sections

I. Introduction

II. Motivation&contribution

III. Extensive Literature
Review Existing
Techniques

IV. Proposed Multimodal
Deep Learning
Framework

V. Result
Analysis&comparison

Show Full Outline

Authors

Figures

References

Keywords

Download PDF

Abstract:

Glaucoma, a leading cause of irreversible blindness, necessitates accurate and early diagnosis to prevent visual impairment. Current methods relying solely on OCT A-scans... **View more**

Metadata

Abstract:

Glaucoma, a leading cause of irreversible blindness, necessitates accurate and early diagnosis to prevent visual impairment. Current methods relying solely on OCT A-scans often fall short in specificity and sensitivity, and may overlook subtle anomalies indicative of early glaucoma. Furthermore, delays in diagnosis can contribute to disease progression. This paper introduces an innovative deep learning model that amalgamates OCT A-scans, fundus images, and visual field data, leveraging the strengths of multi-modal fusion to provide a comprehensive analysis for glaucoma diagnosis. Transfer learning, utilizing pre-trained models like InceptionV3 and ResNet50, was employed to enhance feature extraction, alongside anomaly detection methods including One-Class SVM and Isolation Forest to identify atypical glaucoma presentations. Moreover, the integration of an attention mechanism in segmentation models, specifically V-Net and SegNet, facilitated precise delineation of regions of interest in OCT A-scans. The proposed model significantly outperformed existing methods, enhancing precision by 8.5%, accuracy by 3.9%, recall by 8.3%, AUC by 4.9%, and specificity by 5.5%, while concurrently reducing diagnosis delay by 10.4%. These substantial improvements underscore the potential of our method in revolutionizing glaucoma diagnosis, ultimately contributing to timely intervention and better patient outcomes.

Metrics

More Like This

Published in: 2024 International Conference on Emerging Smart Computing and Informatics (ESCI)

Date of Conference: 05-07 March 2024 **DOI:** 10.1109/ESCI59607.2024.10497193

Date Added to IEEE Xplore: 17 April 2024 **Publisher:** IEEE

► ISBN Information: **Conference Location:** Pune, India

 Contents

I. Introduction

Millions of individuals worldwide suffer from irreparable blindness from glaucoma. Progressive optic nerve injury, frequently linked with elevated intraocular pressure, can cause vision loss if not recognized and treated. Early detection and treatment are essential to preventing this disease's severe effects. OCT A-scans take comprehensive images of the retinal layers to examine the optic nerve head and retinal nerve fiber layer thickness, making glaucoma diagnosis easier. A-scans give significant information, but using them alone can lead to measurement uncertainty and the possibility to miss minor structural changes that indicate early glaucoma [1]–[3]. This can also be done with HVNet operations.

Authors	▼
Figures	▼
References	▼
Keywords	▼
Metrics	▼

[Back to Results](#)

More Like This

Violence Classification Using Support Vector Machine and Deep Transfer Learning Feature Extraction

2021 International Seminar on Intelligent Technology and Its Applications (ISITIA)

Published: 2021

Nonlinear Support Vector Machine Visualization for Risk Factor Analysis Using Nomograms and Localized Radial Basis Function Kernels

IEEE Transactions on Information Technology in Biomedicine

Published: 2008

[Home](#) > [Data Science and Big Data Analytics](#) > Conference paper

Transfer Learning by Fine-Tuning Pre-trained Convolutional Neural Network Architectures for Image Recognition

| Conference paper | First Online: 17 March 2024

| pp 273–287 | [Cite this conference paper](#)



[Data Science and Big Data Analytics](#)
(IDBA 2023)

[Vishwanath S. Mahalle](#) , [Narendra M. Kandoi](#) & [Santosh B. Patil](#)



Part of the book series: [Data-Intensive Research](#) ((DIR))



Included in the following conference series:
[International Conference on Data Science and Big Data Analysis](#)



194 Accesses

Abstract

[https://doi.org/10.1007/97](https://doi.org/10.1007/978-981-99-9179-2_21)

[8-981-99-9179-2_21](https://doi.org/10.1007/978-981-99-9179-2_21)

Print ISBN

978-981-99-9178-5

Online ISBN

978-981-99-9179-2

eBook Packages

Intelligent Technologies
and Robotics

Intelligent Technologies
and Robotics (R0)

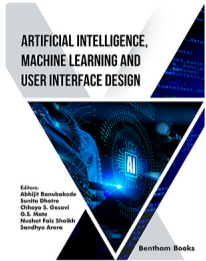
Publish with us

[Policies and ethics](#) 



Search here...

LoginRegisterCart0



Artificial Intelligence, Machine Learning and User Interface Design

Enhancing Efficiency in Content-based Image Retrieval System Using Pre-trained Convolutional Neural Network Models

Author(s): [Vishwanath S. Mahalle](#), [Narendra M. Kandoi](#), [Santosh B. Patil](#), [Abhijit Banubakode](#) and [Vandana C. Bagal](#)

Pp: 241-262 (22)

DOI: [10.2174/9789815179606124010015](#)

Buy Chapters 15

* (Excluding Mailing and Handling)

Abstract

Traditionally, image retrieval is done using a text-based approach. In the text-based approach, the user must query metadata or textual information, such as keywords, tags, or descriptions. The effectiveness and utility of this approach in the digital realm for solving image retrieval problems are limited. We introduce an innovative method that relies on visual content for image retrieval. Various visual aspects of the image, including color, texture, shape, and more, are employed to identify relevant images. The choice of the most suitable feature significantly influences the system's performance. Convolutional Neural Network (CNN) is an important machine learning model. Creating an efficient new CNN model requires considerable time and computational resources. There are many pre-trained CNN models that are already trained on large image datasets, such as ImageNet containing millions of images. We can use these pre-train CNN models by transferring the learned knowledge to solve our specific content-based image retrieval task.

In this chapter, we propose an efficient pre-trained CNN model for content-based image retrieval (CBIR) named as ResNet model. The experiment was conducted by applying a pre-trained ResNet model on the Paris 6K and Oxford 5K datasets. The performance of similar image retrieval has been measured and compared with the state-of-the-art AlexNet model. It is found that the AlexNet architecture takes a longer time to get more accurate results. The ResNet architecture does not need to fire all neurons at every epoch. This significantly reduces training time and improves accuracy. In the ResNet architecture, once the feature is extracted, it will not extract the feature again. It will try to learn a new feature. To measure its performance, we used the average mean precision. We obtained the result for Paris6K 92.12% and Oxford5K 84.81%. The Mean Precision at different ranks, for example, at the first rank in Paris6k, we get 100% result, and for Oxford5k, we get 97.06%.

Keywords: [Content-based image retrieval](#), [Convolution neural network architectures](#), [Transfer learning](#).

Cite as

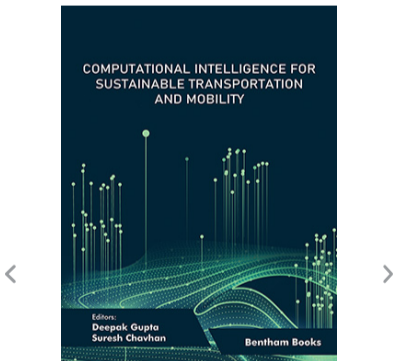
Related Journals



Recent Patents on Computer Science

View More >>

Related Books



Computational Intelligence For Data Analysis

View More >>





Shri Gajanan Shikshan Sanstha's

**SHRI SANT GAJANAN MAHARAJ COLLEGE OF ENGINEERING
SHEGAON - 444203, DIST. BULDANA (MAHARASHTRA STATE), INDIA**

"Recognized by A.I.C.T.E., New Delhi" Affiliated to Sant Gadge Baba Amravati University, Amravati

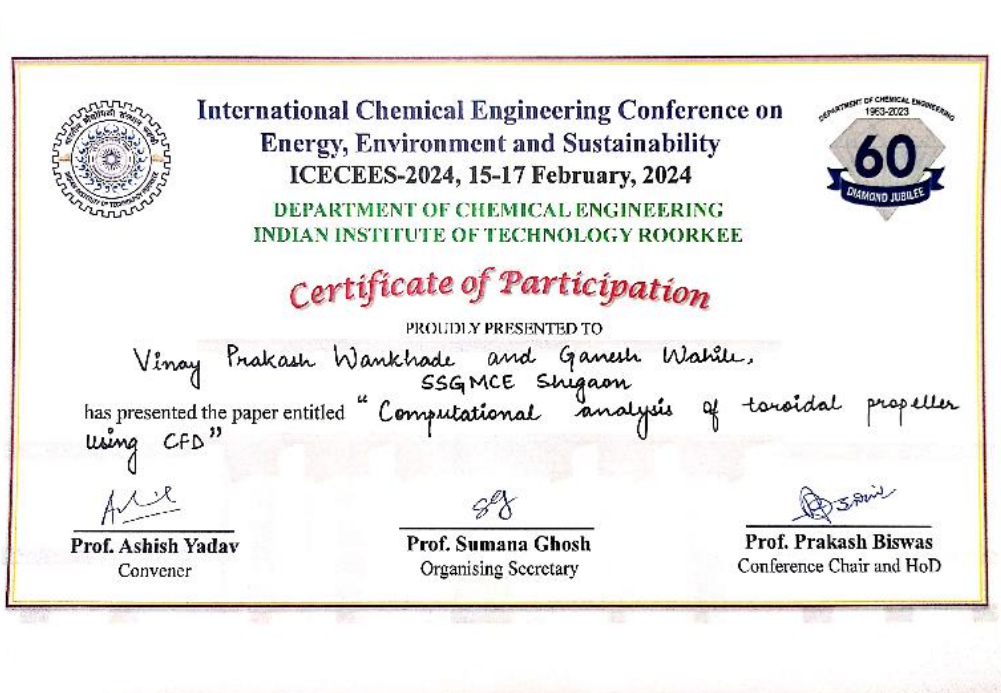
"Approved by the D.T.E., M.S. Mumbai"

Ph : +918669638081/82

Fax : 091-7265-252346

Email: principal@ssgmce.ac.in, registrar@ssgmce.ac.in

Website- www.ssgmce.ac.in



Scanned with OKEN Scanner



Artificial Intelligence, Machine Learning and User Interface Design

Editor(s) : Abhijit Banubakode, Sunita Dhotre, Chhaya S. Gosavi, G. S. Mate, Nuzhat Faiz Shaikh, Sandhya Arora

DOI: 10.2174/97898151796061240101

eISBN: 978-981-5179-60-6, 2024

ISBN: 978-981-5179-61-3

[Back](#)

[Recommend this Book to your Library](#)

[Cite as](#)

Book Web Price:

US \$

Buy Personal Book

59

Order Library eBook

236

Order Printed Copy

85

Order Book + Hard Copy

144

After 20% Discount ↓

115



Artificial Intelligence, Machine Learning and User Interface Design

[Back](#)

[Book Details >>](#)

Enhancing Efficiency in Content-based Image Retrieval System Using Pre-trained Convolutional Neural Network Models

Author(s): Vishwanath S. Mahalle, Narendra M. Kandoi, Santosh B. Patil, Abhijit Banubakode and Vandana C. Bagal

Pp: 241-262 (22)

DOI: 10.2174/9789815179606124010015

Buy Chapters **15**

* (Excluding Mailing and Handling)

[Home](#) > [Data Science and Big Data Analytics](#) > Conference paper

Transfer Learning by Fine-Tuning Pre-trained Convolutional Neural Network Architectures for Image Recognition

Conference paper | First Online: 17 March 2024

pp 273–287 | [Cite this conference paper](#)



[Data Science and Big Data Analytics](#)

(IDBA 2023)

[Vishwanath S. Mahalle](#) , [Narendra M. Kandoi](#) & [Santosh B. Patil](#)

 Part of the book series: [Data-Intensive Research \(\(DIR\)\)](#)

 Included in the following conference series:
[International Conference on Data Science and Big Data Analysis](#)

Access this chapter

[Log in via an institution](#) →

^ Chapter

EUR 29.95
Price includes VAT (India)



A Textbook Quality Assurance

A Textbook Quality Assurance

Dr. Aarti S. Zanwar , Prof. Dr. Abhijit Narayanrao Merekar
, Professor Dr. Smita Abhijit Merekar , Dr. Arvind R.
Bhagat Patil, Dr. Jaikumar M. Patil

Paperback
499.00

e Book
299.00

Pages : 277

Language : English

PAPERBACK Price : 499.00



Add to wishlist



Add to cart



Buy now



ISBN : 978-93-6087-412-4

Category : Academic

About author : Dr. Aarti S. Zanwar is currently working as an Associate Professor in Pharmaceutical Chemistry and Analysis, Department of Pharmacy, Sumandeep Vidyapeeth Deemed to be University, located in Piparia, Waghodia, Vadodara, Gujarat, India. She has 14 year's experience in academics. She has completed her B.Pharm. from Sant Gadge Baba Amravati University and her M.Pharm. in Quality Assurance from Rashtrasant Tukadoji Maharaj Nagpur University. Dr. Aarti has obtained her PhD in Pharmaceutical Sciences from Sumandeep Vidyapeeth Deemed to be University, Gujarat. She has published 43 research papers and review articles in reputed journals. She has written 10 book chapters, authoring one book, and 2 patents are to her credit. Furthermore, she has provided guidance to more than 13 postgraduate students. She is a member of professional bodies like the MPSC and APTI. Her core research area is related to development and validation of different analytical methods using HPLC,



AI-DRIVEN HEALTHCARE

TRANSFORMING DIAGNOSIS FOR
EFFECTIVE TREATMENT

P. V. KALE | A. G. SHARMA | DR. N. M. KANDOI

AI-POWERED DIAGNOSIS
AI-DRIVEN TREATMENT AND CARE
THE FUTURE OF AI IN HEALTHCARE

 **VINSA**
PUBLISHING

AI-Driven Healthcare

Transforming Diagnosis for Effective Treatment

P. V. Kale | A. G. Sharma | Dr. N. M. Kandoi





P. V. Kale

P.V. Kale is employed with the SSGMCE, Shegaon, Department of Information Technology as an Assistant Professor. With twenty years of experience in teaching, she specializes in deep learning, biomedical image processing, and machine learning. She is currently pursuing Ph.D. in Computer Science and Engineering. She holds Bachelor of Engineering in Information Technology and Master of Technology in Information Technology. She has published articles in peer-reviewed journals and is a professional member of ACM and ISTE. In order to succeed in her professional career, she has effectively completed a number of trainings and hands-on workshops. Her study focuses on machine learning in the healthcare industry.



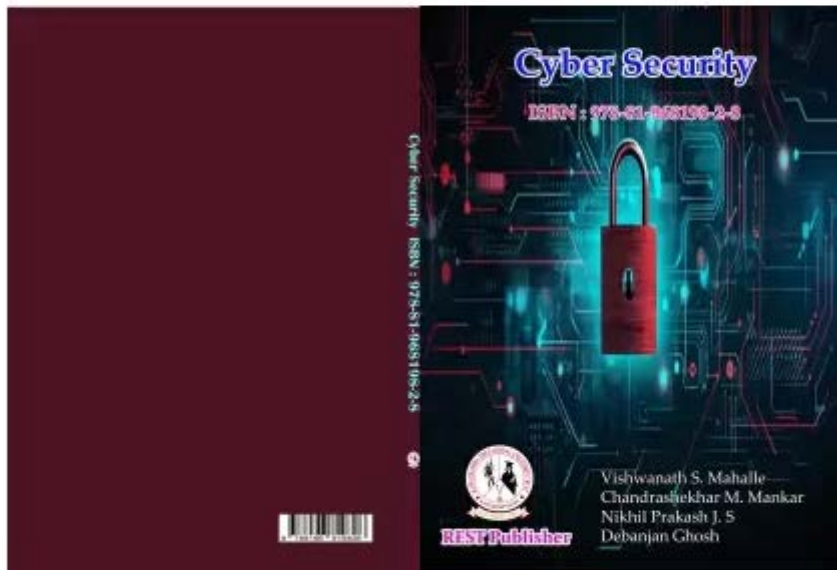
A. G. Sharma

A.G. Sharma is working as an Assistant Professor in Department of Information Technology at the SSGMCE, Shegaon,. He has been teaching for about twelve years, and his areas of specialization are Deep Learning, Neural Networks, Data Science & Statistics, and Natural Language Processing. He is Pursuing Ph.D. in Computer Science and Engineering. He holds Bachelor and a Master degree in Information Technology. In addition to being a member of professional associations like ISTE and ACM, his work published in peer-reviewed journals. To be effective in his line of work, he has successfully completed a number of trainings and hands-on workshops. His field of study is the application of deep learning to the healthcare industry.



Dr. N. M. Kandoi

Dr. N. M. Kandoi is currently serving as an Associate Professor in the Department of Computer Science & Engineering at SSGMCE, Shegaon. With a wealth of 35 years of teaching experience, his specialization in Machine Learning, Blockchain Technology, Web Technology and Security. Dr. Kandoi earned his PhD in Computer Science and Engineering. Additionally, he holds a Master's degree in Computer Science from BITS Pilani and a Bachelor's degree in Computer Science & Engineering. He has contributed to reputed journals with his published articles and holds memberships in professional organizations such as ISTE and ACM. Dr. Kandoi is an active member of the BoS Committee. His current research endeavours are concentrated on the integration of technology in healthcare.



2023 14th International Conference on Computing Communication and Networking Technologies (ICCCNT 2023)

**Delhi, India
6-8 July 2023**

Pages 1-618



**IEEE Catalog Number: CFP2352J-POD
ISBN: 979-8-3503-3510-1**

**Copyright © 2023 by the Institute of Electrical and Electronics Engineers, Inc.
All Rights Reserved**

Copyright and Reprint Permissions: Abstracting is permitted with credit to the source. Libraries are permitted to photocopy beyond the limit of U.S. copyright law for private use of patrons those articles in this volume that carry a code at the bottom of the first page, provided the per-copy fee indicated in the code is paid through Copyright Clearance Center, 222 Rosewood Drive, Danvers, MA 01923.

For other copying, reprint or republication permission, write to IEEE Copyrights Manager, IEEE Service Center, 445 Hoes Lane, Piscataway, NJ 08854. All rights reserved.

****** This is a print representation of what appears in the IEEE Digital Library. Some format issues inherent in the e-media version may also appear in this print version.***

IEEE Catalog Number:	CFP2352J-POD
ISBN (Print-On-Demand):	979-8-3503-3510-1
ISBN (Online):	979-8-3503-3509-5
ISSN:	2162-7665

Additional Copies of This Publication Are Available From:

Curran Associates, Inc
57 Morehouse Lane
Red Hook, NY 12571 USA
Phone: (845) 758-0400
Fax: (845) 758-2633
E-mail: curran@proceedings.com
Web: www.proceedings.com

CURRAN ASSOCIATES INC.
proceedings
.com

TABLE OF CONTENTS

Cyber-Physical Security System in Smart Grid-A Review.....	1
<i>Y Akshatha, A. S. Poornima</i>	
An Effective Detection of Litchi Disease using Deep Learning.....	8
<i>Mansi Dahiya, M. S. Guru Prasad, Tanmay Anand, Khushi Kumar, Sparsh Bansal, H N Naveen Kumar</i>	
Fake News Detection Using Deep Learning and Transformer-Based Model.....	14
<i>Paliwal Mohan Subhash, Deepa Gupta, Suja Palaniswamy, Manju Venugopalan</i>	
An Enhancement to CoAP Protocol for Internet of Medical Things to Reduce Latency	20
<i>Aparna Sreekumar, A R Anjalikrishna, Nima S Nair</i>	
Analyzing the Severity of Air Pollution in an Industrialized Suburb	26
<i>Pritisha Sarkar, Mahesh Kumar Makkenna, Sujoy Saha, Mousumi Saha</i>	
Analysis of Multi-Objective Optimization of Latent Variables in Variational Autoencoders.....	32
<i>A K Punnoose</i>	
Auto-grading C Programming Assignments with CodeBERT and Random Forest Regressor	36
<i>Roshan Vasu Muddaluru, Sharvaani Ravikumar Thoguluva, Shruti Prabha, Peeta Basa Pati, Roshni M Balakrishnan</i>	
Identification Of Users with Social Behavioural Biometrics On Twitter	42
<i>Anudeep Gandla, Vamshi Sunku Mohan, Sriram Sankaran</i>	
A New Hybrid-shaped Complementary Split Ring Resonator for Skin Cancer Detection	49
<i>Madan Kumar Sharma, Doaa Yousuf Alghassani, Basama Mohammed Aldarii, Buthina Abdullha Albadi, Shima Salim Almalki</i>	
Design of a Compact Microstrip Antenna for Wi-Fi, WLAN, X-Band and UWB Applications	54
<i>Sarthak Munjal, Rashmi Roges, Sandeep Sharma, Rishiek Kumar Mishra, Anuradha Bhasin</i>	
AI Based Parameter Estimation of ML Model using Hybrid of Genetic Algorithm and Simulated Annealing	60
<i>Jegadit S Saravanan, Anbazhagan Mahadevan</i>	
Single Image Super-Resolution Network with Enhanced Octave Convolution for Separating Image Frequencies.....	65
<i>Saghar Farhangfar, Aryaz Baradarani, Mohammad Asadpour, Mohammad Ali Balafar, Roman Gr. Maev</i>	
Real-Time Web Application to Classify Diabetic Foot Ulcer	71
<i>Souhrid Nandi, Apoorva Anurag, Veena Mayya, Jayakumar Jeganathan</i>	
In-Depth Network Security for Docker Containers.....	78
<i>Asem Mousa, Wajeeth Tuffaha, Mohammad Abdulhaq, Moath Qadry, M. M. Othman Othman</i>	
Simulation of IoT-based Smart City of Darwin: Leading Cyber Attacks and Prevention Techniques	84
<i>Shujahat Ali Khan, Jawahar Sundaram, Mario Palendeng, Sami Azam, Bharanidharan Shanmugam</i>	

Weed Detection: A Vision Transformer Approach For Soybean Crops	3549
<i>M. Sanjay, Deepashree P. Vaideeswar, Ch. Venkata Rami Reddy, Mithisha Brilent Tavares</i>	
System Complexity Reduction Using 3-D Matrices and Novel Logic Gates	3557
<i>Nameshwari Verma, Pallabi Sarkar</i>	
Comparative Analysis of Deep Learning and Machine Learning Models for Network Intrusion Detection	3562
<i>V. C. Dharaneish, S. Nithin Kumar, V. Hari Varsha, T. Senthil Kumar, T. Gireesh Kumar, Sulakshan Vajipayajula</i>	
Crop Disease Identification in Tomato Leaf using Deep Learning.....	3575
<i>Punith Kumar, H. N Champa</i>	
Enhancing Trustworthiness and Security in Cloud Environments: A Review of Methodologies and Advancements	3582
<i>Manpreet Kaur, Sarpreet Singh</i>	
Resource Optimization based Virtual Machine Allocation Technique in Cloud Computing Domain	3590
<i>Kalka Dubey, S. C. Sharma, Mohit Kumar</i>	
SWAYAM MOOC Reviews: Assessing Acceptability through Sentiment Analysis using Machine Learning	3597
<i>Ishteyaaq Ahmad, Sonal Sharma, Mahesh Kumar Chaubey, Saurabh Dhyani, Sikha Ahmad, Ajay Kumar</i>	
Design and Simulation of 2.45 GHz Microstrip Patch Antenna for S-Band Wireless Applications.....	3602
<i>Sohel Rana, Sheikh Rabiul Islam, Sifat Hossain, Mostafizur Rahman</i>	
Wireless Network for Industrial Application using ESP32 as Gateway	3609
<i>Lopamudra Samal, Pallavi Bute</i>	
Prediction of Cardiac Illness using Machine Learning Algorithms With and Without Feature Selection	3614
<i>Jeethu Philip, Bala Srujan Kumar Reddy Gade, Kameswari Sai Pranamya, Alka, Charan Reddy Guntaka</i>	
Fake News Detection Using Semantic Analysis and Machine Learning Techniques.....	3619
<i>Harveen Kaur</i>	
Using Machine Learning to Predict Patient Health Outcomes	3625
<i>Harveen Kaur, Harpreet Singh, Kashish Verma</i>	
Using Network Analysis to Detect Fake News in Social Media.....	3632
<i>Harveen Kaur</i>	
An Improved Prediction of Polycystic Ovary Syndrome Using SMOTE-based Oversampling and Stacking Classifier.....	3641
<i>Maimuna Akhtar, Kazi Asif Ahmed, Ferdib Al-Islam</i>	
An Empiric Study on Bangla Sentiment Analysis Using Hybrid Feature Extraction Techniques	3647
<i>Shymon Islam, Kazi Masudul Alam</i>	
Exploring KD Trees and KNN Search in the Context of Google Maps: An Insightful Overview	3654
<i>K. Pranith Chowdary, R. Prathap Kumar, M. Tanuja, K. Sri Chandana</i>	

Wireless network for Industrial application using ESP32 as Gateway

IEEE - 56998

Lopamudra Samal

Electronics and communication Engineering

NIT Rourkela, India

Pallavi Bute

Information Technology department

Shri Sant Gajanan Maharaj College of Engineering Shegaon,

Abstract— Modern lighting systems in industrial environments harness the potential of IoT technologies and intelligent industry concepts, facilitated by robust WiFi networks. These systems seamlessly incorporate WiFi-enabled LED lighting, intelligent controls, and real-time monitoring capabilities. By capitalizing on the data transmission capabilities of WiFi networks and employing advanced analytics, industries can make informed decisions, implement predictive maintenance strategies, and optimize operational efficiency. The seamless integration with other smart industry components, facilitated by WiFi network connectivity, allows for comprehensive optimization and fosters sustainable practices. Ultimately, these cutting-edge lighting systems establish interconnected workspaces, empowered by WiFi networks, that enhance productivity, improve well-being, and demonstrate a steadfast commitment to environmental stewardship. In this paper WiFi network is design using ESP32 for smart industrial application, All ESP32 node are behaving like Gateway .

Keywords— *WiFi Network, ESP32, IIOT*

I. INTRODUCTION

In modern industries, lighting systems have undergone significant advancements to prioritize energy efficiency, customization, automation, and connectivity [1]. LED lighting has become the standard, offering long lifespan and cost-effectiveness. Smart lighting control systems integrate features such as occupancy sensors, daylight harvesting, and remote control capabilities, optimizing energy usage. Integration with IoT platforms enables connectivity, data collection, and automation [2,3]. Wireless connectivity options like Wi-Fi and Bluetooth provide flexibility and remote control. Daylighting solutions maximize natural light penetration. Task-specific lighting meets specific operational requirements. Advanced controls allow for customization and adaptability. Energy monitoring and management optimize usage patterns and identify areas for improvement. Maintenance and performance monitoring enable proactive maintenance. Integration with other building systems enhances overall management. These advancements create well-lit, efficient, and connected work environments, improving productivity, reducing costs, and enhancing employee comfort and safety [4-6].

WiFi-enabled lighting systems in industries offer a wide range of advantages through their utilization of wireless connectivity. These systems enable wireless control, remote monitoring, and centralized management of lighting operations. Integration with WiFi networks allows for the seamless incorporation of lighting systems with other IoT devices and platforms, facilitating intelligent automation and optimization. Operators can leverage real-time data and analytics to make informed decisions, optimize energy consumption, and enhance maintenance practices. WiFi connectivity also enables smooth integration with building systems, resulting in improved overall efficiency and occupant comfort. Ultimately, WiFi networks empower

industries to establish efficient, adaptable, and interconnected lighting systems that foster increased productivity and sustainability [7-9].

Production and logistics facilities, such as warehouses, have a significant impact on the environment, [10,11] contributing to greenhouse gas emissions. Heating, cooling, air conditioning, and lighting systems account for a large portion of these emissions. Lighting, in particular, can consume up to 65% of the total energy in warehouses, leading to substantial energy costs [12-14]. As global electricity production and consumption continue to rise, companies are increasingly compelled to reduce energy consumption due to resource scarcity, higher energy prices, and growing environmental consciousness. Industrial energy efficiency initiatives aim to minimize energy requirements for providing products and services. In recent years, there has been a focus on enhancing energy efficiency and adopting renewable energy sources, supported by innovative solutions that span from smart homes to smart grids and envision the future of smart cities and factories [15]. As part of this trend, new lighting technologies have emerged to address energy efficiency challenges and improve sustainability.

The rest of this paper is organized as follows; a brief discussion about project framework is given in section II. methodology is explained in section III. The operation of the proposed circuit is discussed in section IV. Results and discussion are presented in section V and finally we concluded in section VI.

II. FRAMEWORK

The project framework demonstrates the generation of multiple ESP32 nodes by incorporating sensors and electric bulbs/LEDs. These bulbs can be interconnected in parallel to enhance the overall system performance. Communication between the ESP32 nodes is facilitated through the utilization of the ESP-NOW protocol, leveraging the Wi-Fi capabilities of the ESP32 microcontrollers. This communication is established without the need for global internet connectivity, ensuring a self-contained network environment.

During the communication process, each ESP32 node within the network transmits its unique MAC address, enabling identification of the operating node on the display unit. This identification mechanism ensures real-time monitoring and tracking of the active nodes. It is worth noting that the system may encounter various security challenges, which necessitate the development of robust smart industry security software and hardware solutions. Unauthorized attempts to manipulate the network will result in the display of the MAC address of the unauthorized device, thereby reducing security concerns.

The display unit also provides insights into the communication speed, allowing for assessment and



Shri Sant Gajanan Maharaj College of Engineering, Shegaon
Department of Business Administration and Research

3.3.3 - Number of books and chapters in edited volumes/books published and papers published in national/ international conference proceedings per teacher during year

Sr. No.	Name of teacher	Title of Book(Proceeding)	Title of Paper	Conference
1	Dr. H M Jha "Bidyarthi", Dr. P. M. Kuchar, Dr. M. A. Dande, Dr. S. M. Mishra	Case studies on Leading and strategizing for organizations across contexts (Bloomsbury Publication) ISBN - 978-93-56406-84-1	Unchained: The On-going Rise of Chain Business- A case study of Shree Abhay Group of Industries	Dec 2023, International Conference on Management Cases, Bimtech Greater Noida

Case Studies on **LEADING and STRATEGIZING for ORGANIZATIONS ACROSS CONTEXTS**

Editor
Shreya Mishra



BLOOMSBURY

BLOOMSBURY INDIA
Bloomsbury Publishing India Pvt. Ltd
Second Floor, LSC Building No. 4, DDA Complex,
Pocket C - 6 & 7, Vasant Kunj,
New Delhi 110070

BLOOMSBURY, BLOOMSBURY PRIME and the Diana logo are
trademarks of Bloomsbury Publishing Plc

First published in India 2023
This edition published 2023

Copyright © BIMTECH, Greater Noida, 2023

Shreya Mishra have asserted their right under the Indian Copyright Act
to be identified as the editor of this work

All rights reserved. No part of this publication may be reproduced or
transmitted in any form or by any means, electronic or mechanical,
including photocopying, recording or any information storage or
retrieval system, without the prior permission in
writing from the publishers

The book is solely the responsibility of the author and the
publisher has had no role in creation of the content and does not have
responsibility for anything defamatory or libellous or objectionable.

Bloomsbury Publishing Plc does not have any control over, or
responsibility for, any third-party websites referred to or in this book.

All internet addresses given in this book were correct at the time of
going to press. The author and publisher regret any inconvenience caused if
addresses have changed or sites have ceased to exist, but can accept no responsi-
bility for any such changes

ISBN: 978-93-56406-84-1
2 4 6 8 10 9 7 5 3 1

Typeset by Fortune Graphics, Naraina, New Delhi
Printed and bound in India by Replika Press Pvt. Ltd

To find out more about our authors and books, visit
www.bloomsbury.com and sign up for our newsletters

Unchained: The On-going Rise of Chain Business – A Case Study of Shree Abhay Group of Industries

H.M. Jha 'Bidyarthi"', P.M. Kuchar¹, M.A. Dand¹, S.M. Mishra¹ and A.K. Shrivastava²

ABSTRACT

Despite being surrounded by myths of underdevelopment, there are exceptional instances of entrepreneurial ventures in the countryside of India. Some of such instances are truly inborn without the slightest industrial environment in the locality. Shri Anirudh Paldiwal, one of the Directors of Shree Abhay Group of Industries, Shegaon, who took up the responsibility of Shree Abhay Link Chains business in the year 2007—one of the seven businesses of the Group—is one amongst them. Established in 1996, Shri Anirudh Paldiwal drove the company to the position of the biggest player in the market in terms of its production turnover with about 20 per cent market share in a chain business. It was enjoying sales and leveraging the demand and supply gap/supply deficit gap in the Indian Chain market. It didn't feel the need for understanding the market through research and developing its employees or market and products. But the company was left stranded amidst turbulent times due to the struggle in selling their total output because of increased capacity and dumping practices of Chinese Chain manufacturing companies. It is struggling to market its products. Sales became stagnant due to lack of expert marketing team. It posed questions about the revival, survival and growth of the company.

Dilemma: Abhay Group of Industries was enjoying sales and leveraging the demand and supply gap/supply deficit gap in the Indian Chain market. It never realised the dynamism of the chain market and hence did not attempt to develop its employees accordingly or its markets and products. The increase in its production capacity coupled with dumping practices of Chinese Chain manufacturing companies left it stranded in selling its total output and it landed amidst turbulent times and struggle. It is since struggling to market its products. Sales became stagnant due to lack of expert marketing team. What are the strategic alternatives available to him now?

Theory: Strategic Alternatives taught at the MBA 3rd / 4th semester in Strategic Management or Corporate Evaluation and Strategic Management and also Trait Theory of Entrepreneurship.

Type of case: Applied Decisional

Protagonist in a teaching case: Present – Shri Anirudh Paldiwal, Director

¹ Department of Business Administration and Research, Shri Sant Gajanan Maharaj College of Engineering, Shegaon, Buldana, Maharashtra
E-mail: hmjhabidyarthi@rediffmail.com

² Institute of Management, Pt. Ravishankar Shukla University, Raipur, Chhattisgarh
E-mail: hmjhabidyarthi@rediffmail.com

* Corresponding author.

Disclaimer: This case has been developed for academic purposes or classroom discussion and is not intended to illustrate either effective or ineffective handling of an administrative situation or to represent successful or unsuccessful managerial decision-making or endorse the views of the management.

Case questions:

- (a) What are the various Strategic alternatives available with Shree Abhay Link Chains Pvt. Ltd. (SALCPL)?
- (b) What suggestions could help SALCPL to overcome turbulent times?
- (c) What is the risk involved, and what would be the mitigation strategies to be adopted by SALCPL?
- (d) Will SALCPL curtail its expenses on diversification and divert them to focus on niche products like chains?
- (e) What strategy, including relocation of the company, should it adopt for dealing with the problem of unavailability of skilled workers?
- (f) What strategies could be adopted by the Shree Abhay Group of Industries to improve their Sales in the Indian market and abroad?

Keywords: Entrepreneurship and innovation, family business, strategic alternatives, diversification, niche market, link chains, transformational growth, takeovers

INTRODUCTION

The case presents the entrepreneurial journey of Shri Anirudh Paldiwal, the protagonist whose Group of Industries attempted many businesses from Dealership to manufacturing and alongside set up Link chain business in 1996. After the protagonist took over this link chain business he saw it succeed to the paramount level. But the company was struggling in selling the output due to increased capacity and dumping practices of Chinese Chain manufacturing companies. The protagonist faced the challenge of revival, survival and growth of his chain business. The highs and lows experienced during this period and the strategic alternatives available and their choices are lessons of Strategic management and entrepreneurship. The odyssey of Link Chain business of Shree Abhay Group of Industries, Shegaon proves to be a lighthouse in the context of rural entrepreneurship, niche business, transformational approach, diversification and other strategic alternatives.

THEORETICAL PERSPECTIVES OF ENTREPRENEURSHIP AND STRATEGY

Entrepreneurship is a complex term and hard to define (Carree and Thurik, 2005). Hence, the core aspects of entrepreneurship and their consequences cannot be measured with specificity. There have been unforeseen ups and downs in the evolution of entrepreneurial thought process when history is traced back. This includes opportunity construct, international trade, fierce competition oriented market, etc. (Murphy et al., 2006). The extent of risk and allied institutional attributes were the catalysts for entrepreneurial development in ancient and medieval times. Because of the reigning of the military actions, societal status and property/wealth were not true stepping stones for entrepreneurship opportunities (Baumol, 1990). Entrepreneurship is treated as one of the origins for contentment resulting out of the activities of the economic nature. Semantic shades of entrepreneurship are well detected and illustrated by Verin (1982). The first initial usage of the term was seen in case of designs and payments related to civil engineering and the second, the conquests by the Middle Ages Crusades (Sanchez, 2011). 'Essai sur la Nature du Commerce en Général' was the very first instance when the term 'entrepreneur' appeared. The credit for this goes to Cantillon. Van Praag (1999) focused on the factors (envisioned by various authors) turning entrepreneurship a big success. Managerial perspectives and innovation extent are the prerequisite qualities of an ideal entrepreneur (Karlsson et al., 2004). Thus, entrepreneurship reflects business ideation, projection, organization, review and monitoring as well (Panda, 2000).

Planning, profits, allocation of resources are the backbones of classic approach of strategy formulation. Strategy is followed by structure For Chandler (1962). According to Ansoff (1965), long term strategy adoption and allied benefits through reliance on leaders and strengths of the hierarchy are the crucial attributes of this approach. Transformational leadership type best fits to this approach (Kollenscher, 2017). Porter (2008) puts forth that the ways to compete and develop eventually depend upon the vision statements, mission statements, objectives and their honest implementation by the business entity. According to Sloan (1990), pioneering and sustaining strategies result in stability of the business actions.

Evolutionary approach asserts that the organizations are surrounded by the momentum and unpredictability of the macro level parameters/external environment. This influences them in a large manner (Hannan and Freeman, 1984). The most firm organizations are the ones that are truly adaptable and can cope up with the ever changing environment through change and improvement of strategies Freeman and Hannan (1989).

CONVERSATIONAL INTERVIEW

The authors telephonically contacted one of the Directors of Shree Abhay Group of Industries, Shri Bharat Paldiwal, who is also the cousin brother of the protagonist, to take his appointment for the purpose of developing a case on his esteemed organization. There was a preliminary meeting with the authors and the said Director to collect first-hand information about the organization. Since the protagonist who happens to be another Director of Shree Abhay Group of Industries was out of station the second meeting of the authors for data collection was delayed a bit. On arrival of the protagonist to headquarter, the authors again contacted him, took his prior appointment and met him on the appointed day, date and time in the premises of his company. The authors detailed him about the purpose behind developing case and the pre-requisites, i.e. consent from him for the same. The authors also narrated to him their previous case development works on micro-entrepreneurs of the region including Khamgaon, Nandura, Buldhana, etc., of Buldhana district and presented to him the list of entrepreneurs whose organizations were studied by the authors for developing cases during the last ten years. The protagonist was impressed with the track record of case development works of the authors and he accepted in principle to go ahead with developing case on his esteemed organization. The protagonist was even presented a copy of published case for his perusal and he showed interest in going through a copy of similar case of a manufacturing company that the authors had developed and published previously. The authors mailed to him the copy of said case after which followed a series of formal meetings between protagonist and the authors over the following period each meeting extending to two hours or more.

The authors had no or very little knowledge about the targeted organization hence the data collection was done through conversational interview during these meetings. There was no structured questionnaire but the questions followed based on conversation with the protagonist to which the answers were elicited from the later. Meanwhile there also came up a suggestion from the protagonist to modify the title of the case which was duly changed with prior permission of the conference organizer. The conversation led to many relevant questions which finally helped

in collecting detail information about the entrepreneur, the approach of his family, the number of businesses and the background of their origin, the challenges faced, the strategies adopted in attempt to overcome some of these challenges, the dilemma being currently faced, etc. At times there followed telephonic conversations also with the protagonist for certain clarifications and the protagonist extended full cooperation in all these. The authors discussed the draft of the case study with the protagonist over subsequent meetings and after several modifications and revisions it was finalized.

CHRONOLOGY OF JOURNEY OF SHREE ABHAY GROUP OF INDUSTRIES

It all started with Shri. Kewalramji Paldiwal, great great grandfather of the protagonist migrated from Rajasthan to Shegaon in Maharashtra round about the year 1900 and started farming. Years later, Shri. Muktilalji Paldiwal's entrepreneurial instinct led him to start trading in Agricultural Commodities in around 1940. This continued in the family till 1974. Investment in the share/stock market was a novel and untraveled path chosen by this family somewhere around 1970's.

Mr. P.E. Jhunjhunwala, a key person in Hercules Hoist Ltd. approached Shri. Muktilalji Paldiwal and asked for starting the business of manufacturing chain pulley blocks (CPB). Shri. Rajeshji Paldiwal, father of the protagonist, was then pursuing CA with the intention to get employed and earning a handsome salary. Shri. Rajeshji was persuaded to leave the CA course and start a Chain Pulley Block manufacturing business in 1982 and become an employer instead of seeking employment. This is how the seeds of the Shree Abhay Group of Industries were sown by starting the very first company in the name of Shree Abhay Industries (SAI) in manufacturing the Chain Pulley Block for Indef (Hercules Hoists Ltd. – A Bajaj Group Company). There used to be a waiting period of 1 to 2 years in the delivery time of CPB (Chain Pulley Block) in the Indian market. Also, there was strike in Hercules Hoists Ltd. that lasted for about a year and resulted in pending orders of 2–3 years.

Shri. Dineshji Paldiwal, uncle of the protagonist, started Shiv Udyog (Dealership for Indef products) in 1984 which was followed by acquiring Shriram Estate (1987) in about 1 Lakh Sq. feet godowns and around 6 lakh square feet of land in the heart of Shegaon for Warehousing purposes and Abhay Krishi Udyog Pvt. Ltd. (AKUPL) in 1987. A major milestone occurred when a backward integration with the help of Mr. H. A. Nevatia was done by starting the manufacturing of Hand chain/mild steel chain of 5 and 6 mm diameter chain used in CPB with a capacity – 25 Tonnes/month. He also laid a foundation of a Pilot plant of Crane manufacturing in the premises of Abhay Krishi Udyog Pvt. Ltd. in 1998. Shree Abhay Cranes Pvt. Ltd. (SACPL) added colours to the business in 1999 to manufacture cranes on a larger and commercial scale after tasting success and a lucrative market for the cranes.

The plant and machinery of the Indian Link Chains Manufacturers Ltd., Bhandup, Mumbai was taken over in 2005 with the help of Mr. P.K. Nevatia and shifted to Shegaon resulting in increased capacity. Shree Abhay Hoists and Engg. Pvt. Ltd. (SAHEPL) was started with a capacity – 30–35 Tonnes/month to manufacture Load chains/Alloy steel chains.

Shri Anirudh Paldiwal, the protagonist, joined the family business and took over the Link chain business segment in 2007 after completing his formal education in Production Engineering

and Master's in Strategic Entrepreneurship from the University of Southampton, UK. Being a Production Engineer, he was interested more in Mass manufacturing systems. So, he joined the link chain business. After joining the business, he took some aggressive decisions to boost the scale and functioning by hiring the then-highly paid and skilled machine operators and his decisions paid off.

Shri. Bharat Paldiwal, the cousin of the protagonist, joined the family business and took over the Crane manufacturing business segment in 2012 after completing his formal education in Mechanical Engineering and Masters in Business Management from SJMSOM, IIT, Mumbai.

They took over Uniseven Pvt. Ltd., Ambarnath and shifted the machines to the premises of SAHEPL in 2013. This resulted in an increased capacity to 70 Tonnes/month and widened the range of manufacturing the Alloy steel chains from 6 mm to 13 mm. diameter. Hindustan Parsons Pvt. Ltd., Nashik was also taken over and the machines were shifted to the premises of SAHEPL in 2015. This again resulted in an increased capacity to 150 Tonnes/month and widened the range of manufacturing the chains from 6 mm to 36 mm. diameter.

In 2016, Vivek Paldiwal, cousin brother of the protagonist and an Electrical Engineer and Master in Family Business Management from NMIMS, Mumbai entered into Solar EPC (Engineering Procurement and Commissioning) segment of Shree Abhay Group of Industries. He is successfully managing the installation of solar projects of industrial, residential, and commercial scale ranging from 10 KW to 3 MW and is able to provide services to Tier I cities like Mumbai, Bengaluru.

In 2018, two sets of machines of manufacturing Mild Steel Chains were imported from Germany to the premises of AKUPL.

In 2019, SACPL successfully developed wire rope hoists and launched them under their own brand name 'Abhay'. Bharat Paldiwal, cousin brother of the protagonist, was instrumental in using his domain expertise of Mechanical Engineering to accomplish this.

SALCPL was established in 2021 to import ten sets of Mild Steel Chain manufacturing machines and seven sets of Alloy Steel Chain manufacturing machines in 2022. This resulted in an increase in chain manufacturing capacity up to around 400 Tonnes/month and SALCPL emerged as the largest chain manufacturer in India in terms of capacity.

All three brothers and a sister including the protagonist representing the third-generation entrepreneurs of Shree Abhay Group of Industries are professionally highly qualified being engineers of different streams and MBAs in Family Business Management passed out from reputed engineering and management colleges including IIT and the protagonist himself an M.Sc. in Strategic Entrepreneurship from UK besides being an engineer as obvious from the table no. 2 given in the annexure. The second generation of entrepreneurs is also highly qualified and yet they decided to set up their business at a Taluka-Level Village of Shegaon.

There are now seven lines of business entities launched by Shree Abhay Group of Industries as shown below. Amongst these, the chain business is a rising business that occupies a prominent place at the national level.

1. Alloy Steel Chains, Mild Steel Chains, Stainless Steel Chains, Chain Slings and Accessories

2. EOT (Electric Overhead Traveling) and HOT (Hand Operated Travelling) Cranes, Jib Cranes, Stacker Cranes, etc.
3. Wire Rope Hoists and Winches
4. Solar EPC (Engineering Procurement and Commissioning)
5. Warehousing
6. Agriculture and Farming
7. Investment in Stock Market

Thus today there are seven business entities under the Shree Abhay Group of Industries as shown in Chart 2 given in the annexure to this paper. The chronology of the entrepreneurial journey as explained has been presented in the Table 1 along with the family tree in Chart 1 given in the annexure to this paper.

LINK CHAIN PROGRESS BY SHREE ABHAY GROUP OF INDUSTRIES

When the Big companies become even bigger, the smaller companies become weak. The chain manufacturing industry had limited players in the Indian market. Many smaller companies were facing financial crunch and problems keeping their business running. This opportunity was encashed by the Shree Group of Industries to grow in terms of capacity and range making them second largest manufacturer in terms of Range and second to none (leader) in terms of capacity.

Entering into the business of manufacturing chains due to longer waiting times for delivery in 1996 to becoming the largest manufacturer in 2022 has been a phenomenal and transformational growth story. Taking over the sick units in 2005, 2013, 2016, 2018, and 2022 and shifting their machines to remote places like Shegaon required grit.

Hindustan Parsons Pvt. Ltd. was a part of huge group of companies making approx. 5000 Cr. of turnover annually. Their chain manufacturing unit was making around 5 Cr. of revenue. This group was too big to keep operating their chain manufacturing unit and thus they decided to sell this unit. It was bought by SAHEPL and they started making 17–18 Cr. of revenue from the same machines where Hindustan Parsons was able to make only 5 Cr.

One of the companies in a European country was stuck with the problem of not having a successor to look after their business. This compelled them to look for a buyer for their plant and machinery to finally sell it off. It is generally seen in the business families that their current generation has its own dream to create their own destiny by venturing to tread the unconventional path and thus showing no inclination towards carrying forward the legacy and profession of their parents. The Paldiwal family as obvious from its family tree (Chart 1) and family members profession (Table 2) is an exception to the stated existing trends in the business family. Hence this Plant and Machinery from the European country was imported to Shegaon in 2022.

CHALLENGES AND DILEMA

The journey of the protagonist has not been free flowing and he came across several challenges in running his link chain business at a Taluka-village like Shegaon. The nature and magnitude of these challenges as listed below are much diversified requiring professional expertise to deal with.

1. **Unavailability of Skilled Engineers and Labours:** Engineering students have a liking for working in Tier I cities and on handsome packages sitting in cubicles. They appear to be more fascinated towards the glamorous life style of such cities and are also averse towards doing physical works. Add to it is lack of courses, ITIs and other similar skill centres churning out such skilled man power here. Considering the cost of living and other hardships in these cities the Shree Abhay Group of Industries offers better perks, facilities and above all a healthy living at Shegaon yet there is unavailability of good engineers, machine operators, and skilled labours here which poses a great challenge as it is very crucial for this labour-intensive business. The shortage of requisite man power is a great hurdle for a labour intensive industry in its growth at a faster pace.
2. **Absenteeism of Workers:** It is also seen that the BPL families which constitute the major source of labour force get the benefit of a number of schemes offering them subsidised grains and other household commodities. Thus if they work for three to four days in the company their daily wage becomes sufficient for sustaining their family for whole week. This tends them to frequently absent from work affecting the production turnover and hence production cost due to under-utilization of the plant capacity.
3. **Absence of Marketing Consultants and Agencies:** Services of marketing consultants and agencies are not at all available at Shegaon as it is a small place and as it does not offer sizeable consultancy business for them to profitably operate here. It is also experienced that those of similar agencies which are in abundance in Mumbai, Pune etc. show logistical issues along with time constraints to offer their services to Shree Abhay Group of Industries. It inhibits identification of new markets, new customers and understanding of their growing needs for link chain so that the company could modernise its product line and penetrate into newer markets.
4. **Absence of Export Promotion Agencies:** There is a dire need of export promotion agencies either at Shegaon or any other place from where they are willing to connect to Shegaon in order to cater to the needs of foreign customers. The export promotion agencies are conspicuous by their absence in Shegaon.
5. **Overlooked the Importance of Marketing:** Shree Abhay Group of Industries enjoyed for a longer duration the luxury of its supplies being totally consumed by its market. It therefore hardly looked to the marketing side of the business. It didn't pay any attention to enhancing the customer base in India and abroad and promoting their products in the market. But as it grew in capacity and its production enhanced and it noticed the presence of many competitors and smaller companies in the market eating up its own existing market share it was taken aback. It now realizes that it overlooked the importance of marketing.
6. **Dumping Practices from Chinese Companies:** Chinese companies were dumping their products into the Indian market at very lower prices. This posed stiff competition. Moreover, Indian companies needed products at lesser prices and there was huge demand for substandard commercial chains. This is how Chinese companies were dumping their inferior quality goods into the Indian market posing a tough competition for Shree Abhay Group of Industries.

7. **Impact of Steel Index:** There is a huge impact of the Steel index on Shree Abhay Group of Industries as the major raw material is steel. Fluctuating prices of Steel in the commodity market make it difficult to keep the prices constant. Also, it is not possible to change the prices due to already-signed contracts and relations with regular customers.

These challenges pushed Abhay Group of Industries from the state of fully enjoying sales and leveraging the demand and supply gap/supply deficit gap in the Indian Chain market to stagnation. Meanwhile, the consistent increase in its production capacity to expand to lucrative Indian Chain Market coupled with dumping practices of Chinese Chain manufacturing companies left it stranded in selling its total output and it landed amidst turbulent times and struggle. It is since struggling to market its products. Sales became stagnant due to lack of expert marketing team. What are the strategic alternatives available to him now?

STRATEGIES ADOPTED TO DEAL WITH THE CHALLENGES

Getting awareness of the challenges of any business is the beginning in the direction of its dissolution. The protagonist is committed to take forward his business despite several odds and hence resorted to following strategies time and again.

1. **Proper Financial Management:** Shree Abhay Group of Industries has around 400 acres of farming/agricultural land. Moreover, they have been investing in the Share market since 1970. The income from these diversified sources has helped them to infuse capital in expansion plans of lines of manufacturing and EPC business. This is how they never felt the financial crunch and never been on the mercy (laid hands) of the banks/financial institutions. The income from the Share market and farming kept the show going on.
2. **Firm Support from the Family:** The Paldiwal family is still HUF (Hindu Undivided Family). This is strength of the family and expertise from all the members helps in evaluating the strategic alternatives and taking better decisions. This is evidenced from the family tree given in Chart no. 1 in annexure.
3. **In-depth Understanding of the Matter:** All six members of the family from grandfather, father, uncle to three siblings develop an in-depth understanding of the matter at hand and decisions are made thereafter on thorough discussion of the pros and cons. Domain expertise of family members from diversified areas brought to the decision table adds another advantage. Premises and aftermaths are well thought out and consensus is built on the decisions.
4. **Timely Adaptive Approach:** Stiff competition from Chinese companies was fought on a Cost-to-Cost basis by Shree Abhay Group of Industries. At certain times, they ran the business on the BEP (Break Even Point). Dumping practices of China were fought by dialogue with the customers and by making certain changes (altering) in their product mix lines.
5. **Integrity:** 'Work with Integrity evaporates Scarcity' – stands true in their case. Even after the dumping practices from Chinese companies and the challenges of selling products, Shree Abhay Group of Industries refrained itself from indulging in manufacturing inferior and substandard chains. These chains are used in industries and it involves the risk of many lives. They even didn't purchase low-quality Chinese raw materials to help domestic Indian companies grow.

THE FUTURE AHEAD

The protagonist has a vision for the future. As of now, he has the following plans.

1. The Indian market is already saturated and they are one of the largest manufacturers in terms of Capacity and Range/Variety. Hence their future plan is to start exporting their products to overseas market.
2. They envisage maintaining their Leadership position in the chain manufacturing business.

WHY SETUP BUSINESS IN SHEGAON – A TALUKA-LEVEL VILLAGE?

Shree Abhay Group of Industries made a conscious decision through the consensus of its family members to carry out diversified businesses under this umbrella group at a Taluka-Level Village called Shegaon under Buldhana district of Vidarbha region of Maharashtra State. The protagonist advances the following reasons in favour of this decision.

1. **Absence of Undue/Irrelevant Problems of the Workers:** Unlike Tier-I cities and developed Industrial areas, Scattered Labour markets and uninformed labours help in keeping the undue workers' problems at bay. Problems like Strikes, Work outages, and demand for a rise in wages and salaries are negligible here.
2. **Stronghold of Family in Shegaon Town:** Paldiwal family relocated from Rajasthan to Shegaon in 1900 and since then they have been residing as a well-known and a well to do family in Shegaon. This stronghold helps them in access to various resources needed to setup and scale businesses in Shegaon.
3. **Peaceful Life:** Shegaon is a small town and blessed by Shri Sant Gajanan Maharaj which offers peaceful countryside life away from pollution. Availability of nutritious and fresh food of countryside, access to clean natural air, water and soil are other parameters that offer a comfortable life here and hence preference for Shegaon.
4. **Contentment:** The Paldiwal family is very happy with the scale at which they are working right now and feel contented with their achievements. Life is all about satisfaction and happiness and so where else than Shegaon?

CONCLUSIONS

Entrepreneurship and family business have been catalysts in the socio-economic development of the world, specifically, the developing countries. But this hustle and bustle has resulted into some problems as well. Centralization of entrepreneurial ventures, growing size of cities, allied migration can be treated as foremost of them. It is quite interesting that solaces to contemporary problems can be traced into literature of the great people. Years before, he was Mahatma Gandhi who had appealed, 'Come countryside.' Tukdoji Maharaj, a Saint from Maharashtra had emphasized on the significance of the rural area through his classic 'Gram-Geeta'. And alas! It was never possible for most of the Indian ventures. But Shri Anirudh Paldiwal through his Shree Abhay Group of Industries, Shegaon has proved to be a true exemplar of victorious countryside entrepreneurial emergence. Despite the ever-changing turbulent business environment such as changing government regulations, digitalization, demographic shifts, and competition from foreign players, rising costs of raw materials and production, unavailability of skilled man power,

etc., Shree Abhay Group of Industries is successful in raising itself. The countryside family businesses and entrepreneurial ventures have much to learn and adopt from this case because of the unique indigenous approach. However, answers to some questions need to be found out. What are the various Strategic alternatives available with Shree Abhay Group of Industries? What suggestions could help Shree Abhay Group of Industries to overcome turbulent times? What is the risk involved and what would be the mitigation strategies to be adopted by Shree Abhay Group of Industries? Will Shree Abhay Group of Industries curtail its expenses on diversification and divert them to focus on niche products like chains? What strategy including relocation of the company should it adopt for dealing with the problem of unavailability of skilled workers? What strategies could be adopted by the Shree Abhay Group of Industries to improve their Sales in the Indian market and abroad?

REFERENCES

- A. Sloan (1990): *My Years with General Motors, Reissue Edition*, Crown Business, New York, NY, USA.
- Baumol W (1990). Entrepreneurship: Productive, unproductive, and destructive, *J. Polit. Econ.*, 98(5): 893–921.
- Carree M, Thurik R (2006). Understanding the role of entrepreneurship for economic growth. *Entrep. Econ. Growth*, 134(2): 68–79.
- D. Chandler (1962): *Strategy and Structure: Chapters in the History of the American Industrial Enterprise*, Beard Books, New York, NY, USA.
- E. Kollenscher, D. Eden, B. Ronen, and M. Farjoun (2017): 'Architectural leadership: The neglected core of organizational leadership,' *European Management Review*, vol. 14, no. 3.
- H. I. Ansoff (1965): *Corporate Strategy: An Analytic Approach To Business Policy for Growth and Expansion*, McGraw-Hill, Arbor, MI, USA.
- J. Freeman and M. T. Hannan (1989): 'Setting the record straight on organizational ecology: Rebuttal to young,' *American Journal of Sociology*, vol. 95, no. 2, pp. 425–439.
- Karlsson C, Friis C, Paulsson T (2004) Relating entrepreneurship to economic growth, CESIS/JIBS Electronic Working Paper Series.
- M. Hannan and J. Freeman (1993): *Organizational Ecology*, Harvard University Press, London, UK.
- M. Porter (2008): *Competitive Strategy: Techniques for Analyzing Industries and Competitors*, Simon and Schuster, New York, NY, USA.
- M. T. Hannan and J. Freeman (1984): 'Structural inertia and organizational change,' *American Sociological Review*, vol. 49, no. 2, pp. 149–164.
- Murphy PJ, Liao, J, Welsch, HP (2006). A conceptual history of entrepreneurial thought, *J. Manage. Hist.*, 12(1): 12–35.
- Panda NM (2000). What Brings Entrepreneurial Success in a Developing Region? *Journal of Entrepreneurship*, 9(2): 199–212.
- Sanchez JC (2011). Entrepreneurship as a legitimate field of knowledge, *Psicothema*, 23(3): 427–32.
- Van Praag CM (1999). Some Classic Views on Entrepreneurship, *De Economist*, 147(3): 311–35.

ANNEXURE

Table 1: Showing Chronology of Development of Shree Abhay Group of Industries

Year	Incident	Name of Key Person from Family
1900	Great great Grandparents settled in Shegaon, Maharashtra from Rajasthan and started doing Farming	Shri Kewalramji Paldiwal
1940	Started Trading in Agricultural Commodities	Shri Ganulalji Paldiwal
1970	Started doing Investments in the Share/Stock Market	Shri Muktilalji Paldiwal
1982	Shree Abhay Industries (SAI) was started	Shri Rajeshji Paldiwal
1984	Shiv Udyog was started (Dealership for Indef products)	Shri Dineshji Paldiwal
1987	Bought Shriram Estate (About 1 Lakh Sq. feet godowns in the heart of Shegaon for Warehousing purposes.	All the Family members
1996	Started Abhay Krishi Udyog Pvt. Ltd. (AKUPL)	Shri Dineshji Paldiwal
1998	Pilot plant of Crane manufacturing was started in the premises of Abhay Krishi Udyog Pvt. Ltd.	Shri Dineshji Paldiwal
1999	Shree Abhay Cranes Pvt. Ltd. (SACPL) was started to manufacture cranes on a larger and commercial scale after tasting success and a lucrative market for the cranes.	Shri Dineshji Paldiwal
2005	Takeover – The Indian Link Chains Manufacturers. Ltd., Bhandup, Mumbai resulting in increased capacity. Shree Abhay Hoists and Engg. Pvt. Ltd. (SAHEPL) was started to manufacture Load chains / Alloy steel chains Capacity – 30–35 tonnes/month	Shri Rajeshji Paldiwal
2007	Shri. Anirudh Paldiwal joined the family business and took over the Link chain business segment after completing his formal education in Production Engineering.	Shri Anirudh Paldiwal
2012	Shri. Bharat Paldiwal joined the family business and took over the Crane manufacturing business segment after completing his formal education in Mechanical Engineering.	Shri Bharat Paldiwal
2013	Takeover – Uniseven Pvt. Ltd., Ambarnath and shifted the machines to the premises of SAHEPL	Shri Anirudh Paldiwal
2015	Takeover – Hindustan Parsons Pvt. Ltd., Nashik, and shifted the machines to the premises of SAHEPL	Shri Anirudh Paldiwal
2016	Started Solar EPC (Engineering Procurement and Commissioning)	Shri Vivek Paldiwal.
2018	Imported two sets of machines of manufacturing Mild Steel Chains from Germany to the premises of AKUPL	Shri Anirudh Paldiwal
2022	SALCPL imported ten sets of Mild Steel Chain manufacturing machines and 07 sets of Alloy Steel Chain manufacturing machines.	Shri Anirudh and Vivek Paldiwal

Table 2: Showing Educational Background of Family Members of Shree Abhay Group

S. No.	Name of the Family Member	Academic Qualification	Profession and Responsibility
1.	Shri Muktilalji Paldiwal	SSC	Overall Management,
2.	Shri Rajeshji Paldiwal	M. Com., CA (Left to start Shree Abhay Industries)	Compliance and Expansion Decisions of Shree Abhay Group of Industries
3.	Shri Dineshji Paldiwal	M. Com.	

S. No.	Name of the Family Member	Academic Qualification	Profession and Responsibility
4.	Shri Anirudh Paldiwal	Diploma in Production Engineering, from Father Agnel College, Mumbai; B.E. Production Engineering, from VIT, Pune; M.Sc. Strategic Entrepreneurship from the University of Southampton, UK	Joined as CEO, Shree Abhay Link Chain Business in 2007
5.	Shri Bharat Paldiwal	B.E. Mechanical from VNIT, Pune; MBA from SJMSOM, IIT, Mumbai	Joined as CEO, Shree Abhay Cranes business in 2012
6.	Shri Vivek Paldiwal	B.E. Electrical from Ramdeobaba College of Engineering, Nagpur; MBA – Family Business Management from NMIMS, Mumbai	Joined as CEO, the Solar Division of Shree Abhay Industries in 2016
7.	Smt. Prachi	B.Com.; Diploma – Jewellery Design – SNDT, Mumbai; MBA – Family Business Management – NMIMS, Mumbai	

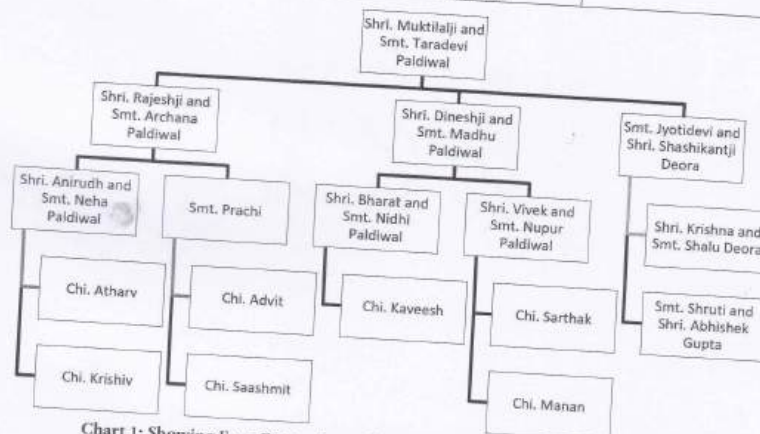


Chart 1: Showing Four Generations of Family Members of Shree Abhay Group

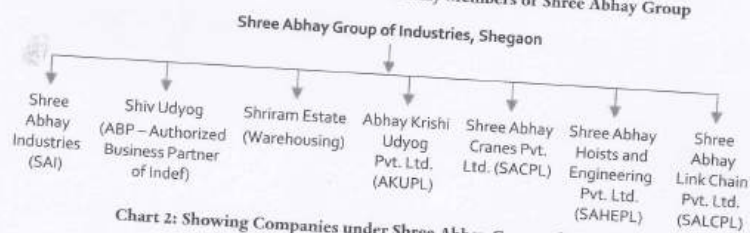


Chart 2: Showing Companies under Shree Abhay Group of Industries



Sahakar Maharshi Late Bhaskarrao Shingne Arts College

Khamgaon, Dist.-Buldhana (NAAC Re-accredited A+)

(Affiliated to Sant Gadge Baba Amravati University, Amravati, M. S.)

Shri R. L. T. College of Science, Akola (NAAC Re-accredited A)

(Affiliated to Sant Gadge Baba Amravati University, Amravati, M. S.)

&

Shri Sant Gajanan Maharaj College of Engineering, Shegaon

(Affiliated to Sant Gadge Baba Amravati University, Amravati, M. S.)

Jointly Organize

***One Day National Level Inter-Disciplinary E-Conference on
Contemporary Dynamics in Humanities, Science & Technology
Monday, 22 April 2024***

CERTIFICATE

This is to certify that Mr./Mrs./Miss/Dr. Dr. Anand Tale participated in the One Day National Level Inter-Disciplinary E-Conference on ***“Contemporary Dynamics in Humanities, Science & Technology”*** on 22 April 2024.

Dr. Saurabh Jadhao
Convener
S.S.G. M.C.E.,
Shegaon

Dr. Pradip Deohate
Convener
Shri R. L. T. College
of Science, Akola

Dr. Dayanand Raut
Convener
S. M. B. S. College,
Khamgaon

Dr. S. B. Somani
Principal
S.S.G.M.C.E.,
Shegaon

Dr. V. D. Nanoty
Principal
Shri R. L. T. College
of Science, Akola

Dr. Sanjay Patil
Principal
S. M. B. S. College
Khamgaon



ज्ञान-विज्ञान विमुक्तये
Peer Reviewed Referred
and UGC Listed Journal
Journal No. 40776

ISSN - 2277 - 5730

An International Multidisciplinary
Quarterly Research Journal

AJANTA



ISO 9001 : 2015 QMS
ISBN / ISSN

Volume - XIII, Issue - II, April - June - 2024

Single Blind Review / Double Blind Review

Impact Factor 2023 - 7.428 (www.sjifactor.com)

Is Herby Awarding This Certificate to

Dr. A. S. Tale

In Recognition of the Publication of the Paper Titled

Effect of Noble Metal (Ag) doping on Hydrogen
Sensitivity of WO₃ Thin Film Sensors

Ajanta Prakashan

Jaisingpura, Near University Gate, Aurangabad. (M.S) 431 004

Mob. No. 9579268077, 9822620877,

ajanta2023@gmail.com, www.ajataprakashan.in

Editor : Vinay S. Hatole



SAHAKAR MAHARSHI LATE BHASKARRAO SHINGNE ARTS COLLEGE

KHAMGAON, DIST. BULDHANA (NAAC Re-accredited A+)

(Affiliated to Sant Gadge Baba Amravati University, Amravati, M.S.)

SHRI R. L. T. COLLEGE OF SCIENCE, AKOLA (NAAC Re-accredited A)

(Affiliated to Sant Gadge Baba Amravati University, Amravati, M.S.)

&

SHRI SANT GAJANAN MAHARAJ COLLEGE OF ENGINEERING, SHEGAON

(Affiliated to Sant Gadge Baba Amravati University, Amravati, M.S.)

Jointly Organize

One Day National Level Inter-Disciplinary E-Conference on

CONTEMPORARY DYNAMICS IN HUMANITIES, SCIENCE & TECHNOLOGY

Monday, 22nd April 2024

CERTIFICATE

This is to certify that **Dr. A. S. Tale**, Department of Physics, Sant Gajanan Maharaj College of Engineering, Shegaon. (Maharashtra) has participated / presented paper entitled **"Effect of Noble Metal (Ag) doping on Hydrogen Sensitivity of WO₃ Thin Film Sensors"** in the One Day National Level Inter-Disciplinary E-Conference on **"Contemporary Dynamics In Humanities, Science & Technology"** on 22nd April 2024.

His/her paper has been published in **Peer Reviewed Refereed & UGC Listed Journal No. - 40776 - AJANTA - ISSN - 2277 - 5730 with Impact Factor - 7.428.**

Dr. Saurabh Jadhao
Convener
Shri Sant Gajanan
Maharaj C.O.E., Shegaon

Dr. Pradip Deohate
Convener
Shri R.L.T. College
of Science, Akola

Dr. Dayanand Raut
Convener
S.M.B.S. College
Khamgaon, Dist. Buldana.

Dr. Sunil Somani
Principal
Shri Sant Gajanan
Maharaj C.O.E., Shegaon

Dr. V. D. Nanoty
Principal
Shri R.L.T. College
of Science, Akola

Dr. Sanjay Patil
Principal
S.M.B.S. College
Khamgaon, Dist. Buldana.



SGBAU/UGC-HRDC/2023-24/RC/NEP/215

UNIVERSITY GRANTS COMMISSION
MALAVIYA MISSION TEACHER TRAINING CENTRE
SANT GADGE BABA AMRAVATI UNIVERSITY, AMRAVATI (M.S.)

Certificate



This is to Certify that

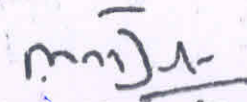
Dr Anand Shriram Tale
Associate Professor

Shri Sant Gajanan Maharaj College of Engineering Shegaon
Affiliated To Sant Gadge Baba Amravati University, Amravati

has participated in the UGC sponsored Refresher Course – National Education Policy And
Its Implementation (Inter Disciplinary) held during 12 Feb 2024 to 24 Feb 2024 and
obtain Grade - A+


Director


Co-ordinator


Vice- Chancellor



सत्यमेव जयते
Government of India



ज्ञान-विज्ञान विमुक्तये
University Grants Commission

CERTIFICATE OF PARTICIPATION

NEP 2020 ORIENTATION & SENSITIZATION PROGRAMME

This is to certify that **Dr.Anand Shriram Tale** from Shri Sant Gajanan Maharaj College of Engineering, Shegaon has completed the NEP 2020 Orientation & Sensitization Programme under Malaviya Mission Teacher Training Programme (MM-TTP) of University Grants Commission (UGC) Organized by Coimbatore Institute of Technology (CIT) from 04/12/2023 to 13/12/2023.

Dr.V.Manikandan

Coordinator (MM-TTC), CIT



Dr.A.Rajeswari

Principal, CIT

Study of Magnesium Doped Zinc Cobaltite Thick Film for Resistive Type H₂S Gas Detection

T. R. Tatte

*Department of Physics, Shri. Dr. R. G. Rathod Arts and Science College,
Murtizapur, 444107, Maharashtra State, India.*

E-mail: truptitatte21@gmail.com

V. D. Kapse

*Department of Physics, Arts, Science and Commerce College,
Chikhaldara 444807, Maharashtra State, India.*

D. R. Patil

*Bulk and Nanomaterials Research Laboratory, Department of Physics,
R. L. College, Parola 425111, Maharashtra State, India.*

M. S. Pande

*Department of Physics, Gajanan Maharaj College of Engineering,
Shegaon, 444203, Maharashtra State, India.*

Abstract:

This work devotes to investigate synthesis of spinel $Zn_{0.7}Mg_{0.3}Co_2O_4$ structure was successfully synthesized by sol-gel method. Surface morphology was examined by means of Scanning electron microscopy (SEM). The gas sensing investigations revealed that $Zn_{0.7}Mg_{0.3}Co_2O_4$ nanostructured based gas sensor exhibited high response (50 ppm) and selectivity towards hydrogen sulfide. Besides, enhanced gas sensing properties of $Zn_{0.7}Mg_{0.3}Co_2O_4$ nanostructures are observed. The excellent gas sensing characteristics of $Zn_{0.7}Mg_{0.3}Co_2O_4$ nanostructures might be attributed to their high porosity and large specific surface area. Moreover, hydrogen sulfide gas sensing mechanism was proposed to explain the high sensor response.

Keywords: Sol-gel; Oxalic acid; Spinel; $Zn_{0.7}Mg_{0.3}Co_2O_4$; XRD.

1. Introduction

Rapid technological and industrial developments continuously result in the emission of hazardous gases, toxins, harmful, flammable and explosive gases and biomolecules. Therefore, sensing of such undesirable chemical or biochemical forms has become a significant research endeavor in recent years [1-3]. The effective detection and removal of toxic gases in the atmosphere is important for human as well as any living organisms. The uncontrolled release of toxic

gases such as CO, H₂S, NH₃, CH₃CH₂OH, etc. from automobiles, industries, laboratories, etc. cause severe health problems and they may even cause death [4-6]. Advanced sensing materials have been adopted in this context to achieve high responsivity combined with less response/recovery time and continuous detection of gas molecules for gas sensors, which are key quality factors that define the sensor performance. In particular, oxides are extensively researched for gas sensing, in view of their robust material properties and their ability to change valence through charge transfer [7-9].

Nanocrystalline ZnCo₂O₄ has also been applied as electro catalyst for many anodic processes such as oxygen evolution [10], photocatalyst [11] and semiconductor gas sensor [12]. In cobalt based ZnCo₂O₄ cubic spinel structure, where Zn divalent ions occupy the tetrahedral and Co trivalent ions occupy octahedral site [13]. Nanostructured ZnCo₂O₄ is stable and cheaper than noble metals [14]. Moreover, it is also active in alkaline solutions.

In this work, we present the synthesis and study of the gas sensing properties of Zn_{0.7}Mg_{0.3}Co₂O₄ nanomaterial for the detection of H₂S. The operating temperature of the material and its interaction mechanism with the H₂S has a crucial effect on the response and selectivity of the sensing device. The results obtained show that the Zn_{0.7}Mg_{0.3}Co₂O₄ nanostructure exhibits an excellent sensing performance for potential applications in H₂S gas sensors.

2. Experimental

2.1 Preparation of Zn_{0.7}Mg_{0.3}Co₂O₄ powder

The appropriate amounts of start materials Co(NO₃)₂·6H₂O (99.0%) and Zn(NO₃)₂·6H₂O (99.0%) were dissolved in ethanol (95.0%), mixed well with each other, and then slowly adding ethanol solution of oxalic acid (99.8%) at room temperature under constant magnetic stirring. The mixture was then stirred for 3 h and then evaporated at 80 °C for 1 h under constant stirring, which led to the formation of a sol. The sol was heated at 100°C for 1 h until a gel was formed. Subsequently dried for 1 h in an electric oven and ground the gel, thus the oxalate precursor powder was attained. The resulting material was calcined at 500°C for 2 h and well-crystallized spinel Zn_{0.7}Mg_{0.3}Co₂O₄ powder was obtained.

2.2. Fabrication of sensor

Appropriate quantity of mixture of organic solvents such as butyl cellulose, butyl carbitol acetate and turpineol was added to the mixture of $\text{Zn}_{0.7}\text{Mg}_{0.3}\text{Co}_2\text{O}_4$ and a solution of ethyl cellulose (a temporary binder). The mixture was then ground to form paste. The paste obtained was screen printed onto a glass substrate in desired patterns. The thick films so prepared were fired at 500°C for 1h.

3. Result and discussion

3.1. X-ray powder diffraction (XRD) analysis

Fig. 1 shows the XRD pattern of the synthesized $\text{Zn}_{0.7}\text{Mg}_{0.3}\text{Co}_2\text{O}_4$ nanomaterial at 500°C for 2 h. It exhibits the diffraction peaks appeared at 2θ values 19.6° , 31.15° , 36.711° , 63.06° , 65.047° and 68.0° correspond to the crystal planes of (111), (220), (311), (222), (422), (511), (440), (620), (533) and (622) respectively which confirms the formation of pure $\text{Zn}_{0.7}\text{Mg}_{0.3}\text{Co}_2\text{O}_4$ spinel structure.

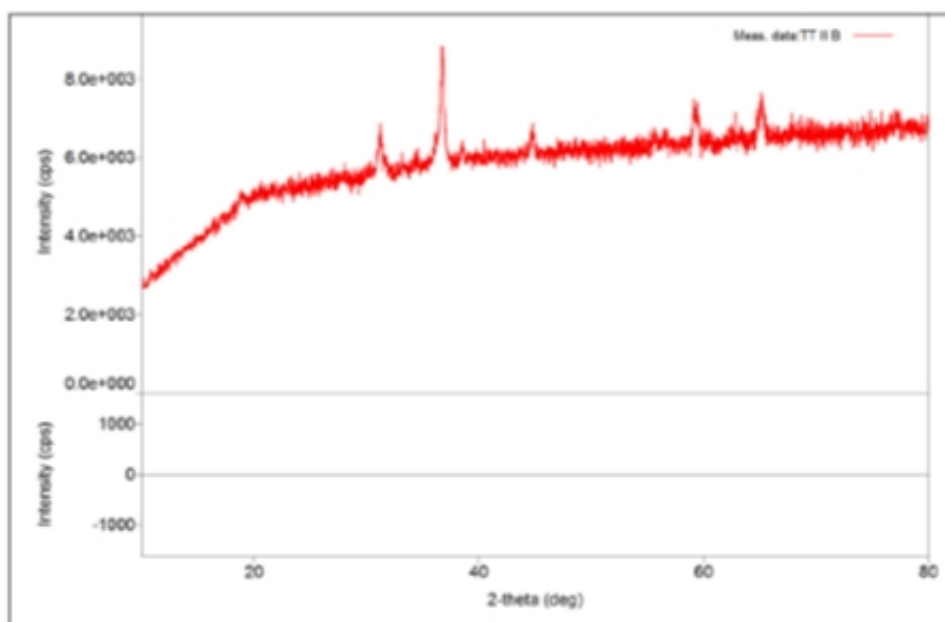


Fig. 1. XRD patterns of $\text{Zn}_{0.7}\text{Mg}_{0.3}\text{Co}_2\text{O}_4$ annealed at 500°C .

The crystallite size was calculated by using the Debye–Scherrer equation.

$$D = \frac{k\lambda}{B\cos\theta} \quad (1)$$

Where, D is the average size of the crystallite, assuming that the grains are spherical, k is 0.9, λ is the wavelength of X-ray radiation,

B is the peak full width at half maximum (FWHM) and θ is the angle of diffraction. The crystalline size of the calcined mixed precursor is found to be 18 nm.

3.2. Fourier transform-Infrared spectra (FT-IR) analysis

$\text{Zn}_{0.7}\text{Mg}_{0.3}\text{Co}_2\text{O}_4$ powder spectrum presented in Fig. 2. Generally, vibrations of metal ions in the crystal lattice are in the range of 400-4000 cm^{-1} in FTIR analysis. From Fig. 2, it can be obtained that the peak at 667 cm^{-1} is attributed to the stretching vibration mode of M–O for the tetrahedrally coordinated metal ions. The band at 573 cm^{-1} can be assigned to the octahedrally coordinated metal ions.

Content of this meant for your information and should not be used for advertisement, evidence or litigation

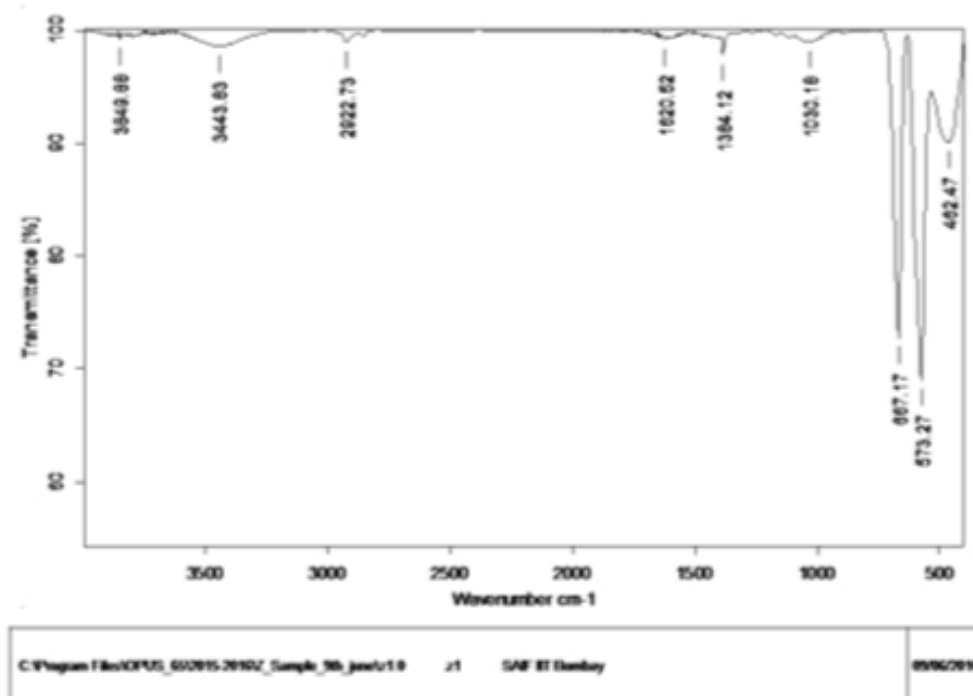


Fig. 2. FTIR spectrum of $\text{Zn}_{0.7}\text{Mg}_{0.3}\text{Co}_2\text{O}_4$ powder.

3.3. Scanning electron microscopy (SEM) analysis

Fig. 3 depicts SEM image of $\text{Zn}_{0.7}\text{Mg}_{0.3}\text{Co}_2\text{O}_4$ thick film. It can be observed that $\text{Zn}_{0.7}\text{Mg}_{0.3}\text{Co}_2\text{O}_4$ thick film show structure having large grains size with soft agglomerations has a regular morphology (polygons). From figure, it shows the formation of the agglomerated particle having grain size is ~ 28 nm.

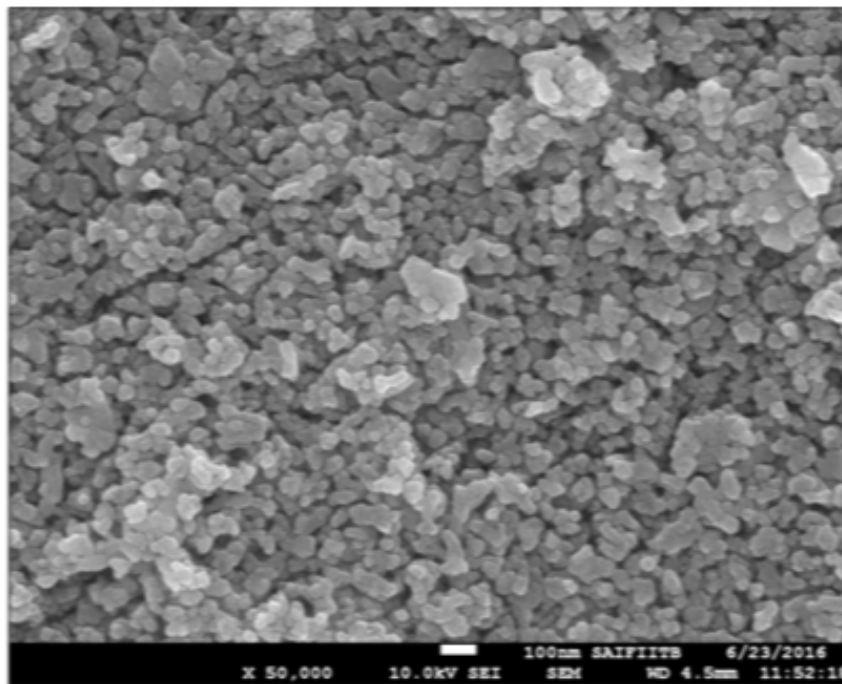


Fig. 3. SEM image of nanosized $\text{Zn}_{0.7}\text{Mg}_{0.3}\text{Co}_2\text{O}_4$.

3.4. Energy dispersion X-ray (EDX) analysis

Fig. 4 shows EDX patterns of the nanosized spinel $\text{Zn}_{0.7}\text{Mg}_{0.3}\text{Co}_2\text{O}_4$. From the EDX spectrum, the presence of Zn, Co and O elements alone in the sample, has been confirmed the absence of any other impurities. EDX results reveal almost the same ratio of Mg/Zn/Co for the synthesized nanoparticle as they were actually added during synthesis process.

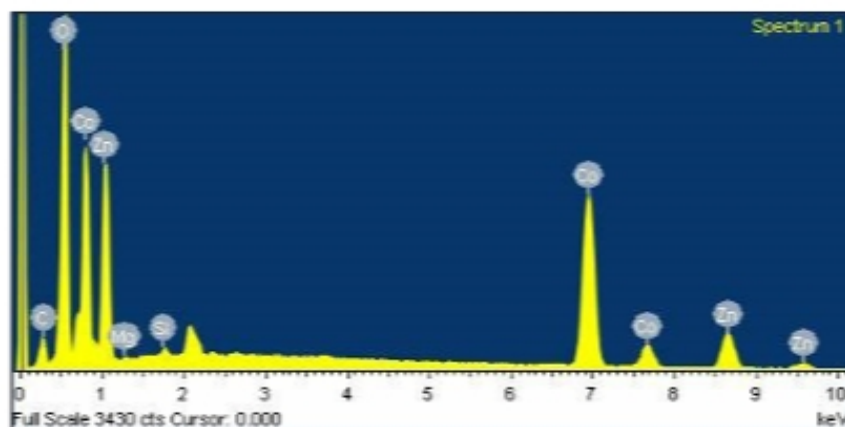


Fig. 4. EDX spectrum for nanosized $\text{Zn}_{0.7}\text{Mg}_{0.3}\text{Co}_2\text{O}_4$.

3.5 Transmission electron microscopy (TEM) analysis

The TEM image of the $\text{Zn}_{0.7}\text{Mg}_{0.3}\text{Co}_2\text{O}_4$ calcined at 500°C for 2 h are shown in Fig. 5(a). It indicates the presence of $\text{Zn}_{0.7}\text{Mg}_{0.3}\text{Co}_2\text{O}_4$

nanoparticles with size 30–40 nm which form beed type of oriental aggregation throughout the region.

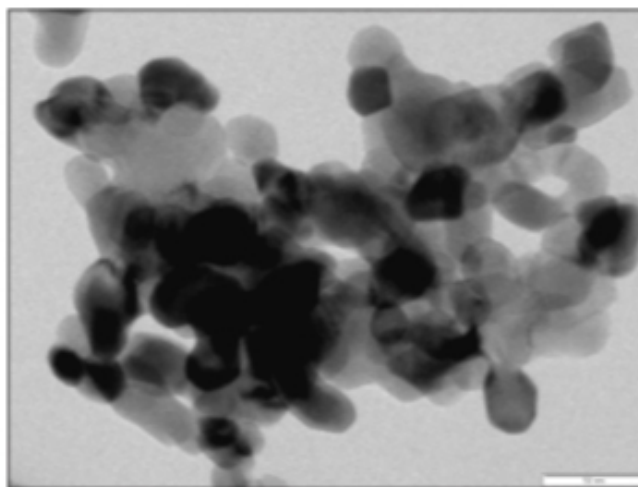


Fig. 5(a). TEM image of nanosized $\text{Zn}_{0.7}\text{Mg}_{0.3}\text{Co}_2\text{O}_4$.

Fig. 5(b) shows the selected area electron diffraction (SAED) pattern the spot type pattern which is indicative of the presence of single crystallite particles. No evidence was found for more than one pattern, suggesting the single-phase nature of the material.

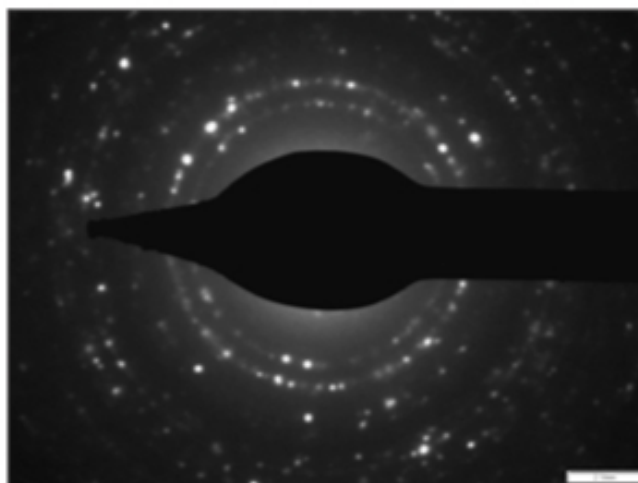


Fig. 5(b). Image of $\text{Zn}_{0.7}\text{Mg}_{0.3}\text{Co}_2\text{O}_4$ nanoparticles with SAED pattern.

4. Gas sensing properties

To study the selective behavior of nanocrystalline $\text{Zn}_{0.7}\text{Mg}_{0.3}\text{Co}_2\text{O}_4$ gas response (S) towards 50 ppm for various test gases such as LPG, NH_3 , CO_2 , H_2S , Cl_2 , H_2 and $\text{C}_2\text{H}_5\text{OH}$ at optimal operating temperature 100°C and is depicted in Fig. 6.

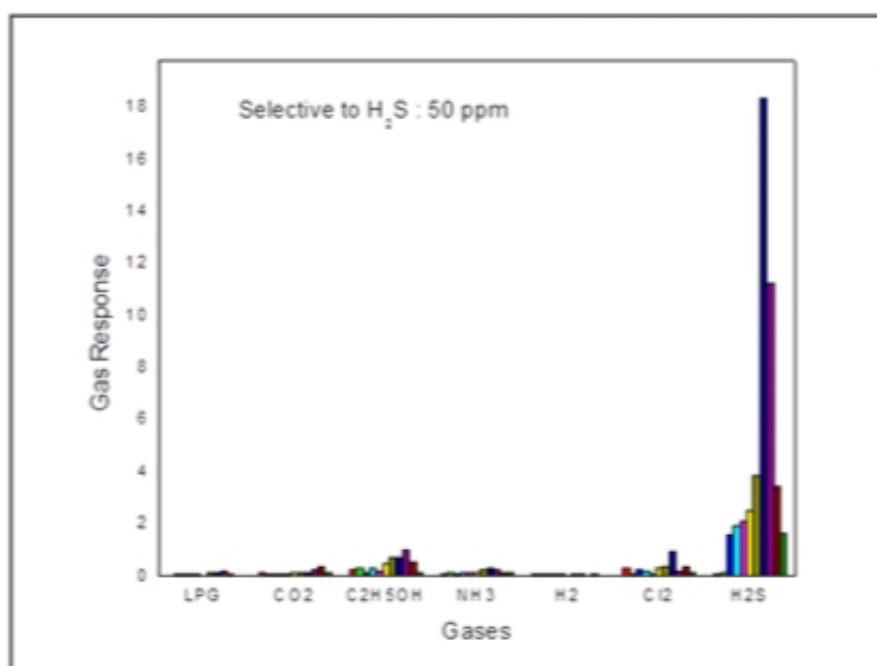
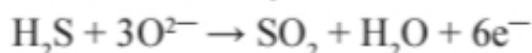


Fig. 6. Selectivity of nanocrystalline $\text{Zn}_{0.7}\text{Mg}_{0.3}\text{Co}_2\text{O}_4$ thick films.

The $\text{Zn}_{0.7}\text{Mg}_{0.3}\text{Co}_2\text{O}_4$ sample exhibited the higher gas response 18.31 towards H_2S . Hence, the $\text{Zn}_{0.7}\text{Mg}_{0.3}\text{Co}_2\text{O}_4$ sensors show maximum selectivity for H_2S gas towards 50 ppm among all the tested gases.

The gas sensing mechanism can be explained as follows. When nanocrystalline ZnCo_2O_4 sensors are exposed to air, oxygen molecules get adsorbed on the surface and form O^- , O_2^- and O^{2-} by capturing free electrons from the conduction band, which results in a high resistance in air. When the semiconductor surface is exposed to H_2S gas at proper temperature, H_2S may react with the surface oxygen species. Thus, the electrons trapped by O^- are released and returned ZnCo_2O_4 . The reaction leads to decrease in resistance of nanocrystalline ZnCo_2O_4 .

The inlet H_2S can react rapidly with the adsorbed oxygen and hydroxyl species, therefore releasing the captured electrons back to bulk. Reducing gases can also react with the lattice oxygen, but the rate is much slower than the surface reaction and can be neglected. The first interpretation of the chemical sensing mechanism considers the negatively charged surface oxygen ions, which react with the gas. The increase of the conductivity in the presence of H_2S may be explained by the reaction below;



According to this reaction, the interaction of H_2S with previously adsorbed O^{2-} ions results in the injection of electrons into the depletion

layer of ZnCo_2O_4 grains. Furthermore, the effect of Mg doping on the gas sensing performance of nanocrystalline ZnCo_2O_4 can be explained. The nanocrystalline $\text{Zn}_{0.7}\text{Mg}_{0.3}\text{Co}_2\text{O}_4$ is highly conductive nature and availability of free electrons in Mg would also cause more electrons to be extracted by adsorbed oxygen. Thus, in the presence of Mg more electrons are extracted, which produce a deeper electron-depleted layer in ZnCo_2O_4 . In addition, the Mg doped nanocrystalline ZnCo_2O_4 has large surface-to-volume ratio and has a high density of active adsorption sites, which helps in showing a relatively higher response than undoped ZnCo_2O_4 .

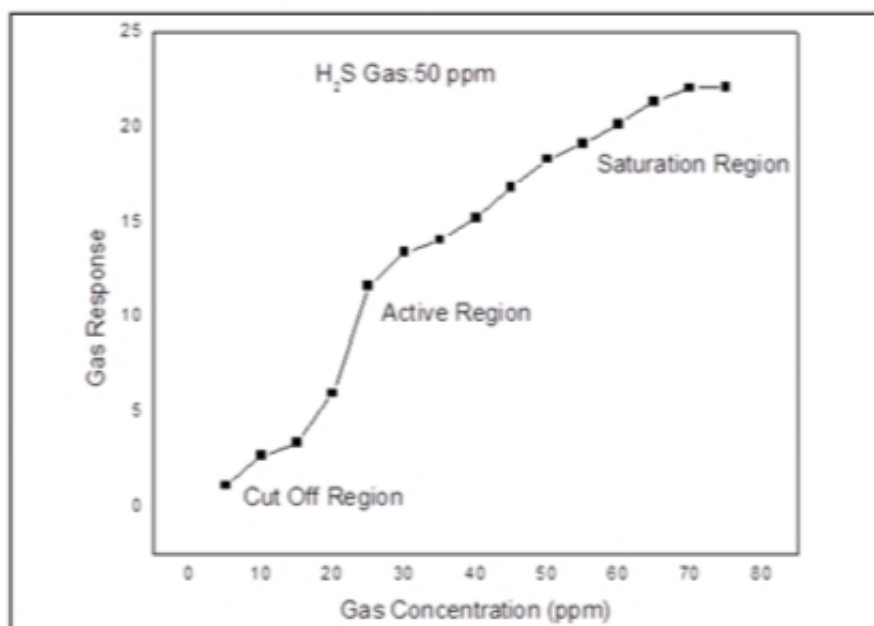


Fig. 7. Gas response of $\text{Zn}_{0.7}\text{Mg}_{0.3}\text{Co}_2\text{O}_4$ as a function H_2S concentration.

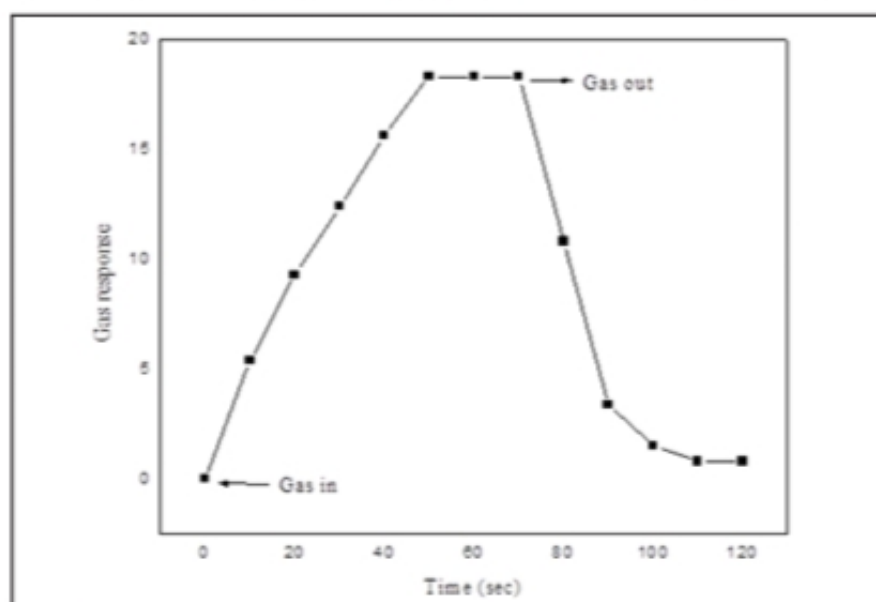


Fig. 8. Response characteristics of $\text{Zn}_{0.7}\text{Mg}_{0.3}\text{Co}_2\text{O}_4$ thick film to 50 ppm H_2S .

The response of $\text{Zn}_{0.7}\text{Mg}_{0.3}\text{Co}_2\text{O}_4$ as a function of H_2S gas concentration at 100°C is shown in Fig. 7. The gas response was observed to increase with increase in the gas concentration and thereafter it remains almost constant. The response and recovery time characteristics of nanocrystalline $\text{Zn}_{0.7}\text{Mg}_{0.3}\text{Co}_2\text{O}_4$ based sensor to 50 ppm H_2S at 100°C are depicted in Fig. 8. The nanocrystalline $\text{Zn}_{0.7}\text{Mg}_{0.3}\text{Co}_2\text{O}_4$ have quick response time 16 s and fast recovery time 52 s. Therefore, nanocrystalline $\text{Zn}_{0.7}\text{Mg}_{0.3}\text{Co}_2\text{O}_4$ based sensor exhibits the good response and recovery time to H_2S .

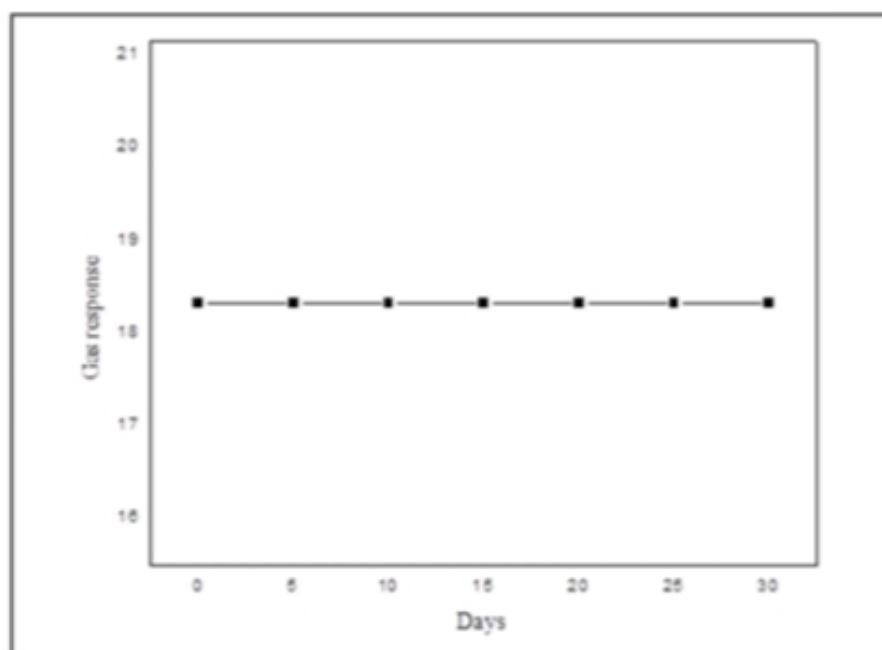


Fig. 9. Stability nanocrystalline $\text{Zn}_{0.7}\text{Mg}_{0.3}\text{Co}_2\text{O}_4$ thick film.

The reproducible nature of nanocrystalline $\text{Zn}_{0.7}\text{Mg}_{0.3}\text{Co}_2\text{O}_4$ based thick film sensor to 50 ppm H_2S was measured for a month in the interval of 10 days and result are shown in Fig. 9. From figure, it was found that nanocrystalline $\text{Zn}_{0.7}\text{Mg}_{0.3}\text{Co}_2\text{O}_4$ based sensor possesses a very good stability and durability.

5. Conclusions

In summary, we have reported the synthesis and investigations of gas sensing properties of $\text{Zn}_{0.7}\text{Mg}_{0.3}\text{Co}_2\text{O}_4$ nanomaterial for the detection of H_2S . The material was fabricated by the sol-gel method. TEM investigation reveals the average crystallite size is in accordance with XRD results. The excellent gas sensing performance

of the prepared $\text{Zn}_{0.7}\text{Mg}_{0.3}\text{Co}_2\text{O}_4$ nanomaterial was attributed to its morphology, the operating temperature and the disparity in the sensing mechanism between H_2S and other reducing gases. The obtained results demonstrate the potential suitability of the application of $\text{Zn}_{0.7}\text{Mg}_{0.3}\text{Co}_2\text{O}_4$ in gas sensing devices for the detection of H_2S .

References

1. K. Wetchakun, T. Samerjai, N. Tamaekong, C. Liewhiran, C. Siri Wong, V. Kruefu, A. Wisitsoraat, A. Tuantranont, S. Phanichphant, *Sens. Actuators, B*, 160 (2011) 580.
2. J. Zhang, Z. Qin, D. Zeng, C. Xie, *Phys. Chem. Chem. Phys.*, 19 (2017) 6313.
3. G. Korotcenkov, *Mater. Sci. Eng., B*, 139 (2007) 1.
4. A. M. Azad, S. A. Akbar, S. G. Mhaisalkar, et al., *J Electrochem Soc.*, 139 (1992) 3690.
5. R. W. Bogue, *Meas Sci Technol.*, 1(1996) 1.
6. Y. R. Wu, J. Singh, *Appl. Phys. Lett.*, 85 (2004) 1223.
7. N. Barsan, D. Koziej, U. Weimar, *Sens. Actuators, B*, 121 (2007) 18.
8. Q. Wang, X. Li, F. Liu, C. Liu, T. Su, J. Lin, P. Sun, Y. Sun, F. Liu, G. Lu, *RSC Adv.*, 6 (2016) 80455.
9. C. Wang, L. Yin, L. Zhang, D. Xiang, R. Gao, *Sensors*, 10 (2010) 2088.
10. B. Chi, J. Li, X. Yang, H. Lin, N. Wang, *Electrochim. Acta*, 50 (2005) 2059.
11. S. V. Bangale, R. D. Prashale, S. R. Bamane, *J. Chem. Pharm. Res.*, 3 (2011) 527.
12. X. Niu, W. Du, W. Du, *Sens. Actuators, B*, 99 (2004) 405.
13. K. Karthikeyan, D. Kalpana, N. G. Renganathan, *Ionics*, 15 (2009) 107.
14. S. Trasatti, J. Lipkowski, P. N. Ross, *The Electrochemistry of Novel Materials*, VCH Publishers, Weinheim, (1994) 207.

Nanocrystalline Spinel Cobalt Aluminate Prepared By Co precipitation Method

S.V. Agnihotri*, V. D. Kapse, T.R. Tatte, P.V. Tumram, M. S. Pande

*Department of Physics, Amolakchand Mahavidyalaya Yavatmal, 445001, Maharashtra State, India.
Department of physics, Arts, Science and Commerce College, Chikhaldara 444807, Maharashtra State India
Department of Physics, Shri. R. G. Rathod Arts and Science College, Murtizapur- 444107, M S, India.
Department of Physics, Amolakchand Mahavidyalaya Yavatmal, 445001, Maharashtra State, India
Department of physics, Gajanan Maharaj College of Engineering, Shegaon 444203
drsva205@gmail.com

Abstract:

Cobalt aluminate (CoAl_2O_4) nanoparticles were synthesized via co precipitation route. Sample was calcinated at 900°C . X-ray diffraction, data confirms the formation of single-phase cubic structure and the average grain sizes were evaluated. The XRD result revealed the production of a sharp single cubic spinel structure of prepared sample without any impurity peak with the crystallite size of about 21.6 nm. The high and low frequency absorption bands of CoAl_2O_4 were investigated using FT-IR analysis. The microstructural features were examined by scanning electron microscopy (SEM).

Keywords: Nanocrystalline, Cubic-Spinel, XRD, FT-IR, SEM.

Introduction:

Cobalt aluminate spinel (CoAl_2O_4) is known for its blue colour and it is widely used as pigments for ceramics, paints, fibres and so on. CoAl_2O_4 is a material which have excellent thermal stability, high melting point and electrical properties. The structure of CoAl_2O_4 also plays a key role in determining the material's behaviour in different environments making it an important consideration in various fields of science and engineering [1]. The materials have high thermal stability, colour stability, resistance to moisture and humidity also make it suitable for use in harsh environments [2-7].

Materials and Methods:

There are several methods use to synthesize Cobalt aluminate nanoparticles, including the mixed oxide method, citrate-nitrate method, hydrothermal synthesis and combustion methods [8,9]. Among all the methods, co precipitation is one of the most efficient routes and human-friendly method to develop spinel oxide materials in a short span of time while utilizing less energy [10].

Sample CoAl_2O_4 was synthesized by co-precipitation method in an air atmosphere. The starting materials were weighed according to the stoichiometric ratio. The raw materials $\text{Al}(\text{NO}_3)_3(99.0\%)$, $(\text{Co}(\text{NO}_3)_2 \cdot 6\text{H}_2\text{O})$, were dissolved in distilled water mixed well with each other at 80°C temperature under constant magnetic stirring, where in the molar ratio of Co/Al was 1:2. In this process, ammonia was used as precipitant. The mixed materials were dried in an oven for 24 h. The dried materials were put into the alumina crucible and calcined in a muffle furnace at 900°C for 4 h and then the white powder was obtained. Thick film was prepared from this powder by screen printing method.

There are many reports available on semiconducting metal oxide. Among these cobalt aluminate gas sensor is a potential candidates of the gas sensing device. In this paper

characterization of the spinel was carried out by using powder X-ray diffraction, infrared spectra and scanning electron micrograph.

Techniques:

The X-ray measurement of various mixed solids was carried out using a BRUKER D8 advance diffractometer (Germany). The patterns were run with Cu K α radiation at 40 kV and 40 mA with scanning speed in 2 θ of 2° min⁻¹. The crystallite size of CoAl₂O₄ crystallites present in the investigated solids was based on X-ray diffraction line broadening and calculated by using Scherrer equation [11]

$$d = \frac{k\lambda}{\beta \cos \theta}$$

where d is the average crystallite size of the phase under investigation, k is the Scherrer constant (0.89), λ is the wave length of X-ray beam used, β is the full-width half maximum (FWHM) of diffraction and θ is the Bragg's angle. The XRD patterns of these powders showed several peaks at 31.44, 37.02, 44.94, 55.78, 59.46 and 65.30 corresponding to (h k l) reflection at (2 2 0), (3 1 1), (4 0 0), (4 2 2), (5 1 1) and (4 4 0) respectively [12]. These peaks could be indexed with space group Fd3m.

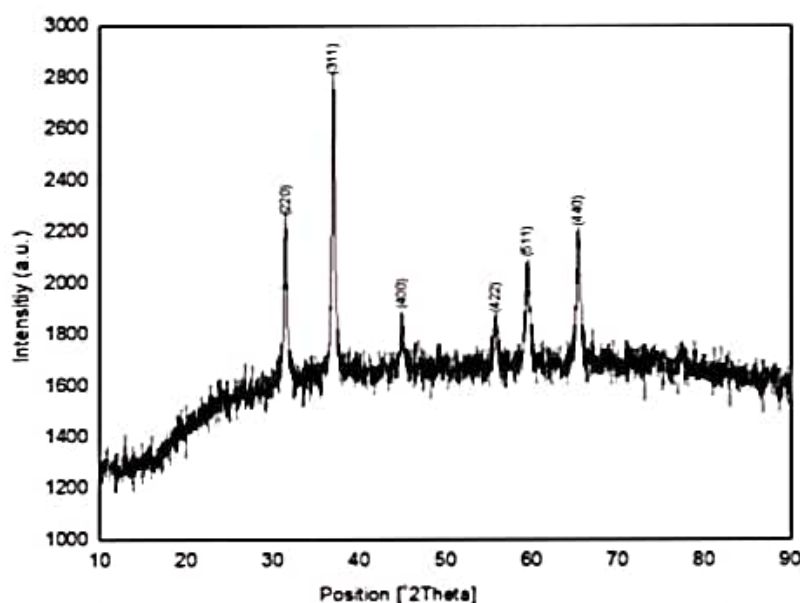


Fig. 1: XRD pattern of CoAl₂O₄ powder calcinated at 900°C.

Infrared spectra of given sample as shown in fig. 2. Spectra shows three bands in the region 500 to 700 cm⁻¹. These three bands are attributed to the vibration modes of the CoAl₂O₄ phase [13]. These results are in good agreement with XRD analysis.

Scanning electron micrographs (SEM) were recorded on JEOL JSM 7600F. SEM micrographs of the sample CoAl₂O₄ thick film are presented in fig. 3. The film was synthesized by screen printing method. Figure shows agglomerates of different shapes and the particle size between the range 45.1- 45.4 nm.

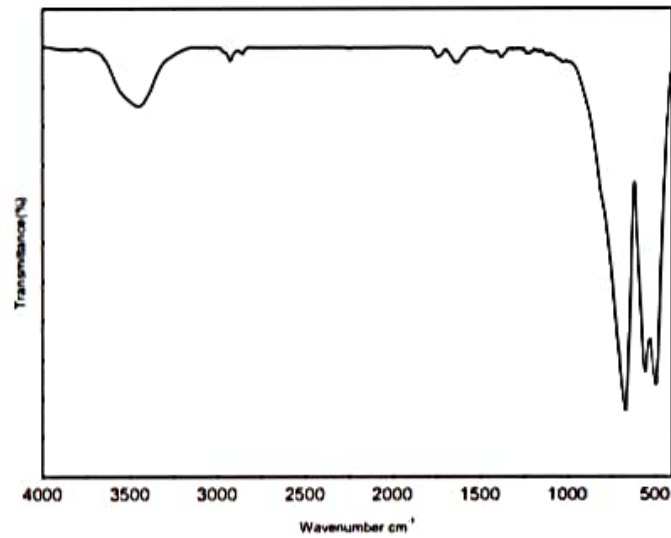


Fig.2: FTIR spectra of CoAl_2O_4 powder calcinated at 900°C .



Fig. 3: SEM image of Nanocrystalline CoAl_2O_4 thick film.

Conclusion:

In summary, CoAl_2O_4 nanoparticles have been successfully synthesized through co precipitation method. The sample was heated upto 900°C . The heat treatment blue powders with a direct spinel structure (CoAl_2O_4). The vibrational stretching frequencies corresponding to the composites were confirmed by FT-IR spectroscopy. Scanning electron micrograph shows homogenous morphology; it consists in agglomerates of primary particles of quasi-spherical shape with a size in the range 45.1 to 45.4nm.

References:

1. S. Bid and S.K. Pradan, *Materials Chemistry and Physics* (2003) 82-27.
2. R.E. Ayala and D.W. Marsh, *Ind. Chem. Res.* (1991) 30-55.
3. Y. Tang, C. Wu, Y. Song, Y. Zheng, K. Zhao, Effects of colouration mechanism and stability of CoAl_2O_4 ceramic pigments sintered on substrates, *Ceram. Int.* 44 (2018) 1019–1025.
4. S. Obata, M. Kato, H. Yokoyama, Y. Iwatara, M. Kikumoto, O. Sakurada, Synthesis of nano CoAl_2O_4 pigment for ink-jet printing to decorate porcelain, *J. Ceram. Soc. Japan* 119 (2011) 208–213.
5. Y. Song, Y.L. Zheng, Y.F. Tang, H.B. Yang, Fabrication and stability of CoAl_2O_4 ceramic pigment for 3D printing, *MSF* 898 (2017) 1935–1939.
6. P. Xiaojin, C. Jinshu, Y. Jian, J. Na, K. Junfeng, H. Yansheng, Z. Qi, Environmental blue CoAl_2O_4 pigment co-doped by Zn^{2+} and Mg^{2+} : synthesis, structure and optical properties, *Adv. Appl. Ceram.* 117 (2018) 303–311.
7. M. Abhishek, K. Manjunatha, V. Jagadeesha Angadi, E. Melagiriappa, B.N. Anandaram, H.S. Jayanna, M. Veena, K.S. Acharya, Structural and magnetic properties of Eu^{3+} substituted Mg-Cd nanoferrites: a detailed study of influence of high energy γ -rays irradiation, *Chem. Data Collect.* 28 (2020).
8. G. Aguilar-Rios, M. Valenzuela, P. Salas, H. Armendariz, P. Bosch, G. Del Toro, R. Silva, V. Bertin, S. Castillo, A. Ramirez-Solis, I. Schifter, *Appl. Catal. A.Gen.* 127 (1995) 65-75.
9. J. Wrzyszczy, M. Zawadzki, J. Trawczyński, H. Grabowska, W. Miśta, *Appl. Catal. A Gen.* 210 (2001) 263–269.
10. C.O. Arean, B.S. Sintes, G.T. Palomino, C.M. Carbonell, E.E. Platero, J.B. P. Soto, *Microporous Mater.* 8 (1997) 187.
11. B.D. Cullity, *Elements of X-ray Diffraction*, Addison-Wesley Publishing Co. Inc. 1976 (chapter 14)
12. N. Ouahdi, S. G. Fritsch, Durand, El Bernard, Ouattib, Rachida, Er Rakho, Lahcen, R. Moussa, A. Samdi, *J. of Euro. Ceram. Soc.* 28 (10) (2008) 1987-1994.
13. X. Duan, M. Pan, F. Yu, D. Yuan, Synthesis, structure and optical properties of CoAl_2O_4 spinel nanocrystals, *J. Alloys Compd.* 509 (2011) 1079-1083.

Preparation of Zinc doped Magnesium Ferrite Nanoparticles by Sol-Gel Method

T. R. Tatte*, V. D. Kapse, M. S. Pande

**Department of Physics, Shri. Dr. R. G. Rathod Arts and Science College, Murtizapur, 444107, Dist. Akola, Maharashtra State, India.*

Department of Physics, Arts, Science and Commerce College, Chikhaldara, 444807, Maharashtra State, India.

Department of Physics, Gajanan Maharaj College of Engineering, Shegaon, 444203, Maharashtra State, India.

1. Introduction

During the last decade, the world has seen huge interest in developing and understanding the matter of nanometric scale. It has allowed the scientists to develop and characterize materials with prominent properties and nanometric sizes. Due to the note-worthy properties, exhibited by nonmaterial, they have become centre of attention in the scientific community. The fabrication of spinel-structured ferrite nanoparticles has been intensively investigated in recent years due to their unique physical and chemical properties, as well as technological applications in ferrofluids [1], high-density magnetic recording media [2], biomedicine [3] and radar-absorbent materials [4].

Spinel ferrites, MFe_2O_4 ($M = Mg, Mn, Fe, Co, Ni, Zn, Cu, Cd$, etc.) are a technologically important group of materials. Among different ferrites, magnesium ferrite ($MgFe_2O_4$) enjoys a special attention because of its vast applications in high density recording media, heterogeneous catalysis, adsorption, sensors and magnetic technologies. $MgFe_2O_4$ is a partially inverse spinel and its degree of inversion is sensitive to the thermal history of the sample, microstructure and preparative parameters. Nanoparticles of $MgFe_2O_4$ have good photo electrical properties [5-7]. To fabricate various types of nanoparticles, a large number of methods are used such as physical, chemical, biological and hybrid methods. The nanoparticles synthesized using each method exhibit particular properties. So, the synthesis of nanostructured materials has become a particularly important area of research.

There are several methods for synthesizing nanosized spinel ferrite particles such as hydrothermal, co-precipitation, combustion, sol-gel, precursor, spray drying and freeze drying, microemulsion and reverse micelle method [8-15]. To prepare nanoferrites with simple routes by using cheap, non-toxic and eco-friendly precursors are still the core issue, among other proven synthesis methods [16]. Among these methods, the nanoparticles prepared by sol-gel method have been studied, although this synthesis provides a quick and easy way to prepare nanoparticle, it usually produces sample with large size distribution and less defined crystal chemistry.

Herein, the purpose of this work is to prepare nanocrystalline Zn doped Mg spinel ferrite by a sol-gel method with a low calcination temperature involving low cost metal nitrates as raw materials and study of their structural properties.

2. Experimental

Preparation of nanocrystalline $\text{Mg}_{0.5}\text{Zn}_{0.5}\text{Fe}_2\text{O}_4$ powder was synthesized by the sol-gel technique. All chemicals were of analytical grade and were used without further purification. The stoichiometric molar amounts of Ferric nitrate [$\text{Fe}(\text{NO}_3)_3 \cdot 9\text{H}_2\text{O}$], Magnesium nitrate [$\text{Mg}(\text{NO}_3)_2 \cdot 6\text{H}_2\text{O}$], Zinc nitrate [$\text{Zn}(\text{NO}_3)_2 \cdot 6\text{H}_2\text{O}$] and Citric acid [$\text{C}_6\text{H}_8\text{O}_7 \cdot \text{H}_2\text{O}$] were weighed separately with a ratio 0.5M:0.25M:0.5M. These reagents were mixed with distilled water and volume made up to 100 ml. The solution mixture was stirred and heated at 60°C for 3 h and followed by 80°C, until the mixture changed to gel form. The gel was then dried in an oven at 100°C for 24 h. The obtained powder was then calcined in a muffle furnace at 700°C for 2 h to improve the crystallinity of the prepared material. Finally, brown color powder was obtained. Taken solid phase sample was grinded in a mortar to make it powder for further analysis.

The phase confirmation was determined using XRD (Bruker, AXD D8-Discover using Cu K α radiation with an accelerating voltage 40 kV). FT-IR image was recorded using 3000 Hyperion Microscope with Vertex 80 (Bruker, Germany) to provide information about the structural coordination in the powder sample. The TEM image was recorded using CM 200 (Philips) with an accelerating voltage of 20-200 kV.

Appropriate quantity of mixture of organic solvents such as butyl cellulose, butyl carbitol acetate and turpineol was added to the mixture of $\text{Mg}_{0.5}\text{Zn}_{0.5}\text{Fe}_2\text{O}_4$ and a solution of ethyl cellulose (a temporary binder). The mixture was then ground to form paste. The paste obtained was screen printed onto a glass substrate in desired patterns. The thick films so prepared were fired at 500°C for 1 h. Surface morphology of thick film was observed by using SEM (JSM-7600F microscope) with an accelerating voltage of 0.1 to 30 kV.

3. Result and discussions

3.1 XRD analysis

The X-ray diffraction pattern of $\text{Mg}_{0.5}\text{Zn}_{0.5}\text{Fe}_2\text{O}_4$ calcinated at 700°C for 2 h was exhibited in Fig. 1. Main peaks were found at 2θ values = 29.90°, 35.21°, 56.58°, 62.14° and 73.48° which were identified as corresponding to Miller index (220), (311), (400), (511) and (440) respectively (JCPDS card no. 73-2211). The XRD peaks and their positions with the calculated lattice parameter confirm that all the compositions exhibit single-phase cubic spinel structure with Fd3m space group. No peaks from other phases are detected, indicating high purity of the products.

The average crystallite size (D) was calculated from XRD peaks broadening using the Debye-Scherrer approximation, which is defined as

$$D = \frac{K\lambda}{\beta \cos \theta} \quad (1)$$

where, D is the average crystallite size, k is a constant equal to 0.9, λ is the X-ray wavelength and β is the peak full width at half maximum (FWHM) and θ is the angle of diffraction.

However, the lattice constant of as-synthesized ferrite powder was $a = 8.421 \text{ \AA}$. A similar linear variation of lattice constant with Zn content has been observed by El-Sayed [17] and Kakatkar et al. [18] for M-Zn ferrites with $M = \text{Ni, Co, Cu, Mg}$. The average crystallite size was determined from the XRD powder pattern using Debye-Scherrer formula and was found to be 30 nm.

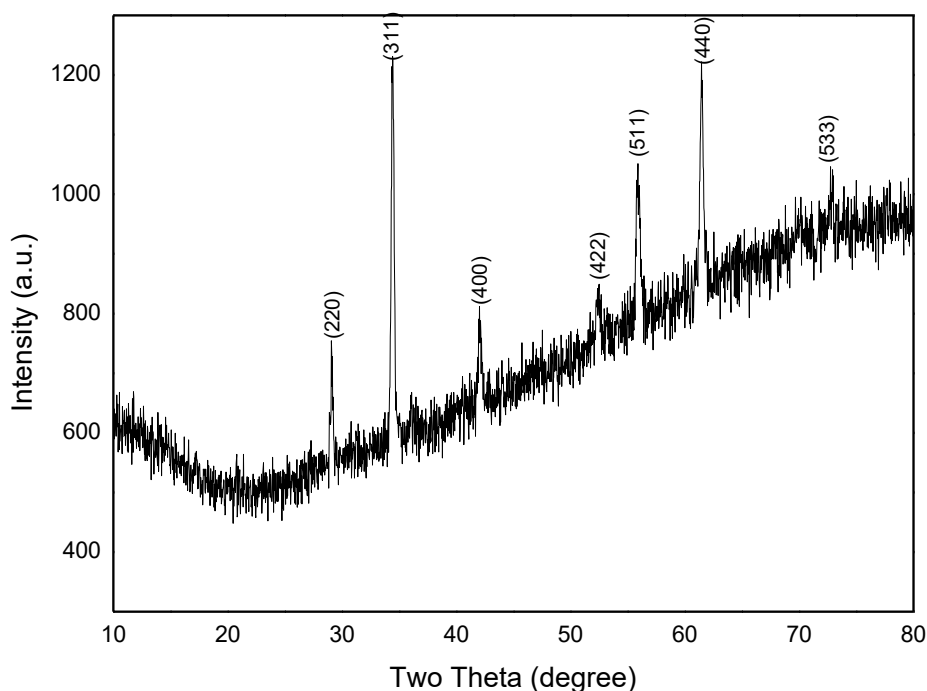


Fig. 1. XRD pattern of $\text{Mg}_{0.5}\text{Zn}_{0.5}\text{Fe}_2\text{O}_4$ calcined at 700°C .

3.2 FT-IR analysis

FT-IR spectrum of $\text{Mg}_{0.5}\text{Zn}_{0.5}\text{Fe}_2\text{O}_4$ nanoparticle was presented in Fig. 2. Vibrations of ions in the crystal lattice were usually observed in the range of $4000 - 400 \text{ cm}^{-1}$ in IR analysis. Two main broad metal-oxygen bands were seen in the IR spectra relative to spinel ferrite compounds. Infrared spectrum shown in Fig. 2 had two absorption bands near about 400 cm^{-1} and 600 cm^{-1} for octahedral and tetrahedral sites



respectively. Waldron [19] attributed the higher absorption band position (600 cm^{-1}) to the intrinsic stretching vibrations of tetrahedral complexes and the lower absorption band position (400 cm^{-1}) to octahedral-metal stretching because of the difference in $\text{Fe}^{3+}-\text{O}^{2-}$ distances for the octahedral and tetrahedral sites respectively. The Mg^{2+} ions occupy mainly the octahedral sites but fraction of these ions may be migrated into tetrahedral sites. This would explain the existence of a weak shoulder in the range of $690-710\text{ cm}^{-1}$. This confirms that the Mg ferrite has a partially inverse spinel structure.

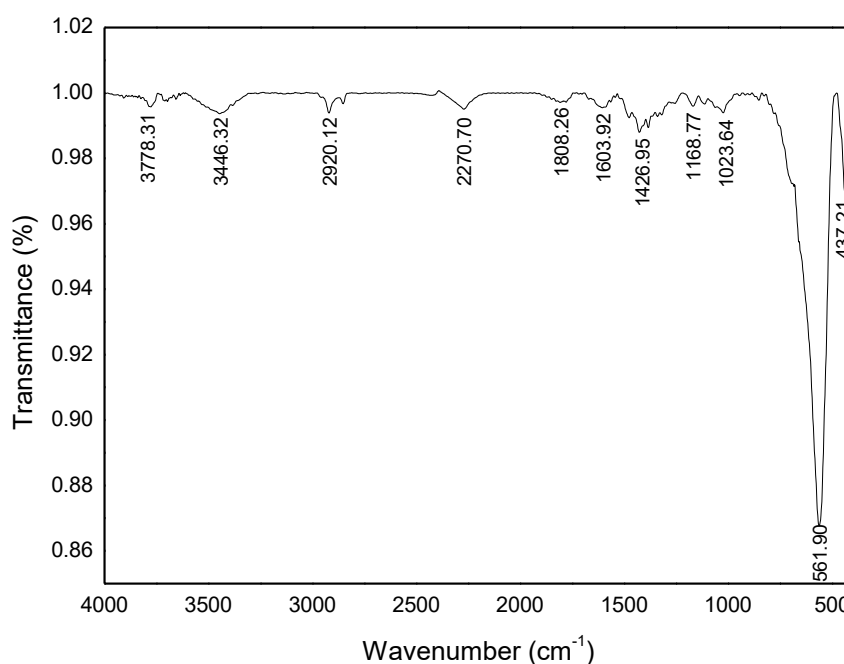


Fig. 2. FTIR spectrum of nanocrystalline $\text{Mg}_{0.5}\text{Zn}_{0.5}\text{Fe}_2\text{O}_4$.

3.3 TEM analysis

The size and morphology of the obtained $\text{Mg}_{0.5}\text{Zn}_{0.5}\text{Fe}_2\text{O}_4$ nanocrystal was characterized by TEM observation. Fig. 3(a) shows TEM image of $\text{Mg}_{0.5}\text{Zn}_{0.5}\text{Fe}_2\text{O}_4$ nanoparticle. The corresponding SAED pattern is shown in Fig. 3(b). As can be seen from Fig. 3(a) and (b), the prepared product consists of small sized nanocrystals with irregular shapes. It appears that a higher temperature reaction favors a particle with larger grain sizes, because a higher temperature enhanced the atomic mobility and caused the grain growth to result in a better crystallinity. As it can be seen that the result estimated from TEM micrograph was in good accordance with the XRD

analysis. The selected area aperture used in this study sufficed to reveal all the corresponding bright rings of the spinel structure. It was observed that the spot type pattern which is indicative of the presence of single crystallite particles and no evidence was found for more than one pattern, suggesting the singlephase nature of the material.

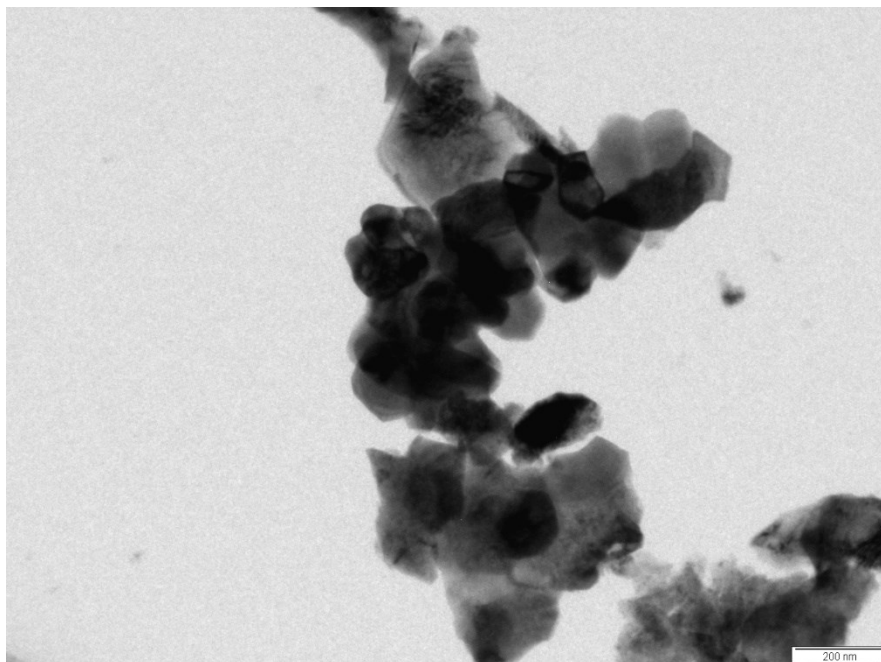


Fig. 3(a). TEM image of nanocrystalline $\text{Mg}_{0.5}\text{Zn}_{0.5}\text{Fe}_2\text{O}_4$.

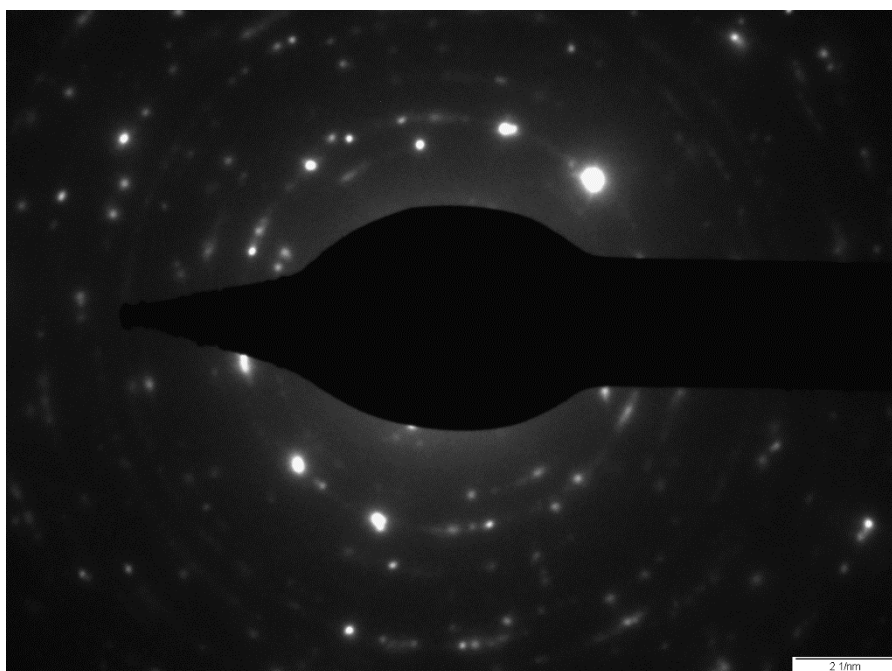


Fig. 3(b). SAED micrograph of nanocrystalline $\text{Mg}_{0.5}\text{Zn}_{0.5}\text{Fe}_2\text{O}_4$.

3.4 SEM analysis

SEM technique was employed for finding morphology of the thick film. Fig. 4 shows SEM image of the nanocrystalline spinel $\text{Mg}_{0.5}\text{Zn}_{0.5}\text{Fe}_2\text{O}_4$. The SEM technique was employed for finding morphology of the powder; it shows formation of the agglomerated particle. SEM image shows that the sample exhibit large grains structure having irregular morphology (polygons) with the presence of soft agglomerations.

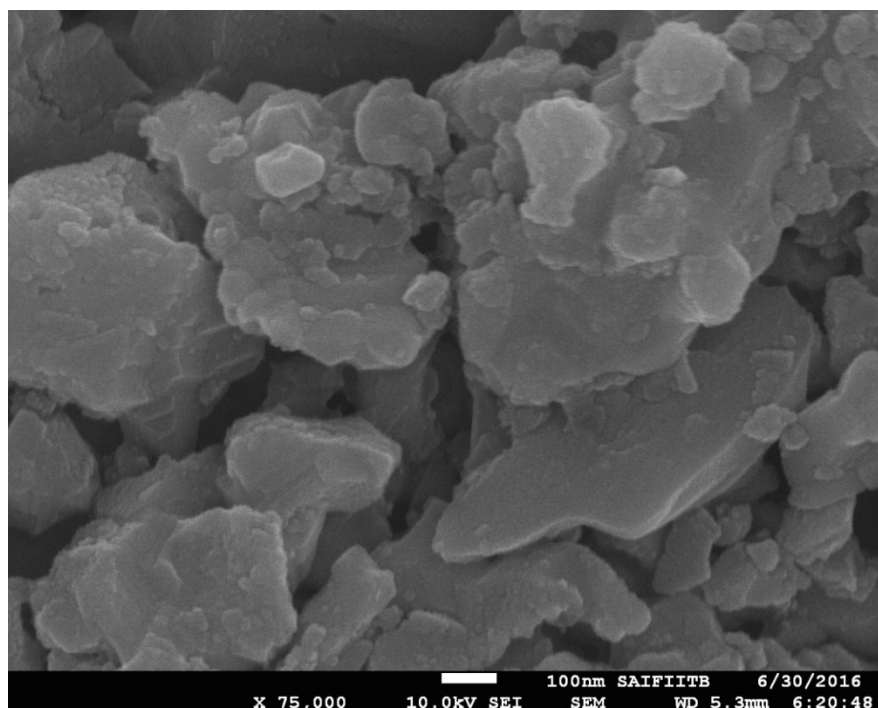


Fig. 4. SEM image of nanocrystalline $\text{Mg}_{0.5}\text{Zn}_{0.5}\text{Fe}_2\text{O}_4$.

3.5 Energy dispersion X-ray analysis

Energy dispersion X-ray analysis (EDX) was investigated the elemental composition of synthesized $\text{Mg}_{0.5}\text{Zn}_{0.5}\text{Fe}_2\text{O}_4$ thick film. EDX spectrum of the nanocrystalline $\text{Mg}_{0.5}\text{Zn}_{0.5}\text{Fe}_2\text{O}_4$ is as shown in Fig. 5. The EDX analysis exhibit the presence of Mg, Zn, Fe and O and EDX spectrum reveal almost the same ratio of Mg/Zn/Fe for the nanocrystalline $\text{Mg}_{0.5}\text{Zn}_{0.5}\text{Fe}_2\text{O}_4$ as they were actually added during synthesis process. Hence, confirms the purity of nanocrystalline $\text{Mg}_{0.5}\text{Zn}_{0.5}\text{Fe}_2\text{O}_4$.

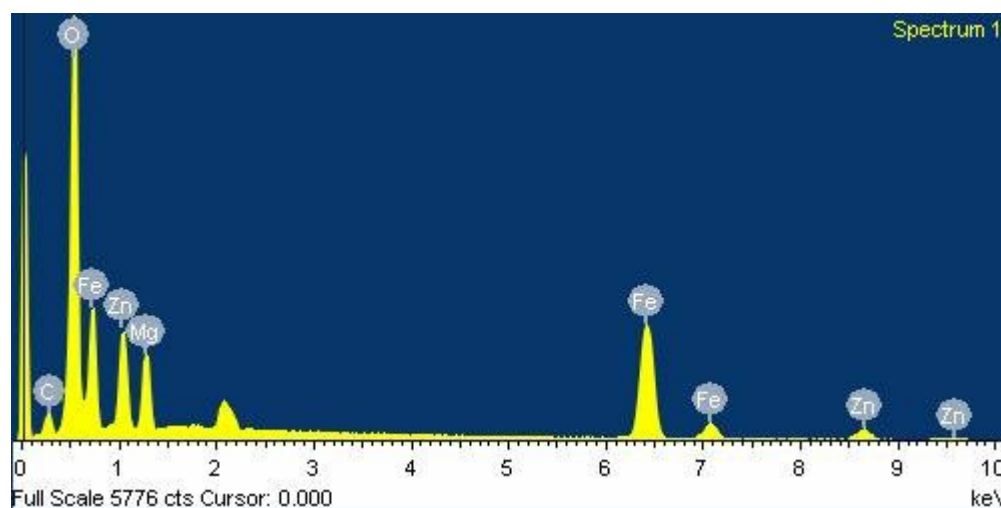


Fig. 5. EDX spectrum for nanocrystalline $\text{Mg}_{0.5}\text{Zn}_{0.5}\text{Fe}_2\text{O}_4$.

4. Conclusions

Zinc doped magnesium ferrite nanoparticles ($\text{Mg}_{0.5}\text{Zn}_{0.5}\text{Fe}_2\text{O}_4$) was prepared using less expensive, environment-friendly and low temperature sol-gel method using citric acid as anionic surfactant calcined at 700°C . XRD pattern reveals that the synthesized ferrite consists of nano crystalline particle with average crystallite size 30 nm. The FT-IR spectrum exhibits main absorption bands around 561 cm^{-1} and 437 cm^{-1} corresponding to the vibration modes of the tetrahedral and octahedral sites respectively. The crystallite size from TEM analysis matches well with XRD results confirming the usefulness of sol-gel method for the synthesis of nanocrystalline $\text{Mg}_{0.5}\text{Zn}_{0.5}\text{Fe}_2\text{O}_4$. The morphological investigations from SEM showed the sample surface is fully covered by grains with irregular shape. The EDX confirmed the presence of Mg, Zn, Fe and O with values as per the initial precursor concentration.

Acknowledgements

I would like to thank Sophisticated Analytical Instrument Facility (SAIF), Indian Institute of Technology (I.I.T.), Bombay for carrying out FT-IR, SEM-EDX and TEM-ED characterizations and Department of Physics, Vidyabharati Mahavidhyalaya, Amravati for providing the XRD facility.

References

- [1] K. Raj, R. Moskowitz, J. Magn. Mater., 85 (1990) 233.
- [2] A. Moser, K. Takano, D. T. Margulies, M. Albrecht, Y. Sonobe, Y. Ikeda, S. Sun, E. E. Fullerton, J. Phys. D: Appl. Phys., 35 (2002) R157.
- [3] J. M. Bai, J. P. Wang, Appl. Phys. Lett., 87 (2005) 152502.

-
- [4] R. C. Che, L. M. Peng, X. F. Duan, Q. Che, X. L. Liang, *Adv. Mater.*, 16 **(2004)** 401.
- [5] A. M. Duncan, H. D. Rouvaray, *Microclusters*, *Sci. Am.*, 12 **(1989)** 110.
- [6] A. Pradeep, P. Priyadharsini, G. Chandrasekaran., *J. Magn. Mag. Mater.*, 320 **(2008)** 2779.
- [7] Ü. Özgür, Y. Alivov, H. Morkoç, *J. Mater. Sci.: Materials in Electronics*, 1 **(2009)** 169.
- [8] S. Komarneni, E. Fregeau, E. Breval, R. Roy, *J. Am. Ceram. Soc.*, 71 **(1998)** C-26.
- [9] Q. Chen, A. J. Rondinone, B. C. Chakoumakos, Z. J. Zhang, *J. Magn. Magn. Mater.*, 194 **(1999)** 1.
- [10] K. Suresh, N. R. S. Kumar, K. C. Patil, *Adv. Mater.*, 3 **(1991)** 148.
- [11] A. S. Albuquerque, J. D. Ardisson, W. A. A. Macedo, *J. Magn. Magn. Mater.*, 192 **(1999)** 277.
- [12] N. S. Gajbhiye, S. Prasad, G. Balaji, *IEEE Trans. Magn.*, 35 **(1999)** 2155.
- [13] H. F. Yu, A. M. Gadalla, *J. Mater. Res.*, 11 **(1996)** 663.
- [14] M. P. Pileni, N. Moumen, *J. Phys. Chem.*, 100 **(1996)** 1867.
- [15] C. Liu, B. Zou, A. J. Rondinone, Z. J. Zhang, *J. Am. Chem. Soc.*, 122 **(2000)** 6263.
- [16] B. B. Dora, S. Kumar, R. K. Kotnala, B. C. Raulo, M. C. Sahu, *Int. J. Pharm Sci. Rev. Res.*, 30 **(2015)** 294.
- [17] A. M. ElSayed, *Ceramic Inter.*, 28 **(2002)** 363.
- [18] S. V. Kakatkar, S. S. Kakatkar, R. S. Patil, A. M. Sankpal, S. S. Suryavanshi, D. N. Bhosale, S. R. Sawant, *Phy. Stat. Sol.(b)*, 198 **(1996)** 853.
- [19] R. D. Waldron, *Phys. Rev.*, 9 **(1955)** 1727.

Review on Nanocrystalline perovskite (ABO₃): A potential material for solid state gassensor

Manisha S. Pande ^{a*}, V. D. Kapse ^b, S.V.Agnihotri ^c, T.R.Tatte^d

^{a*} Department of Physics, Shri Sant Gajanan Maharaj College Of Engineering, Shegaon-444203, India.
manisha031082@gmail.com

^b Department of Physics, Arts, Science and Commerce College, Chikhaldara-444807, India.
vdk.nano@gmail.com

^c Department of Physics, Amolakchand Mahavidyalaya, Yavatmal-445001, India.drsva205@gmail.com

^d Department of Physics, Shri Dr. R. G. Rathod Arts & Science College, Murtizapur-444107, India.
truptitatte21@gmail.com

ABSTRACT

This paper concentrates on nanocrystalline powders of ABO₃ structure were synthesized by the various. Solid state gas sensor is a very effective sensor compared to other sensors because it can detect different harmful gases and it can be used in variety of applications. Given the intense market rivalry, it would be ideal for gas sensors to become more dependable and of higher quality. High sensitivity, high precision, and cost-effective compatible gas sensors have garnered a lot of interest. Research on sensing materials has been broadly targeted in order to provide good gas sensing. This paper review on solid state gas sensor. The creation of effective and efficient gas sensors is the result of advancements in nanotechnology and the use of various materials.

Keywords: Nanomaterials, gas sensors, perovskite, etc.

1. Introduction

In day today modern life detection of different gases play a vital role. The significant area of research towards gas sensing that leads to the fabrication of gas sensing devices which detect various harmful gases. Human body suffers from different diseases due to the emission of various toxic and hazardous gases. Solid-state sensors are among the most versatile of all sensors, as they detect a wide variety of gases, and can be used in many different applications. Among the unique attributes of the solid-state sensor are the abilities of the sensor to detect both low ppm levels of gases, as well as high combustible levels. Solid state gas sensors, are the excellent candidates to the fabrication of commercial gas sensors for a wide range of applications [1-5]. The development of high precision gas sensors is crucial for the monitoring of harmful (exhaust) gases in the environment. A variety of dangerous gases, such as CH₄, NO₂, LPG, NH₃, SO₂, CO, H₂S, NO₂, Acetone, H₂ethanol, and methanol, are constantly released by industry, transportation, and agricultural activities. Many of these gases are hazardous to human health as well as the environment, even at levels measured in parts per million, or ppm. Some of these gases, like H₂, are naturally explosive when exposed to air.

In recent years, nanomaterials based on perovskite have been used in a variety of sustainable applications. Their structural properties enable researchers to investigate functionalities in a variety of directions, including solar cells, LEM devices, transistors and sensors, etc. Perovskite nano-materials have been shown to have remarkable sensing performance to a wide range of chemical and biological species, both in solids and solutions. In particular, they are able to detect small molecules (e.g., oxygen, nitrogen dioxide, carbon dioxide, etc.). In addition, Solid-state gas sensors are emerging as a viable substitute for the intended real-

time functions in light of recent developments in the materials sciences and advancements in processing and downsizing techniques. The greatest options for the development of commercial gas sensors for a broad range of such applications are solid state gas sensors, which are based on a variety of concepts and materials. [6-10].

2. Structure, Stability and Properties of Perovskites

Perovskite is the name given to the compounds that have the formula type ABX_3 with different sized 'A' and 'B' cations bonded to anion X [11]. ABO_3 Perovskites exhibit good thermal stability with an eV band gap of 3–4, which is why they were used in a lot of gas sensing studies [12]. Perovskite materials can be employed as sensors for gaseous species because their stability was significantly disrupted when exposed to gaseous environments, such as NO_2 , CH_4 , NH_3 , C_2H_5OH , acetone, etc. [13]. The chemiresistive I–V, phosphorescence, and fluorescence responses of these perovskite materials can be used to record the sudden changes in them. However, in these sensing investigations, the opto- electronic characteristics of perovskites are crucial. Renowned contenders with remarkable attributes including electrical conductivity, ferroelectricity, superconductivity, catalytic activity, etc. are perovskite oxides. There are several ways to synthesis the nanocrystalline perovskite material, including the hydrothermal, sol-gel, and chemical co-precipitation processes, etc. Because of the remarkable stability of the perovskite structure, structural flaws can be created when one or both of the cations in the A and B sites are partially substituted with other metals that have a different oxidation state.

3. Review of solid state gas sensor

Soil, water, and air pollution are the three categories into which environmental contamination falls. Of these three categories, air and water pollution are the main contributors to disasters since they spread quickly over a wide area in a short amount of time. Since industrial progress has dramatically expanded environmental pollution to such a level that public concern is now so great that it cannot be ignored any longer, environmental monitoring and management are absolutely necessary. Therefore, in order to address these environmental issues, thorough study has been done to quickly identify these contaminants and lower their levels to within the regulatory allowed concentrations. These factors have contributed to the advancement of solid-state gas sensor research and development in recent years. Gas sensors with metal oxides as the sensing medium have been widely used in gas detection applications. In fact, there is growing interest in gas sensing for nanocrystalline semiconducting metal oxides with regulated compositions, which also represent an intriguing new area of fundamental research [14]. Because of its oxide stability, high response, low production cost, and ability to respond to a wide spectrum of chemicals, semiconductor metal oxide nanostructures are the most preferred of all the solid state gas sensing materials. They respond quickly, are robust, dependable, and reasonably priced. Different types of solid state gas sensors are semiconductor gas sensor, optical gas sensor,

electrochemical gas sensor, etc. Semiconductor gas sensors (SGS), known sometimes as chemoresistive gas sensors, are typically based on metal oxides (e.g. SnO_2 , TiO_2 , In_2O_3 , WO_3 , NiO , etc.). Recent applied research and product releases in this sector of gas sensors have revealed some noteworthy developments regarding the use of nanotechnologies and gas-sensing layers. In the sensing industry, optical gas sensors are crucial for measuring chemical and biological quantities. Changes in the absorption spectrum were used to measure the first optical chemical sensors. Chemical sensors and biosensors currently employ a wide range of optical techniques, such as ellipsometry, surface plasmon resonance (SPR), spectroscopy (luminescence, phosphorescence, fluorescence, Raman), interferometry (white light, modal, and optical waveguide structures), spectroscopy of guided modes in optical waveguide structures (grating coupler, resonant mirror), and interferometry (white light,

phosphorescence, and fluorescence). Electrochemical gas sensors use an electrochemical cell, which is made up of two terminals (an anode and a cathode) of the same composition and a casing that holds a collection of chemical reactants (electrolytes or gels) in contact with the environment. A membrane on the top of the gas sensor enclosure allows the gas sample to pass through it. At the anode, oxidation happens, and at the cathode, reduction happens.

4. Conclusion

In this review study, the materials chosen for the construction of such gas sensors, and the sources of emission and regulatory standards of air pollutants are briefly reviewed. It has been addressed how advances in material science have led to the development of potential solid-state gas sensors, with the aim of comprehending the underlying technology and offering targeted functionality for a particular application.

References

- [1] P. T. Moseley, B. C. Tofield (eds.), *Solid State Gas Sensors*, Adam Hilger, Bristol and Philadelphia (1987).
- [2] M. J. Madou, S. R. Morrison (eds.), *Chemical Sensing with Solid State Devices*, Academic Press, New York, 1989.
- [3] A. Mandelis, C. Christofides (eds.), *Physics, Chemistry and Technology of Solid State Gas Sensor Devices*, Wiley (1993).
- [4] P. T. Moseley, *Meas. Sci. Technol.* 8, 223 (1997).
- [5] I. Lundström, *Sensors and Actuators B* 35-36, 11 (1996).
- [6] P. T. Moseley, B. C. Tofield (eds.), *Solid State Gas Sensors*, Adam Hilger, Bristol and Philadelphia (1987).
- [7] M. J. Madou, S. R. Morrison (eds.), *Chemical Sensing with Solid State Devices*, Academic Press, New York, 1989.
- [8] A. Mandelis, C. Christofides (eds.), *Physics, Chemistry and Technology of Solid State Gas Sensor Devices*, Wiley (1993).
- [9] P. T. Moseley, *Meas. Sci. Technol.* 8, 223 (1997).
- [10] I. Lundström, *Sensors and Actuators B* 35-36, 11 (1996)
11. T.M., Fthenakis, V.M., Eds.; Academic Press: Cambridge, MA, USA, 2018; pp. 233–254.
12. Varignon, J.; Bibes, M.; Zunger, A. Origin of band gaps in 3d perovskite oxides. *Nat. Commun.* 2019, 10, 1658.
13. Zhu, Z.; Sun, Q.; Zhang, Z.; Dai, J.; Xing, G.; Li, S.; Huang, X.; Huang, W. Metal halide perovskites: Stability and sensing-ability. *J. Mater. Chem. C* 2018, 6, 10121–10137.
14. N. Barsan, M. Schweizer-Berberich, W. Göpel, *Fresenius J. Anal. Chem.* 365, 287 (1999).